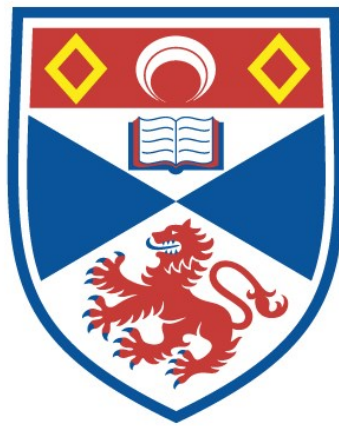


THE ORDOVICIAN ROCKS OF THE BAIL HILL AREA,
SANQUHAR, SOUTH SCOTLAND : VOLCANISM AND
SEDIMENTATION IN THE IAPETUS OCEAN

M. J. McMurtry

A Thesis Submitted for the Degree of PhD
at the
University of St Andrews



1979

Full metadata for this item is available in
St Andrews Research Repository
at:
<http://research-repository.st-andrews.ac.uk/>

Please use this identifier to cite or link to this item:
<http://hdl.handle.net/10023/15275>

This item is protected by original copyright

The Ordovician rocks of the Bail Hill
area, Sanquhar, South Scotland :
volcanism and sedimentation in the
Iapetus Ocean.

by

M. J. McMurtry

Thesis presented for the degree of Doctor
of Philosophy in the Faculty of Science of
the University of St. Andrews.

November 1979

ProQuest Number: 10171302

All rights reserved

INFORMATION TO ALL USERS

The quality of this reproduction is dependent upon the quality of the copy submitted.

In the unlikely event that the author did not send a complete manuscript and there are missing pages, these will be noted. Also, if material had to be removed, a note will indicate the deletion.



ProQuest 10171302

Published by ProQuest LLC (2017). Copyright of the Dissertation is held by the Author.

All rights reserved.

This work is protected against unauthorized copying under Title 17, United States Code
Microform Edition © ProQuest LLC.

ProQuest LLC.
789 East Eisenhower Parkway
P.O. Box 1346
Ann Arbor, MI 48106 – 1346

Th 9297

C E R T I F I C A T E

I hereby certify that Michael J. McMurtry engaged in research for 9 terms at the University of St. Andrews, that he has fulfilled the conditions of Ordinance No. 12 and Resolution of the University Court, 1967, No. 1, and that he is qualified to submit the accompanying thesis in application for the degree of Doctor of Philosophy.

E.K. WALTON.

I certify that the following thesis is of my own composition, that it is based on the results of research carried out by me, and that it has not previously been presented in application for a higher degree.

M.J. McMurtry.

For

Kay and Jack

"We are now in the Amazon system of rivers", he announced with satisfaction one day. "You see, the water is running south." But almost immediately they crossed a stream flowing in the opposite direction. "Very curious", said Dr. Messinger. "A discovery of genuine scientific value."

E.W.

"Hold to the centre", he said to himself, "as you move on. The future's not everything." And he dug his stick into the earth, with his eyes on the ground.

J.C.P.

The Ordovician rocks of the Bail Hill area, Sanquhar, South Scotland : volcanism and sedimentation in the Iapetus Ocean.

by

M.J.McMurtry

ABSTRACT

The Bail Hill area lies in the "Northern Belt" of the Southern Uplands and contains sedimentary and volcanic rocks of Llandeilo/Caradoc age.

The sedimentary succession has been divided into four formations - the Glenflossh, Kiln, Spothfore and Guffock Formations. The Glenflossh and Guffock Formations are mainly arenaceous and were largely deposited by turbidity currents flowing to the southwest. They typically consist of T_{ae} units. The fine-grained sandstones and siltstones of the Kiln Formation were also deposited by turbidity currents. Parallel-laminated units in the lower part of the formation represent "overbank" deposits, whilst lenticular-bedded units in the upper part are interpreted as channel-mouth deposits. Bouma sequences are not common in these lithologies. The Spothfore Formation consists of rudites deposited by a variety of sediment and fluid gravity flows close to a feeder system.

The petrography of greywackes within the formations shows no significant variation across strike, in contrast to successions studied to the southwest. The provenance of detritus in the sediments is believed to be the north-westerly Laurentian continent with a significant but variable intrabasinal contribution of sedimentary and volcanic debris. A stratigraphic succession for the area is proposed, although graptolite evidence for the relative ages of the formations is equivocal.

A new stratigraphic unit, the Bail Hill Volcanic

Group, is proposed and the petrography and field relations of the subdivisions within this group are discussed. Field relations suggest that the Bail Hill volcano was a composite, central-type structure. Early basaltic lavas were succeeded by more differentiated lithologies and pyroclastic activity increased with time.

The mineral and whole-rock chemistry indicates the Bail Hill Volcanic Group has differentiated along the sodic alkaline series (alkali basalt - hawaiite - mugearite - trachyte). Gabbroic and dioritic xenoliths in the extrusive rocks are believed to be fragments of a large sub-volcanic intrusive mass that underlay the Bail Hill volcano in Ordovician times. The volcanic pile as a whole has undergone metamorphism to zeolite facies grade. Higher grade assemblages in the xenoliths suggest that they were hydrothermally altered prior to incorporation in the extrusive rocks.

It is concluded that the Bail Hill Volcanic Group represents the remnants of a seamount within the Iapetus Ocean, whilst the sedimentary rocks record the transition from the abyssal plain into a Lower Palaeozoic trench. Northwesterly subduction of the Iapetus Ocean crust resulted in the accretion of the Bail Hill area on to the facing edge of the northwesterly Laurentian continent.

CONTENTS

	<u>Page</u>
CHAPTER 1 : INTRODUCTION	1
1.1 LOCATION OF AREA	1
1.2 HISTORY OF PREVIOUS RESEARCH	3
1.3 AIMS OF PROJECT	7
 PART 1 - THE SEDIMENTARY ROCKS (CHAPTERS 2-5)	 9
 CHAPTER 2 : STRATIGRAPHY	 10
2.1 INTRODUCTION	10
2.2 GLENFLOSH FORMATION	11
2.2.1 General	
2.2.2 Characteristic lithologies	
2.2.3 Age relations	
2.3 KILN FORMATION	12
2.3.1 General	
2.3.2 Characteristic lithologies	
(a) Black shales	
(b) Fine to medium-grained sandstones and siltstones	
(c) Greywackes	
(d) Volcanic rocks	
2.4 SPOTHFORE FORMATION	17
2.4.1 General	
2.4.2 Characteristic lithologies	
2.4.3 The clasts	
2.4.4 Field relations	
2.5 GUFFOCK FORMATION	22
2.5.1 General	
2.5.2 Characteristic lithologies	
(a) Black shales and cherts	
(b) Greywackes	

	<u>Page</u>
5.3 KILN FORMATION	49
5.3.1 Black shales and cherts	
5.3.2 Fine-grained sandstones and siltstones	
5.3.3 Greywackes	
5.4 SPOTHPORE FORMATION	54
5.5 CONCLUSIONS	57
 PART 2 - THE VOLCANIC ROCKS (CHAPTERS 6-9)	 59
 CHAPTER 6 : STRATIGRAPHY AND PETROGRAPHY	 60
6.1 INTRODUCTION	60
6.2 CAT CLEUCH FORMATION	61
6.2.1 General	
6.2.2 Field relations	
6.2.3 Petrography	
6.3 BUGHT CRAIG MEMBER	64
6.3.1 General	
6.3.2 Field relations	
6.3.3 Petrography	
6.4 PEAT RIG FORMATION	68
6.4.1 General	
6.4.2 Tongue Sike area	
6.4.3 Grain Burn area	
6.4.4 Peat Rig area	
6.4.5 Guffock Hill area	
6.5 GRAIN BURN FORMATION	73
6.5.1 General	
6.5.2 Field relations	
6.5.3 Petrography	
6.6 UNDIFFERENTIATED INTRUSIONS	75
6.7 OUTLYING TUFF MEMBERS	76
6.7.1 General	
6.7.2 Field relations	
(a) Stoodfold Member	
(b) Penfrau Member	
(c) Back Burn Member	
(d) Craignorth Member	

	<u>Page</u>
6.7.3 Petrography	
6.8 SUMMARY OF VOLCANIC ACTIVITY	84
CHAPTER 7 : MINERALOGY	90
7.1 INTRODUCTION	90
7.2 PYROXENES	90
7.2.1 General	
7.2.2 Sector-zoned pyroxenes	
7.3 AMPHIBOLES	105
7.4 PRIMARY MICAS AND SECONDARY CHLORITES	111
7.5 FELDSPARS	112
7.6 APATITES	115
7.7 ZEOLITES	116
7.8 PREHNITE	117
7.9 CONCLUSIONS	121
CHAPTER 8 : GEOCHEMISTRY	123
8.1 INTRODUCTION	123
8.2 ALTERATION	130
8.2.1 Geochemical constraints	
8.2.2 Petrographical constraints	
8.3 MAJOR AND TRACE ELEMENT DATA	132
8.3.1 Aluminium	
8.3.2 Iron and Magnesium	
8.3.3 Calcium	
8.3.4 Sodium	
8.3.5 Potassium	
8.3.6 Manganese	
8.3.7 Titanium	
8.3.8 Phosphorus	
8.3.9 Chromium and Nickel	
8.3.10 Strontium	
8.3.11 Barium	
8.3.12 Rubidium	
8.3.13 Lithium	
8.3.14 Zirconium and Yttrium	

	<u>Page</u>
8.4 INTERPRETATION	144
8.4.1 Nature of alteration	
8.4.2 Igneous spectrum and alkali elements	
8.4.3 Normative analyses	
8.4.4 AFM data	
8.4.5 Minor oxides and trace elements	
8.5 CONCLUSIONS	155
CHAPTER 9 : PETROGENESIS	157
CHAPTER 10: DISCUSSION	166
10.1 INTRODUCTION	166
10.2 THE VOLCANIC ROCKS	167
10.3 SEDIMENTATION AND FOREARC TECTONICS	172
10.4 MODEL FOR THE BAIL HILL AREA	184
ACKNOWLEDGEMENTS	188
REFERENCES	190
APPENDICES	
Appendix 1 List of graptolite specimens	
Appendix 2 Greywacke point-counting data	
Appendix 3 Orientation of folds in the area	
Appendix 4 Methods of sampling and chemical analysis of igneous rocks	
Appendix 5 Accuracy and precision of geo- chemical and mineralogical data	
Appendix 6 Samples localities	
Appendix 7 Logged sequences in the Glenflossh and Kiln Formations	
Appendix 8 Field maps of outlying tuff members	

LIST OF FIGURES

	<u>Page</u>
Figure 1 : (a) Location of area. (b) Regional geology (from O.S. Sheet 15).	2
Figure 2 : (a) Point-counting data plotted on triangular diagram (Glenflossh and Guffock Formations). (b) Point-counting data plotted on triangular diagram (Kiln and Spathfore Formations).	28
Figure 3 : Triangular diagram of feldspar, rock fragments and matrix components in grey- wackes for formation means.	29
Figure 4 : (a) Plot of Bail Hill pyroxenes on pyroxene quadrilateral. (b) Trend of Bail Hill pyroxenes compared with typical alkaline and subalkaline trends.	96
Figure 5 : Illustration of the sector-zoned pyroxene.	97
Figure 6 : Traverse from core to margin of sector- zoned pyroxene.	100
Figure 7 : Major-element oxide concentrations vs. SiO ₂ .	133
Figure 8 : Trace-element concentrations vs. SiO ₂ .	134

(Continued)

List of Figures (continued)

- Figure 9 : (a) Bail Hill rocks in relation to the igneous spectrum. 147
(b) Plot of total alkalis vs. SiO_2 for Bail Hill rocks.
- Figure 10 : (a) Iron-magnesium-alkali variation in the Bail Hill rocks. 151
(b) Ti-Y-Zr plot for the Bail Hill extrusive rocks.
- Figure 11 : (a) Zr vs. Zr/Y plot for Bail Hill extrusive rocks. 154
(b) Zr vs. P_2O_5 plot for Bail Hill extrusive rocks.

LIST OF TABLES

	<u>Page</u>
Table 1 : Greywacke formation means (point counting).	29
Table 2 : Comparison of greywacke formation means (point counting).	30
Table 3 : Pyroxene analyses (electron microprobe).	91
Table 4 : Sector-zoned pyroxene analyses (electron microprobe).	104
Table 5 : Pargasite and ferroan pargasite analyses (electron microprobe).	106
Table 6 : Secondary amphibole in xenoliths (electron microprobe).	107
Table 7 : Biotite and chlorite analyses (electron microprobe).	110
Table 8 : Plagioclase feldspar analyses (electron microprobe).	113
Table 9 : Zeolite and prehnite analyses (electron microprobe).	119
Table 10 : Partial analyses of apatites (electron microprobe).	120
Table 11 : Chemical compositions (oxides, wt%) and trace-element abundances (ppm) of xenoliths from the Bail Hill Volcanic Group.	124
Table 12 : Chemical compositions (oxides, wt%) and trace-element abundances (ppm) of basalts from the Bail Hill Volcanic Group.	125

(continued)

List of tables (continued)

	<u>Page</u>
Table 13 : Chemical compositions (oxides wt%) and trace-element abundances (ppm) of intermediate lavas from the Bail Hill Volcanic Group.	126
Table 14 : Chemical compositions (oxides wt%) and trace-element abundances (ppm) of pyroclastic rocks from the Bail Hill Volcanic Group.	127
Table 15 : Chemical compositions (oxides wt%) and trace-element abundances (ppm) of intrusives from the Bail Hill Volcanic Group.	128
Table 16 : Groundmass analyses (electron microprobe).	129

LIST OF PLATES

		<u>Between</u> <u>pages</u>
Plate 1	(a) Greywackes of the Glenflossh Formation. (b) Base of Spothfore Formation.	23-24
Plate 2	(a) Thick greywacke unit in Kiln Formation. (b) Trace fossil on greywacke base.	23-24
Plate 3	(a) Spothfore Formation rudites. (b) Spothfore Formation rudites.	23-24
Plate 4	(a) Guffock Formation greywackes. (b) Sole-markings on greywacke base.	23-24
Plate 5	(a) Lithologies of the Kiln Formation. (b) Lithologies of the Kiln Formation.	23-24
Plate 6	(a) Sediments of the Spothfore Formation. (b) Clast from cobble-conglomerate unit of the Spothfore Formation.	23-24
Plate 7	(a) Clast from Spothfore Formation cobble conglomerates. (b) Sediments of the Spothfore Formation.	23-24
Plate 8	(a) Sediments of the Spothfore Formation. (b) Sediments of the Spothfore Formation.	23-24
Plate 9	(a) Sediments of the Spothfore Formation. (b) Clasts in Spothfore Formation rudites.	23-24
Plate 10	(a) Photomicrograph of typical Glenflossh Formation greywacke. (b) Photomicrograph of Kiln Formation greywacke.	36-37

(Continued)

List of Plates (continued)		<u>Between</u>
		<u>pages</u>
Plate 11	(a) Photomicrograph of porphyritic lava clast in Spothfore Formation greywacke. (b) Photomicrograph of Guffock Formation greywacke.	36-37
Plate 12	Photomicrograph of arenite from Kiln Formation.	36-37
Plate 13	(a) Folding in rocks of the Kiln Formation. (b) Folding in rocks of the Glenfloss Formation.	45-46
Plate 14	(a) Auto-brecciated basaltic lavas of the Cat Cleuch Formation. (b) Amygdaloidal patches in Cat Cleuch Formation lavas.	89-90
Plate 15	(a) Photomicrograph of amygdale in basal Cat Cleuch Formation lavas. (b) Photomicrograph of amygdaloidal patch in Cat Cleuch Formation auto-brecciated basalts.	89-90
Plate 16	(a) Photomicrograph of Cat Cleuch Formation basalt. (b) Photomicrograph of hawaiite/mugearite lava.	89-90
Plate 17	(a) Photomicrograph of Bught Craig Member Matrix. (b) Photomicrograph of euhedral feldspar phenocryst.	89-90

(Continued)

List of Plates (continued)		<u>Between</u>
		<u>pages</u>
Plate 18	(a) & (b) Photomicrograph of hawaiite/ mugearite lava.	89-90
Plate 19	(a) Photomicrograph of late-stage intrusion. (b) Photomicrograph of "apatite-rock".	89-90
Plate 20	(a) Peat Rig Formation lavas containing crystal clots. (b) Ultramafic xenolith in Peat Rig lavas.	89-90
Plate 21	(a) Matrix and xenoliths of Bught Craig Member. (b) Matrix and xenoliths of Bught Craig Member.	89-90
Plate 22	(a) Xenoliths in lava matrix of Bught Craig Member. (b) Gabbroic xenolith in Bught Craig Member.	89-90
Plate 23	(a) Leucocratic gabbro xenolith in Bught Craig Member. (b) Melanocratic gabbro xenolith from Bught Craig Member.	89-90
Plate 24	(a) Melanocratic dioritic xenolith from Grain Burn Member. (b) Gabbroic xenolith in Bught Craig Member.	89-90
Plate 25	(a) Photomicrograph of gabbro xenolith. (b) Photomicrograph of melanocratic gabbro xenolith.	89-90

(Continued)

List of Plates (continued)		<u>Between</u>
		<u>pages</u>
Plate 26	(a) & (b) Photomicrograph of gabbro xenolith.	89-90
Plate 27	Photomicrograph of diorite xenolith.	89-90
Plate 28	(a) Pyroclastic rocks of outlying tuff members. (b) Pyroclastic rocks of outlying tuff members.	89-90
Plate 29	(a) Pyroclastic rocks of outlying tuff members. (b) Pyroclastic rocks of outlying tuff members.	89-90
Plate 30	(a) Pyroclastic rocks of outlying tuff members. (b) Pyroclastic rocks of outlying tuff members.	89-90
Plate 31	(a) Pyroclastic rocks of outlying tuff members. (b) Pyroclastic rocks of outlying tuff members.	89-90
Plate 32	(a) Laminated siltstones with bubble-cavity texture. (b) Photomicrograph of bubble-cavity texture.	89-90
Plate 33	(a) Photomicrograph of lithic tuff. (b) Photomicrograph of lithic tuff.	89-90
Plate 34	Sector-zoned pyroxene.	104-105

(Continued)

List of Plates (continued)

		<u>Between</u>
		<u>pages</u>
Plate 35	Sector-zoned pyroxene.	104-105
Plate 36	Sector-zoned pyroxene.	104-105
Plate 37	Sector-zoned pyroxene.	104-105

CHAPTER 1 : INTRODUCTION

1.1 LOCATION OF AREA

The area studied comprises some 15 sq km situated to the northwest of the Crawick Water, near Sanquhar in Dumfriesshire (Fig.1). It lies within the "Northern Belt" of the Southern Uplands of Scotland and is covered by O.S. sheets NS71SE, NS71SW, NS71NE and NS81NW. The area is bounded to the south by the Crawick Water, to the west by the Carboniferous rocks of the Sanquhar Coal Basin, to the north by the watershed of tributaries draining into the Crawick Water and to the east by grid line NS81.

The terrain is hilly, undulating between 200 and 500 metres. The highest point on the area, Polholm Rig, has an elevation of 495 metres (1610 feet). Bail Hill itself is an inconspicuous hill rising to 454 metres (1474 feet) close to the Ordovician-Carboniferous boundary in the southwest of the area. The Ordovician tableland is deeply dissected by streams and it is in these tracts that the underlying strata are exposed. Only on the flanks of Bail Hill are good exposures developed away from such stream sections.

The rocks constitute a series of Ordovician sediments and volcanics. The sediments cover 12 sq km of the total area and consist of greywackes, conglomerates, breccias, siltstones, shales and cherts. The volcanic rocks consist of lavas, pyroclastics and volcanoclastics.

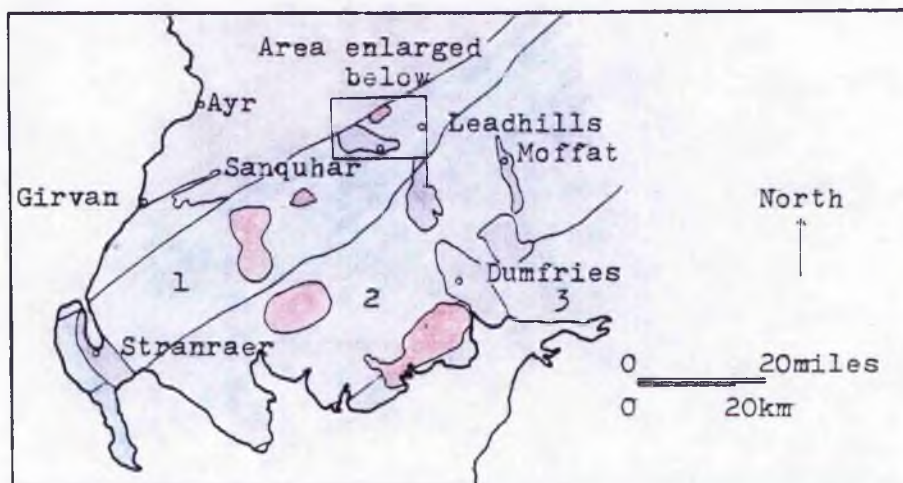


Figure 1(a): Location of the area. Purple = post Lower Palaeozoic; red = intrusive rocks; blue = Lower Palaeozoic rocks. (1 = Northern Belt; 2 = Central Belt; 3 = Southern Belt).

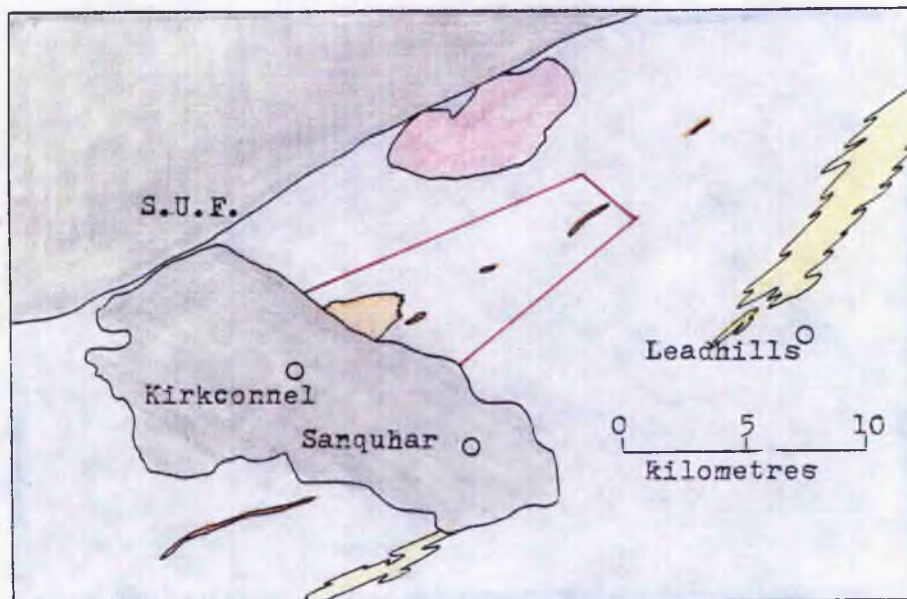


Figure 1(b): Regional geology (from Sheet 15). Grey = post-Ordovician; red = Spango granite; yellow = Leadhills line; orange = volcanic rocks; blue = greywackes. S.U.F. = Southern Uplands Fault. Red line indicates outline of area mapped.

Poor exposure and deep weathering pose many problems in subdividing successions.

All four, six or eight figure grid references in this thesis should be prefixed by the letters NS, unless otherwise indicated. For reasons of brevity the letters have been omitted.

1.2 HISTORY OF PREVIOUS RESEARCH

The first published account of the area is that by the Geological Survey of Scotland in 1871, as part of their "Explanation of Sheet 15". The account subdivides the Silurian rocks into two districts (Leadhills and Sanquhar) on topographical and geological grounds. The Sanquhar District includes the whole of the area covered in this thesis and the 1871 account of this is summarised below.

The general structure is taken as a broad synclinal fold which is interrupted by smaller isoclinal folds in the vicinity of Sanquhar itself. The rocks are assigned a Llandeilan age and attain an estimated minimum thickness of 13,100 feet (4000 metres) in the Scottish Survey's succession.

The igneous nature of the volcanic rocks is not recognised, the site being described as "... a remarkable area of metamorphism." The Scottish Survey note that the "metamorphic rocks" are found along an horizon in which the greywackes are feldspathic. This was thought to be one of the determining factors as to why these particular strata should be metamorphosed.

The volcanic nature of the rocks outcropping on Bail Hill was first recognised by Peach and Horne in their "Memoir on the Silurian Rocks of Scotland" (1899). In contrast to the earlier survey Peach and Horne envisaged the total thickness of strata spanning Arenig to Caradocian times as less than 4000 feet (1200 metres), and the succession to be repeated by isoclinal folding. Their stratigraphic succession has Arenig volcanics at the base, followed by radiolarian cherts (late Arenig-mid-Llandeilo), Glenkiln shales and, finally, greywackes and conglomerates.

The main Bail Hill volcanic pile is assigned by Peach and Horne to the basal Arenig episode, although they report the occurrence of interbedded volcanics and Glenkiln shales in nearby stream sections. The presence of pillow-lavas at Bail Hill is noted, although none were observed by the present author and no localities are given in the Memoir. It is thought by the present author that large round fragments in the lavas and pyroclastic rocks were mistakenly identified as pillows.

The lavas are variously described as andesites, diabase-porphyrates and biotite-andesites. The pyroclastic rocks include tuffs and agglomerates containing augite, hornblende and biotite. The agglomerates are reported to contain xenoliths of gabbro, diorite, granite, andesite and lava-types which do not outcrop in the area.

The sedimentary rocks are described as greywackes and conglomerates with cherts and shales. It is clear from the Memoir that the conglomerates of the Bail Hill area were not thought of as "Haggis Rock", despite

the indication to the contrary on Sheet 15. Peach and Horne suggest the conglomerates are indicative of uplift and erosion during Llandeilo and Caradoc times and they note that clasts in the conglomerates are all of rock-types found in the vicinity.

Peach and Horne conclude that the Southern Uplands succession "clearly indicates an oceanic phase of sedimentation ...", with the Bail Hill area representing the remnants "of an old volcano in Arenig time."

Scott (1914) described some augites from Bail Hill, giving details of their optical properties and a bulk chemical composition. From the chemical analysis Scott concludes that the augites are intermediate between non-titaniferous pyroxenes characteristic of calcic rocks and the titanaugites of the alkalic rocks, in agreement with the mildly alkalic nature of the Bail Hill rocks.

The "Haggis Rock" and other conglomerates in the Northern Belt are discussed in a paper by Ritchie and Eckford (1935). It is clear that they restrict the term "Haggis Rock" to the conglomerates found in the Fingland Burn, traceable via Kilbucho to Leadburn in the northeast, outcropping to the north of the present area. Other conglomerates, including those of the Bail Hill area, are described separately.

The conglomerates of the Bail Hill area are not assigned a position in their stratigraphic succession, although the volcanics are assigned to a mid-Llandeilo horizon. The Bail Hill conglomerates are described as being coarser than the "Haggis Rock", although the nature

of the clasts was not known. Ritchie and Eckford suggest the conglomerates represent a local stratigraphic break in the Bail Hill area, attributing their formation to the mechanism of "tidal scour" during Glenkiln times.

Volcanic fragments in the "Haggis Rock" are recognised as being petrographically similar to varieties found at Bail Hill and are attributed by Ritchie and Eckford to derivation from the same volcanic horizon.

Kennedy (1936), in a little-known paper, describes an apatite-rich rock from Bail Hill. A detailed description of the siting of the rock enabled the present author to visit the exact location. Unfortunately, it is now overgrown and in an attempted excavation only lapilli tuffs were uncovered.

Kennedy discusses the field relations, petrography and geochemistry of the "apatite-rock". He concludes that it is a pneumatolytically altered calcareous sediment and invokes fumarolic activity as the likely cause of alteration. His belief that the apatites in the Bail Hill rocks are of secondary origin is in contrast with the primary origin envisaged by Teall in the Memoir by Peach and Horne (1899).

The volcanic rocks are said to be of Caradoc age, although Kennedy does not state how this date was ascertained.

The Bail Hill volcanics were first systematically mapped and studied during the 1930's by Mrs.V.A.Eyles. An unpublished account of her work is kept in the I.G.S. building in Edinburgh. It is this work that is quoted by

Pringle (1948) and referred to by Greig (1971).

In her account the field relations and petrography of the volcanic rocks are discussed at length, and the outlying areas of pyroclastic rocks in the Kiln and Spothfore Burns and in Brown's Cleuch are correlated with the Bail Hill rocks. Four chemical analyses are presented, including that of a syenitic xenolith.

Harris et.al. (1965) obtained a potassium-argon date of 445 m.y. from biotites in the Bail Hill rocks. They suggest this as a minimum age for the Caradoc.

Churkin et.al. (1977) recalculated the date obtained by Harris et.al. (1965) using a refined decay constant and obtained an age of 456 m.y.

Piper (1978) obtained palaeomagnetic data from lithologies at five sites within the Bail Hill volcanic pile. The evidence is used to support the postulated existence of an ocean in Lower Palaeozoic times, separating the northwestern and southeastern forelands of the Caledonian orogen.

1.3 AIMS OF THE PROJECT

The aims of the project are as follows:-

1. To map Bail Hill and its environs, subdividing the sedimentary and volcanic successions where possible and constructing a stratigraphic column for the area.

2. To examine the nature of the sedimentary rocks and to determine their source(s) and depositional mechanism(s) and environment(s).

3. To examine the petrography, mineralogy and geochemistry of the volcanic rocks and to determine the nature of the volcanism and the petrotectonic affinities of the magma(s).

4. To determine the sediment-volcanic relationship and to assess the extent to which sedimentation was influenced by the volcanism.

5. To incorporate information from 1-4 into a regional model for the Lower Palaeozoic rocks of Britain.

A map showing the distribution and structure of the various stratigraphic units can be found at the back of the thesis.

Part 1 : The sedimentary rocks.

CHAPTER 2 : STRATIGRAPHY

2.1 INTRODUCTION

The sedimentary rocks have been subdivided into large units that can be traced along and across strike. Formations are based on sedimentary facies, with each formation characterised by a particular lithology, although they are generally a mixture of lithologies.

Throughout this section the term "greywacke" is used in the sense of Pettijohn (1957) to refer to a poorly sorted arenaceous rock with abundant interstitial argillaceous matrix. "Shale" is restricted to fissile rocks containing under 50% silt material. "Siltstone" refers to laminated or non-laminated rocks containing over 50% silt size material. Difficulties were encountered in trying to distinguish between shale and siltstone in the field. For this reason the sandstone:shale ratio, used by many authors in elucidating sediment types, has not been used in this research area. Furthermore in the Kiln Formation difficulties were encountered in distinguishing fine-grained greywackes from better-sorted sandstones and some siltstones in the field. Because of this and the fact that all three lithologies form significant sections of the Kiln Formation the less definitive term "sandstone" has been used for lithologies in this formation.

Four formations have been recognised in the area and these are, moving north to south:-

4) Guffock Formation (minimum thickness 800m) - greywackes with subordinate siltstones, black shales and cherts.

3) Spothfore Formation (300-800m) - rudites with subordinate siltstones.

2) Kiln Formation (700-900m) - fine-grained sandstones and siltstones with subordinate greywackes, black shales and cherts.

1) Glenfloss Formation (minimum thickness 900m) - greywackes with subordinate siltstones.

The Kiln and Spothfore Formations form a continuous stratigraphic succession and are fault bounded to the south against the Glenfloss Formation (Eller Fault) and to the north

against the Guffock Formation (Howcon Fault). The bottom of the Glenfloss Formation and the top of the Guffock Formation do not occur within the confines of the area.

2.2 GLENFLOSS FORMATION

2.2.1 General

The Glenfloss Formation is the most poorly exposed of the formations and attains its maximum outcrop in streams and road cuttings on the flanks of Glenfloss Hill. It also crops out in the lower reaches of the Kiln, Polcraig and Back Burns and in Hay Cleuch on the south-east bank of the Crawick Water. In the Kiln, Polcraig and Back Burns thick vegetation obscures exposure and thus detailed observations were only possible in the Spothfore Burn and in road cuttings opposite Nether Cog.

2.2.2 Characteristic lithologies

The dominant lithology is dark blue-grey greywacke with units grading from coarse or medium sand at the base to fine sand or silt at the top. Parallel and/or cross-lamination are occasionally observed in the upper part of units. Sole markings are locally developed but are not common. Units attain a maximum thickness of 1.2 m but are generally 0.3-0.6 m thick. Thin siltstone partings, with or without lamination, normally occur between units although amalgamated units are locally developed. Plate 1(a) illustrates a typical outcrop of Glenfloss greywackes.

Interbedded with the graded greywacke units are

siltstones with sandy laminae. These occur as packets up to 2.5 m thick and are strongly cleaved parallel to bedding. The sandy laminae are not graded but frequently display parallel or cross-lamination. Lensing of the sandy laminae was not observed although poor exposure inhibited tracing individual units for more than a metre along strike. Locally the siltstones form up to 50% of the succession, although overall they constitute less than 20%.

2.2.3 Age relations

Fossil evidence was not obtained from this formation. However, Peach and Horne (1899) obtained graptolites from shales outcropping on Duntercleuch Rig (840160) which are along strike from the Glenfloss Formation. Peach and Horne (1899) conclude that the assemblages are transitional between Glenkiln and Hartfell faunas. H. Williams (pers. comm., 1979) states that the faunas listed by Peach and Horne (1899) from the Back Burn locality are from the N. gracilis and C. peltifer zones, whilst those from Duntercleuch Burn range in age from N. gracilis to D. clingani.

2.3 KILN FORMATION

2.3.1 General

The Kiln Formation is best exposed in the Kiln Burn and its tributaries. Good sections also occur in the Polcraig, Spothore and Back Burns, in Brown's Cleuch and in cuttings on the flanks of Craignorth Hill.

2.3.2 Characteristic lithologies

The dominant lithology is fine sandstone and siltstone, although greywackes, black shales and volcanic rocks also crop out.

(a) Black shales : Black shales crop out at the base of the formation. They crop out in all the major stream sections and also on the B740 road at Eller Scar. In the Kiln Burn they are associated with green and grey radiolarian cherts. The relationship between the two lithologies is obscured by incomplete exposure. The cherts, however, crop out to the south of the black shales and if the northerly younging direction, widely observed elsewhere in the area, is tenable would lie below the black shale horizon.

The shales are highly folded and faulted and their total thickness is unknown. They are, however, no more than a few tens of metres thick, a more accurate estimate being precluded by incomplete exposure.

The shales are characteristically fossiliferous and graptolite faunas from the N.gracilis zone were collected in the Kiln and Polcraig Burns and in cuttings on the B740 at Eller Scar (see Appendix 1 for faunal lists).

In the Spothfore Burn black graptolitic shales and cherts are found in a fault-bounded slice with associated volcanics within the Kiln Formation. The shales yield a N.gracilis fauna (see Appendix 1 for faunal lists) and in places are seen to overlies green radiolarian cherts. Black shales and green and grey radiolarian cherts also crop out in the southwest of the area in the Cat Cleuch. Here, black shales yielding a N.gracilis fauna (see

Appendix 1 for faunal lists) are overlain by the basal lavas of the Bail Hill Volcanic Group (see Section 6.2.1). The cherts are inferred to underlie the black shales in this section.

The black graptolitic shales are internally structureless (i.e. without lamination) and silt- and sand-size particles are notably absent.

(b) Fine to medium-grained sandstones and siltstones :

The characteristic lithology of the Kiln Formation is fine-medium-grained sandstone with or without siltstone and shale horizons. Parallel and cross-lamination are the most common sedimentary features of the sandstones.

In subaerial exposures the rocks are well-cleaved parallel to bedding and internal features are masked. The latter are best displayed in subaqueous outcrops where surfaces have been smoothed and polished.

In the lower part of the formation parallel lamination is dominant over cross-lamination. Units of fine-grained sandstone or siltstone alternate every few cms with units of fine siltstone or shale (see Plate 5(a)). Units show sharp tops and bases and are very rarely graded. In the terminology of Campbell (1967) individual units are "thin beds" or "laminae" and show "even parallel stratification".

In the Kiln Burn pale-grey sandstones alternate with poorly laminated siltstones. The sandstones are not laminated but occasionally show grading at the top of units into the overlying siltstone units.

In the Back Burn pale-green, non-fossiliferous

shales up to 5 cm thick are found in a siltstone and sandstone sequence (see Plate 5(a)). Sandstones are not as common as in the Kiln Burn and often display cross-lamination.

These rhythmically parallel laminated rocks form sequences tens of metres thick, separated by graded, massive or cross-laminated greywackes. The fine-medium-grained sandstones are generally better sorted than the greywackes and in the terminology of Dott (1964) many of them are arenites rather than wackes.

In the Stoodfold and Kiln Burns and in Brown's Cleuch siltstones are interbedded with lithic tuffs (see Section 6.7.1). Lamination in these siltstones is due to variation in grain-size with units up to a few cms thick. At (76901386) some of the silt laminae show normal grading, with decrease in the percentage of silt particles visible in thin-section. It is in this lithology that the bubble-cavity texture is found (see Section 6.7).

In the upper part of the formation fine sandstones and siltstones containing cross-laminated lenticular horizons crop out (see Plate 5(b)). In Campbell's (1967) terminology the rocks are described as "discontinuous, wavy, non-parallel bedding", but are more accurately described as lenticular bedding with single and connected lenses (Reineck and Singh, 1973).

The sandy laminae are moderately sorted and contain abundant matrix (15%+). The single and connected lenses display cross-lamination, with both lee and stoss laminae occasionally visible in the same ripple. The

material separating the sandy lenses is fine sandstone or siltstone containing thin "stringers" of sand that when traced along strike frequently terminate as starved ripples. The sand "stringers" preserve the paths of the ripples as they migrated across the sediment-water interface. Shales are not found in this succession.

The lenticular bedded sands are well displayed in the Kiln Burn at (768139), in the Spothfore Burn at (78431520) and in the Back Burn at (79251569). The lenticular bedded lithologies are interrupted by occasional coarse greywacke units.

(c) Greywackes : Interbedded with the fine-medium grained sandstones and siltstones are thick, coarse greywacke units. The lower parts of units are generally structureless or graded, whilst the upper parts may show parallel and/or cross-lamination. One unit in the Kiln Burn at (772135) is 3.3 m thick and displays reverse grading in the bottom 30 cms before grading normally to fine sand (see Plate 2(a)). More commonly units are 0.3-0.5 m thick. Sole markings are locally developed and one unit displays a series of sinuous ridges which originated as furrows on the underlying siltstone unit, formed by some organism(s) migrating across the surface (see Plate 2(b)).

Although locally abundant the greywacke units are subordinate to the finer-grained lithologies.

(d) Volcanic rocks : Interbedded with the sediments of the Kiln Formation are volcanic rocks of pyroclastic origin. They crop out in the Stoodfold and Kiln Burns, in Brown's Cleuch and in the Spothfore and Back Burns. The rocks

include lithic and crystal tuffs, agglomerates and volcaniclastic sediments. They are considered in detail in Section 6.7.

2.4 SPOTHFORE FORMATION

2.4.1 General

The Spothfore Formation is exposed in the Kiln, Spothfore and Back Burns, on the flanks of Guffock Hill and in stream cuttings near Corsebank farm. The best exposures are in the Spothfore Burn, after which the formation is named.

2.4.2 Characteristic lithologies

The lithologies of this formation are coarse-grained sandstones and rudites. Following the classification of Davies and Walker (1974) the following types have been recognised :-

1. Cobble-boulder and cobble conglomerates (see Plates 3(a), 3(b) and 9(b)).
2. Coarse-pebble conglomerates and breccias (see Plates 8(b) and 9(a)).
3. Fine-pebble conglomerates and breccias (see Plate 7(b)).
4. Granule-sandstones (± rare cobbles) (see Plates 6(a) and 8(a)).
5. Laminated fine sandstones and siltstones. Lithology 5 is a continuation of the lenticular bedded material found in the upper part of the Kiln Formation

(see Section 2.3.2).

2.4.3 The clasts

All clasts over 0.4 cm diameter are of intrabasinal origin, with sediments constituting 95% and volcanic rocks 5% of the total. The sedimentary clasts include greywackes, siltstones, shales and cherts. Limestones, non-greywacke sandstones and rudite clasts are not found. The volcanic clasts include lavas, pyroclastics and volcaniclastics. In the classification of Kelling and Holroyd (1978) the rocks are intrabasinal autochthonous rudites.

The largest observed clasts are of greywacke and siltstone. Clasts of up to 2 m were observed, whilst at some localities clasts of 5 m+ were inferred. The greywacke clasts commonly display smooth, rounded outlines and are internally structureless. Some clasts display almost perfect spherical outlines with diameters of 10-25 cms. The outer skin of these clasts is usually porous and is texturally different from the rudite matrix. At the centre of these clasts there is usually a fragment (2-5 cms) of siltstone or shale (see Plate 7(a)). The significance of this is discussed in Section 5.4. The grain-size of the greywacke clasts rarely reaches coarse sand grade and fine-medium grained clasts are most abundant in the cobble-boulder and cobble conglomerates and in the coarse-pebble conglomerates.

Siltstone clasts are usually subrounded, elongate and rarely more than 30 cms in length. Lamination is often

preserved in such clasts and in some instances the laminae are contorted and twisted, indicating the clast was "plastic" when transported. Siltstone clasts are found in all rudite types.

Shale fragments occur as small subangular clasts of under 10 cms and as elongate shale rafts up to 2 m in length. From two such clasts graptolite faunas were collected (see Appendix 1 for faunal lists). The shales are black and non-laminated.

Chert fragments are rarely more than 20 cms in size (for exceptions see Section 2.4.4), displaying subrounded to subangular outlines. Grey, green, chocolate-brown, red and black varieties occur and included radiolaria were often observed.

The volcanic clasts are porphyritic lavas and tuffaceous sandstones of intermediate (hawaiite/mugearite) composition. The material is often porous and displays subangular to subrounded outlines. The largest observed clast, a biotite-amphibole-plagioclase feldspar-bearing lava, was 25 cms long.

Shales, cherts and volcanic clasts are found in all rudite types.

2.4.4 Field relations

The conglomerates and breccias are generally characterised by an absence of sedimentary features of use in distinguishing units. Where units were distinguished they were 0.6-2.5 m thick, with planar tops and bases. Channeling and erosion of the underlying units was only

observed at (77561520) where a cobble conglomerate cuts into the underlying siltstone unit to a depth of 0.7m.

The lithologies are typically chaotic, showing no internal grading (normal or reverse), stratification or imbrication. The only exceptions to this occur in the Spothfore Burn at (78421521) where a fine-pebble breccia displays lamination and imbrication (see Plate 7(b)), and in the Kiln Burn at (76801429) where coarse-tail grading can be seen in granule-sandstone units.

In the Spothfore and Kiln Burns units of red and green chert crop out within the Spothfore rudite sequences. Although at several localities they appear to be conformable with the dip and strike in the rudites (e.g. 78031526), they are believed to be large exotic clasts and not interbedded units. At (78301527) the base of a large green chert clast is separated from underlying fine pebble conglomerates by a thin (1-5 cm) parting of khaki-coloured clay material. In the gully upstream (78231529) well-bedded cherts with ashy(?) partings crop out. Occasional rudite units indicate that the chert sequence is not continuous, although the contact between the two lithologies is not exposed. On the banks above the gully, along strike from the chert units, clastic rocks crop out and cherts are not found. As there is no evidence for faulting in this area, it is suggested that the cherts are large clasts and therefore discontinuous along strike.

Further evidence for an exotic origin for the cherts is found at (78201530). Here folded red and green cherts show considerable variation in the attitude of the

folds and display possible thickening of units near fold hinges. Nearby rudite units are apparently unfolded. It is suggested that the chert deformation is pre-tectonic and possibly related to their incorporation in the rudites.

At (78051527) the upper contact between cherts and cobble conglomerates is exposed. The contact is sharp, with bedding in the chert slightly oblique to the basal conglomerate. Flashes of chert are seen to pass up into the conglomerate indicating that the chert was not fully consolidated when the conglomerate was deposited. If it is assumed that there is a simple chert-rudite relationship (i.e. tectonic, interbedded or with the cherts as clasts in the rudites) then this sharp top contact can only be resolved with the three features mentioned above (nature of bottom contact, discontinuity along strike and folding of cherts) if the cherts are large exotic blocks in the Spothore rudites. The dimensions of the blocks are not known as they are only visible in the stream section and cannot be traced laterally. It seems probable, however, that the blocks attain dimensions of up to several tens of metres.

Fine sandstone and siltstone units with parallel and cross-lamination are interbedded with the rudites at several localities (e.g. (76511448), (79231579) and (806166)). These form packets of up to 20 m thick and are similar to lithologies in the Kiln Formation.

2.5 GUFFOCK FORMATION

2.5.1 General

The Guffock Formation is the most northerly unit of the stratigraphic sequence and is poorly exposed. It crops out in the burn draining the southwest flank of Guffock Hill, in the upper reaches of the Kiln, Spothfore and Back Burns and in Glenaners Burn.

2.5.2 Characteristic lithologies

Greywackes are dominant over siltstones, black shales and cherts.

(a) Black shales and cherts : Black shales and cherts crop out at the base of the formation. In the Grain, Kiln and Sow Burns dark grey and green cherts are poorly exposed. Radiolarian-rich, chocolate-brown varieties were observed in the Kiln Burn section. The cherts are generally well-bedded, with units 10-25 cms thick. Individual units are separated by thin yellow ashy(?) bands. Pale green siltstone/shale units crop out in close proximity to the cherts, although the relationship between the two lithologies is not known.

In the Polholm, Back and Polthistly Burns black graptolitic shales crop out which yield faunas characteristic of the N.gracilis zone. The shale outcrop in the Back Burn is particularly impressive. The graptolites are in excellent preservation and two new species have been identified at this locality (see Appendix 1 for faunal lists). The shales are strongly fractured and faulted and

this together with the incomplete exposure precludes an accurate estimate of the thickness of this lithology. In Back Burn, however, the shales crop out on both banks for upwards of 50m.

(b) Greywackes : The dominant lithology of the Guffock Formation is dark blue-grey greywacke. Grading from coarse or medium sand to fine sand or silt is ubiquitous. In the Glenaners Burn the base of some units is pebbly sandstone, with clasts of shale, red chert and quartz. Some of these shale clasts show signs of "plastic" deformation. Units are generally 0.3-0.6 m thick and only in the Back and Glenaners Burns do thicker units crop out. Sole markings (flutes and long ridges) are locally abundant, particularly in the Guffock Hill Burn (see Plate 4(b)). A typical outcrop of Guffock Formation greywacke units is illustrated in Plate 4(a).

The greywacke units are separated by packets of well-cleaved siltstone, 0-20 cms thick, although in the Back Burn they reach a metre or more. Poorly developed parallel and cross-lamination was observed in these lithologies, although their well-cleaved nature obscures internal sedimentary features.



Plate 1(a): Greywackes of the Glenfloss Formation. Typical example of T_{ae} units, younging left to right. Eller Scar, B740 road.



Plate 1(b): Base of the Spothfore Formation. Hammer rests on a cobble conglomerate unit which is interbedded with lenticular sandstones of the upper part of the Kiln Formation. Sequence youngens left to right. Back Burn.



Plate 2(a): Greywacke unit in the Kiln Formation. Unit is 3.3 m thick and displays reverse grading in lower 30 cms (right) before grading normally to fine sand (left). Tape measure (centre right) is 1 m long. Kiln Burn.



Plate 2(b): Trace fossil on turbidite base (Cosmorhape). Sinuous grooves on underlying siltstone unit preserved as cast on greywacke base. Grooves originated by migration of organism(s) across silt-water interface. Kiln Formation, Kiln Burn.



Plate 3(a): Spothfore Formation rudites. Siltstone clasts in cobble conglomerate. Weathering on clast at centre bottom accentuates lamination in clast. Kiln Burn.



Plate 3(b): Spothfore Formation rudites. Cobble-boulder conglomerates containing intrabasinal sedimentary and volcanic clasts. Kiln Burn.



Plate 4(a): Guffock Formation greywackes. Thick, medium sand-grade turbidite units with thin siltstone partings. Younging right to left. Back Burn.



Plate 4(b): Sole-markings on greywacke base. Flute-casts on base of turbidite unit in the Guffock Formation indicate a current flowing to the southwest. Coin (5p) at centre for scale. Back Burn.



Plate 5(a): Lithologies of the Kiln Formation. Parallel-laminated siltstones (dark grey) and shales (medium grey) from the lower part of the Kiln Formation. Siltstones contain thin, lenticular sandstone laminae. Specimen collected in Back Burn section.

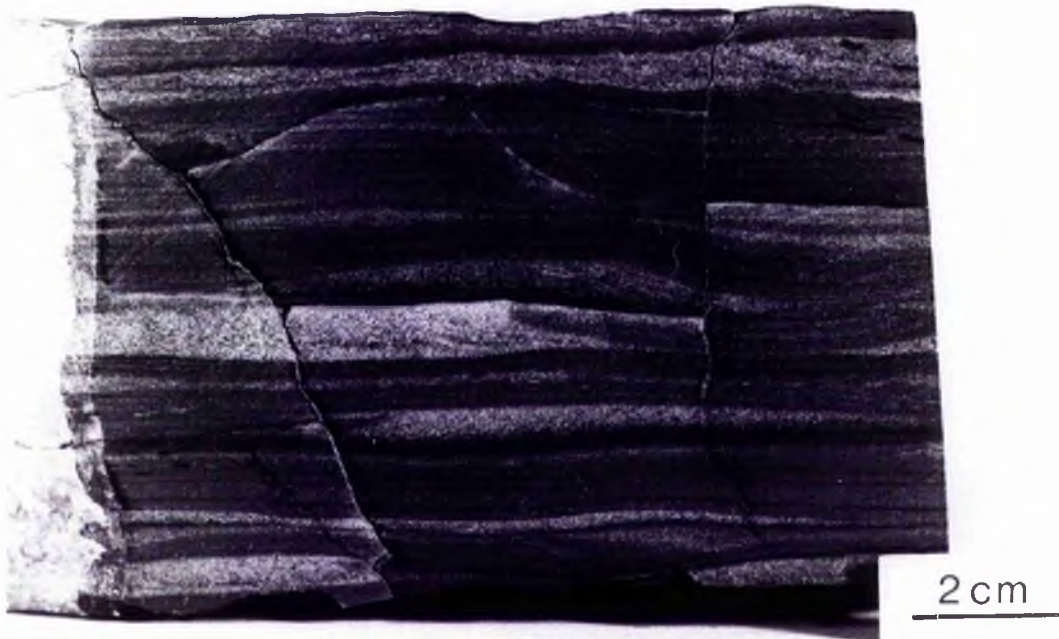


Plate 5(b): Lithologies of the Kiln Formation. Lenticular bedded sandstones and siltstones from the upper part of the Kiln Formation. Specimen collected in Back Burn.



Plate 6(a): Sediments of the Spothfore Formation. Amalgamated pebbly sandstone units from the base of the Spothfore Formation. Two porphyritic lava clasts can be seen at the base of the second unit. Specimen collected in Back Burn section.



Plate 6(b): Clast from cobble-conglomerate unit of the Spothfore Formation. Volcaniclastic sandstone with thin mud veneer (bottom right). Specimen collected in Back Burn section.



Plate 7(a): Clast from Spothfore Formation cobble-conglomerates. Spheroidal sandstone clast with mudstone nucleus. Specimen collected in Spothfore Burn section.



Plate 7(b): Sediments of the Spothfore Formation. Lamination and imbrication in fine-pebble breccia from the base of the Spothfore Formation. Imbrication indicates a current flowing to the southeast. Specimen collected in Spothfore Burn section.



Plate 8(a): Sediments of the Spothfore Formation. Granule-sandstone from unit displaying coarse-tail grading. Granules are composed of quartz, intrabasinal sediments and porphyritic lavas. Specimen collected in the Kiln Burn section.



Plate 8(b): Sediments of the Spothfore Formation. Coarse-pebble conglomerate containing predominantly chert clasts, although greywacke fragment is visible at top left. Matrix to clasts is of greywacke composition. Specimen from Spothfore Burn section.



Plate 9(a): Sediments of the Spothfore Formation. Coarse-pebble conglomerate containing material that was brittle (veined clasts to left and right) and plastic (streaky material, bottom left) when incorporated in rudite unit. Specimen from Back Burn section.

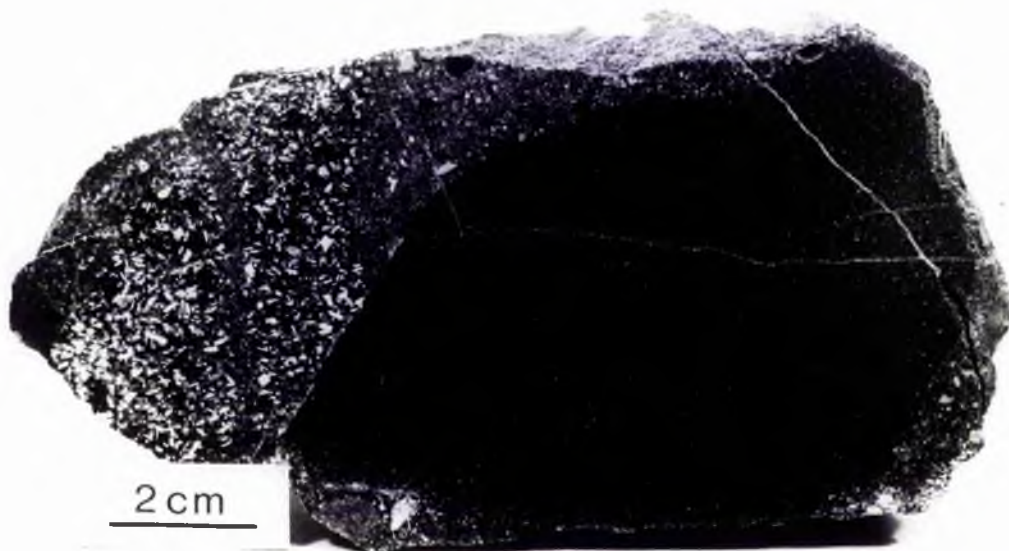


Plate 9(b): Clasts in Spothfore Formation rudites. Greywacke clast (right) and porphyritic lavas (left) in cobble-boulder conglomerate with greywacke matrix. Specimen collected on flanks of Craignorth Hill.

CHAPTER 3 : PETROGRAPHY

3.1 INTRODUCTION

This chapter is an account of the petrography of the greywackes from the four sedimentary formations and how they equate with equivalent formations to the southwest. The petrography of the fine-grained sandstones from the Kiln Formation is discussed in a separate section at the end of the chapter.

Variation in the petrography of Southern Uplands greywackes has proved a useful tool in subdividing and correlating successions. Kelling (1961, 1962), Welsh (1964) and Floyd (1975) have studied greywackes along strike from the present area and Floyd (1975) used petrographic criteria to subdivide his succession into formations. This approach was not used in the present area and formations are based on sedimentary facies rather than petrographic criteria. However, greywackes occur in all formations and specimens were collected in order to ascertain the nature and significance of any petrographic variation and to aid correlation with other areas.

Grid sampling was not feasible due to poor exposure and the scarcity of suitable lithologies where outcrop was found. Over three-quarters of the specimens were collected from the three main stream sections, the Kiln, Spothfore and Back Burns. The remainder were collected from key localities such as the Guffock Hill Burn and from cuttings on the B740 road to Crawfordjohn.

Each formation was sampled across strike in at least one stream section, with specimens collected every 100-200 m. Additional samples were collected wherever suitable lithologies were found. At several localities adjacent or nearby units were sampled to see if there were significant differences between neighbouring units.

Where possible, units with a maximum grain-size of coarse sand were selected for modal analysis. However, some finer-grained varieties were incorporated wherever there was a scarcity of suitable lithologies.

Sample localities are given in Appendix 2.

3.2 MODAL ANALYSIS

3.2.1 The constituents

In the study 1000 points were counted in successive traverses across a thin-section and assigned to one of eight categories. Cross-cutting veins were not included in the count. A total of 68 specimens were used in the study.

The eight categories are :-

1. Quartz, including all mono- and poly-crystalline grains, but excluding metamorphic and sedimentary quartzite fragments:
2. Feldspar, including all discrete grains of alkali and plagioclase feldspar:
3. Basic igneous rock fragments, including all clasts of melanocratic igneous rocks (basalts, spilites, andesites and related rocks, gabbros, diorites and volcanic

glass):

4. Acid igneous rock fragments, including all clasts of leucocratic igneous rocks (granites, granophyres and quartz bearing fine-grained igneous clasts):

5. Metamorphic rock fragments, including all clasts of slate, phyllite, schist and quartzite:

6. Sedimentary rock fragments, including all clasts of chert, shale, siltstone, sandstone (including greywackes) and limestone:

7. Ferromagnesian minerals, including all detrital grains of pyroxene, amphibole, epidote and olivine:

8. Matrix, including all material under 0.01mm, heavy minerals, micas and material not covered in 1-7.

3.2.2 Sources of error

There are several possible sources of error in assigning grains to one of these categories, the chief of which are mentioned below :-

1. Feldspar : Fresh untwinned alkali feldspar can be confused with quartz. Plagioclase that has broken down largely to white mica can be confused with siltstone or shale. Plagioclase that has altered to carbonate material can be confused with detrital calcite (matrix) or limestone.

2. Fine-grained sedimentary material can be confused with matrix, especially as some shale and siltstone clasts are "squeezed" between grains.

3. Acid-igneous fine-grained material can be confused with chert or devitrified volcanic glass.

4. Polycrystalline quartz can be mistaken for sedimentary or metamorphic quartzite, or coarse acid-igneous fragments.

Individual techniques for avoiding such errors result in individual operator-bias. Thus, whereas results and correlation may be fairly reliable where only one operator is involved, there are uncertainties in correlating between operators. To ascertain any errors inherent in comparison between operators two of J.D.Floyd's specimens were point-counted by the present author and the results compared with those of Floyd. It was found that there was very close correlation on quartz and matrix counts. Basic and acid igneous, metamorphic and ferromagnesian categories also showed close agreement for both specimens. The feldspar and sedimentary categories showed close agreement on one count but were disparate on the other. The order of magnitude, however, was similar. It is concluded that tentative correlation of greywacke types, using certain categories of constituent, can be made between the Bail Hill area and those of west Nithsdale.

3.2.3 Point counting results

The results of the modal analyses of 68 greywacke specimens are listed in Appendix 2 and summarised in Table 1. It can be seen from Figure 3 that the greywackes of the four formations fall close together near the lithic/feldspathic greywacke boundary. The greywackes of the Guffock Formation and the greywacke matrix to the Spothfore Formation rudites both lie in the feldspathic greywacke field, whilst

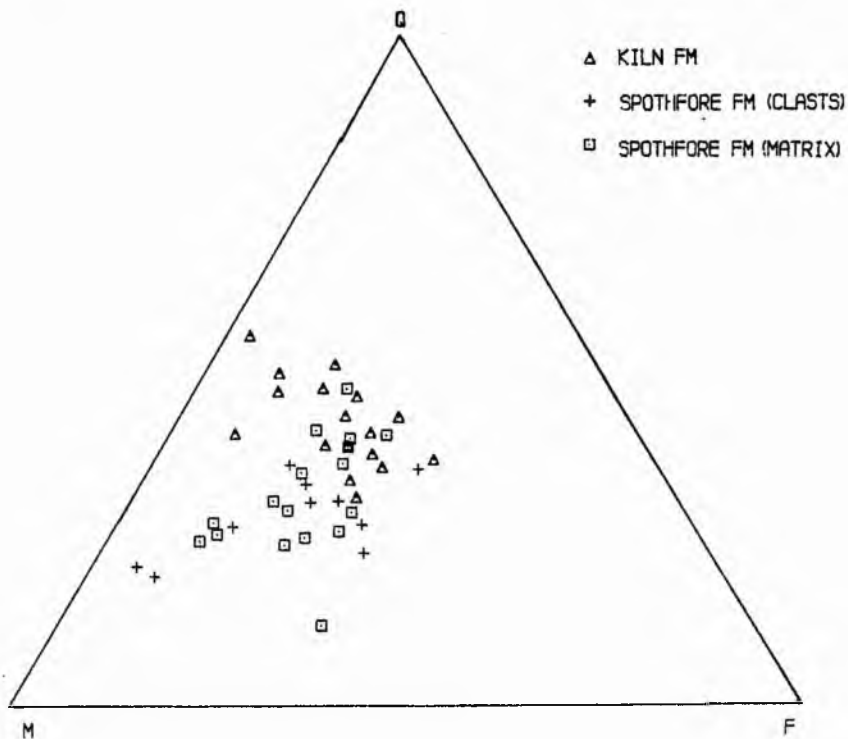
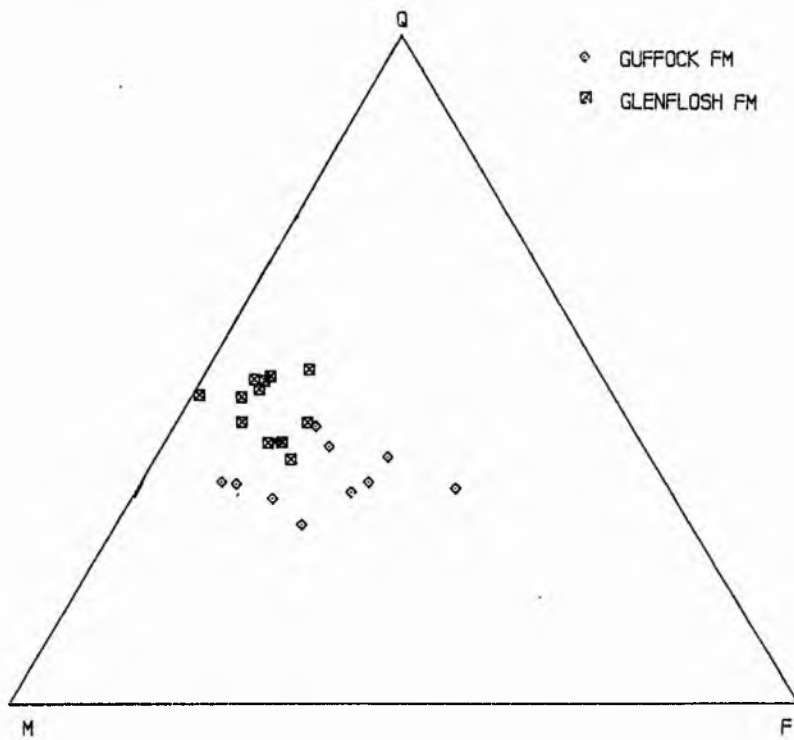


Figure 2: Point-counting data for greywacke samples plotted on triangular diagram.

Q= Quartz + acid igneous + metamorphic; E= Feldspar + basic igneous + ferromagnesian minerals; M= Matrix + sedimentary.

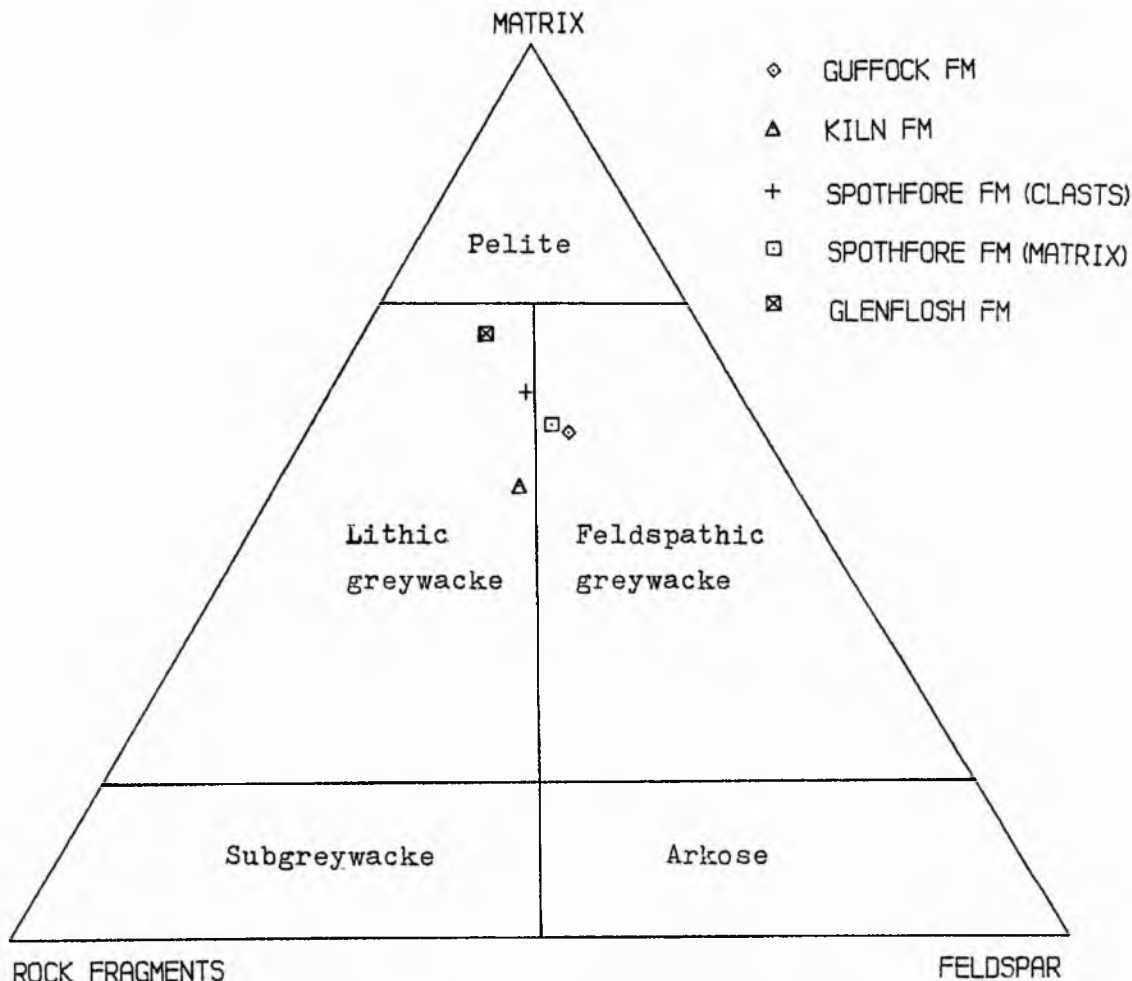


Figure 3: Triangular diagram for components feldspar, rock fragments and matrix. Data are from the formation means in Table 1, and are recalculated to 100%. Diagram based on Pettijohn (1957).

Table 1. Greywacke formation means (point counting).

Component	Glenflosch	Kiln	Spothfore (Mx)	Spothfore (Clasts)	Guffock
Quartz	41.2	37.5	27.3	25.4	30.1
Feldspar	6.9	14.5	16.6	13.9	17.4
Basic ig.	3.6	6.3	5.4	8.1	4.8
Acid ig.	1.2	2.2	2.4	1.5	2.4
Metamorphic	2.0	1.6	1.4	1.4	1.8
Sedimentary	5.3	6.2	5.0	4.0	3.9
Ferromags.	-	-	0.1	0.2	0.1
Matrix	39.8	31.7	41.8	45.5	39.5

see Appendix 2 for full data

Table 2. Comparison of greywacke formation means (point counting).

(a) MCMURTRY (this thesis: see Appendix 2 for full data)

Component	Formation Means				
	Glenflossh	Kiln	Spothfore Matrix	Spothfore Clasts	Guffock
Quartz	41.2	37.5	27.3	25.4	30.1
Feldspar	6.9	14.5	16.6	13.9	17.4
Basic ig.	3.6	6.3	5.4	8.1	4.8
Acid ig.	1.2	2.2	2.4	1.5	2.4
Metamorphic	2.0	1.6	1.4	1.4	1.8
Sedimentary	5.3	6.2	5.0	4.0	3.9
Ferromags.	-	-	0.1	0.2	0.1
Matrix	39.8	31.7	41.8	45.5	39.5
n (68)	12	17	17	11	11

(b) FLOYD (1975, Table 5)

	Marchburn	Afton	Blackcraig	Shinnel	Scar
Quartz	14.9	48.3	33.4	56.7	20.3
Feldspar	44.3	14.1	15.8	14.9	49.5
Basic ig.	7.1	4.4	13.6	2.0	4.3
Acid ig.	3.5	0.9	2.6	1.2	2.3
Metamorphic	1.0	2.7	4.2	0.7	1.4
Sedimentary	1.6	1.4	1.3	2.0	1.5
Ferromags.	1.5	0.2	6.1	0.2	1.7
Matrix	26.1	28.0	23.0	22.3	19.0
n (152)	22	50	20	30	30

(c) WELSH (1964, Table 13)

	Lochryan	Cairnerzean	Boreland	Glenwhan
Quartz	28.5	13.7	19.0	4.8
Feldspar	7.4	15.3	21.6	13.9
Basic ig.	18.7	27.7	17.5	47.5
Acid ig.	9.8	5.9	8.7	4.3
Metamorphic	9.6	10.0	1.9	2.2
Sedimentary	5.2	2.9	1.2	3.8
Ferromags.	-	7.1	-	5.4
Matrix	20.8	17.4	30.0	18.1
n (92)	39	27	5	21

(d) KELLING (1962, Tables 2 and 3)

	Corsewall	Kirkcolml	Galdenoch	Port. Acid	Port. Basic
Quartz	16.6	29.6	26.2	17.2	8.6
Feldspar	17.5	11.1	9.7	18.6	30.9
Basic ig.	17.7	9.0	10.2	14.6	29.4
Acid ig.	17.4	13.3	13.2	15.5	5.5
Metamorphic	0.8	4.8	2.8	1.6	0.6
Sedimentary	1.1	5.0	1.8	3.6	2.3
Ferromags.	10.3	0.6	7.8	3.5	13.4
Matrix	18.3	26.8	28.0	25.4	9.3
n (74)	24	37	3	5	5

n = number of specimens

the Glenflossh and Kiln Formations together with greywacke clasts in the Spothfore Formation rudites lie in the lithic greywacke field.

3.3 SUMMARY OF THE PETROGRAPHY OF THE FORMATIONS

3.3.1 General

The categories which show most variation through the succession are quartz, feldspar, basic igneous and matrix. In addition the ferromagnesian count which is of significance elsewhere (Kelling, 1962; Welsh, 1964; Floyd, 1975) is commented on, although it shows little variation in the present area.

3.3.2 Glenflossh Formation

The formation is characterised by quartz-rich, feldspar-poor greywackes without significant ferromagnesian mineral contribution (see Fig.2(a)).

The feldspar is generally a mixture of alkali and plagioclase (albite), although no plagioclase was counted in PB152 and SPB3 contains only four alkali feldspar counts. The few ferromagnesian minerals that do occur are epidotes. Zircon is the most abundant heavy mineral and occurs in all sections. The micas include muscovite and biotite and it is noticeable that slides poor in plagioclase feldspar are poor in biotite. Acid igneous, metamorphic and sedimentary clasts usually constitute less than 10% of the total. The sedimentary clasts are all of intra-basinal lithologies, with siltstone and shale the most

common.

3.3.3 Kiln Formation

The formation is characterised by moderately high contents of quartz and feldspar (see Fig.2(b)). Quartz grains are over twice as abundant as feldspar, but locally ratios are nearer 1:1 (KB137). Ferromagnesian minerals are scarce or absent.

Acid igneous, metamorphic and sedimentary clasts show little variation, together totalling 9-14%. Basic igneous clasts vary from 2-14%. Alkali feldspar is usually dominant over plagioclase. Heavy minerals include zircon, apatite and garnet. Among the basic igneous clasts are fragments of porphyritic biotite-amphibole-plagioclase feldspar-bearing lavas, similar to lithologies on Bail Hill (see Plate 10(b)), although spilites are more common.

At two localities greywackes from neighbouring units were collected and point counted. It can be seen from analyses of the KB123 and KB125 specimens (see Appendix 2) that stratigraphically adjacent units show large variations in feldspar and basic clast concentrations. This intraformational variation is as great as the interformational variations.

3.3.4 Spothfore Formation (Matrix)

The greywacke matrix of the rudites is a quartz-poor, intermediate-feldspar sand without significant ferromagnesian contribution. The sands are matrix-rich, averaging over 40% (see Fig.2(b)).

Alkali feldspar is dominant over plagioclase. The basic-igneous material is mainly spilitic, but includes biotite-amphibole-plagioclase feldspar-bearing lavas similar to those on Bail Hill (see Plate 11(a)). Sedimentary clasts are locally very abundant (e.g. KB139) and are all of intrabasinal lithologies (mainly siltstones, shales and cherts). Acid igneous and metamorphic clasts generally constitute less than 5% of the total. Zircon is the most abundant heavy mineral and among the micas biotite is subordinate to muscovite.

3.3.5 Spothfore Formation (Clasts)

The petrography of the greywacke clasts in the Spothfore rudites varies from quartz-poor, feldspar-rich sands (SPB45C), through intermediate quartz and feldspar sands (KB143C), to matrix-rich, quartz-and feldspar-poor varieties (KB177) (see Fig.2(b)).

The clasts never attain coarse sand grade and the fine-grained nature of the clasts has rendered identification of material difficult. Matrix-rich varieties have low counts in the feldspar and basic igneous categories and in many instances this may be due to replacement of this material by a secondary carbonate cement (see Section 3.3.6). Ferromagnesian minerals constitute less than 1% in all specimens.

3.3.6 Guffock Formation

The greywackes of this formation are moderately quartz-rich and contain, on average, 17% feldspar (see

Fig.2(a)). Ferromagnesian minerals are scarce or absent.

The greatest variation occurs in the basic igneous category, which varies from less than 1% (GHB124) to 18% (BB32). Those specimens that are low in basic igneous material are often matrix-rich and the original greywacke matrix has been replaced by carbonate material. The carbonate matrix is seen to replace some of the feldspars and basic igneous fragments and this would account for their low totals. Some of the feldspars in this formation are of andesine composition (e.g. BB85DS) and their calcic nature would make them more susceptible to this type of alteration. Overall, however, plagioclase is subordinate to alkali feldspar. The few ferromagnesian minerals that were counted are green amphiboles and epidotes. Muscovite and biotite are present in approximately equal proportions, whilst the heavy minerals are mainly zircons and apatites.

3.4 COMPARISON WITH OTHER AREAS

The work of Kelling (1962), Welsh (1964) and Floyd (1975) provides a suitable frame of reference for comparing the greywackes of the present area with those to the southwest (see Table 2). Floyd (1975) concluded that although there were significant differences in the absolute data between his area and those of Kelling (1962) and Welsh (1964), the relative figures did compare. All three authors found a ferromagnesian-poor and a ferromagnesian-rich formation outcropping to the north of the Leadhills line or its equivalent on the coast. However,

in the present area there is no ferromagnesian-rich formation north of the Leadhills line.

The Glenflossh, Kiln and Guffock Formations bear similarities to Floyd's Afton Formation, with high quartz, intermediate feldspar and low basic igneous contents, together with an absence of a significant ferromagnesian content. The presence of andesine feldspar in the Guffock Formation suggests affinities with Floyd's Blackcraig Formation. The greywacke clasts and matrix of the Spothfore Formation are matrix-rich and this inhibits comparison with other areas. However, the absence of a significant ferromagnesian contribution would suggest the Spothfore rocks are the equivalents of Floyd's Afton Formation.

It is noticeable that the equivalent formations of Kelling (1962) and Welsh (1964) are depleted in quartz and enriched in basic and acid igneous material and metamorphic clasts when compared with the inland exposures of west Nithsdale and Bail Hill. In view of individual operator-bias the significance of this cannot be assessed. It is noted, however, that neighbouring areas show fairly good correlation (viz. the Bail Hill area and west Nithsdale, and the adjacent areas bordering Loch Ryan), whereas the correlation between areas is not good. This possibly indicates a difference in the composition of the greywackes between the coastal and inland exposures and is not merely due to individual operator-bias.

3.5 FINE-GRAINED SANDSTONES OF THE KILN FORMATION

The fine-grained sandstones of the Kiln Formation are petrographically distinct from greywackes of the same formation. The rocks are often arenites rather than wackes, containing less than 15% argillaceous matrix. Lithic clasts and quartz are less abundant than in the Kiln greywackes, whilst feldspar is more abundant and is often oligoclase or andesine in composition. Pleochroic amphibole fragments are also common, as well as crystal fragments of apatite and biotite. Green chlorite is also noticeable in thin section. Many of the crystals display some euhedral faces and this together with their pristine nature suggests they have not been transported for any great distance and/or have not been subject to appreciable weathering. A typical example of this lithology is illustrated in Plate 12.

3.6 CONCLUSIONS

The petrography of the greywackes in the Bail Hill area does not vary significantly amongst formations. Intraformational variation is as great as interformational variation. The categories which show the greatest variation between and within formations are quartz, feldspar, basic igneous and matrix. There is no significant ferromagnesian content in any of the greywackes of the Bail Hill area, in contrast with areas along strike that have been examined. This, together with the differences between coastal and inland greywackes, suggests that the petrography of Northern Belt greywackes varies along as well as across strike.

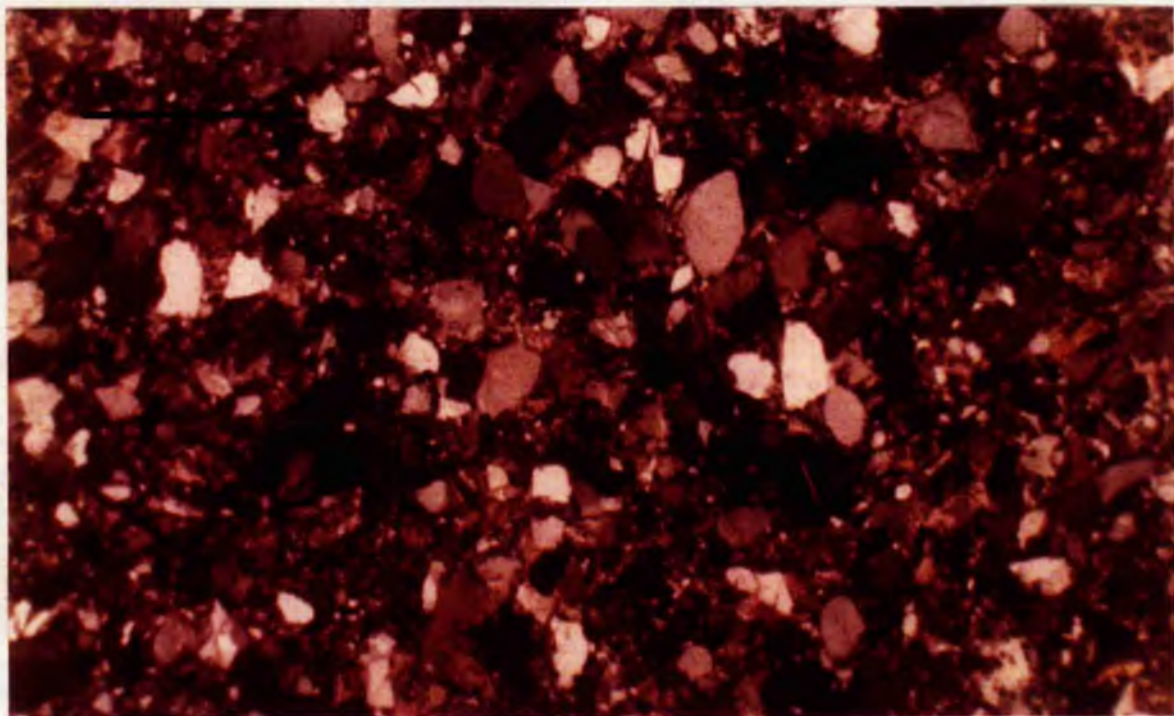


Plate 10(a): Photomicrograph of typical Glenfloss Formation greywacke. Its quartz-rich, feldspar-poor nature is apparent. Few lithic clasts are visible. Scale-bar is 1 mm . Cross-polarised light.

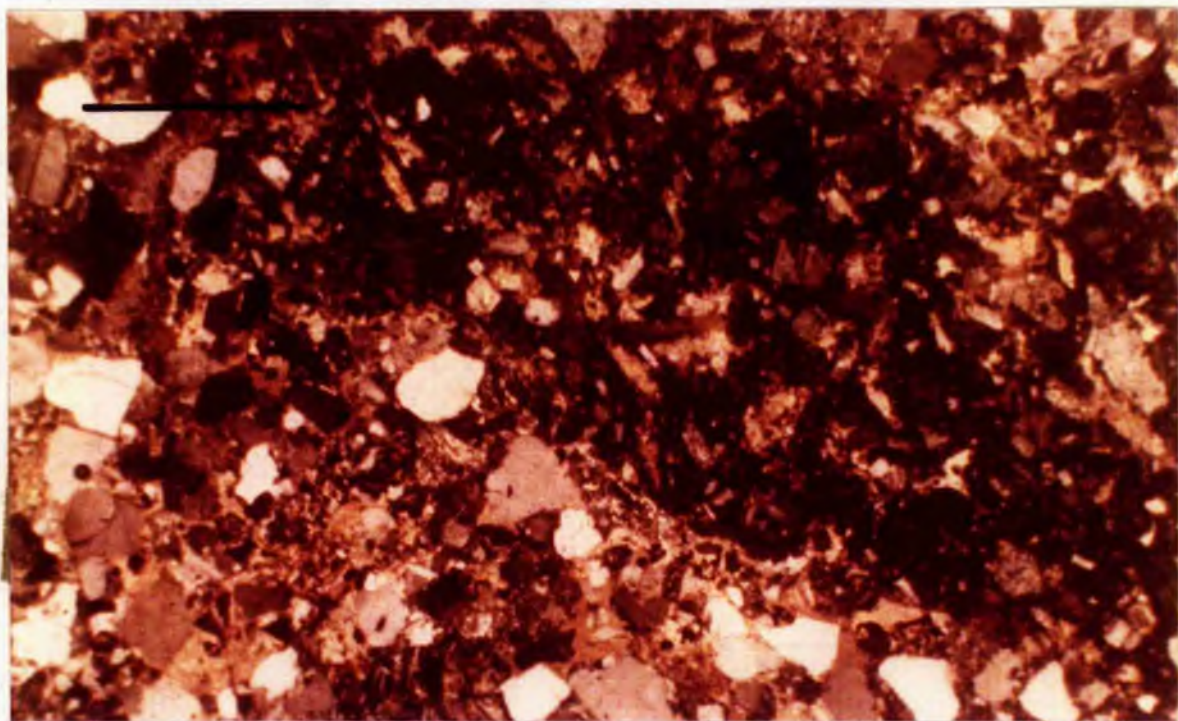


Plate 10(b): Photomicrograph of Kiln Formation greywacke. Volcanic detritus is abundant, with porphyritic lava clast running top left to bottom right and spilite clast (bottom left). Secondary carbonate cement is present. Scale-bar is 1 mm. Cross-polarised light.

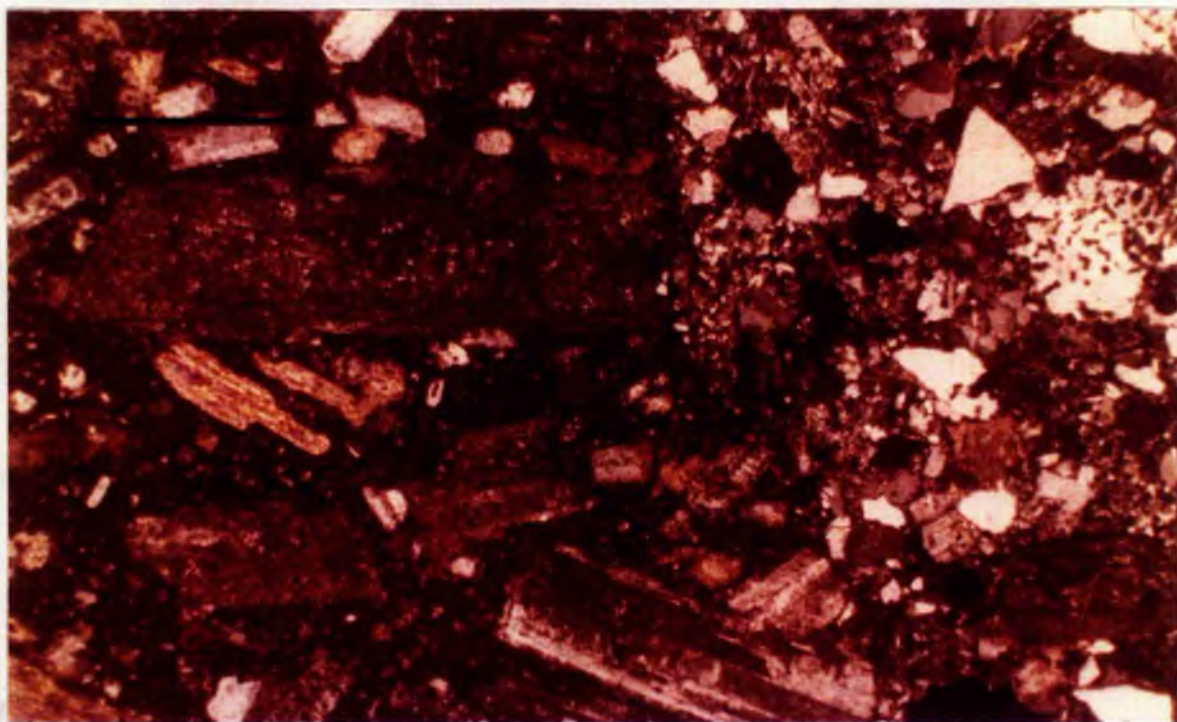


Plate 11(a): Photomicrograph of porphyritic lava clast in Spothfore Formation greywackes. Plagioclase feldspar (oligoclase) and biotite phenocrysts in mugearite lava. Greywacke contains quartz with vermicular chlorite (right). Scale-bar is 1 mm across. Cross-polarised light.

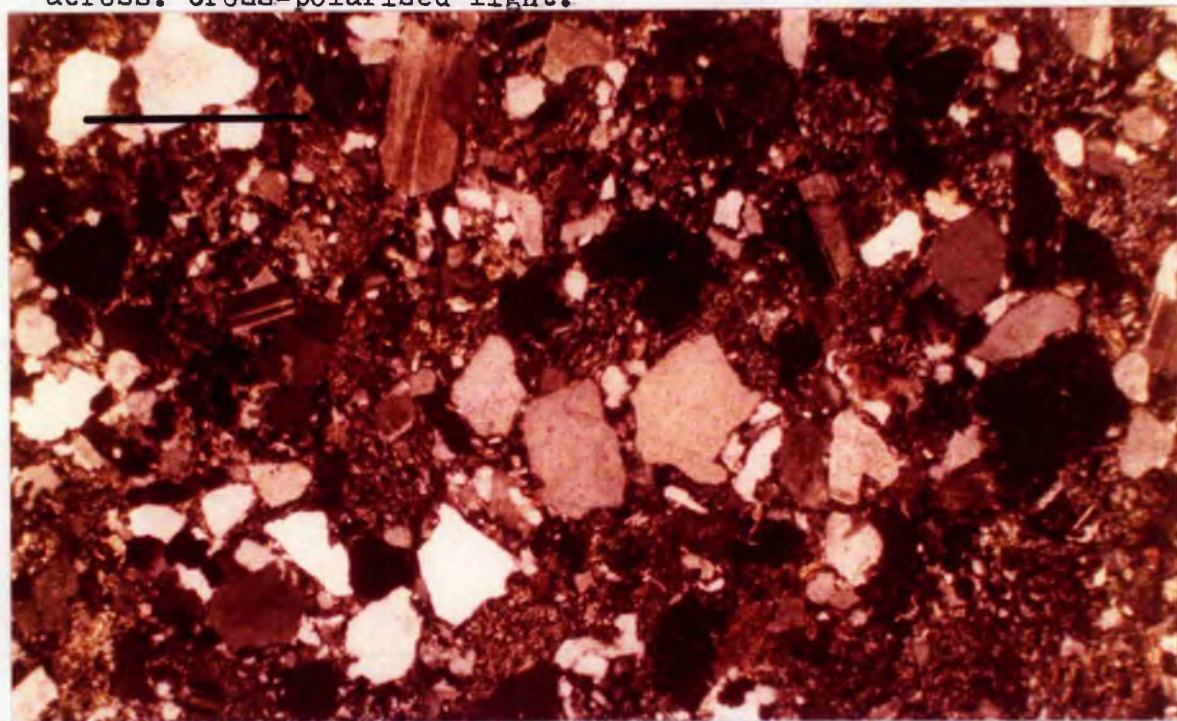


Plate 11(b): Photomicrograph of Guffock Formation greywacke. Feldspar and lithic clasts are relatively abundant, but overall the rock is still quartz-rich. Scale-bar is 1 mm across. Cross-polarised light.

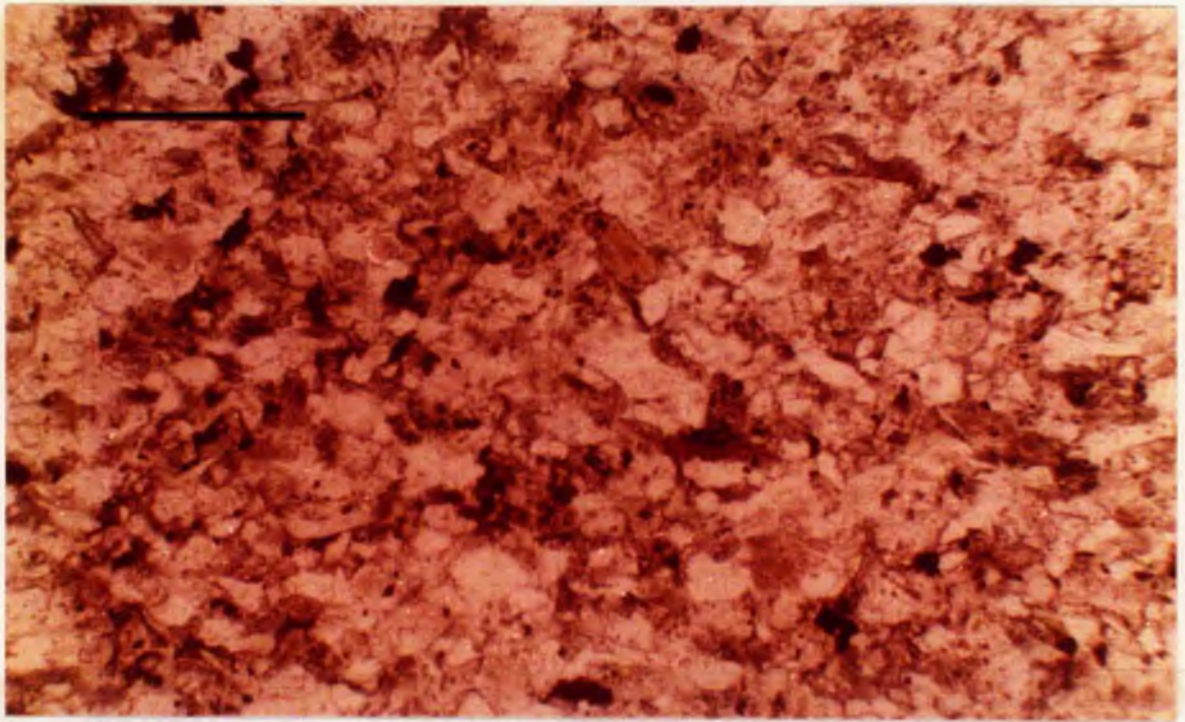


Plate 12(a): Photomicrograph of arenite from the Kiln Formation. These units are believed to be current winnowed lithologies of "bottom-current" origin. Note the absence of an argillaceous matrix, the presence of green chlorite, dark-brown biotite and pale-brown amphibole (centre). The amphibole is optically similar to pargasites of the Bail Hill Volcanic Group. Scale-bar is 0.5 mm across. Plane-polarised light.

CHAPTER 4 : STRUCTURE4.1 DISTRIBUTION OF FORMATIONS4.1.1 Glenfloss Formation

The Glenfloss is the most southerly of the four sedimentary formations and attains an outcrop width of 1 km in the Kiln Burn area. This is a minimum thickness for the formation as the base does not occur within the confines of the area. The formation can be traced to the northeast where it crops out north of the Leadhills line (B.C.Hepworth, pers.comm., 1979).

The bedding displays a typically Caledenoid trend, striking 060-075°E and dipping northwest at upward of 60°. Way-up criteria (sole markings, grading, cross-lamination) indicate the formation youngs northwest. Southerly younging directions were only observed near the top of the formation in Hay Cleuch and these were subordinate to northwesterly younging directions. It should be stressed, however, that exposure is poor and observations few.

4.1.2 Kiln Formation

The Kiln Formation outcrops in a belt up to 1 km wide, lying to the north of the Glenfloss Formation. The base of the formation is marked by a sequence of black shales and cherts which are the surface expression of a strike-parallel, high-angle fault (Eller Fault), similar in style to the NE faults of Walton (1965b).

to next p. - nt are

The coarse "chaotic" rudites of this formation obscure structural features. Way-up criteria were only discerned in graded granule-sandstone units and in the lenticular bedded sandstones and siltstones associated with the rudites. These indicate the formation youngs northwest and no southerly younging strata were observed.

Units show more varied strike than in the other formations, with $060-090^{\circ}\text{E}$ being the most common values. Strikes of over 100°E were observed, particularly in the northeast of the area. Beds dip vertically or steeply northwest.

4.1.4 Guffock Formation

The Guffock Formation is the most northerly of the sedimentary formations and attains an outcrop width of 0.9 km in the Back Burn section. This gives a minimum thickness for the formation as the top does not occur within the confines of the area.

The base of the formation is marked by a sequence of strongly tectonised black shales and cherts. This sequence is the surface expression of a strike-parallel, high-angle fault (Howcon Fault), which separates the Spothfore and Guffock Formations.

Above this tectonised basal zone in the Kiln, Spothfore, Glenaners and Guffock Hill Burns, the strata show a Caledenoid strike of $060-090^{\circ}\text{E}$ and dip vertically or steeply northwest. In the Back Burn, however, the rocks strike $070-090^{\circ}\text{E}$ and vary considerably in dip from 40°N or S, through vertical. In this section the basal strata are

Above the tectonised basal zone the rocks display typical Caledenoid strike of $060-075^{\circ}\text{E}$. In the Kiln and Spothfore Burns and on the flanks of Craignorth Hill the units dip northwest at upwards of 60° . In the Back Burn, however, units more commonly dip vertically or steeply south. It is observed from way-up criteria (sole markings, grading, cross-lamination, load features) that the formation youngs northwest, although southerly younging strata are found on the short limbs of folds (see Section 4.2). In the Kiln Burn the volcanic strata cropping out south of the confluence of the Kiln and Stoodfold Burns dip at moderate angles and young to the southeast. However, the top and bottom of this lithology is fault-bounded and the sediments and volcanics on either side dip vertically and young northwest.

4.1.3 Spothfore Formation

The Spothfore Formation has a maximum outcrop width of 0.8 km in the region of the Kiln and Spothfore Burns. To the southwest it terminates against the volcanic rocks of Bail Hill, whilst in the northwest there is a marked thinning of the formation across the Spothfore Burn section.

The southern boundary of the Spothfore Formation is conformable with the underlying Kiln Formation. The passage from the fine-grained rocks of the Kiln Formation to the rudites of the Spothfore Formation is well displayed in the Kiln Burn at (76801423), in the Spothfore Burn at (78421521) and in the Back Burn at (79251569) (see Plate 1(b)).

folded and young alternately northwest and southeast. Fold closures are rarely seen and in the middle and upper parts of the formation the strata young only to the northwest. Elsewhere, way-up criteria (sole markings, grading, cross-lamination) indicates the formation youngs northwest.

4.2 FOLDING

In the course of mapping the area details of any folds were recorded in order to aid correlation with other areas. Poor inland exposure and massive, thick lithologies resulted in the observation of only 17 fold axes (see Appendix 3). All are in thin-bedded fine-grained sandstones and siltstones, the majority of which are from the Kiln Formation. In addition, two observations were obtained from the basal strata of the Guffock Formation and one each from the Spothfore (infaulked siltstone block) and Glenflosch Formations.

The common style is a fold pair, anticline and syncline, with the syncline to the south (see Plate 13(a)). Strata on the southerly dipping limb young southeast, but as the limb is rarely more than a few tens of centimetres in length the predominant younging direction is to the northwest. Folds are tight rather than isoclinal, with axial planes subparallel to the regional strike ($050-090^{\circ}\text{E}$). There are two maxima, one at 055°E and another at 084°E . Axial planes dip southwest or northeast at angles up to 60° , but more commonly at less than 35° .

This style of folding has been reported from elsewhere in the Southern Uplands and its continuation

into Longford-Down (Craig and Walton, 1959; Walton, 1965b; Anderson and Cameron, in press). It is interesting to note that Kelling (1961) on rocks along strike from the present area has two fold axes maxima at 055°E and 075°E , corresponding closely to the two maxima mentioned above.

In contrast to other reported occurrences in the Southern Uplands and Longford-Down an s_1 fabric is very rarely developed in the Bail Hill area. A few localities within Kiln Formation rocks in the Spothfore Burn show traces of a possible s_1 fabric, but elsewhere it is conspicuously absent.

In addition to these tight fold pairs more open structures, with wavelengths of tens of metres, were observed in the Stoodfold and Back Burns. In the Stoodfold Burn the axial plane is parallel to the small fold pairs and probably correlates with the F_2 of Rust (1965). This differs only in style from F_1 and is incorporated in the F_{1-2} of Walton (1965b) and F_1 of Anderson and Cameron (in press). In the Back Burn the axial plane differs markedly from the other structures in the area (115°E , 55°S). This is tentatively correlated with the F_3 of Rust (1965).

In Brown's Cleuch and the Stoodfold Burn recumbent fold structures are seen to overlies fault planes. Only five such structures were observed and generalisation is therefore not possible. It seems likely, however, that the folds are related to localised drag on fault planes.

4.3 FAULTING

Very few faults were directly observed in the

course of mapping, although field relations suggest they are common. They are divided into two categories, strike faults and wrench faults, and are summarised below.

4.3.1 Strike faults

These trend parallel to the regional strike and include the two major faults at the base of the Kiln and Guffock Formations, the Eller and Howcon Faults. Smaller strike-parallel faults are found in proximity to the volcanic horizon in the Stoodfold, Kiln and Spothfore Burns and in Brown's Cleuch. Recent evidence (Eales, 1978) suggests that the strike-parallel faults may have originated as low angle thrusts and were subsequently rotated into their present-day near-vertical orientation. Evidence elsewhere in the Southern Uplands suggests that lines of black shale and chert are the surface expression of major reverse faults that control outcrop distribution (e.g. Walton, 1965b; Floyd, 1975). By inference the Eller and Howcon Faults belong to this style of faulting.

In two tributaries of the Spothfore Burn the basal fault of the Guffock Formation has an orientation of 100°E , rather than the more usual 060°E . Across this there is a significant change in the thickness of the Spothfore Formation from 800 to 250m. There is no evidence for the relative ages of this feature and the adjacent Howcon Fault. It is tentatively identified as part of the Howcon Fault system.

4.3.2 Wrench faults

Wrench faults were rarely observed in the sedimentary lithologies, although this is probably a function of incomplete exposure and the difficulties inherent in recognising such features in lithologically monotonous successions. In the volcanic rocks lithological contrast and more complete exposure enabled observation of a number of wrench faults with an orientation between 140-160°E. Sense of movement was only observed on one fault plane and was sinistral.

4.4 GENERAL STRUCTURE

The major feature of the area is of steeply dipping, northwesterly younging strata separated by major strike-parallel, high-angle faults. This association has been widely reported from elsewhere in the Southern Uplands (Kelling, 1961; Walton, 1965b; Floyd, 1975). The major faults are marked at the surface by lines of black shales and cherts along which decollement has taken place (Fyfe and Weir, 1976). These pass up into coarser sediments which are locally folded into syncline-anticline pairs. The dominant northwesterly younging direction is only locally reversed on the short limb of the fold pairs. No S_1 penetrative fabric is associated with these or later more open folds.

The relative ages of the four formations is problematical. From field evidence it is clear that the Kiln and Spothfore Formations form a more or less continuous stratigraphic sequence, with the Spothfore Formation

overlying the Kiln Formation. However, these two formations are separated from the Guffock and Glenfloss Formations by the Howcon and Eller Faults, respectively. Elsewhere in the Southern Uplands major strike-parallel reverse faults have been inferred to explain the apparent paradox of northwesterly younging greywackes with southerly younging graptolite zones (e.g. Craig and Walton, 1959; Walton, 1965b; Floyd, 1975). At Bail Hill, however, although the clastic rocks young northwest the graptolite faunas from the Guffock and Kiln Formations fall within the N.gracilis zone and their relative ages cannot be distinguished (R.B.Rickards, pers.comm., 1979).

It is noted that Peach and Horne (1899) assign faunas from the horizon representing the Howcon Fault to the Glenkiln, whereas faunas from the Eller Fault horizon are transitional between Glenkiln and Hartfell. This suggests the base of the Guffock Formation is older than the base of the Kiln. Likewise, if the Duntercleuch Rig faunas (Peach and Horne, 1899) represent the base of the Glenfloss Formation then the base of the Glenfloss Formation would be younger than the basal Kiln Formation rocks (see Sections 2.2.2 and 2.3.1). This would give the following stratigraphic sequence :-

4. Glenfloss Formation (youngest)
3. Spothfore Formation
2. Kiln Formation
1. Guffock Formation (oldest)

It is stressed, however, that this sequence is derived by inference and that modern knowledge of Ordovician graptolite

zones does not permit the resolution of relative age relations such as those practised by Peach and Horne (1899).

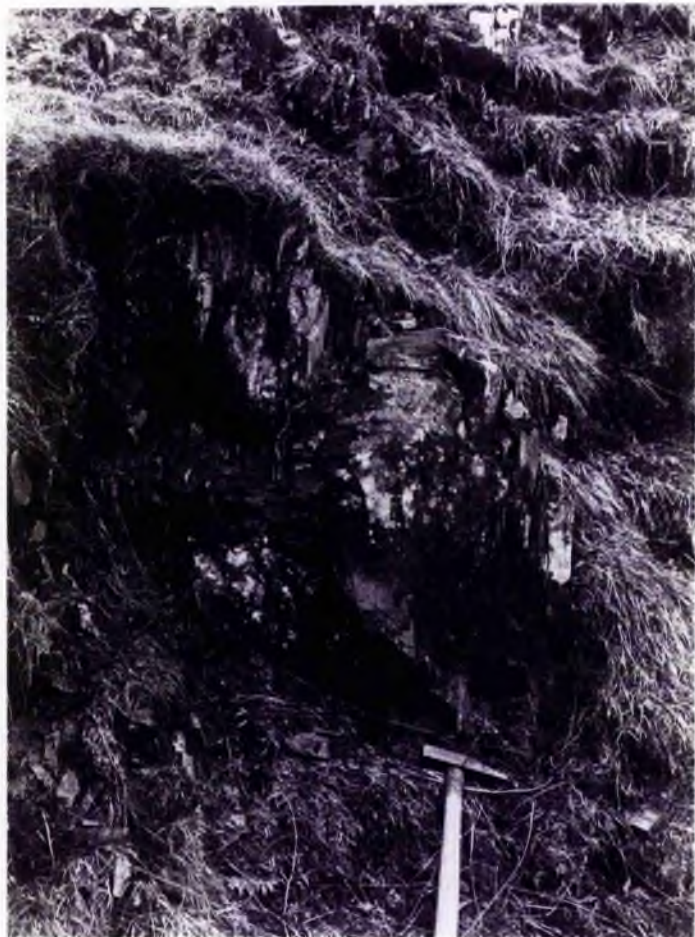


Plate 13(a): Folding in rocks of the Kiln Formation. Syncline-anticline pair in siltstones. Synclines are invariably found to the south of anticlines. Back Burn.



Plate 13(b): Folding in rocks of the Glenfloss Formation. Syncline in siltstones in the Hay Cleuch section. An s_1 cleavage is not developed.

CHAPTER 5 : SEDIMENTOLOGY

5.1 INTRODUCTION

This chapter is an account of the sedimentology of the four sedimentary formations with particular reference to recent ideas on fan models and gravity-transport mechanisms. The terminology of Middleton and Hampton (1973) is used for the various sediment and fluid gravity flows and their deposits. Many criteria diagnostic of certain deep-water sediments were not available as a result of incomplete exposure and a complex tectonic history (e.g. determination of continuity along strike, fining/coarsening upward cycles, palaeocurrent data). Nevertheless, those features that could be observed are sufficient to give some insight into the nature and depositional environment of the sediments.

In view of the lithological similarities between the Glenflossh and Guffock Formations the two are considered together.

5.2 GLENFLOSSH AND GUFFOCK FORMATIONS

The greywackes of the Glenflossh and Guffock Formations were deposited by turbidity currents. Turbidity currents are the best understood of the four sediment gravity flow mechanisms (Middleton and Hampton, 1973) and explain the following salient features in the units of the two formations :-

1. Grading from coarse or medium sand at the

base to fine sand or silt at the top :

2. Sharp, flat-based beds with or without sole marks :
3. Regular bedding with continuity across outcrop :
4. Occurrence of parallel and/or cross-lamination near the top of units :
5. Occurrence of thin siltstone partings between graded units :
6. Occasional amalgamation of graded units.

Greywacke units generally consist of a graded T_a division and, except in amalgamated sequences, a thin siltstone parting (T_e). Parallel and/or cross-lamination (T_{bcd}) were occasionally observed. Although poor exposure and weathering tends to mask such features they were observed in less than 1 in 10 units and are relatively uncommon.

The majority of units are, therefore, T_{ae} turbidites typical of a proximal environment (Walker, 1976). The relatively thick nature of units (up to 1.2 m), coarse grain-size and the occasional amalgamation of units are all in accordance with this.

The fact that the T_e divisions are siltstones rather than shales and their laminated nature suggests they are not background hemipelagic sediments but "instantaneous" deposits (Rupke and Stanley, 1974). Thus T_e is not used in the sense of Bouma (1962) but corresponds to the e_t division of Kuenen (1964) or the e division of Hesse (1975). These siltstones are believed to be suspension and traction deposits from the tail of the turbidity current

that deposited the underlying T_a unit or subsequent low-density currents. Background sedimentation (e_p of Kuenen (1964), f of Hesse (1975)) constitutes an insignificant part of the succession except at the base of the Guffock Formation (black shales).

The thicker packets of siltstone with sandy horizons (see Sections 2.2.2 and 2.5.2) contain abundant evidence for deposition by tractional mechanisms. Parallel and cross-lamination are both common. The absence of grading in the sandy laminae and the presence of sharp bases and tops indicate that they are not distal turbidites (Mutti, 1977). Bouma sequences cannot be applied to such lithologies and although in nature and association they resemble Mutti's (1977) interchannel facies, the more general term "overbank" deposit is preferred. It is envisaged that these formed by overflow of turbidity currents from nearby channelised areas, where T_{ae} sequences were being deposited.

Palaeocurrent data are reasonably abundant in the Guffock Hill Burn but elsewhere are scarce. In both formations the data from flute marks consistently indicate currents flowing to the southwest (4 observations in the Glenfloss Formation, 7 in the Guffock Formation). Non-directional data in the Guffock Formation (long-ridges) indicate a current flowing to the southwest or northeast.

The sedimentology of the black shales and cherts found at the base of the Guffock Formation is considered in Section 5.3.1.

5.3 KILN FORMATION

The Kiln Formation consists of three different sedimentary lithologies. Black shales and cherts at the base of the formation are overlain by fine-grained sandstones and siltstones, with occasional interbedded medium-coarse-grained greywacke units. The sedimentology of each lithology is considered below.

5.3.1 Black shales and cherts

Peach and Horne (1899) considered the cherts to have accumulated as radiolarian oozes, whilst the black shales accumulated as muds on the fringe of terrigenous sedimentation. Interpretation of these deposits has not changed in the intervening years, although the depositional environment is better understood. Radiolarian oozes and hemipelagic muds both accumulate in deep-water environments well away from the influence of terrigenous clastic sedimentation, such as in the abyssal plains of modern oceans.

In the absence of any studies on these lithologies in the Bail Hill area, the interpretation outlined above is accepted. The complete absence of lamination and the scarcity of silt particles in the black shales is in accordance with their inferred hemipelagic origin. The black shales and cherts at the base of the Guffock Formation are similar in all respects to those of the Kiln Formation.

5.3.2 Fine-grained sandstones and siltstones

The fine-grained sandstones and siltstones are

subdivided into two, corresponding to the lower and upper parts of the Kiln Formation. Parallel lamination is dominant in the lower part, cross-lamination in the upper.

Parallel laminated rocks in the lower part of the Kiln Formation include well-sorted sands (arenites) and non-fossiliferous green shales, although matrix-rich siltstones and fine-grained sandstones are more common.

In the Stoodfold Burn at (76701381) and in the Kiln Burn at (76901386) the parallel laminated siltstones and sandstones are interbedded with lithic tuffs. Adjacent tuff units are petrographically similar but are separated by a metre or more of sediment. The thin nature of the tuff units (usually less than 20 cms) together with their petrographically similar nature suggests they represent minor episodes from the middle-stage activity of the Bail Hill volcano (see Section 6.8). The time period between eruptions of adjacent tuff bands is unlikely to be more than a few hundreds or thousands of years. During this time a metre or more of sediment would be deposited, giving a sedimentation rate of the order of 1 m per 1000 years.

Sedimentation rates for contourites are less than 10 cms per 1000 years (Stow and Lovell, 1979), for dilute turbidity currents 23 cms per 1000 years (Rupke and Stanley, 1974), both much lower than the probable sedimentation rate for the Kiln Formation. However, Piper (1978) has reported an overall sedimentation rate of 1800 m per million years (1.8 m per 1000 years) for silt turbidites in the Aleutian Trench. Thus it would appear that turbidity currents are the only depositional mechanism capable of

It seems likely, therefore, that turbidity current mechanisms resulted in the deposition of these parallel-laminated lithologies, in agreement with their graded nature noted above.

The absence of interbedded hemipelagics, the presence of well-sorted sands, the scarcity of Bouma sequences and the high sedimentation rates indicate that they are not distal turbidites (Nelson et.al., 1975). The presence of grading in some laminae indicates that settling from suspension of a turbidite flow could take place. More commonly, however, grading is not visible and parallel lamination is the only internal sedimentary feature. This is typical of the waning stages of turbidite flow when deposition from suspension becomes subordinate to tractional processes - as in the T_b and T_d divisions, for example. It is envisaged that the sands, silts and muds with poor to moderate sorting were deposited by weak or waning turbidity currents. Similar lithologies have been described by Piper (1978) and assigned to a proximal environment close to the fan-valley feeder systems.

The well-sorted sands show features typical of current-winnowed lithologies formed by reworking of material by bottom currents (Nelson et.al., 1975). The associated shales are also of bottom-current origin (see below). Although the well-sorted sandstones and shales are "bottom current" deposits it is not clear whether these currents were related to large-scale ocean-circulation systems (Bouma and Hollister, 1973) or turbidite-related currents (Mutti, 1977). In view of this and in the absence of any palaeocurrent criteria the term "bottom-current deposit"

is preferred to "contourite".

The high volcanic content of the well-sorted sands (see Section 3.5) suggests the bottom currents moved across a mixed volcanic and turbidite terrain. The sandy material would be deposited by tractional (cross-laminated) and suspensional (structureless or graded) mechanisms. Clay and mud particles would be kept in suspension until the boundary layer became supersaturated with clay flocs when a shale or silt layer would be deposited (Stow and Bowen, 1978). The shales in these sequences are therefore "instantaneous" deposits and not background sedimentation as in the case of the black shales. Their laminated and unfossiliferous nature is in accordance with this.

No palaeocurrent data were obtained from this sequence.

The upper part of the Kiln Formation shows a dominance of lenticular bedded lithologies, generally matrix-rich, of poorly sorted sandstones and siltstones. Similar lithologies have been described from tidal environments (Reineck and Singh, 1973), but in view of the associated deep-water lithologies this is not the case here. In places the lenticular bedded lithologies are interbedded with rudites of the Spothfore Formation. The similarity in palaeocurrent data suggests a related source (see Section 5.4). In view of this it is interesting to note that Mutti (1977) has described similar lenticular bedded lithologies which he ascribes to an inner-fan, channel-mouth environment.

The dominance of tractional features and the absence of T_2 divisions indicate that fluid gravity flow

was responsible for deposition of these lithologies. The lenticular bedded lithologies of this area are succeeded by coarse rudites indicative of a proximal environment close to the feeder system and in view of this they are equated on a uniformitarian basis with the channel-mouth facies of Mutti (1977). The lenticular bedded lithologies of this area are succeeded by coarse rudites of the inner-fan environment and in view of this they are equated on a uniformitarian basis with the channel-mouth facies of Mutti (1977).

Isolated ripples in the lenticular bedded sandstones and siltstones indicate currents flowing to the southeast or east.

5.3.3 Greywackes

Interbedded with the fine-grained sandstones and siltstones are massive greywacke units. Units generally begin with a T_a division which may or may not show grading. Those units which do not show grading pass abruptly into the lithologies described above (see Section 5.3.2). Those that are graded show parallel and/or cross-lamination at the top of units and generally show a more complete Bouma sequence than greywackes in the Glenflossh and Guffock Formations (see Section 5.2).

Two directional and one non-directional palaeo-current indicators were observed, with currents flowing to the southwest, and southwest or northeast, respectively. However, in view of the relatively great petrographic variation within the greywackes of this formation (see Section 3.3.3) the possibility that some of the thick and

coarse-grained units are related to the northwesterly channels supplying the fine-grained sandstones and siltstones cannot be overlooked.

5.4 SPOTHFORE FORMATION

The clasts in the rudites of the Spothfore Formation are all of deep-water intrabasinal lithologies. Shallow-water (continental shelf) lithologies are not found. The underlying and interbedded siltstones and sandstones were deposited in a deep-water environment, whilst the nearby volcanic pile at Bail Hill was erupted in a submarine environment (see Section 6.8). These associations together with the features in the rudites themselves indicate this formation was deposited in a deep-water environment well below wave base.

Deep-water conglomerates of turbidite association have been described by many authors (Hendry, 1971; Rochleau and Lajoie, 1974; Davies and Walker, 1974; Walker, 1975; Winn and Dott, 1977; Stanley et al., 1978; Kelling and Holroyd, 1978). However, with the exception of the latter two references, all the examples cited differ from the Spothfore Formation rudites in that the clasts are of extrabasinal origin. It is evident that many of the Spothfore Formation clasts were "plastic" when transported. Greywacke clasts possess porous outer skins suggesting that these were not brittle when transported but semi-consolidated, low-density, water-saturated masses. Clearly the type of flow required to transport such material is not so extreme as that required to transport similar-sized, brittle, dense,

fully-lithified material (Kelling and Holroyd, 1978).

The spheroidal sandstone clasts with the mudstone nucleus (see Section 2.4.3) are believed to have formed by movement of a plastic mud or silt nucleus in a muddy sand medium. Material adhering to the mud or silt nucleus would contain sufficient clay material between sand grains to retain a cohesive outer shell. The clast would then grow "snowball" fashion. They are not "armoured mud balls" as the grain size is never greater than medium sand and the sandy skin is thicker than the mud nucleus. The clast would stop growing on cessation of rotation or loss of its cohesive outer skin. They are similar in structure, formation and association to the mudstone-nucleus sand spheroids of Stanley (1964).

The scarcity of fluid gravity flow features (imbrication, lamination etc.) suggests the rudites were emplaced by sediment gravity flows (Middleton and Hampton, 1973). In accordance with this three features suggest that there was little internal turbulence and that many of the clasts were "floated" or rafted quietly in, in the manner of debris flows (Middleton and Hampton, 1973). Firstly, many of the clasts possess a mud veneer, less than a mm thick, although the matrix itself is sandy. If appreciable grain-grain interaction had taken place this veneer would have been abraded away. Secondly, in the Kiln Burn at (76761442) a perfectly preserved inarticulate brachiopod shell was found in the matrix of a cobble-conglomerate. For such a delicate structure to be preserved abrasion between grains would have to be negligible.

Thirdly, clasts believed to have been plastic at the time of transportation show textural differences with the rudite matrix. The "snowball" sandstones are such a case and this indicates that these had formed prior to transportation and were "floated" in debris flows into the present area. The presence of clasts showing plastic deformation is not incompatible with the above model as this deformation could be a result of either, transportation prior to initiation of the debris flow, or transportation in the non-rigid part of a debris flow (Middleton and Hampton, 1973).

Some rudite units show characteristics of other types of sediment and fluid gravity flows. The coarse-tail grading observed in granule-sandstones in the Kiln Burn (see Section 2.4.4) indicates deposition from suspension by turbidity current mechanisms. The absence of parallel and/or cross-lamination and interbedded hemipelagics at the top of such units would make them Bouma T_a units. Units in the Spothfore Burn were deposited particle by particle to produce lamination and imbrication (see Section 2.4.4) and fluid gravity flow was therefore the depositional mechanism.

The interbedded lenticular bedded sandstones and siltstones are similar to lithologies in the upper part of the Kiln Formation and are likewise interpreted as channel-mouth deposits (see Section 5.3.2).

Only one palaeocurrent direction was obtained from the rudite units. Imbrication in fine-pebble breccias from the Spothfore Burn at (78431520) indicates a current flowing to the southeast. The isolated ripples in the

lenticular bedded sandstones and siltstones indicate currents flowing to the southeast or east. A further indication of the source of the rudites is obtained from graptolite specimens from shale clasts within rudite units. Two faunas were obtained, both of which are from the N. gracilis zone. However, the fauna obtained from a clast in the Spothfore Burn is from low down in the N. gracilis zone and is older than faunas collected in the Eller and Howcon Fault zones. The overall trend in the Southern Uplands is for the graptolite zones to get progressively younger to the south. On this basis the clasts in the rudites would be derived from lithologies lying to the north of the present area.

5.5 CONCLUSIONS

The greywackes of the Glenflossh and Guffock Formations are T_{ae} turbidites typical of a mid-fan environment (Walker and Mutti, 1973). Sole markings indicate the turbidites were deposited by currents flowing to the southwest. Overflow from channels where T_{ae} sequences were being deposited resulted in the deposition of overbank silts and sands. Background (hemipelagic) sedimentation is masked by turbidity-current activity except at the base of the Guffock Formation. Distal turbidites were not observed in either formation.

In the Kiln Formation deposition of radiolarian ooze and hemipelagic muds was succeeded by rapid sedimentation of silt turbidites. These were subject to local reworking by bottom currents, which also incorporated

volcanic material from the nearby Bail Hill volcano in the sandstones and shales. These were in turn succeeded by channel-mouth sands and silts, indicative of a proximal environment close to the feeder system. These sands and silts were formed by reworking of material dropped by by-passing turbidity currents stemming from the northwest or west. Proximal, medium-coarse-grained sand turbidites were still active, although some coarse-grained units may be related to the northwesterly feeder system supplying the channel-mouth sands, rather than the northeasterly-derived turbidites typical of the Guffock and Glenfloss Formations.

The rudites of the Spothfore Formation were deposited by both sediment and fluid gravity flow mechanisms in an inner-fan environment. The majority of units were deposited by debris flows, although turbidity currents and tractional mechanisms were responsible for the deposition of some fine-pebble breccias and granule-sandstones. Palaeo-current evidence is scarce but consistent with interbedded channel-mouth sands and palaeontological data in suggesting a source to the northwest.

Part 2 : The volcanic rocks.

CHAPTER 6 : STRATIGRAPHY AND PETROGRAPHY6.1 INTRODUCTION

It is proposed that the lithologies hitherto known as the Bail Hill volcanics should henceforth be known as the Bail Hill Volcanic Group. The following subdivisions have been recognised within the Bail Hill Volcanic Group :-

1. Cat Cleuch Formation
2. Bught Craig Member
3. Peat Rig Formation
- 3(a). Grain Burn Member
4. Undifferentiated intrusions
5. Tuff members in outlying streams
 - (a) Stoodfold Member
 - (b) Penfrau Member
 - (c) Back Burn Member
 - (d) Craignorth Member.

In addition to the problems posed by poor exposure, mapping of the volcanic rocks is further complicated by rapid lateral and vertical variation in lithology, and difficulties in determining dip and strike. In the absence of way-up criteria there are also uncertainties over age relations. For these reasons a detailed sequence of events for the volcanic activity is not attempted, although early, middle and late stage activity is distinguished (see Section 6.8). For the same reasons no attempt has been made to estimate the thickness of individual units, unless there is good evidence for the dip and strike and continuity of the succession.

Although volumetrically subordinate to the main volcanic pile, the tuff members in the outlying streams are of great importance and have therefore been examined in detail. Their occurrence not only provides information on the nature of the volcanism, but also on volcanic-sediment relationships as a result of their interbedded nature with sediments of the Kiln Formation.

6.2 CAT CLEUCH FORMATION

6.2.1 General

The Cat Cleuch Formation is well exposed in low crags around the Cat Cleuch and its unnamed tributary stream. Similar lithologies were also observed in and west of the Grain Burn section. The formation consists mainly of auto-brecciated basaltic lavas and is distinguished in the field by the characteristic appearance of large clinopyroxene phenocrysts.

6.2.2 Field relations

In the Cat Cleuch tributary at (75781325) there is good evidence to suggest the lavas of this formation were erupted on to black graptolitic muds. Here, black shales yielding a N. gracilis fauna (see Appendix 1 for faunal lists) are vertical and in conformable contact with vesicular lavas. The shales immediately south of the lavas are hard and poorly cleaved, suggesting they have been baked. This would imply a northwesterly younging direction; it is corroborated by exposures in the Spothfore Burn

(see Section 6.7.2) and is in accordance with the dominant northwesterly younging direction observed in the sedimentary sequence (see Section 5.1). As the black shales represent the basal strata of the Kiln Formation it follows that the lavas in contact with them represent the earliest volcanic activity preserved in the Bail Hill area.

Within the formation itself there is very little evidence for the dip and strike of lithologies. Poor exposure and deep weathering have obscured the field relations of the two additional outcrops of this formation in and west of the Grain Burn section. In view of their position within the volcanic succession it is possible that these outcrops represent further extrusion(s) of basaltic lava in the middle stages of volcanic activity.

6.2.3 Petrography

The basal lavas are massive, vesicular rocks with occasional amygdales of clay minerals (illite?) displaying a well-developed comb-structure (see Plate 15(a)). Microphenocrysts of untwinned feldspar displaying fluidal texture are set in a dark-brown microcrystalline ground-mass. Large glomeroporphyritic (?) xenocrysts of andesine feldspar and euhedral clinopyroxene phenocrysts were occasionally observed. Within a few metres of the base the lavas become blocky and rubbly with an increase in the content of pyroxene phenocrysts and the occasional presence of amphiboles. These lavas in turn pass up into typical auto-brecciated lavas of the Cat Cleuch Formation, which are well exposed on the right bank of the Cat Cleuch

tributary.

The auto-brecciated lavas can easily be mistaken for pyroclastic rocks (Peach and Horne, 1899; Scott, 1914) due to their brecciated, knobbly appearance on weathering. However, when sectioned the rocks reveal red or yellow amygdaloidal patches containing euhedral pyroxenes and feldspar, surrounded by green, non-amygdaloidal patches containing broken pyroxene and feldspar euhedra (see Plates 14(a) and (b)). In thin section the red or yellow patches are seen to consist of a microcrystalline groundmass with amygdales of calcite, zeolites and analcite (see Plate 15(b)), whilst the green patches consist of non-amygdaloidal, shattered, glassy and hyaloclastic material.

The crystals in both patches show similar optic properties, with the pyroxenes displaying sector and concentric zoning (see Section 7.2.2) and the feldspars concentric zoning (see Plate 16(a)). However, the crystals in the green patches have been shattered and display euhedral and anhedral faces. A notable feature of the feldspars in these rocks is the intergrowth of crystals to produce a stellate structure.

Apatite is fairly common as crystals of up to 1 mm in the lower parts of the formation in the Cat Cleuch and its tributary and also in the Grain Burn exposures. In the auto-brecciated basalts, however, it is only present as small inclusions within pyroxene and feldspar phenocrysts. Many of the feldspar phenocrysts have been wholly or partially altered to K-feldspar, carbonate or white mica (see Section 7.5).

6.3 BUGHT CRAIG MEMBER

6.3.1 General

A number of low crags in the vicinity of the Cat Cleuch tributary expose a heterogeneous mixture of coarse- and fine-grained igneous fragments in a lava matrix. The Bught Craig Member is named after the largest of these crags, although the best exposures are found 150 m north-west of Bught Craig at (75741352).

6.3.2 Field relations

The Bught Craig Member was not observed in contact with any of the surrounding lithologies. Nearby lithic tuffs are of unknown affinities and may belong to this member. The distribution of outcrops suggests the overall trend of the member is at right-angles to the dominant NE-SW orientation observed elsewhere in the area and is in accordance with its interpretation as neck material infilling a volcanic vent (see Section 6.8).

6.3.3 Petrography

The matrix to the clasts is a highly porphyritic, poorly vesicular lava of hawaiite/mugearite composition (see Plates 16(b) and 17(b)). Euhedral phenocrysts of amphibole, plagioclase feldspar, biotite/phlogopite and apatite are all common in a microcrystalline groundmass of feldspar, apatite, iron-titanium oxides and (?) devitrified glass. The amphibole and plagioclase feldspar crystals are commonly zoned. Biotite/phlogopite phenocrysts

frequently contain pods of prehnite along the cleavage. Xenocrysts of clinopyroxene, occasionally sheathed in pargasitic amphibole, are widespread. The lava is hard, compact and very fresh in appearance.

The clasts form up to 5% of the total rock. With the exception of occasional fragments of baked shale and chert, the clasts are all of igneous origin. The fine-grained clasts include pyroxene-bearing lavas of the Cat Cleuch Formation, porphyritic intermediate rocks similar in composition to the lava matrix, as well as spilitic and feldspathic varieties which do not outcrop on Bail Hill. The coarse-grained xenoliths include gabbros, diorites and monomineralic amphibole and clinopyroxene clots. Typical examples of lithologies from the Bught Craig Member are illustrated in Plates 21(a) and (b).

Among the fine-grained lithologies which do not outcrop on Bail Hill are pyroxene-bearing, non-porphyritic lavas with a mesostasis of equigranular laths of albite to andesine composition. It is possible that the material was originally basaltic and has been arrested in the process of spilitisation. True spilites with albite-chlorite-iron oxide mineralogies are also found and in some instances display strongly weathered rims, although the material around them is fresh. This suggests these clasts had been through one cycle of weathering before incorporation in the Bught Craig Member. Amphibole-bearing clasts with a poorly fluidal crystalline feldspathic mesostasis are optically similar to the amphibole-bearing lavas of Bail Hill, suggesting the clasts may be derived

from shallow intrusions or lavas belonging to the Bail Hill Volcanic Group which are not found as outcrop at the present day. Apatite, an abundant accessory in the Bail Hill Volcanic Group, is present in these clasts, corroborating their inferred derivation from the Bail Hill episode.

The gabbroic clasts have primary mineralogies of clinopyroxene and plagioclase feldspar. Iron-titanium oxides and apatite, ubiquitous as accessories in the dioritic and extrusive rocks, are notably absent. In one specimen from (75731345) possible pseudomorphs after olivine were observed in a melanocratic gabbro clast (see Plate 25(a)), although olivine was not observed in any other rock type. The clinopyroxenes show varying degrees of alteration to pale-green amphibole and associated chlorite. The amphibole frequently forms a rim around the clinopyroxene, although another common occurrence is as a radiating cluster with a mass of chlorite crystals as a core (see Plates 26(a) and (b)). The amphiboles and chlorites frequently form interconnected "stringers", with thin vein-like lines joining up large equant mosaics of the two minerals which often contain remnant clinopyroxene in the core. Chlorite was not observed directly replacing the clinopyroxene and it is possible that the chlorite represents the later stages of clinopyroxene replacement, after the bulk of the material has altered to amphibole. The plagioclase feldspar has partially altered to white mica in gabbroic clasts.

Although compositional banding was not observed

in the gabbroic xenoliths, two features suggest a cumulate origin for these rocks. Firstly, alignment of crystals is noticeable in several clasts at outcrop, suggesting an original layering in the rocks (see Plates 22(a) and (b)). Secondly, there is considerable variation in the feldspar: clinopyroxene ratio amongst clasts, which, if the fragments originate from a single plutonic mass, indicates large-scale compositional banding (see Plates 23(a) and (b)).

The dioritic clasts contain primary plagioclase feldspar, amphibole, biotite/phlogopite, iron-titanium oxides and apatite, with or without remnant clinopyroxene. The material is generally very fresh, although the feldspar (albite/oligoclase/andesine) can be partially altered to carbonate or white mica and the biotite/phlogopite crystals contain pods of prehnite along the cleavage. The feldspars and amphiboles are zoned, the former strongly so.

There is a continuous range from melanocratic diorites, composed almost exclusively of pargasitic amphibole and iron-titanium oxides, through to leucocratic varieties containing very little amphibole and iron-titanium oxides, but with over 85% plagioclase feldspar, with minor amounts of apatite and biotite/phlogopite. Typical examples of melanocratic and leucocratic varieties are illustrated in Plates 24(a) and 27, respectively.

Mrs. Eyles reports the occurrence of syenitic xenoliths in this lithology, although none were observed by the present author.

The largest observed clast was a gabbro over 30 cms in diameter. More commonly clasts were under 10 cms

with rounded to subangular outlines.

6.4 PEAT RIG FORMATION

6.4.1 General

The Peat Rig Formation is not in itself a lithologically distinct formation, including, as it does, all volcanic lithologies outcropping on Bail Hill not covered in categories 1, 2 and 4 (see Section 6.1). In the area of the Grain Burn exposures permit the recognition of a Grain Burn Member within the rocks of this formation (see Section 6.5). Elsewhere, the formation crops out on the flanks of Bail Hill and Peat Rig as low crags that are so widely spaced and lithologically diverse as to make further subdivision impractical. The formation has been subdivided into four geographical areas which are described individually.

6.4.2 Tongue Sike area

In the three tributaries of the Tongue Sike lavas of intermediate composition (hawaiite/mugearite) crop out. The lavas are strongly porphyritic, with large amphiboles (up to 1 cm), plagioclase feldspars and apatites (up to 7 mm). The amphiboles have altered to mixtures of carbonate, chlorite, epidote and iron oxides and identification is based on their hexagonal basal sections and remnant cleavage. The feldspars are turbid and show alteration to carbonate, white mica, chlorite and possible K-feldspar. Zoning in feldspar is preserved as patches of differential

alteration. The apatites are fresh and occur as phenocrysts. They can frequently be identified in hand specimen by their vitreous, translucent, yellow-green nature. The microcrystalline matrix is red to chocolate-brown in colour and is mainly composed of secondary chlorites and iron oxides with some primary feldspar and apatite.

Some lithologies show good evidence for strike at $070-090^{\circ}\text{E}$ and vertical dip.

6.4.3 Grain Burn area

Lithic tuffs and agglomerates of intermediate (hawaiite/mugearite) composition crop out in the Grain Burn and its tributaries. The rocks are porous and deeply weathered, hindering petrographical observation. It would appear, however, that the pyroclastic rocks are composed of petrographically similar fragments to the lavas of the nearby Grain Burn Member (see Section 6.5) and are probably different expressions of the same volcanic activity.

The "apatite rock" (Kennedy, 1936) occurs within lithic tuffs of this formation in a tributary of the Grain Burn at (749140) (see Plate 19(b)). Kennedy (1936) indicates the rock is conformable with the tuffs, although his interpretation of the rock as a pneumatolytically altered sediment precludes any knowledge of its intrusive/extrusive nature. The apatites in the "apatite rock" and in the extrusive and intrusive rocks of Bail Hill are undoubtedly of primary magmatic, not hydrothermal, origin (see Section 7.6) and Kennedy's interpretation is therefore rejected. In view of the conformable nature of the "apatite rock"

with the lithic tuffs and the scarcity of lavas of this composition the rock is reinterpreted as a late-stage, pegmatitic infilling.

The field relations with the neighbouring Grain Burn Member are discussed in Section 6.5. Because of their deeply weathered, porous nature the dip and strike was rarely discerned in this lithology.

6.4.4 Peat Rig area

On the flanks of Peat Rig auto-brecciated lavas of intermediate composition (hawaiite/mugearite) are sporadically exposed. Similar lithologies crop out on Laganaweel Knowe and in a disused quarry on the east flank of Bail Hill. The lavas are all poorly vesicular, with phenocrysts of amphibole, plagioclase feldspar, biotite/phlogopite and apatite in varying states of preservation. The feldspars show degrees of alteration to carbonate, white mica and possible K-feldspar, although some material is fresh enough to allow identification by optical techniques. Zoning and homogeneous overgrowths were observed. Amphiboles have generally altered to mixtures of chlorite, carbonate, epidote and iron oxides. Biotite/phlogopite show varying degrees of alteration to chlorite and contain prehnite along the cleavage. Apatite is in pristine condition. The groundmass of the lavas is a microcrystalline mixture of primary feldspar and apatite with secondary chlorite and iron-oxides. An unusually pristine example of this lithology is illustrated in Plates 18(a) and (b).

No information on field relations was forthcoming

from these lithologies.

6.4.5 Guffock Hill area

On the south flank of Guffock Hill, west of the Grain Burn, a number of low crags expose auto-brecciated lavas of similar primary and secondary mineralogies to those of the Peat Rig area (see Section 6.4.4). This locality (746142) is particularly interesting as the lavas contain diffuse patches of euhedral plagioclase feldspar, amphibole, biotite/phlogopite and apatite with little interstitial fine-grained groundmass (see Plate 20(a)). In addition, sharp-bounded, coarse-grained xenoliths are found in both the lava matrix and the crystal-rich patches (see Plate 20(b)).

The diffuse crystal-rich patches are mineralogically similar to phenocrysts occurring in the lava matrix and it is evident from the field relations that these were patches of semi-solid "crystal-mush" in the extrusive rocks. The similarity in their geochemistry (see Chapter 8) corroborates the mineralogical similarity and suggests they are different expressions of the same activity.

The sharp-bounded, coarse-grained xenoliths include gabbros (in the lava matrix) and diorites and ultramafic clasts (in the lava matrix and the crystal-rich patches). The clinopyroxenes in the gabbros and the ultramafic clasts show varying degrees of alteration to pale green amphibole and chlorite in a similar manner to the association in xenoliths in the Bught Craig Member (see Section 6.3.3). The gabbroic clasts are similar to

the varieties in the Bught Craig Member (see Section 6.3.3). The ultramafic clasts, however, contain clinopyroxene, brown pargasitic amphibole and iron-titanium oxides with minor amounts of plagioclase. Secondary minerals include pale-green amphiboles, chlorites (both replacing clinopyroxene) and carbonate material, possibly barytes, pseudomorphing feldspar (see Sections 8.3.11 and 8.4). The clinopyroxene is also sheathed in brown amphibole in some sections. However, in view of the primary nature of the brown pargasitic amphibole (see Section 7.3) this is believed to be an igneous phenomenon and not a secondary metamorphic feature as in the case of the pale-green amphiboles and chlorites. From this it can be inferred that the clinopyroxene represents an earlier crystallising phase than the brown amphibole.

The dioritic xenoliths contain amphibole (brown or olive green), plagioclase feldspar, biotite/phlogopite, iron-titanium oxides and apatite. They are petrographically similar to varieties in the Bught Craig Member (see Section 6.3.3), although they do not show the range from leucocratic to melanocratic specimens, being mainly composed of approximately 70% plagioclase feldspar and 30% amphibole, primary mica, iron-titanium oxide and apatite.

All xenoliths observed were less than 20 cms in diameter. No information on field relations was forthcoming from these lithologies.

6.5 GRAIN BURN MEMBER

6.5.1 General

The Grain Burn Member crops out in the gully carved out by the Grain Burn. The lavas of this member are distinguished from the surrounding Peat Rig Formation by the dominantly pyroclastic nature of the latter in this section. The petrographically similar nature of the lavas of the Grain Burn Member with the pyroclastic rocks of the Peat Rig Formation suggest they are different expressions of the same volcanic activity, hence the lavas have been assigned "Member" status within the Peat Rig Formation.

6.5.2 Field relations

The porous nature of the rocks and the resultant deep weathering has obscured many features in the lavas. The dip and strike was rarely determined with certainty and only then at contacts between the lavas and thin intercalated pyroclastic rocks. These contacts are generally vertical and conformable, although younging directions were not ascertained. There is considerable variation in strike, with values of $035-110^{\circ}E$ recorded. The contact with the Peat Rig Formation was observed at (75151402), where a vertical, conformable contact separates lavas to the south from lithic tuffs to the north.

6.5.3 Petrography

The lavas of this formation are strongly porphyritic hawaiites and mugearites. Phenocrysts of

amphibole, biotite/phlogopite and plagioclase feldspar are variously dominant at different localities in the section, whilst apatite is an ubiquitous accessory phenocryst. These occur in a red-brown microcrystalline groundmass of feldspar, apatite and secondary chlorite and iron oxides. The phenocryst feldspars are of oligoclase/andesine composition and show zoning and adcumulus growth. They are turbid in thin-section and show degrees of alteration to carbonate, white mica and possible K-feldspar. The amphiboles have altered to mixtures of carbonate, chlorite, iron oxides and, occasionally, epidote. Their hexagonal basal sections and remnant cleavage allow identification. The biotite/phlogopite phenocrysts are in varying stages of alteration to chlorite and include pods of prehnite along the cleavage. It is from the biotites of this member that Harris et.al. (1965) obtained a date of 445 m.y. for the Bail Hill rocks. In view of the extreme weathering of this lithology it is possible that the biotites may have suffered argon-loss. This would give a minimum age for the rocks rather than an absolute age, a fact acknowledged by Harris et.al. (1965) but ignored by Churkin et.al. (1977) in their recalculated age of 456m.y. Apatite is present as pristine crystals up to 3mm in length.

The rocks themselves are commonly vesicular, often extremely so, and are massive or crudely columnar at outcrop.

Coarse-grained xenoliths of melanocratic dioritic material were obtained from crudely columnar lavas at (75131401) and (74961381). The largest xenolith was over 10 cms in size, although most were under 5 cms. The xenoliths are comparatively fresh, containing pargasitic amphibole (olive-green to brown), iron-titanium oxides and subordinate amounts of biotite/phlogopite, plagioclase feldspar and apatite. The amphiboles show simple and

concentric zoning, visible as colour changes in thin section. In addition, a coarse-grained clast of uncertain affinities (dioritic/gabbroic?) was observed in a vertically bedded agglomerate, interbedded with lavas of this member, at (748137).

6.6 UNDIFFERENTIATED INTRUSIONS

Intrusions with trachytic affinities were observed in the Cat Cleuch (intrusive into cherts and shales) and in the Grain Burn (intrusive into agglomerates and lavas).

Two varieties have been recognised, the first of which is only found in the Cat Cleuch and is less differentiated than the second variety (see Table 15). The first variety is the more northerly of the two intrusions in the Cat Cleuch area and is massive or columnar at outcrop. The rock is holocrystalline, with andesine feldspars in fluidal texture together with subordinate apatite, biotite/phlogopite and pseudomorphs after amphibole. The feldspars are dusted with inclusions and ubiquitously zoned. The mineralogy and geochemistry (see Chapter 8) suggest it is the intrusive equivalent of the middle-stage extrusive activity at Bail Hill (see Section 6.8).

The second variety is the most acid rock-type found in the Bail Hill area. Biotite/phlogopite and apatite are subordinate to albite and oligoclase feldspars in fluidal texture (see Plate 19(a)). The feldspars are usually zoned and dusted with inclusions. Occasional amygdales of calcite were observed. At outcrop the rocks are massive and grey or red-grey in colour. This variety

has been found at the base of the volcanic pile in the Cat Cleuch and near the top of the volcanic pile in the Grain Burn at (75351412). In the Cat Cleuch close to the Ordovician-Carboniferous contact this lithology passes into a poorly consolidated, friable mass of crystals. In thin section this material is petrographically similar to the more compact material outcropping to the north and it is suggested that its poorly consolidated nature is due to tectonic activity and/or subaerial exposure during or after deposition of the Carboniferous sediments.

In the Cat Cleuch the intrusions are conformable with bedding suggesting they were originally injected as shallow sills. The geometry of the intrusion in the Grain Burn is not known.

6.7 OUTLYING TUFF MEMBERS

6.7.1 General

The volcanic rocks in the outlying stream sections are all of pyroclastic origin. Lithic tuffs and agglomerates are the most common lithologies, although crystal tuffs and associated rocks are found in the Stoodfold Member. Four separate members were identified within the confines of the area, all occurring within the sedimentary sequence of the Kiln Formation. To the northeast of the area, however, volcanic strata outcrop in the Nether Whitecleuch Burn, and in the Glentewing and Glenliscleuch Burns, south of Crawfordjohn. The exposure in the Nether Whitecleuch Burn was visited by the present author and, although exposure

is extremely poor, interbedded pyroclastic and clastic sedimentary units were observed. Petrographically, the igneous material is similar to lithologies found in Brown's Cleuch and there is little doubt that it is related to the Bail Hill volcanic episode. Peach and Horne (1899) state that the igneous material outcropping in the Glentewing and Glenliscleuch Burns is petrographically similar to the material in the Nether Whitecleuch and Kiln Burns, the latter locality corresponding to the Stoodfold Member. It is tentatively inferred that this material is related to the Bail Hill volcanic episode.

6.7.2 Field relations

(a) Stoodfold Member : The Stoodfold Member is the best exposed of the four tuff members, cropping out in the Stoodfold and Kiln Burns. In the Stoodfold Burn evidence for the interbedded nature of the volcanics and sediments is found at (76701381). Here, at least 18 individual tuff units crop out in a 10 m sequence (see Plate 28(a)). Thick units (50 cms +) have erosive bases and contain "rip-up" clasts of siltstone that were clearly "plastic" when transported. Thinner units have planar tops and bases and do not disturb the underlying sediments. The sequence here youngs north-west. Graptolites from the N. gracilis zone were collected from this locality (see Appendix 1 for faunal lists).

Immediately downstream from the confluence of the Kiln and Stoodfold Burns the volcanic horizon crops out as a southerly-younging, fault bounded block. Here, massive, basal lithic tuffs are overlain by 10-15 m of crystal tuffs and volcanoclastics which display grading, scouring, parallel

and cross-lamination (see Plate 31(a)). These are in turn succeeded by more massive lithic tuffs (with units up to 1.5 m thick) some of which display erosive bases and contain "rip-up" clasts of mudstone (see Plates 30(a) and (b)). These are in turn overlain by a thick agglomerate unit (see Plate 29(b)). To the north and south the fault-bounded block passes out into northwesterly younging sediments. On the northern side the sediments are interbedded with highly porous lithic tuff bands up to 30 cms thick (see Plate 28(b)). The sediments (siltstones) contain flattened blocks of pumiceous material and are packed with small flecks of white material (see Plate 31(b) and Section 6.7.3). The flecks are found in a 30 m sequence and are randomly distributed through laminae, although they decrease in abundance upstream. Graptolites were collected from the siltstones at this locality (76901386) and indicate a N.gracilis age for the sediments and interbedded tuffs (see Appendix 1 for faunal lists).

(b) Penfrau Member : Three volcanic units crop out separated by fault-bounded slices involving black shale and chert. In view of the stratigraphic similarity between the three units they are believed to be the same horizon repeated by faulting. The member is fault-bounded to the north and south against the greywackes and fine-grained sandstones of the Kiln Formation.

The most southerly volcanic unit is an extensively carbonated breccia, cropping out on the right bank of the stream. The unit is of unknown thickness and is underlain

by strongly tectonised shales and cherts. The main agglomerate unit lies upstream and forms a prominent waterfall. Shales yielding a N. gracilis fauna crop out at the base of the waterfall (see Appendix 1 for faunal lists) and are seen to be eroded by the agglomerate. The conformable but erosive contact between the two lithologies is well exposed at the waterfall itself and the sequence is seen to young northwest. The lower contact of the black shales at the base of the waterfall was observed to be in vertical and apparently conformable contact with green cherts on the left bank. This is the only contact between the cherts and black shales observed in the area and it suggests the latter overlie the cherts.

The 9 m agglomerate unit forming the waterfall contains large (up to 25 cms) rounded clasts of amygdaloidal porphyritic lava which are well-displayed on the water-smoothed section above the waterfall. The agglomerate is fault-bounded on the northern side, passing into a strongly deformed sequence of shales and cherts which are in turn overlain by a third agglomerate unit. The contact between the sediments and the third agglomerate unit is sharp and is not tectonic. There is, however, no evidence for tectonism in the agglomerate, despite the extreme folding and faulting in the shales and cherts. The possibility that some or all of the deformation in the cherts and shales is syn-sedimentary cannot be overlooked, although a more detailed analysis is precluded by weathering and incomplete exposure. The agglomerate unit is fault-bounded on its northern margin by a mineralised unit that forms a

prominent linear feature cropping out 15 m upstream from the confluence of the Spothfore and Penfrau Burns. The agglomerate strikes obliquely into this feature and has a minimum thickness of 9 m.

(c) Back Burn Member : The Back Burn Member is the smallest and most poorly exposed of the four tuff members. It is not indicated on O.S. Sheet 15 or mentioned in the Silurian Memoir (Peach and Horne, 1899) and is believed to be a hitherto undiscovered locality of the volcanic rocks. It crops out at (79441547) as a single 1.5 m lithic tuff unit and is interbedded with graded greywackes and fine-grained sandstones.

(d) Craignorth Member : The Craignorth Member crops out as a series of lithic tuffs and agglomerates with interbedded siltstones in Brown's Cleuch, on the flanks of Craignorth Hill. The sequence here has been strongly tectonised and no attempt has been made to draw up a sequence of events. The main volcanic units crop out on the right bank of Brown's Cleuch at (810162). Here, a 7 m agglomerate unit is interbedded with siltstones and erodes into those on the south side, indicating the sequence youngs northwest. At least two lithic tuff units, 0.3 and 0.5 m thick, occur above and below the main agglomerate unit (see Plate 29(a)) within a few metres of it. The units are separated by poorly laminated siltstones.

Forty metres upstream on the right bank further lithic tuff and volcanoclastic units crop out. The interbedded siltstones contain graptolites from the N. gracilis zone (see Appendix 1 for faunal lists) and inarticulate

brachiopods.

Thin, structureless lithic tuff units are interbedded with siltstones at (80931623). The tops and bases of the units are planar and sharp and do not disturb the adjacent sediments.

6.7.3 Petrography

The lithic tuffs and the matrix of the agglomerates are characteristically very well sorted, with grains 1-5 mm in size. Smaller fragments and a fine-grained groundmass are notably absent and material is in grain-grain contact. Individual grains display subangular to angular outlines and rare interstices between grains are infilled with chloritic or opaque material. The interstices form less than 5% of the total rock. Typical examples of the lithic tuffs are illustrated in Plates 33(a) and (b).

The grains in the lithic tuffs and agglomerate matrix are all of porphyritic lava. In the Stoodfold, Back Burn and Craignorth Members the lava is of hawaiite/mugearite composition, with phenocrysts of plagioclase feldspar, biotite/phlogopite, apatite and amphibole. Many of the feldspars are remarkably fresh and display simple and concentric zoning in oligoclase and andesine compositions. The biotite/phlogopite and apatite phenocrysts are also fresh, although the micas contain pods of prehnite along the cleavage. The amphiboles are only identifiable by their hexagonal basal sections and remnant cleavage, having altered to mixtures of chlorite, carbonate and iron oxides.

In the Penfrau Member the clasts are of basaltic,

rather than intermediate, composition. Phenocrysts of labradorite/bytownite feldspar, amphibole and clinopyroxene are common, whilst apatite is scarce and biotite/phlogopite is not found. The feldspars are usually fresh and are ubiquitously zoned, although some show partial alteration to carbonate and white mica. The amphibole is in pristine condition and is optically similar to pargasites found on Bail Hill itself. The clinopyroxenes display sector and hourglass zoning and are similar in all respects to varieties in the Cat Cleuch Formation.

In all four tuff members there is variation in the nature and amount of groundmass between phenocrysts within individual grains. However, the homogeneity of the phenocryst phases within individual units and, on a broader scale, within individual tuff members suggests that each unit/member had a homolithic source and the variation in the nature and amount of groundmass is no more than would be expected from a single eruption or cycle of eruptions. The large round clasts in the agglomerates are petrographically similar to the grains of the tuff matrix in which they are found. Although many are cut through by veins of carbonate material others contain pristine phenocryst mineralogies (see Plate 17(a)). The clasts attain a maximum size of 0.5 m and are commonly vesicular or amygdaloidal.

The crystal tuffs and associated rocks of the Stoodfold Member consists of a series of thin-bedded units of crystal debris, submillimetre lithic fragments, silt and mud. Coarser units contain abundant carbonate

material between crystal fragments of feldspar, apatite and biotite/phlogopite. The remainder of the material was too fine-grained to be identified in thin-section.

The siltstones containing white flecks in the Stoodfold Member (see Section 6.7.2) were sectioned in order to ascertain the nature of the white material (see Plates 32(a) and (b)). The white flecks form patches of up to 1 mm in size that are homogeneously infilled with a colourless cryptocrystalline material containing small green rods. The composition of this material is not known, although it is possibly a cryptocrystalline silica aggregate containing rods of chlorite.

This feature is very similar to the bubble-cavity textures of Reineck and Singh (1973). However, Reineck and Singh (1973) indicate that this feature forms in near-surface, shallow-water sediments by decomposition of organic matter or entrapment of air. Subsequent burial of the sediment leads to compression of the bubble-cavities until they are barely recognisable. The siltstones from the Stoodfold Member differ in several respects from the examples of Reineck and Singh (1973). Firstly, the sediments are of deep-water association and are unlikely to have contained appreciable organic matter or air. Secondly, the cavities have not been compressed, even though they were buried under sediments of the upper Kiln Formation and rudites of the Spothfore Formation. Thirdly, the cavities have been infilled with homogeneous material. Fourthly, the cavities are randomly distributed through the siltstone laminae. From these features it can be inferred that the

cavities formed after the sediment had been partially or wholly compacted (hence their non-flattened nature and random distribution) and that the material forming the cavities crystallised in situ as a silica aggregate and does not represent a later infilling (hence the homogeneous nature of infillings).

In view of the proximity of the strata containing this feature to the volcanic horizon it is tentatively suggested that they originated by the migration of volcanic fluids. It is envisaged that late-stage volcanic fluids percolated through a partially compacted sequence of sediments and crystallised within this sequence when they were unable to migrate further.

6.8 SUMMARY OF VOLCANIC ACTIVITY

The lavas of the Cat Cleuch Formation represent the earliest phase of volcanicity preserved in the Bail Hill area. They were erupted in a deep-water submarine environment on to black graptolitic muds of N.gracilis age. Massive and rubbly lavas soon gave way to phenocryst-rich, auto-brecciated basalts. The auto-brecciation was caused by shattering of the lava as it was chilled by contact with sea-water. Some patches were insulated against the sea-water and these cooled and vesiculated as material with a microcrystalline matrix containing amygdales. The green patches (see Section 6.2.3) represent the material that chilled against sea-water, setting up internal stresses that resulted in shattering of phenocrysts and vitrification of the liquid portion of the lava. The absence of pillow-

structures from these basalts suggests that the viscosity of the lava was too high and/or the volatile content too great to allow the quiet effusion necessary for pillow development (Bonatti, 1970).

Following the early basaltic activity the middle-stage activity, represented by the Peat Rig Formation and the Bught Craig and Grain Burn Members, consisted of extrusion of lavas and pyroclastic rocks of hawaiite/mugearite composition.

The Bught Craig Member is a vent conglomerate representing one of the feeder systems. The term "vent conglomerate" is used as the matrix is a lava, not pyroclastic material as in the case of a "vent agglomerate". The great variety of igneous fragments occurring as clasts in this member attests to material being torn off walls at depth (gabbros, diorites), at shallow sub-volcanic levels (holocrystalline amphibole-bearing intrusive material) and from the underlying volcanic lithologies (Cat Cleuch Formation basalts, baked shale and chert fragments). Some fragments are undoubtedly related to the Bail Hill volcanic episode, although they are not found at outcrop. Other types (spilites) may be fragments from the basal (Arenig?) volcanic horizon of the Southern Uplands succession (Peach and Horne, 1899). It is clear, however, that the rocks outcropping at present are not representative of the volcanic and intrusive rocks that were present at the Bail Hill area in Ordovician times.

The blocks present in the Bught Craig Member represent neck material of a feeder system that filled

with lava of hawaiite composition, resulting in the feeder system becoming inactive. The nature and geometry of the Bught Craig Member, together with the absence of dykes that could act as feeder systems and the overall geometry of the volcanic pile suggest that the Bail Hill volcano was a composite volcano subject to central, rather than fissural, eruptions.

The massive hawaiite/mugearite lavas represented by the matrix of the Bught Craig Member and of the Peat Rig Formation around Tongue Sike were succeeded by massive, blocky and auto-brecciated lavas of similar composition found near Peat Rig, Guffock Hill and in the Grain Burn. These were accompanied by petrographically identical pyroclastic rocks, found in both the Peat Rig Formation and the Grain Burn Member. The occurrence of coarse-grained xenoliths and crystal-rich patches in these rocks attests to material being brought up from depth. As a result of incomplete exposure the proportion of lava to pyroclastic rocks in the main Bail Hill volcanic pile cannot be assessed. It is clear from field exposures, however, that pyroclastic activity played a more important role with time.

The final or late-stage activity of the Bail Hill volcanic episode was the injection of small trachytic intrusions into and under the volcanic pile. However, it would seem from some lithologies in the Cat Cleuch and clasts in the Bught Craig Member that high-level intrusive rocks were being emplaced during the middle-stage volcanic activity as well.

There is no evidence to suggest the volcanic column ever broke through sea-level. Early lavas were erupted on to black graptolitic muds of deep-water association and were therefore submarine. However, the succeeding lavas and pyroclastics contain few features of use in distinguishing the environment of eruption. Two factors suggest that activity was confined to a submarine environment. Firstly, at (75371430) in a tributary of the Grain Burn, lithic tuffs were observed in contact with overlying conglomerates of deep-water association (see Section 5.4). The contact is sharp and there is no evidence for either substantial erosion of the volcanic rocks, or, a tectonic discontinuity between the two lithologies. If the volcanic rocks were erupted in a subaerial environment one of these two features would have to be present in order to succeed subaerial extrusion with submarine deposition. From their absence it is inferred that the upper part of the volcanic pile was erupted in a submarine environment and eventually covered by conglomerates of deep-water association. Secondly, the sediments along strike from the main volcanic pile in which the outlying tuff members are interbedded are also of deep-water association (see Section 5.3). This suggests that both early and middle-stage activity took place in a deep-water environment, well below wave-base.

The pyroclastic rocks in the outlying streams originated from eruptions of the nearby Bail Hill volcano. As eruptions were proceeding the material thrown out into the aqueous medium would be sorted as it settled from

suspension. The first material to settle through the water column would be the relatively dense lithic fragments and volcanic bombs. These would accumulate on the flanks of the volcano and would periodically slough away into deeper water, as material became unstable. The flows would be warm, soggy slurries, some of which were able to erode the underlying strata. In a subaerial environment the slurries would manifest themselves as ash-flows.

The lithic tuffs and agglomerates of the four tuff members represent the flows of material that settled from suspension during or immediately after individual eruptions. The large round clasts in the agglomerates are volcanic bombs thrown out during the more violent eruptions. The absence of grading or internal structure suggests individual units were subject to mass emplacement. Their well-sorted nature and the absence of a fine-grained groundmass between grains suggest "grain flow" was the operative mechanism (Middleton and Hampton, 1973). The steep slopes required for the initiation of grain flow would have been readily available on the flanks of the volcano.

On cessation of an eruption the less dense crystal debris, small lithic fragments, volcanic dust and pumiceous material would settle from suspension. These are represented by the crystal tuffs and associated rocks of the Stoodfold Member. This material would accumulate on the flanks of the volcano and would be transported into deeper water by a variety of sediment and fluid gravity flow mechanisms (Middleton and Hampton, 1973).

Both the lithic tuffs and agglomerates and the crystal tuffs and associated rocks are very similar to the subaqueous volcanic deposits described by Fiske (1963) and Fiske and Matsuda (1964). From the petrography of the various members it is clear that pyroclastic equivalents of the early lavas of the Cat Cleuch Formation (Penfrau Member) and the middle-stage activity of the Peat Rig Formation and Grain Burn Member (Stoodfold, Back Burn and Craignorth Members) are represented.

Basal lavas are underlain by N.gracilis shales. Middle-stage pyroclastic rocks are interbedded with and overlain by siltstones containing a N.gracilis fauna. From this it is inferred that the lifespan of the Bail Hill volcano was confined to a part of N.gracilis times.

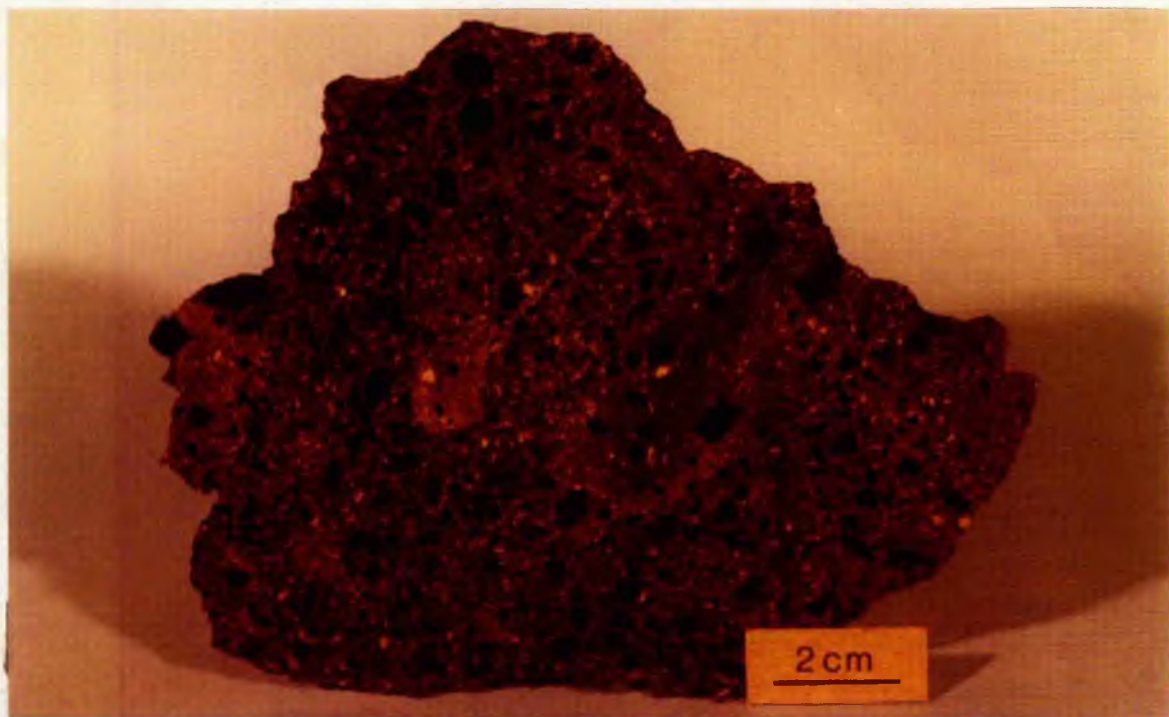


Plate 14(a): Auto-brecciated basaltic lavas of the Cat Cleuch Formation. Sector-zoned pyroxenes (black) and plagioclase feldspars (grey-white) in hyaloclastic (green) and microcrystalline (grey-yellow) material.



Plate 14(b): Amygdaloidal patches containing euhedral pyroxenes and feldspars (left) and brecciated hyaloclastic material containing broken euhedra (right). Cat Cleuch Formation specimen.

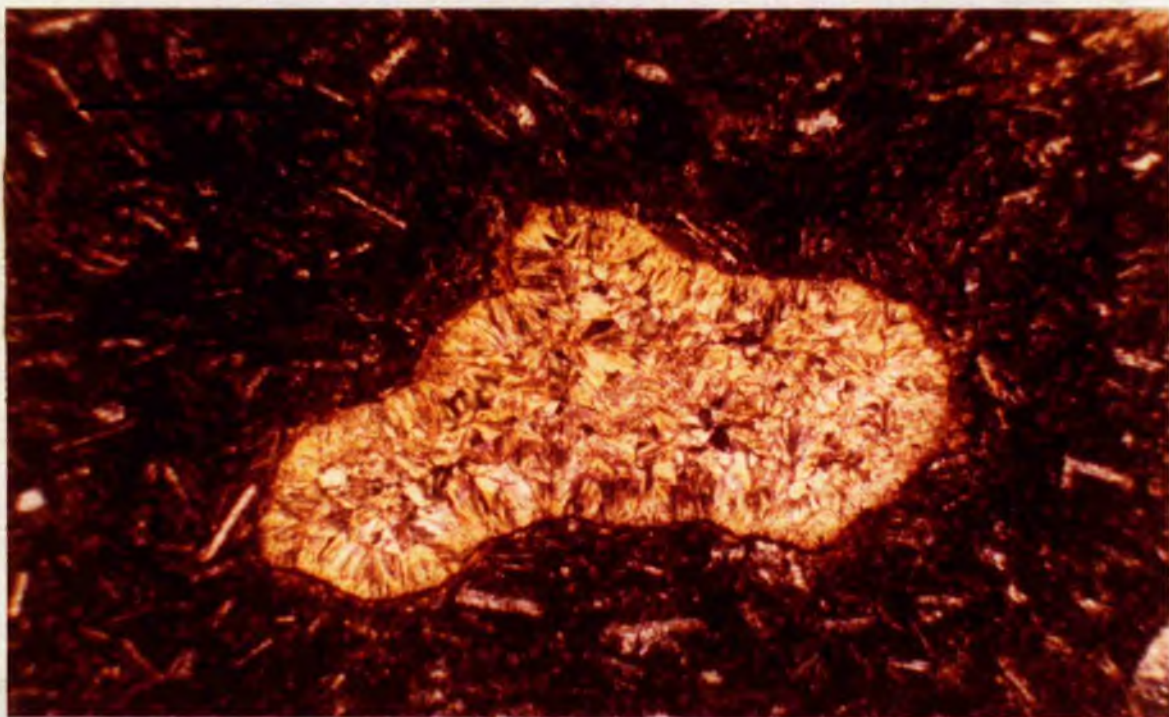


Plate 15(a): Photomicrograph of amygdale in basal Cat Cleuch Formation lavas. Material infilling vesicle is probably a clay mineral. Note also fluidal texture in feldspar microphenocrysts. Scale-bar is 0.5 mm across. Cross-polarised light.

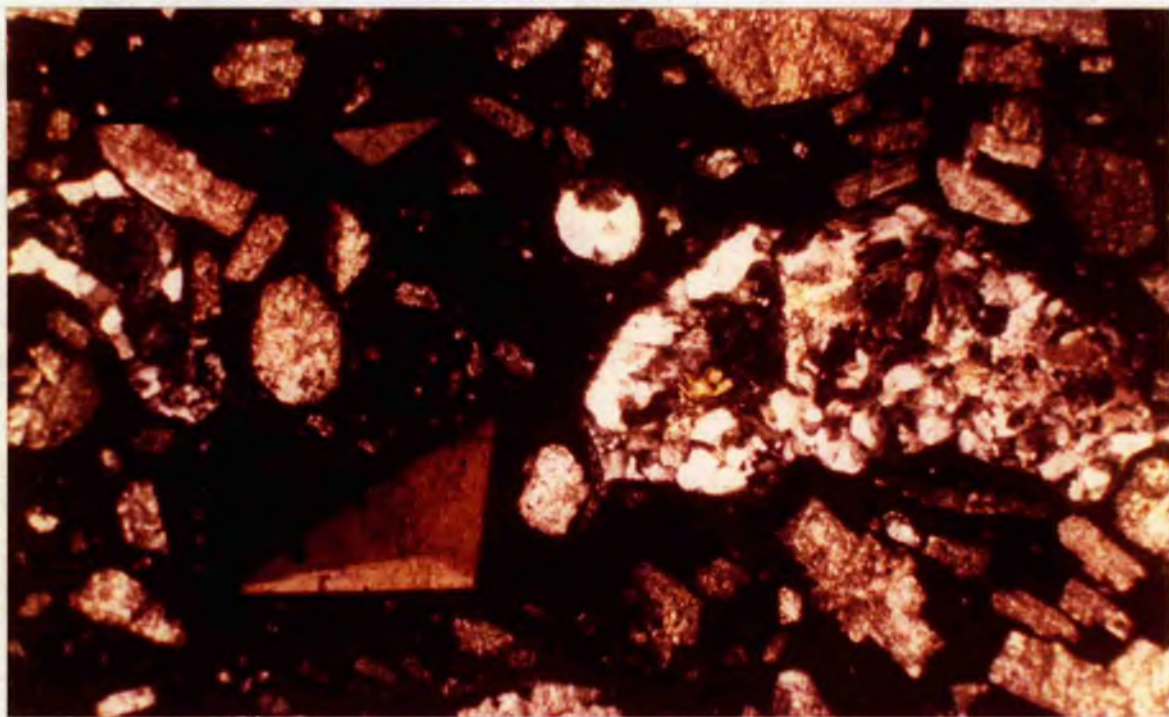


Plate 15(b): Photomicrograph of amygdaloidal patch in Cat Cleuch Formation auto-brecciated basalts. Zeolites (low birefringence), carbonate (high birefringence) and chlorite (anomalous birefringence) infilling vesicles. Plagioclase feldspar has altered to K-feldspar and white mica. Sector-zoned pyroxene at bottom left. Scale-bar is 1 mm across.

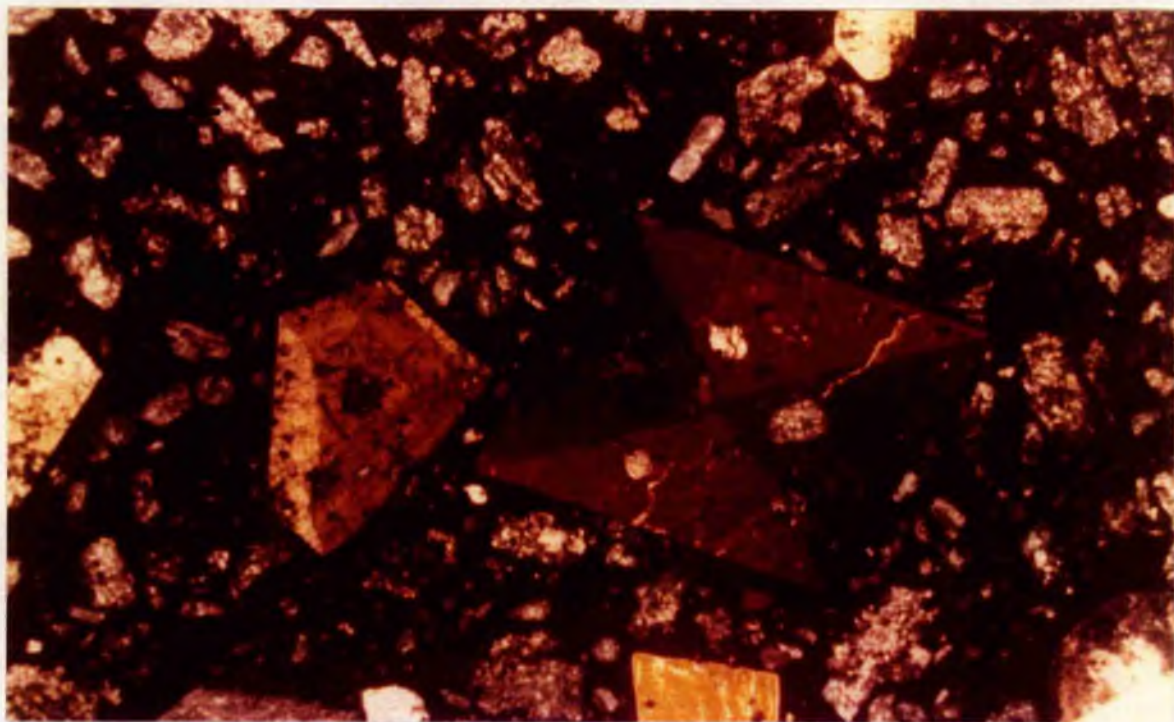


Plate 16(a): Photomicrograph of Cat Cleuch Formation basalt. Sector-zoned pyroxenes and plagioclase feldspar phenocrysts in microcrystalline matrix. Inclusions of feldspar occur within the large pyroxene which shows hourglass zoning. Scale-bar is 1 mm. Cross-polarised light.

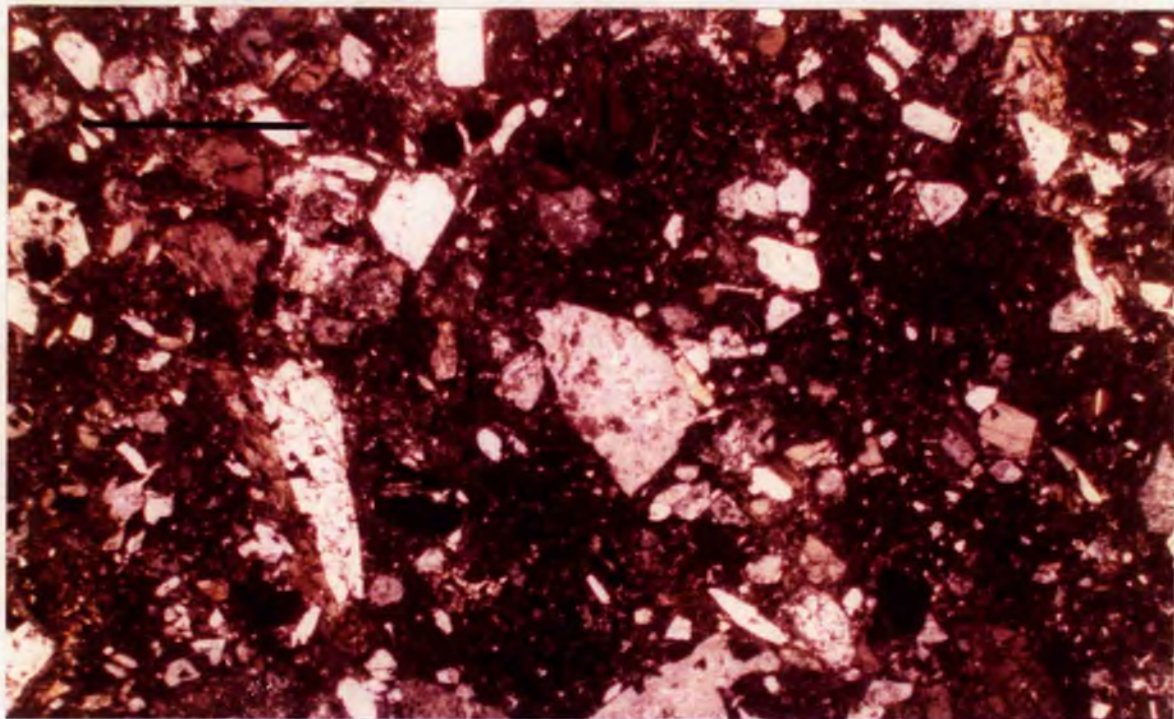


Plate 16(b): Photomicrograph of hawaiite/mugearite lava. Phenocrysts of pargasitic amphibole (simple twinned crystal, left of centre) and plagioclase feldspar (low birefringence) in fine-grained microcrystalline matrix. Bught Craig Member. Scale-bar is 1 mm.

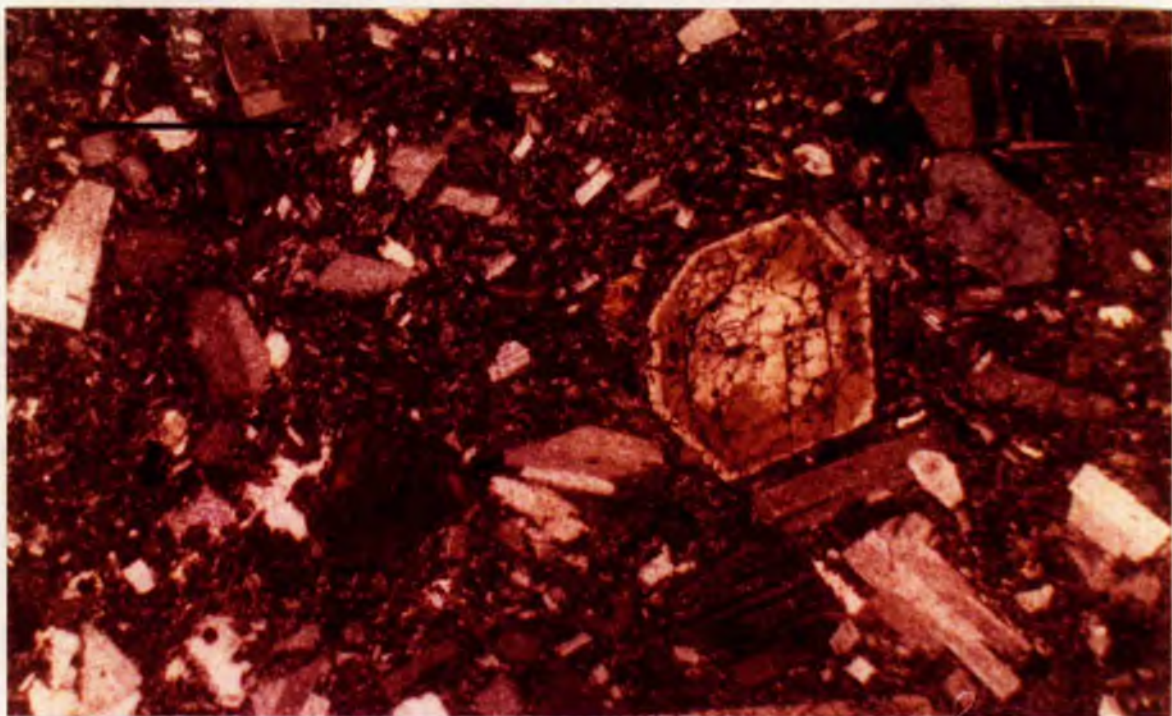


Plate 17(a): Photomicrograph of Bught Craig Member matrix. Phenocrysts of pargasite (olive green crystal displaying concentric zoning), apatite (medium grey crystal, top right) and plagioclase feldspar in felsic groundmass. Scale-bar is 1 mm. Cross-polarised light.



Plate 17(b): Photomicrograph of euhedral feldspar phenocryst. Concentric zoning is visible at the margins, whilst the core has partially altered to carbonate. Specimen from bomb in agglomerate. Stoodfold Member. Scale-bar is 1 mm. Cross-polarised light.

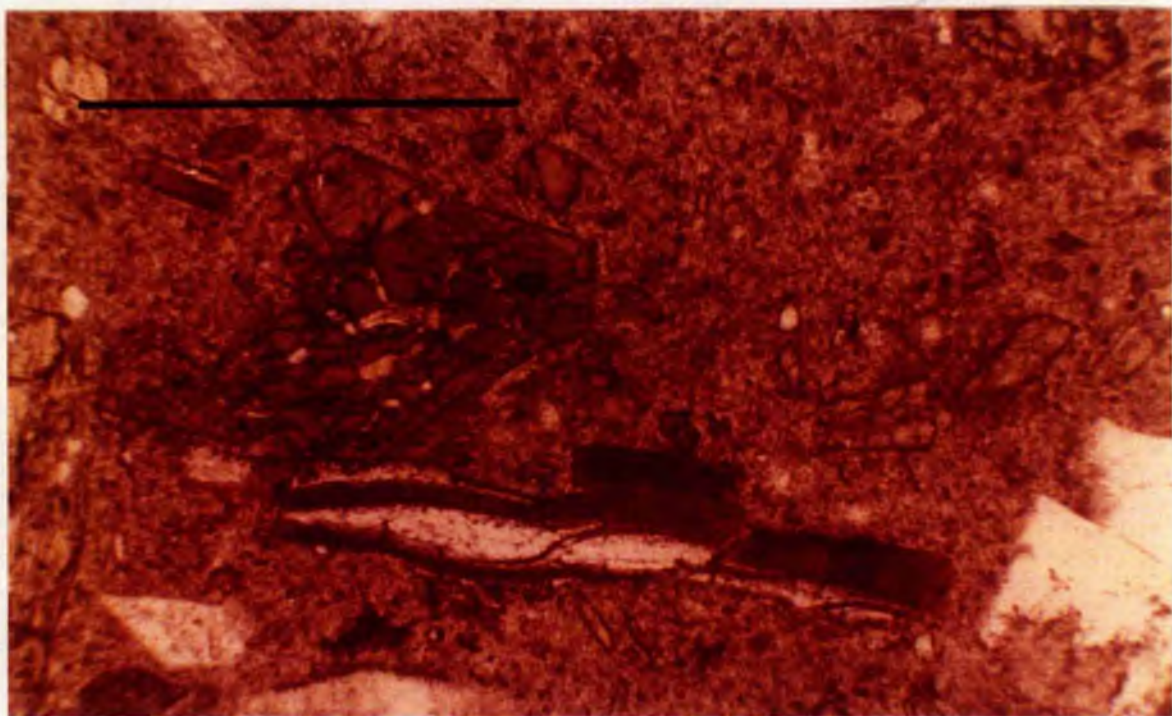


Plate 18(a): Photomicrograph of hawaiite/mugearite lava. Pargasite (olive green), biotite/phlogopite (dark brown) and feldspar (white) are the phenocryst phases. Mica contains pod-like inclusion of prehnite. Scale-bar is 1 mm.

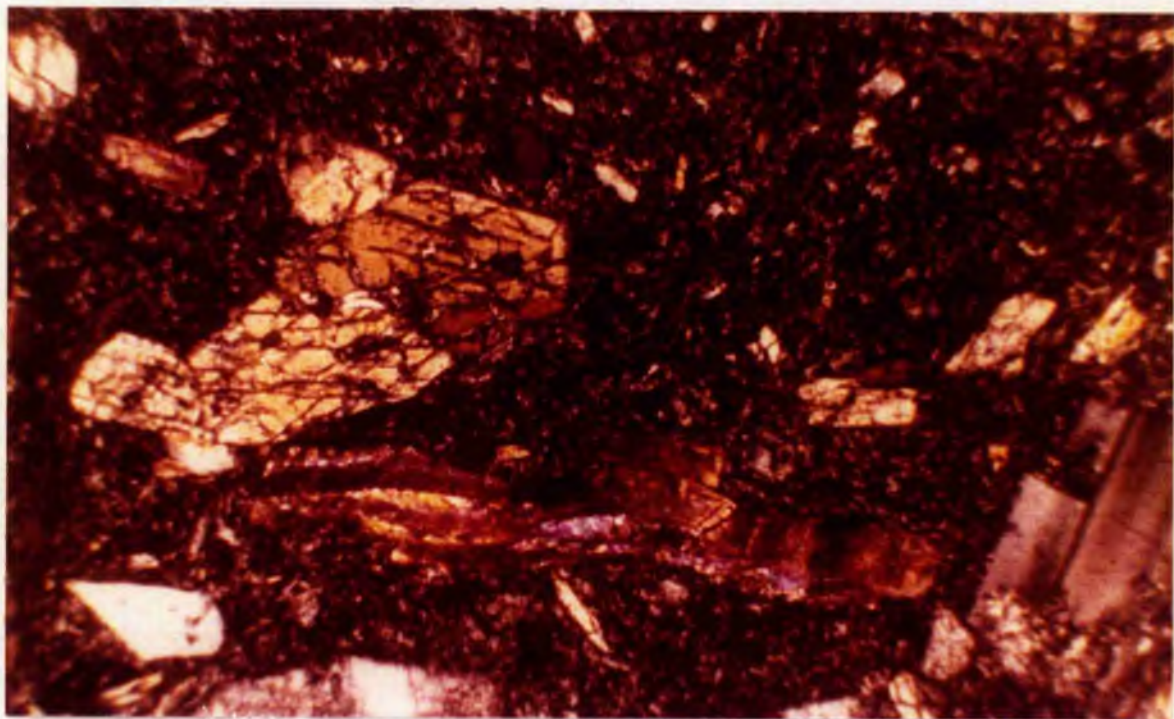


Plate 18(b): As above in cross-polarised light. Cleavage in mica is seen to bow around the prehnite.

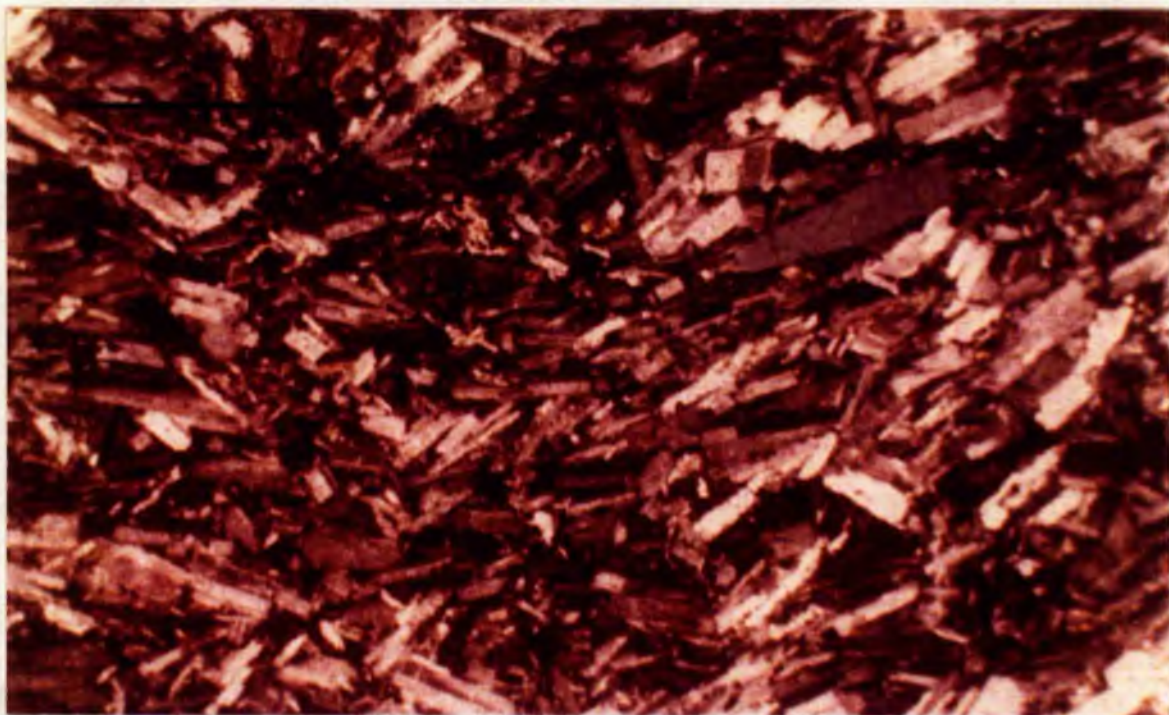


Plate 19(a): Photomicrograph of late-stage intrusion. Sodic trachyte displaying fluidal feldspars (albite/oligoclase) and large apatite (top right). Scale-bar is 1 mm. Cross-polarised light.

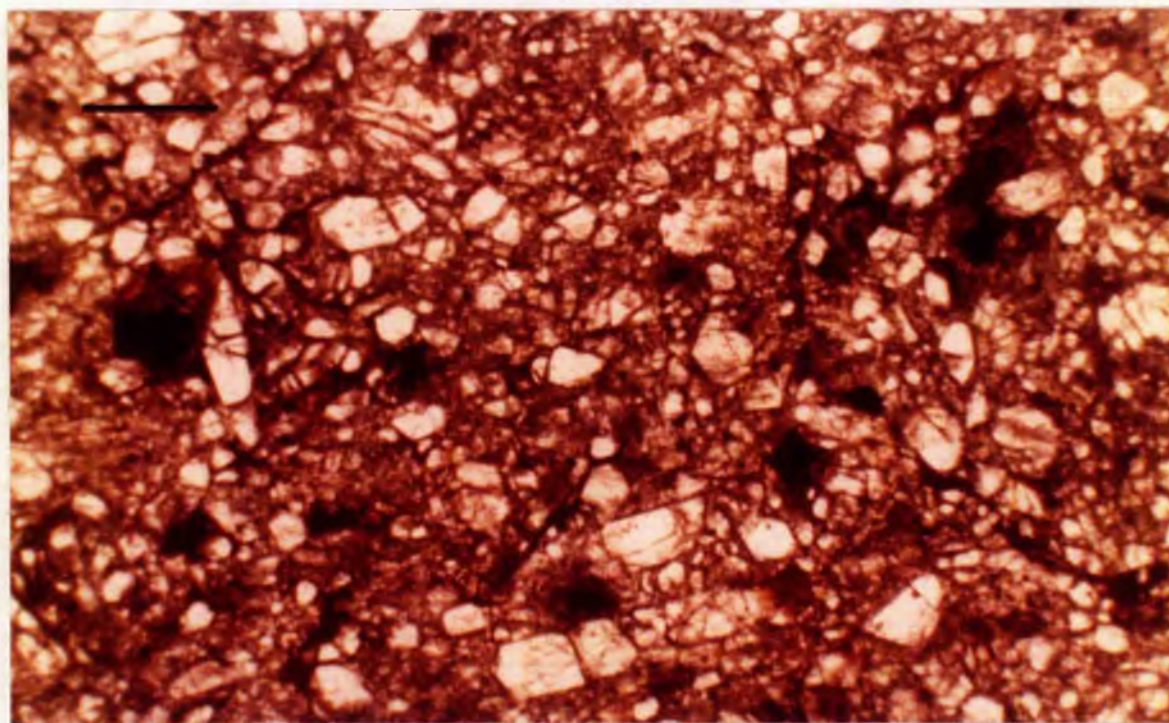


Plate 19(b): Photomicrograph of "apatite rock". Euhedral apatites in a carbonate matrix, with some iron-titanium oxides and biotite/phlogopite. Scale-bar is 1 mm. Plane-polarised light.



Plate 20(a): Peat Rig Formation lavas containing crystal clots. Hawaiite/mugearite lavas (grey-brown) containing diffuse patches of crystal-rich material, (red patches). Phenocrysts in lavas are identical to material in crystal clots.



Plate 20(b): Ultramafic xenolith in Peat Rig lavas. A black, strongly-chloritised clast is found within a lava matrix. The clast is rimmed by pinkish material reminiscent of the crystal clots in plate 20(a).

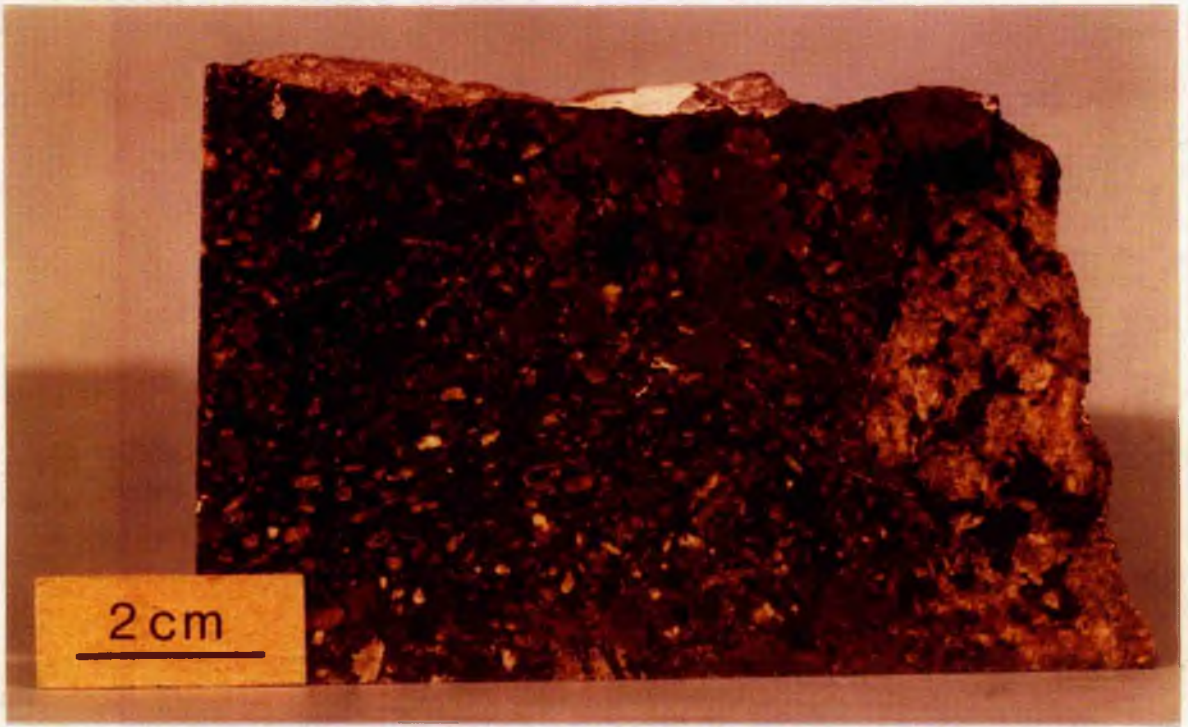


Plate 21(a): Matrix and xenoliths of the Bught Craig Member. Hawaiiite/mugearite lava matrix containing clasts of diorite (far right) and pyroxene and amphibole-bearing lavas (top centre and right). Note phenocryst-rich nature of matrix.

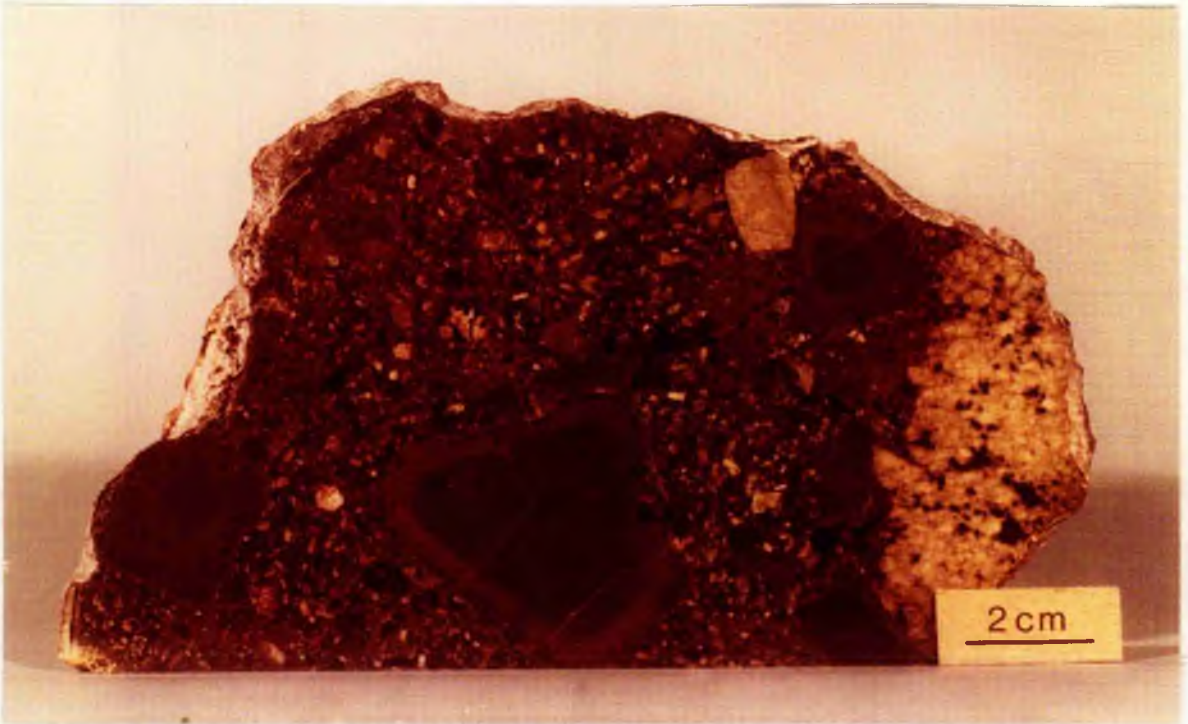


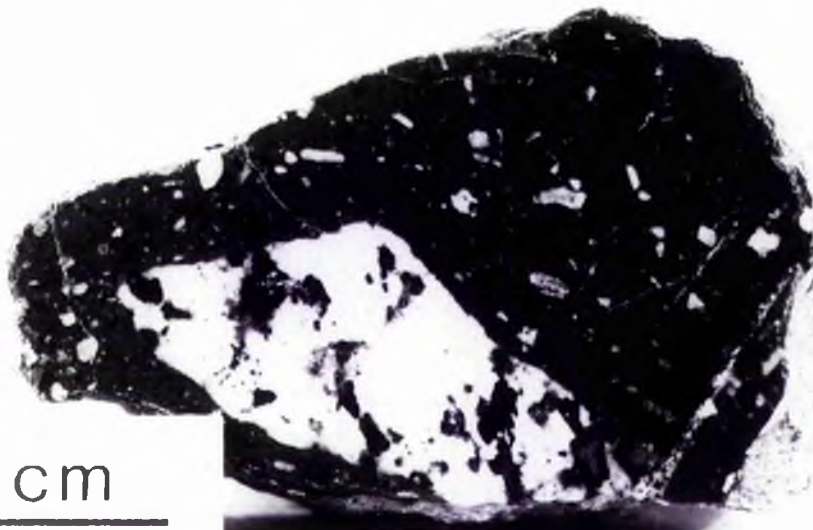
Plate 21(b): Matrix and xenoliths of the Bught Craig Member. Xenoliths include a leucocratic gabbro (far right), porphyritic lavas (left and right of centre) and aphyric lavas with weathered rims (centre and top right). Large feldspar xenocryst at top right.



Plate 22(a): Xenoliths in lava matrix of Bught Craig Member. Gabbroic (centre left) and fine-grained aphyric (bottom right) clasts are visible. The gabbro clast shows a marked layering of crystals.



Plate 22(b): Gabbroic xenolith in Bught Craig Member. Layering of the crystals is apparent.

A photograph of a leucocratic gabbro xenolith specimen. The rock is dark with numerous white phenocrysts of plagioclase feldspar and black amphibole. A scale bar labeled "2 cm" is positioned to the left of the specimen.

2 cm

Plate 23(a): Leucocratic gabbro xenolith in Eught Craig Member. The porphyritic nature of the lava matrix is apparent, with phenocrysts of plagioclase feldspar (white) and amphibole (black).

A photograph of a melanocratic gabbro xenolith specimen. The rock is dark with numerous white phenocrysts of bytownite feldspar. A scale bar labeled "2 cm" is positioned below the specimen.

2 cm

Plate 23(b): Melanocratic gabbro xenolith from Bught Craig Member. Primary mineralogy consists of chromian diopside and bytownite feldspar.

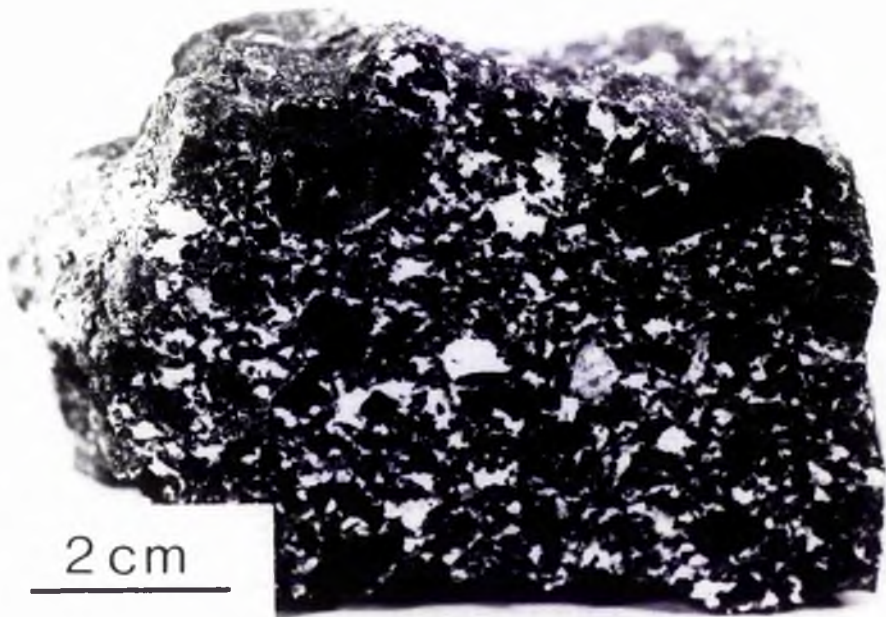


Plate 24(a): Melanocratic dioritic xenolith from Grain Burn Member. Pargasitic amphibole and iron-titanium oxides are the major constituents, with subordinate amounts of plagioclase feldspar, biotite/phlogopite and apatite.



Plate 24(b): Gabbroic xenolith in Bught Craig Member. A weak layering is developed in the xenolith, the chemical analysis of which is given in Table 11 (analysis 3). The clast was 35 cms across.

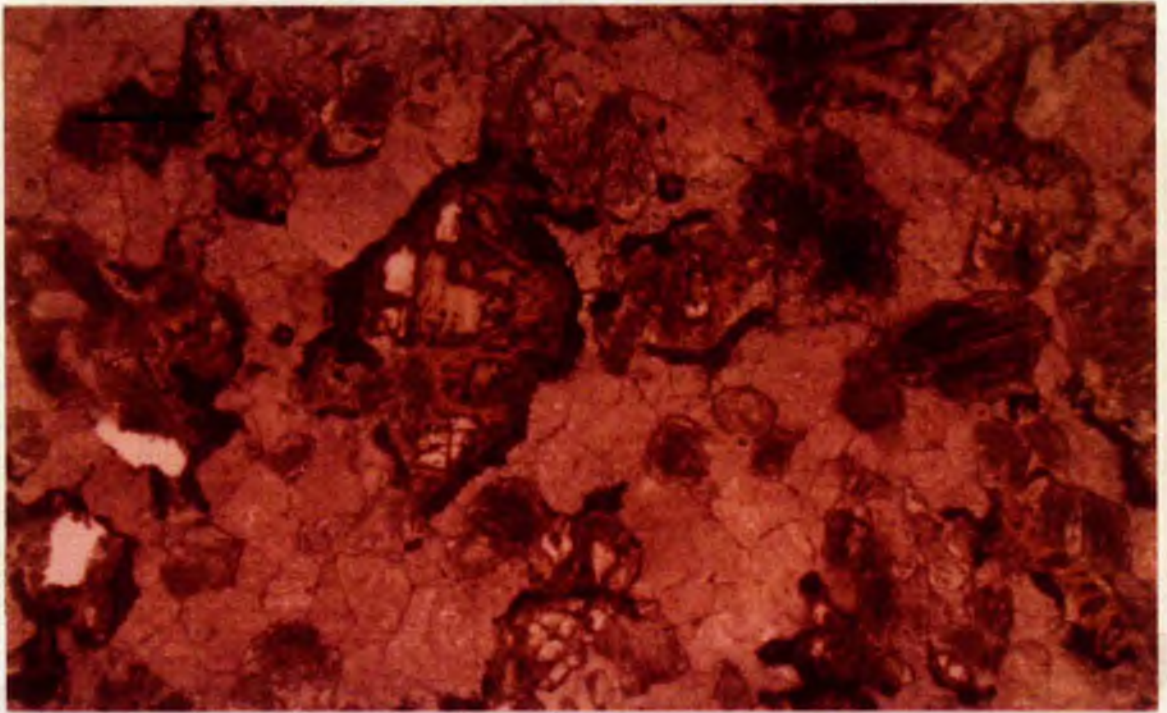


Plate 25(a): Photomicrograph of gabbro xenolith. Melanocratic gabbro containing possible pseudomorphs after olivine (centre). Other phases are feldspar (pale-pink), which has partially altered to white mica, and clinopyroxene (grey). Scale-bar is 1 mm. Plane-polarised light.



Plate 25(b): Photomicrograph of melanocratic gabbro xenolith. Diopside shows second-order colours and is in pristine condition, whilst plagioclase has partially altered to white mica, although original calcic material is visible between alteration. Scale-bar is 1 mm.

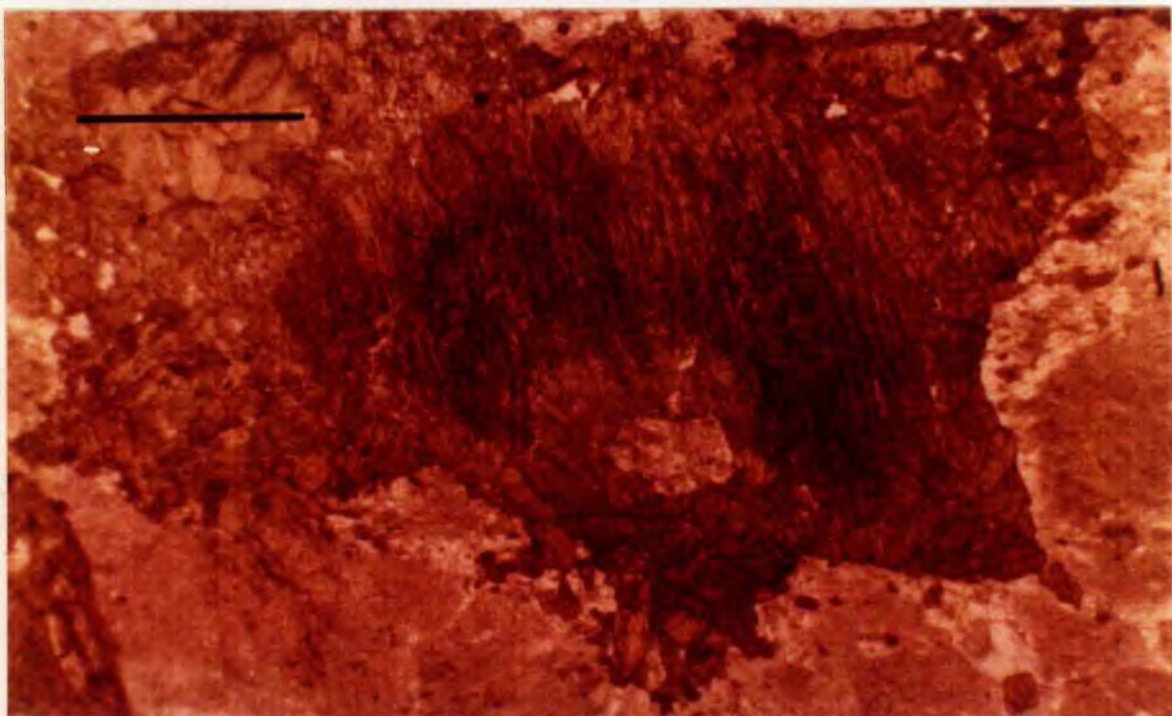


Plate 26(a): Photomicrograph of gabbro xenolith. Diopside (centre) with rim of actinolitic amphibole (green) and chlorite clusters (top left). Plagioclase has partially altered to white mica. Scale-bar is 1 mm.

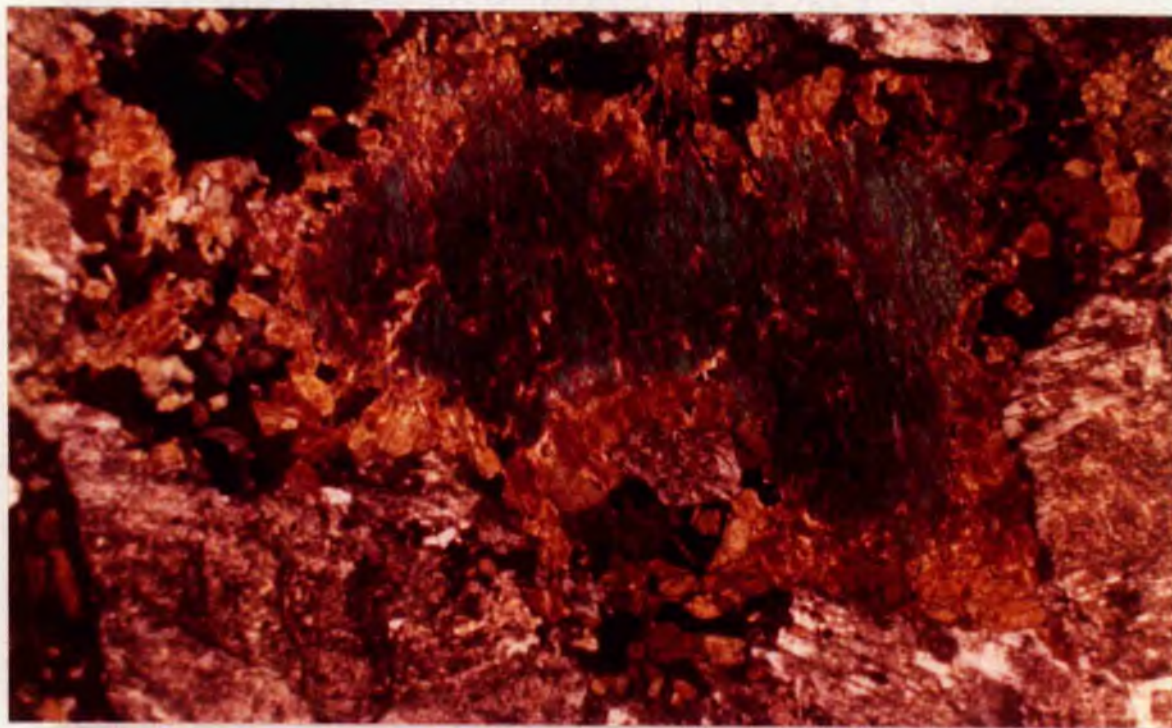


Plate 26(b): As above in cross-polarised light. Chlorite shows black and purple birefringence. Remnant calcic plagioclase is visible through alteration patches.

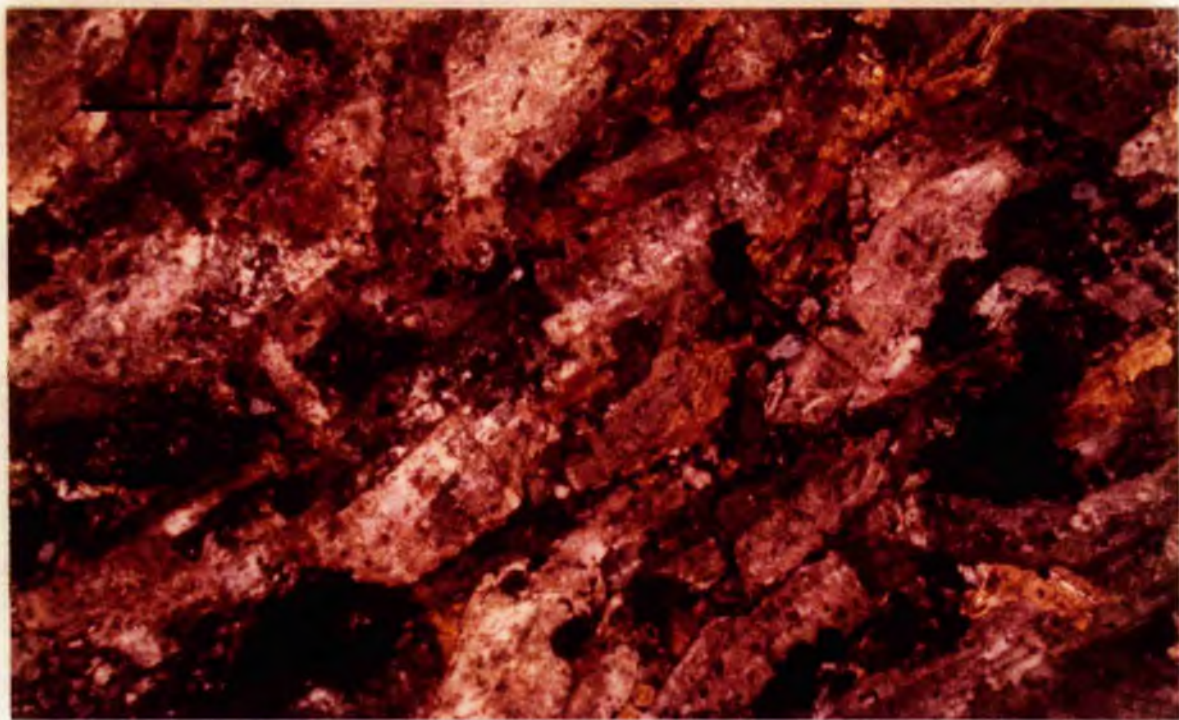


Plate 27: Photomicrograph of diorite xenolith. Large prismatic plagioclase feldspars, small apatites (centre and top right) and biotite/phlogopite (high birefringence), with orientation (?layering) of crystals running bottom left to top right. Scale-bar 1 mm.



Plate 28(a): Pyroclastic rocks of outlying tuff members. Lithic tuffs with erosive base overlying fossiliferous siltstones. "Rip-up" clasts of siltstone are visible in the upper part of the tuff unit. Stoodfold Member, Stoodfold Burn.



Plate 28(b): Pyroclastic rocks of outlying tuff members. Thin, highly-porous ash band interbedded with siltstones of the Kiln Formation. Stoodfold member, Stoodfold Burn.



Plate 29(a): Pyroclastic rocks of outlying tuff members. Lithic tuff unit interbedded with fossiliferous siltstones of the Kiln Formation. Craignorth Member, Brown's Cleuch.



Plate 29(b): Pyroclastic rocks of outlying tuff members. Agglomerate containing bombs of kawaiite/mugearite lava in a lithic tuff matrix. Stoodfold Member, Stoodfold Burn.

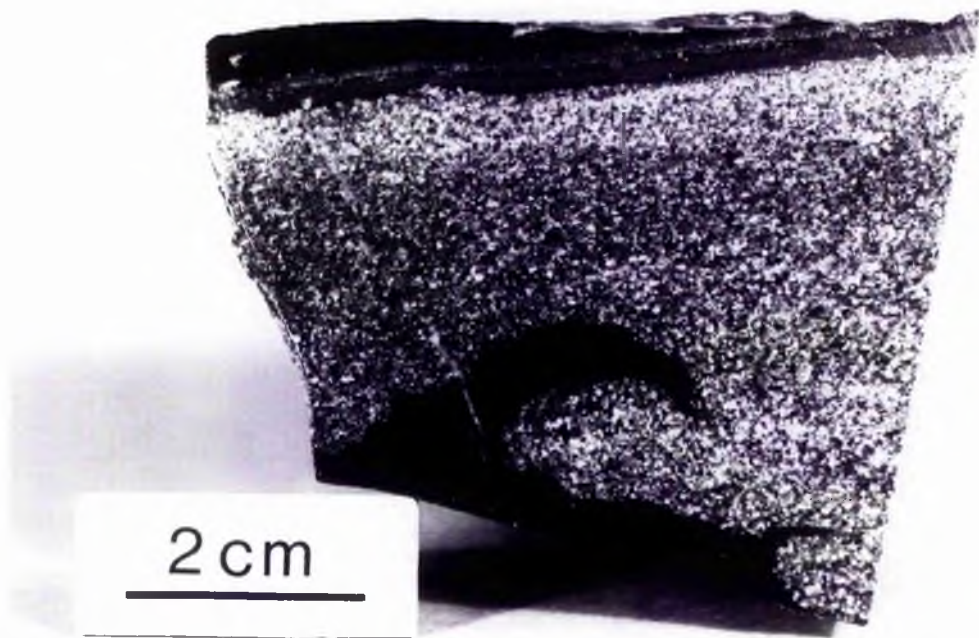


Plate 30(a): Pyroclastic rocks of outlying tuff members. Flame structure in Stoodfold Member. Bottom unit is volcanoclastic mudstone, top unit is lithic tuff. Specimen collected in Kiln Burn section.



Plate 30(b): Pyroclastic rocks of outlying tuff members. Erosive base of lithic tuff unit, containing large lava clasts (centre left) and "rip-up" clasts of siltstone (top right). Specimen from Stoodfold Member, Stoodfold Burn.



Plate 31(a): Pyroclastic rocks of outlying tuff members. Scouring, grading and lamination in crystal tuffs and volcaniclastic sediments. Specimen collected from 10-15 m sequence between lithic tuff units in the Kiln Burn. Stoodfold Member.

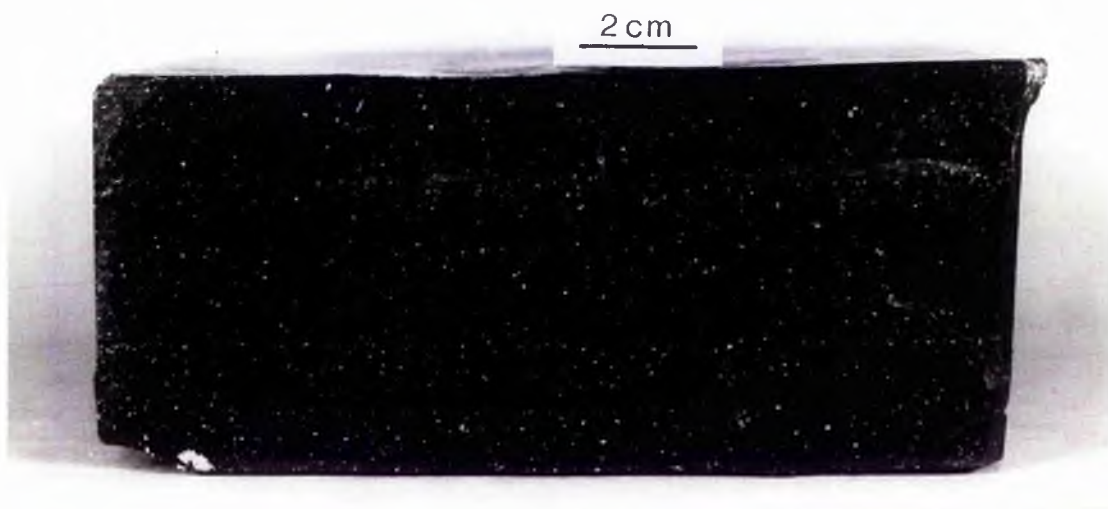


Plate 31(b): Pyroclastic rocks of outlying tuff members. Laminated siltstones of the Kiln Formation containing white flecks of cryptocrystalline material of supposed volcanic origin. Specimen collected in the Kiln Burn from Stoodfold Member.

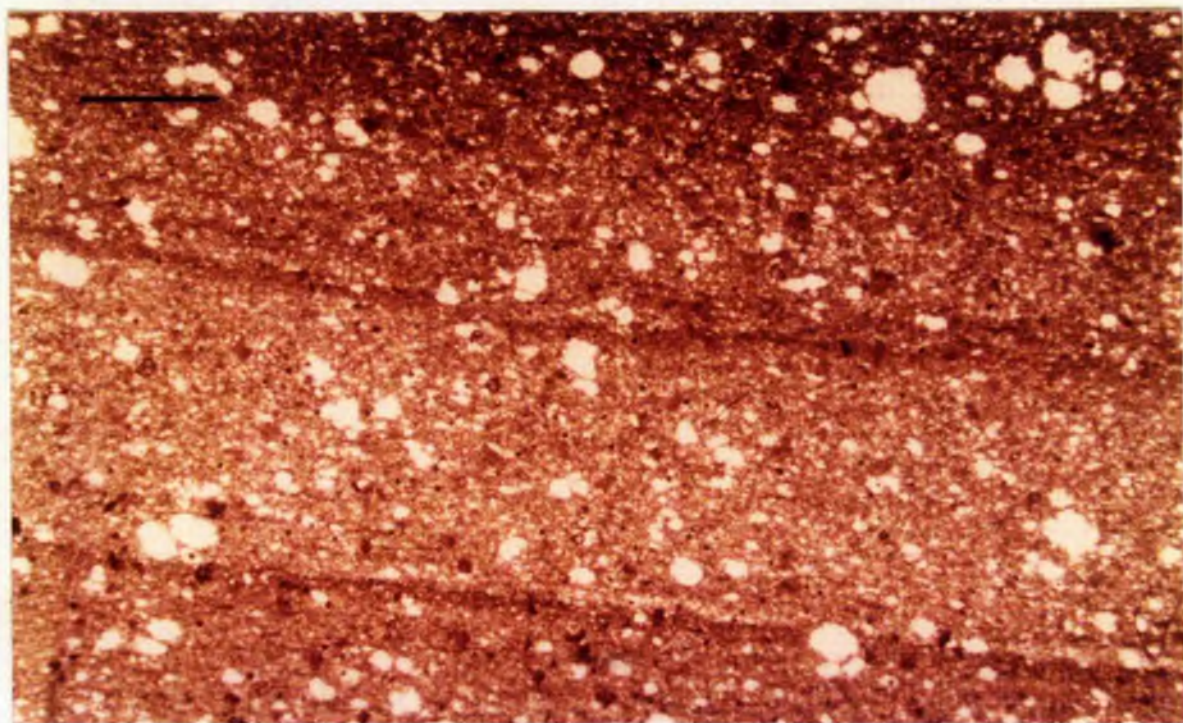


Plate 32(a): Laminated siltstones with bubble-cavity texture. Photomicrograph illustrating random distribution and varying size of cavities (white). Host material is turbiditic siltstone. Scale-bar is 1 mm. Plane-polarised light.

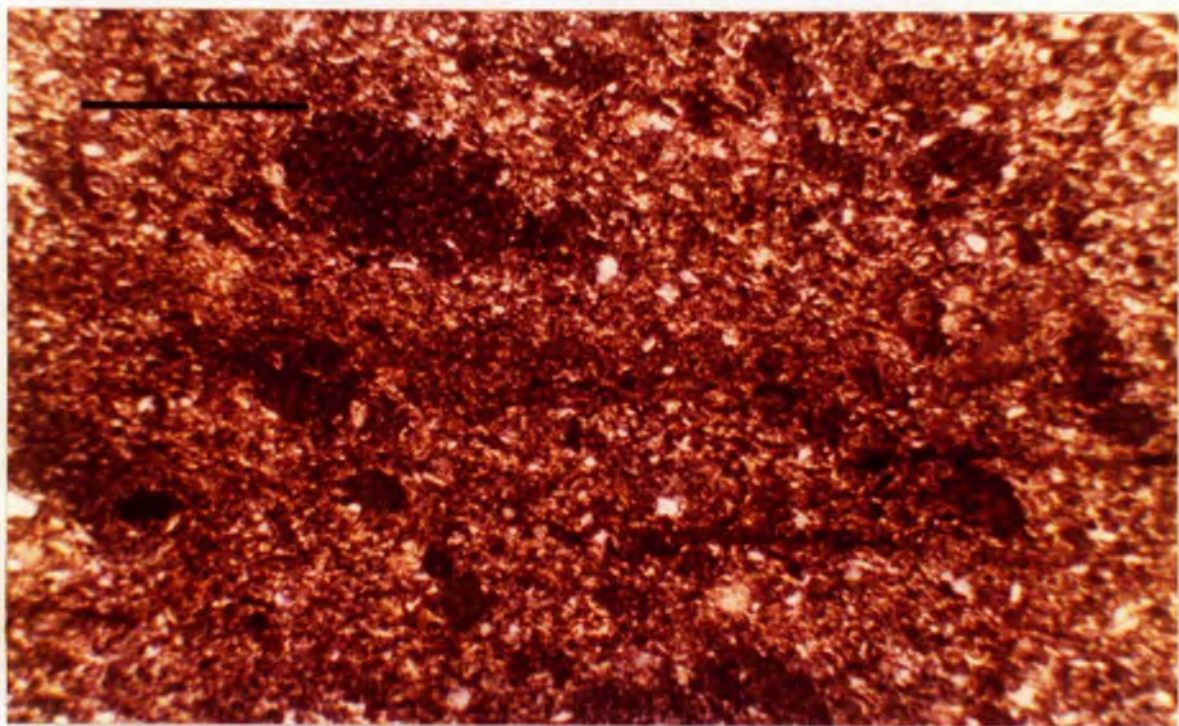


Plate 32(b): Photomicrograph of bubble-cavity texture. Close-up of cavities shows cryptocrystalline nature of infilling and lack of flattening of bubbles. Scale-bar is 0.5 mm. Cross-polarised light.

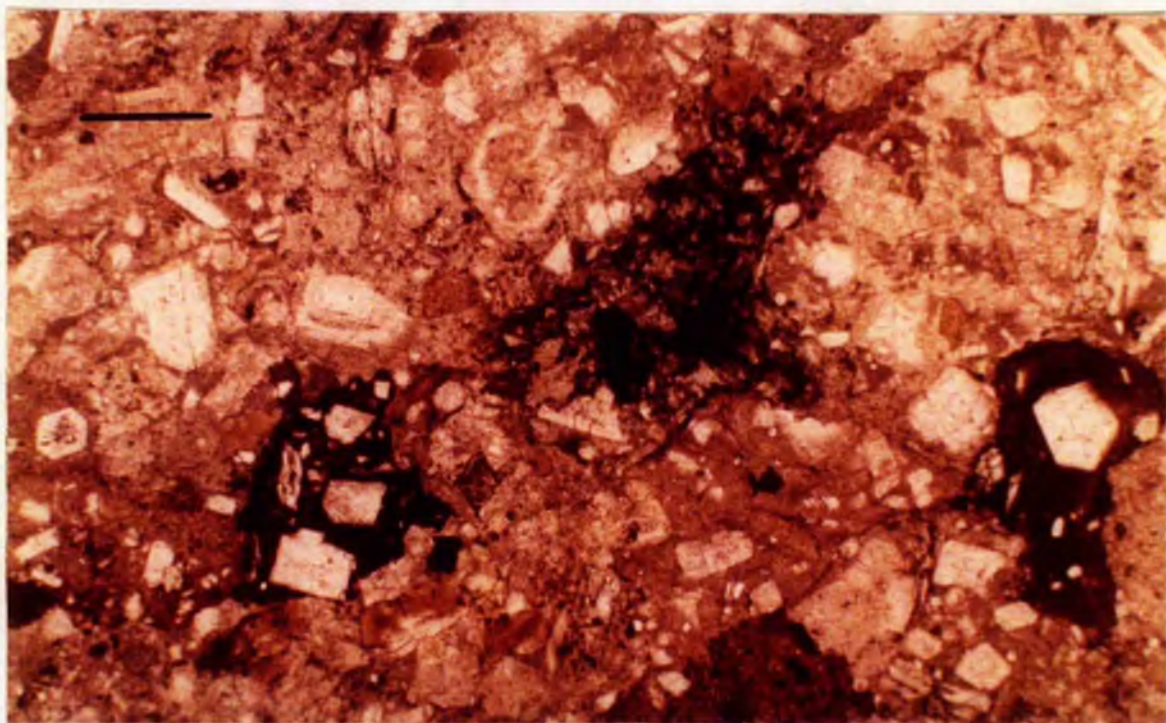


Plate 33(a): Photomicrograph of lithic tuff. Fragments of feldspar-phyric lavas with phenocrysts of biotite/phlogopite (red-brown), apatite (white crystal on right). Material is in grain-grain contact. Scale-bar is 1 mm. Plane-polarised light.

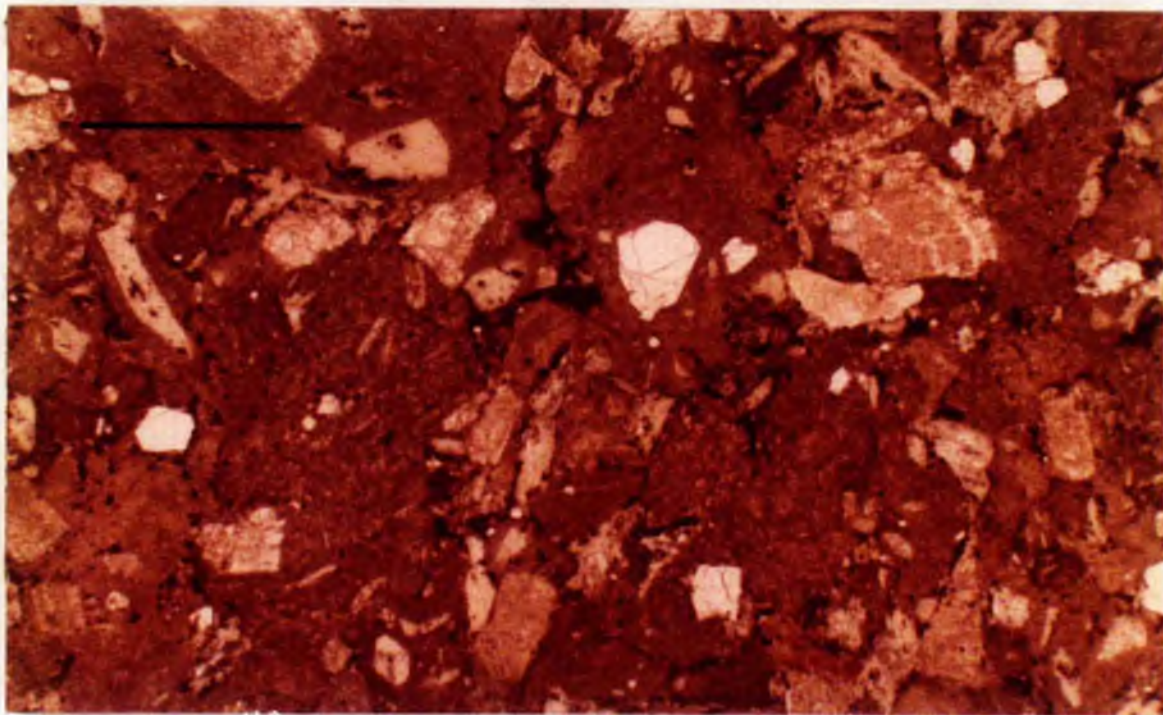


Plate 33(b): Photomicrograph of lithic tuff. Hawaiite/mugearite lavas containing phenocrysts of apatite (centre), feldspar, biotite/phlogopite (bottom right) and pseudomorphs after amphibole (green crystal, top left). Scale-bar is 1 mm. Plane-polarised light.

CHAPTER 7 : MINERALOGY

7.1 INTRODUCTION

Electron microprobe analyses of the principal mineral phases in 26 samples of the xenoliths and lavas from the Bail Hill Volcanic Group were obtained in order to ascertain the relationship between the volcanics and the xenoliths and to determine the petrochemical affinities of the magma(s). The material studied is not representative of the Bail Hill Volcanic Group, as certain major lithologies are unsuitable for analysis, due to weathering and alteration of phenocrysts. Therefore, the volumetrically subordinate pyroxene-bearing rocks have been studied in detail, whilst the more abundant amphibole and biotite/phlogopite-bearing lithologies have received little attention. Nevertheless, in view of the inferred derivative nature of the amphibole and biotite/phlogopite-bearing lithologies by differentiation of the more basic members (see Chapters 8 and 9) it should be possible to achieve the aims outlined above by studying the xenoliths and early volcanic activity.

Details of the analytical techniques used, standards, accuracy and precision of data are given in Appendices 4-6.

7.2 PYROXENES

7.2.1 General

Analyses of clinopyroxenes from coarse-grained

Table 3. Pyroxene analyses (electron microprobe).

	1	2	3	4	5	6	7	8	9	10	11	12	13
SiO ₂	51.87	53.46	52.67	51.58	51.09	50.63	50.86	50.58	51.35	49.74	49.58	46.79	52.56
TiO ₂	0.41	0.26	0.54	0.73	1.25	0.42	1.11	1.00	0.87	0.87	0.86	1.38	0.09
Al ₂ O ₃	2.81	1.91	2.69	3.41	3.96	5.10	3.58	4.32	3.91	5.18	4.52	7.30	1.16
Cr ₂ O ₃	0.32	0.33	0.28	0.36	0.70	0.38	0.57	0.30	0.99	0.09	0.04	0.02	N.D.
FeO*	4.31	4.49	4.65	5.15	5.07	5.46	5.92	6.01	5.87	6.17	6.38	7.90	11.61
MnO	0.06	0.21	0.20	0.13	0.18	0.25	0.17	0.12	0.20	0.06	0.16	0.17	3.01
MgO	15.51	16.14	15.53	15.21	14.79	15.36	14.56	14.92	14.72	14.30	14.98	13.20	10.87
CaO	23.57	23.07	22.63	23.44	22.02	21.23	22.85	22.41	21.07	22.74	22.13	22.13	20.40
Na ₂ O	0.13	N.D.	N.D.	N.D.	N.D.	0.47	N.D.	N.D.	0.31	N.D.	N.D.	N.D.	1.01
Total	98.99	99.87	99.19	100.01	99.06	99.30	99.62	99.66	100.09	99.15	98.89	98.89	100.71

Number of ions on the basis of 6 oxygens

Si	1.921	1.958	1.942	1.899	1.893	1.865	1.887	1.873	1.892	1.851	1.887	1.756	1.978
Al ^{IV}	0.079	0.042	0.058	0.101	0.107	0.135	0.113	0.127	0.108	0.149	0.153	0.244	0.022
Al ^{VI}	0.043	0.041	0.059	0.047	0.066	0.087	0.044	0.061	0.062	0.079	0.046	0.079	0.030
Ti	0.011	0.007	0.015	0.020	0.035	0.012	0.031	0.028	0.024	0.024	0.024	0.039	0.003
Fe ⁺³	0.013	0.000	0.000	0.003	0.000	0.048	0.000	0.002	0.000	0.018	0.057	0.087	0.060
Cr	0.009	0.010	0.008	0.010	0.023	0.011	0.017	0.009	0.029	0.003	0.001	0.001	0.0
Mg	0.856	0.881	0.854	0.835	0.817	0.843	0.805	0.823	0.808	0.793	0.832	0.738	0.610
Fe ⁺²	0.120	0.138	0.143	0.156	0.157	0.121	0.184	0.124	0.181	0.174	0.141	0.161	0.305
Mn	0.002	0.007	0.006	0.004	0.006	0.008	0.005	0.004	0.006	0.002	0.005	0.005	0.096
Ca	0.935	0.906	0.894	0.925	0.874	0.838	0.909	0.889	0.863	0.907	0.893	0.890	0.823
Na	0.009	0.0	0.0	0.0	0.0	0.034	0.0	0.0	0.022	0.0	0.0	0.0	0.074
Mg	44.5	45.6	45.0	43.4	44.0	45.4	42.3	43.3	43.5	41.9	43.2	39.2	32.2
Fe**	7.0	7.5	7.9	8.5	8.8	9.5	9.9	10.0	10.1	10.2	10.5	13.5	24.3
Ca	48.5	46.9	47.1	48.1	47.2	45.1	47.8	46.7	46.4	47.9	46.3	47.3	43.5

* total iron as FeO

N.D. not detected

** (Fe⁺² + Fe⁺³ + Mn)

1. Average of 6 analyses in gabbroic xenolith (28/4).
 2. Average of 2 xenocrysts in hawaiite (27/2).
 3. Average of 3 analyses in gabbroic xenolith (27/3).
 4. Average of 3 analyses in gabbroic xenolith (27/8).
 5. Single analysis in ultramafic xenolith (103/70).
 6. Average of 2 analyses in gabbroic xenolith (27/23).
 7. Average of 2 analyses in xenolith (103/7).
 8. Average of 4 analyses in gabbroic xenolith (27/11).
 9. Average of 2 analyses in ultramafic xenolith (103/51).
 10. Average of 4 analyses from basalt (16W).
 11. Average of 6 analyses in basalts of Cat Cleuch Formation [111] sector.
 12. Average of 8 analyses in basalts of Cat Cleuch Formation. [100], [110] & [010] sectors.
 13. Average of 3 analyses in dioritic xenolith (27/1).
- Analyses 1-7, chromian diopsides; analyses 8 & 9, chromian salites; analyses 10-12, salites; analysis 13, augite.

xenoliths and lavas are given in Table 3 and their positions on the pyroxene quadrilateral illustrated in Figure 4.

The gabbroic and ultramafic xenoliths contain a single pyroxene, a chromian salite or diopside. Average analyses from xenoliths show a continuous range from $\text{Ca}_{48.5}:\text{Mg}_{44.5}:\text{Fe}_{7.0}$ to $\text{Ca}_{46.4}:\text{Mg}_{43.5}:\text{Fe}_{10.1}$. The most iron-poor variety occurs in a melanocratic gabbro containing possible olivine pseudomorphs, suggesting that it is the most primitive of the xenoliths studied. In the other gabbroic xenoliths pyroxene is subordinate to plagioclase feldspar and it is possible that as the Fe-content of the pyroxenes increased the rate of precipitation of the phase itself decreased, with concomitant increase in the rate of precipitation of plagioclase feldspar. In the ultramafic xenoliths (Table 3, analysis 9) chrome salite occurs with pargasitic amphibole and iron-titanium oxides with minor amounts of plagioclase feldspar. Petrographic evidence suggests that the clinopyroxene precipitated before the amphibole and iron-titanium oxides (see Section 6.4.4).

The Bail Hill diopsides and salites show some notable differences from the analyses given in Deer et.al. (1978). Firstly, the xenolith pyroxenes from Bail Hill show slightly above-average TiO_2 contents (0.73% in the Bail Hill crystals, against an average of 0.54% in Deer et.al. (1978)). The TiO_2 contents of analyses 3, 4, 5 and 7 (Table 3) are particularly unusual as Deer et.al. (1978) state that TiO_2 contents over 0.5% are confined to salites. However, this slightly above-average TiO_2 contents of xenolith diopsides and salites is in agreement with the

observations of Verhoogen (1962) who indicates that Ti would be expected to preferentially enter silicates in the early stages of crystallisation, before the appearance of magnetite as a liquidus phase. The absence of iron-titanium oxides from the gabbroic xenoliths has been noted (see Section 6.3.3), whilst in the ultramafic xenoliths it is a later precipitating phase than the pyroxene (see above and Section 6.4.4). The entry of Ti into silicates is enhanced at high temperatures and in silica-undersaturated melts (Verhoogen, 1962), both of which are inferred for the Bail Hill magma at this time (see Chapter 9).

A second feature of the Bail Hill pyroxenes (both xenolith and phenocryst varieties) is the very low Na₂O contents. In many of the analyses Na₂O was below the detection limits, although there is no evidence to suggest loss of Na₂O from the pyroxene structure. It is therefore believed to be a primary feature of the crystals. In contrast to this, the analyses presented in Deer et al. of chrome-bearing diopsides contain more Na₂O than their chrome-free equivalents, reflecting the higher contents of Na in pyroxenes crystallising from alkaline magmas. However, the Na-content of pyroxenes is indirectly related to the oxygen fugacity of the magma, as this determines the amount of Fe³⁺ in the system (Gibb, 1973). This in turn determines the roles of the CaFe²⁺Si₂O₆ (hedenbergite) and NaFe³⁺Si₂O₆ (aegirine) molecules in the sequence of crystallisation, with pyroxenes differentiating to one or other of these end members. It is therefore suggested

that the pyroxenes in the Bail Hill xenoliths and volcanics crystallised under relatively low oxygen fugacities, resulting in little Fe^{3+} being available to allow substitution of Na in the pyroxene structure. The scarcity of Fe^{3+} in the structural formulae (see Table 3) is in agreement with this, although it is stressed that this has been calculated according to the charge-balance equation of Papike et.al. (1974) and involves Na in the calculation.

A third feature of the xenolith pyroxenes is the occurrence of chrome-salite at Bail Hill (Table 3, analysis 9). The substitution of Cr in pyroxene is related to the Mg-content of the crystal (Wedepohl, 1969). The occurrence of chrome-salite, however, suggests that substitution of Cr in pyroxene is dependent on factors other than the Mg-content of the crystal. This crystal has no counterpart in the analyses presented in Deer et.al. (1978) and no explanation of this feature is offered.

Phenocryst analyses (Table 3, analyses 10-12) are all from lavas of the Cat Cleuch Formation. In the lower part of the formation, unzoned salite phenocrysts (analysis 10) show compositional continuity with the xenolith pyroxenes (see Figure 4). The presence of Cr_2O_3 and the absence of detectable Na_2O in the phenocrysts further suggest a genetic relationship with the xenolith pyroxenes. Analyses 11 and 12 are averages from sector-zoned pyroxenes. The similarity in composition between the 100, 110 and 010 sectors allows them to be considered together. The differences among these three sectors and the $\bar{1}11$ sector is evident in Table 3. The sector-zoned

pyroxenes are discussed in detail in Section 7.2.2.

The analysis falling in the augite field on Figure 4 is from a dioritic xenolith in the Bught Craig Member (Table 3, analysis 13). The xenolith contains similar feldspars, amphiboles, micas and apatites to those found as phenocrysts in the extrusive rocks, indicating that it is undoubtedly related to the Bail Hill episode. The pyroxene is rimmed by pargasitic amphibole and may be an earlier crystallising phase than the other minerals. However, the most notable feature of this pyroxene, the anomalously high MnO concentration, is reflected in micas from the same specimen (Table 7, analysis 1).

The Bail Hill extrusives and xenoliths contain a single Ca-rich pyroxene, typical of the association found in alkaline magmas (Wilkinson, 1956, 1967, 1970). The typically tholeiitic association of co-existing Ca-rich and Ca-poor pyroxenes is not found. In the past much emphasis has been placed on using pyroxene data to distinguish between alkaline and subalkaline magmas. Trends on the pyroxene quadrilateral (Wilkinson, 1973), silica, titanium and aluminium relations (Kushiro, 1960; LeBas, 1962) and TiO_2 -MnO- Na_2O plots (Nisbet and Pearce, 1977) have all been used in an attempt to differentiate between magma types. However, the plots of Kushiro (1960), LeBas (1962) and Nisbet and Pearce (1977) are only applicable to ground-mass pyroxenes, not phenocrysts and xenolith varieties. Furthermore, mildly alkaline magmas can give erroneous results when discrimination of magma type is based on these plots (Barberi *et al.*, 1971; Gibb, 1973). It is

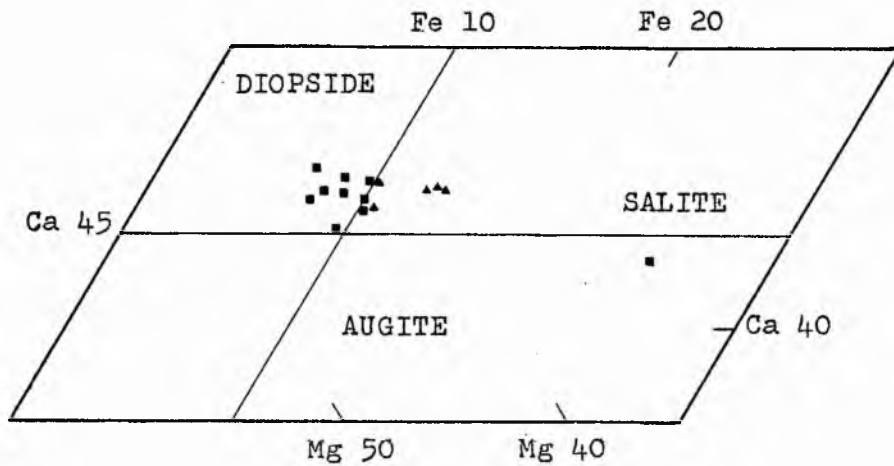


Figure 4(a): Plot of Bail Hill pyroxenes on pyroxene quadrilateral. Squares represent average analyses for xenolith pyroxenes, triangles represent phenocryst varieties.

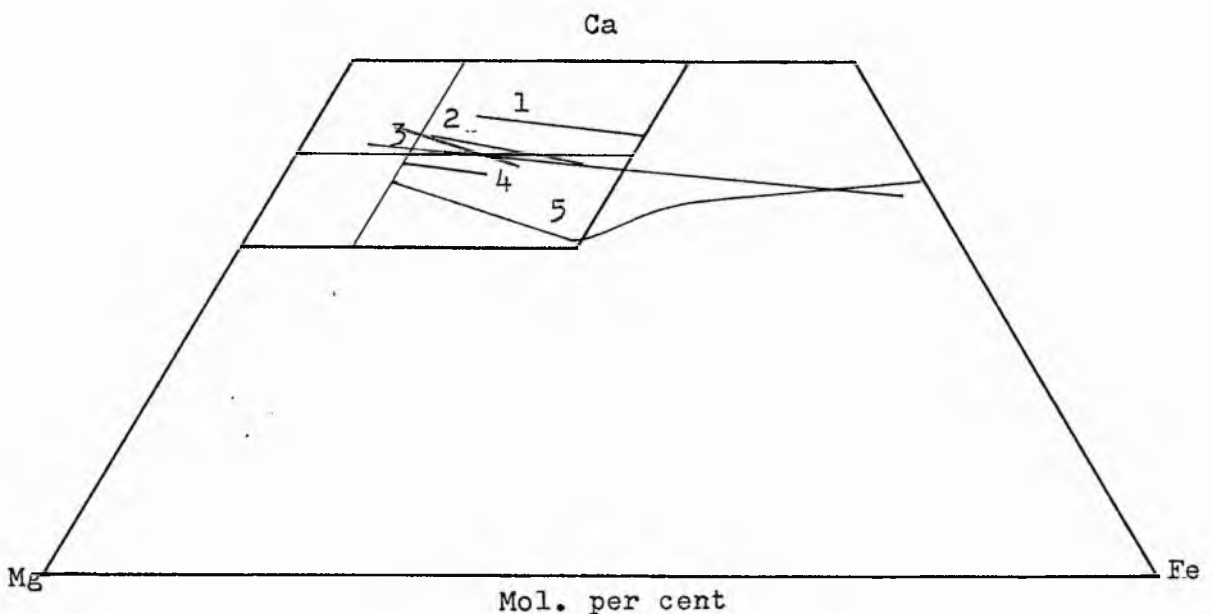


Figure 4(b): Trend of Bail Hill pyroxenes compared with typical alkaline and subalkaline trends. Bail Hill trend in red; 1-4, trends for alkaline pyroxenes after Wilkinson (1956), Murray (1954), Gibb (1971) and Aoki (1959). Subalkaline trend, no. 5, after Wager and Brown (1967).

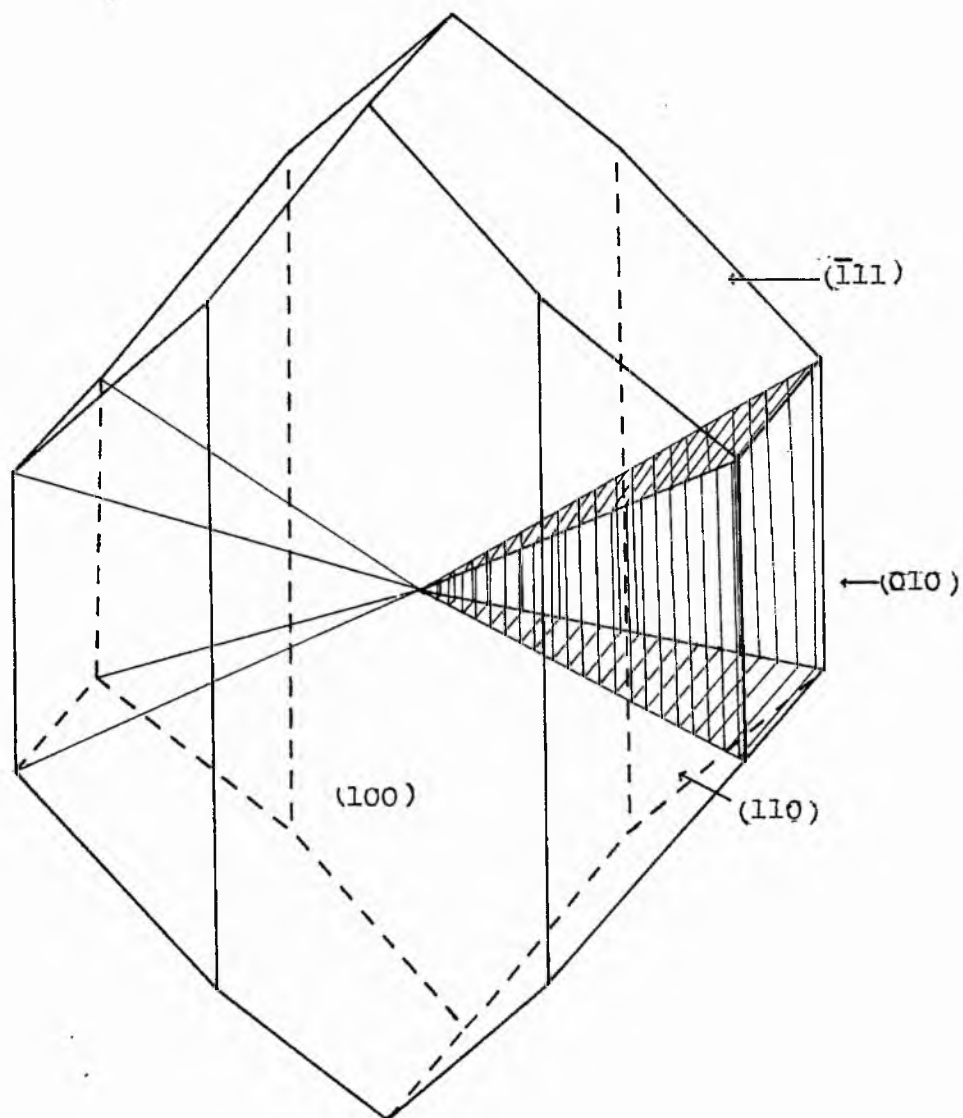


Figure 5: Illustration of the sector-zoned pyroxenes of the Cat Gleuch Formation. The two sectors in the $\{010\}$ form are shown and the nature of the concentric zoning indicated.

inferred from this data that discrimination between the two magma types (alkaline and subalkaline) for the Bail Hill data could not be achieved on these plots and they have, accordingly, not been used.

Under certain physicochemical conditions mildly alkaline magmas can crystallise pyroxenes with tholeiitic (subalkaline) affinities (Barberi et.al., 1971). The converse situation (a tholeiitic magma crystallising pyroxenes with alkaline affinities) is not likely to be realised in a natural system (Barberi et.al., 1971). Thus, the close affinity of the Bail Hill pyroxenes with pyroxenes of known alkaline affinities (see Figure 4) is likely to be a reliable indicator of the magma from which they crystallised. Moreover, according to Deer et.al. (1978) diopsides and salites are the typical pyroxenes found in rocks of alkali olivine basalt parentage.

7.2.2 Sector-zoned pyroxenes

Pyroxenes from the Cat Cleuch Formation display euhedral outlines with the $\{100\}$, $\{110\}$, $\{010\}$ and $\{\bar{1}11\}$ forms present. In some simple-twinned crystals the $\{001\}$ form is developed on the upper surface, the twin plane being $\{100\}$.

In thin section the crystals display sector and concentric zoning and the hourglass structure is well developed. Individual sectors are pyramidal in shape, with the apex at the crystal centre and one of the crystal faces as a base (see Figure 5). All sectors that have for their base faces in the same form are collectively

known by the face characterising that form. Thus the crystals of the Cat Cleuch Formation are made up of 12 interlocking pyramids as follows: 2 in the $\{100\}$ form, 4 in the $\{110\}$ form, 2 in the $\{010\}$ form and 4 in the $\{\bar{1}11\}$ form.

Sector and concentric zoning are visible by small variations in the colour and birefringence within crystals (see Plates 34, 35, 36, 37). The colour varies from pale yellow, through lemon yellow to pale green (n.b. examples illustrated in Plates 34-37 are greater than 30 microns thick). Strongly coloured varieties are pleochroic to pale yellow. The relationship between colour and chemistry is discussed below.

Because the crystals are large and euhedral it was possible to cut individual specimens at right angles to crystallographic axes in order to observe the zoning and relate it to crystal axes and faces. Sections were then polished and studied on the electron microprobe. It is evident that there are consistent significant differences between sectors, with the most marked variation between the $\{\bar{1}11\}$ sector and the other three (see Table 4). Within each sector there are also differences due to concentric zoning, although there is no overall zoning from core to margin (see Figure 6).

Figure 6 is a traverse from the core to margin in the $\{100\}$ sector of a single crystal. Analyses were obtained at approximately 0.1 mm intervals across the crystal and the results are plotted to show the variation due to concentric zoning. Al_2O_3 and TiO_2 show the greatest

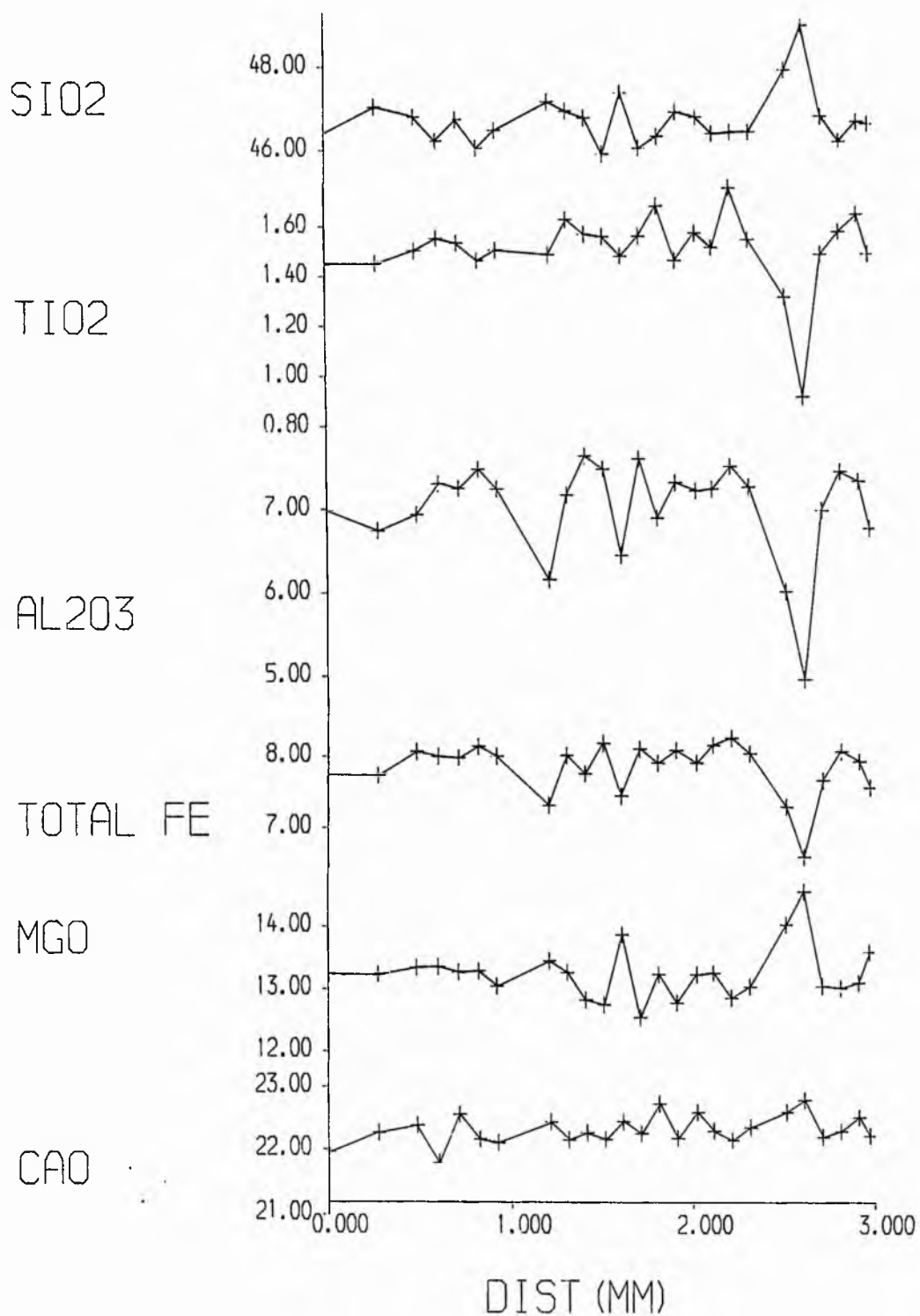


Figure 6: Traverse from core to margin of sector-zoned pyroxene showing relative oxide variation.

variation and are both sympathetic with total iron. SiO_2 and MgO vary antipathetically to these three elements, whilst CaO remains almost constant. Minor amounts of MnO , Cr_2O_3 , NiO and Na_2O were found but have been omitted for simplicity. Similar variations were found in the other three sectors where, although the absolute concentrations differ, the relative variations are the same.

The pyroxene composition shows strong correlation with crystal colour, pale-yellow sectors and bands contain lower Al_2O_3 , TiO_2 and total iron and higher SiO_2 and MgO than lemon-yellow and pale-green sectors and bands.

The concentric zoning is also picked out by trains of inclusions (iron-titanium oxides, feldspars, apatites and devitrified glass) oriented parallel to the crystal face forming the base of a particular sector. The inclusions allow two scales of concentric zoning to be distinguished :-

1. Coarse-bands, approximately 0.1 mm thick, differing slightly in colour and birefringence from adjacent coarse bands. These are bounded by sharp discontinuities, marked by lines of inclusions and colour change:

2. Fine bands, approximately 0.01 mm thick, occurring within the coarse bands. These do not display sharp boundaries but merge into adjacent fine bands with slightly different colour and birefringence.

There is no systematic colour variation in either the coarse or the fine bands.

With banding on such a scale an average crystal

50 mm across contains over 2500 concentric zones per sector. Some of the more distinct bands can be traced from one sector to another, indicating that the bands are primary growth phenomena and that crystals had euhedral outlines at all stages of their growth. The chemical differences were therefore produced on the surfaces of simultaneously growing crystal faces. This feature together with the rapid changes in composition marked by the concentric zoning are not likely to be produced by large-scale changes in the composition of the magma, but by disequilibrium crystallisation in which the material added to rapidly growing crystal faces is controlled by the varying diffusion rates of elements in the liquid (Thompson, 1972; Deer et.al., 1978). The rapid growth would not allow equilibration of the growing surface with the crystal interior before the next growth layer was added (Hollister and Gancarz, 1971). Material would only equilibrate if there was a pause in growth allowing equilibration to take place between the liquid and the surface of the crystal.

The two scales of banding correspond to growth without time for equilibration (fine bands) and a temporary cessation of growth allowing surface equilibration to take place (coarse bands). The trains of inclusions and sharp colour discontinuities therefore represent periods of no growth. The merging of the fine bands is due to variation in the diffusion rates of ions to the growing surface, with colour increasing with the amount of Fe^{3+} and Ti^{3+} in the growth layer (Ferguson, 1973).

A number of models have been proposed to account

for sectoral differences (Hollister and Gancarz, 1971; Nakamura, 1973; Dowty, 1976). All require rapid growth rates and relate sectoral differences to the differing atomic arrangements on crystal/growth surfaces. The results from the Cat Cleuch Formation pyroxenes support the model of Hollister and Gancarz (1971) and Dowty (1976) who predict decreasing concentrations of Ti, Al and Fe^{3+} from $\{100\}$ through $\{010\}$ and $\{110\}$ to $\{\bar{1}11\}$ (see Table 4).

The nature of the sector-zoning is also dependent on the composition of the parental magma (Nakamura, 1973). Tholeiitic (subalkaline) magmas produce sector zoning in $\text{Ca}/(\text{Mg}+\text{Fe})$ (e.g. Hollister and Hargraves, 1970), whilst alkaline (silica-undersaturated) magmas display sector zoning with respect to Ti and Al (Hollister and Gancarz, 1971; Thompson, 1972; Ferguson, 1973; Downes, 1974; Rahman, 1975). The Cat Cleuch Formation shows all the characteristics of having crystallised from a silica-undersaturated magma, corroborating the mildly alkaline trend of the Bail Hill pyroxenes on the pyroxene quadrilateral (see Section 7.2.1).

A noticeable feature of many of the pyroxenes from the Cat Cleuch Formation is the marked curvature of faces in the $\{100\}$ form and the edges between faces in the $\{\bar{1}11\}$ form. This is best viewed perpendicular to $\{010\}$. The faces in the $\{100\}$ form are notably convex. The edge between faces in the $\{\bar{1}11\}$ form is occasionally concave, as indicated by Scott (1914), but more commonly shows a marked break of slope near the acute angle between faces in the $\{100\}$ form and the edge between faces in the $\{\bar{1}11\}$ form (see Plate 35). In thin section the curvature of

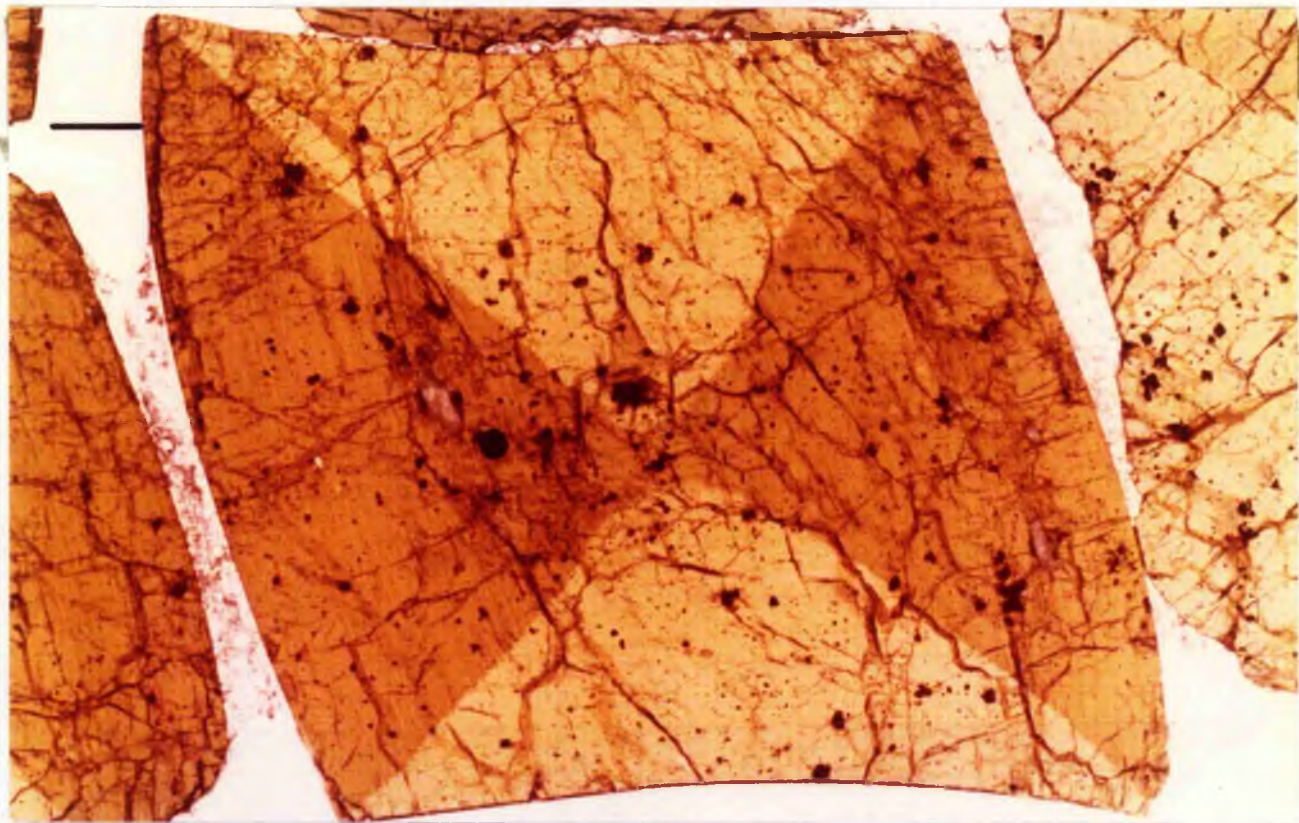


Plate 34: Sector-zoned pyroxene. Sector and concentric zoning are visible in this crystal and the hourglass structure is well developed. The $\{100\}$ (dark) and the $\{\bar{1}11\}$ (light) sectors are present and concentric zones run parallel to the crystal edges. Scale-bar is 1 mm. Photograph of polished thin section.

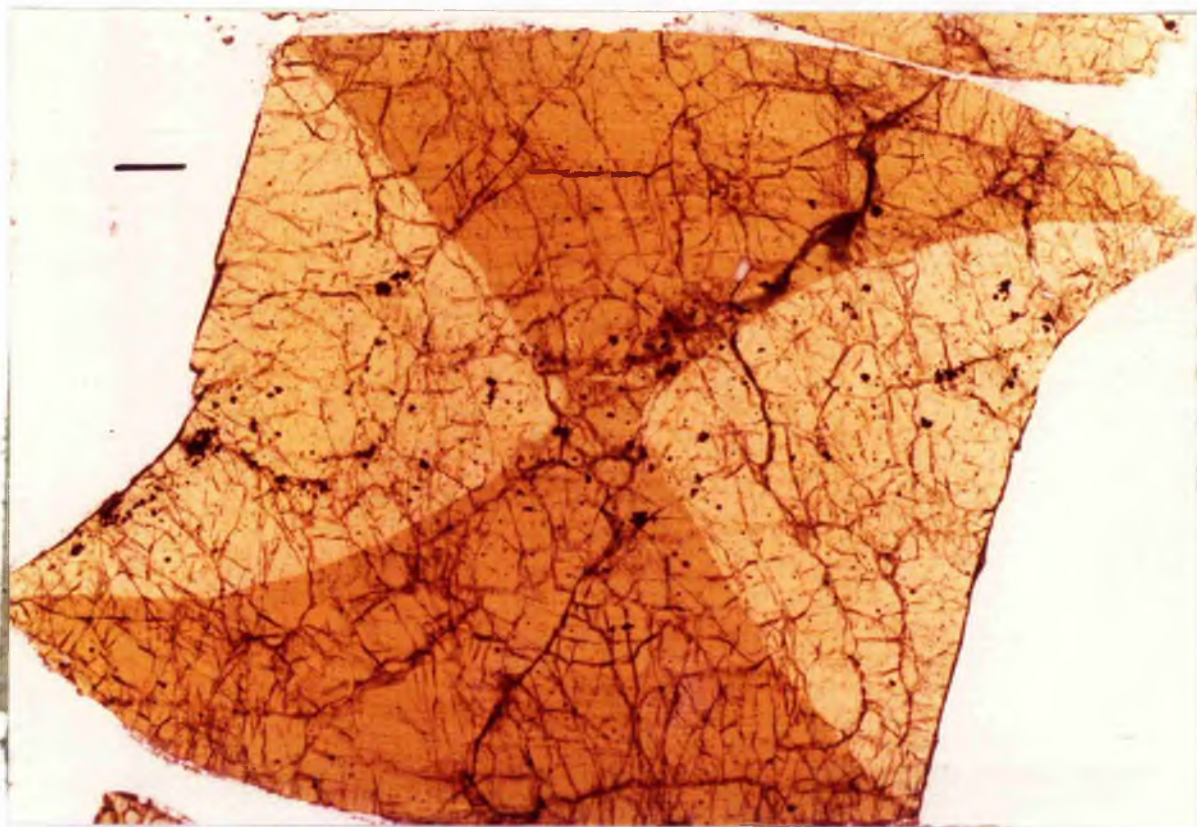


Plate 35: Sector-zoned pyroxene. The crystal has been cut perpendicular to $\{010\}$ revealing the $\{100\}$ (dark) and $\{\bar{1}11\}$ sectors. The non-planar nature of faces in these forms is exhibited in the curvature of faces in the $\{100\}$ form and the sudden change in orientation of faces in the $\{\bar{1}11\}$ form (manifest as a marked change of slope). Note that each sector has one straight and one curved boundary with its adjacent sectors. The increasing curvature of the "curved" boundaries away from the crystal centre suggests that the "deformation" of the crystal is a growth phenomena and is not of secondary origin. Scale-bar is 1 mm. Photograph of polished thin section.

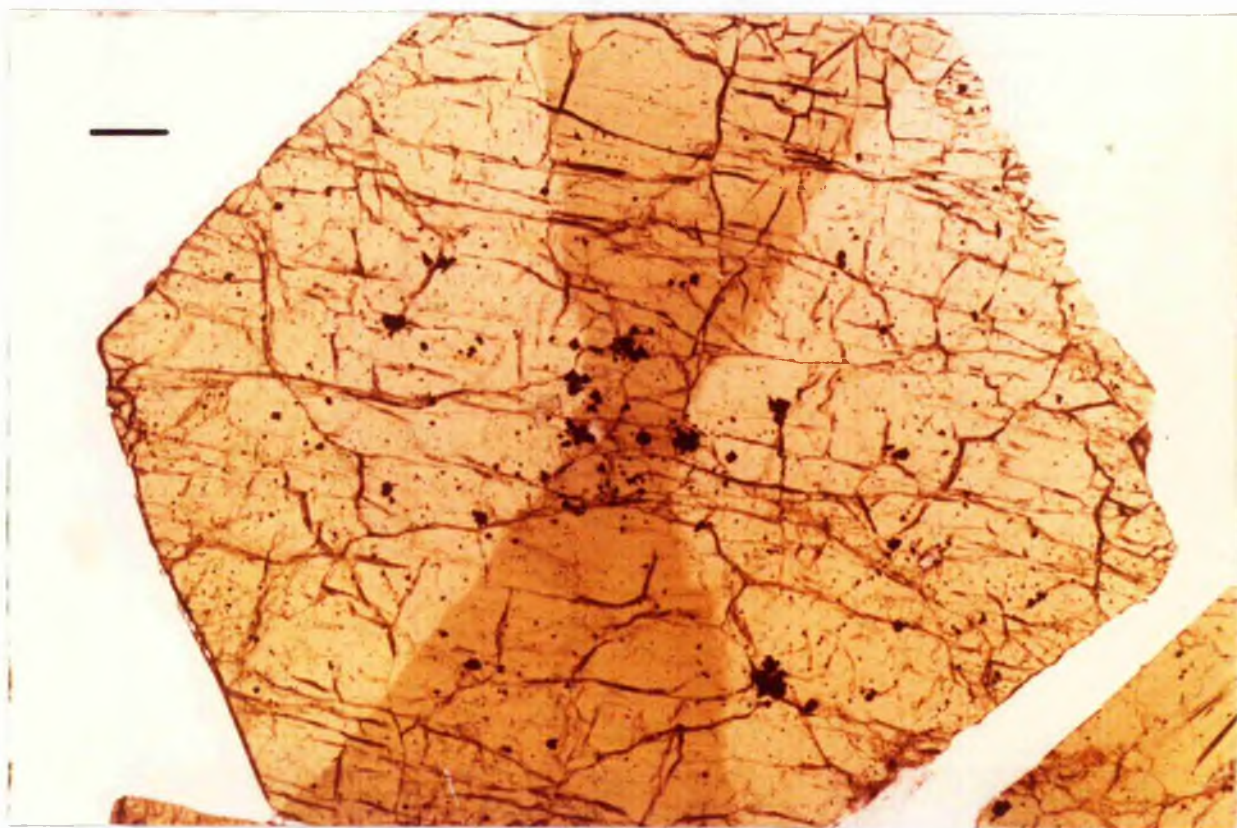


Plate 36: Sector-zoned pyroxene. The crystal has been cut perpendicular to $\{100\}$. The dark-green colouration corresponds to the Ti and Al rich $\{010\}$ sectors, whilst the pale-green corresponds to the Si and Mg rich sectors of the $\{\bar{1}11\}$ zone. Scale-bar is 1 mm. Photograph of polished thin section.



Plate 37: Sector-zoned pyroxene. Simple-twinned crystal cut perpendicular to $\{010\}$. Curvature of the faces is apparent in the lower part of the crystal and is reflected in the curved boundary between the $\{100\}$ (dark) and $\{\bar{1}11\}$ (light) sectors. In the upper part of the crystal there is no curvature and the boundary between sectors is straight. Scale-bar is 1 mm. Photograph of polished thin section.

Table 4. Sector-zoned pyroxene analyses (electron microprobe).

	Crystal 1		Crystal 2		Crystal 3		Crystal 4		
	{100}	{111}	{110}	{100}	{110}	{010}	{111}	{010}	{110}
SiO ₂	46.68	49.44	46.59	46.27	47.21	47.42	49.08	45.90	46.68
TiO ₂	1.50	0.92	1.26	1.50	1.25	1.36	0.98	1.54	1.35
Al ₂ O ₃	6.99	4.62	7.39	7.51	7.39	6.55	4.69	7.99	7.34
FeO*	7.80	6.48	7.66	7.93	7.88	7.44	6.54	8.18	7.86
MnO	0.15	0.16	0.07	0.16	0.12	0.12	0.20	0.19	N.D.
MgO	13.21	14.90	12.94	12.96	13.37	13.55	14.85	12.63	12.78
CaO	22.17	22.25	22.38	22.23	22.49	22.31	22.35	22.00	22.38
Total	98.50	98.77	98.29	98.56	99.71	98.75	98.69	98.43	98.39

Number of ions on the basis of 6 oxygens

Si	1.759	1.845	1.758	1.744	1.755	1.780	1.834	1.734	1.762
Al ^{iv}	0.241	0.155	0.242	0.256	0.245	0.220	0.166	0.266	0.238
Al ^{vi}	0.070	0.048	0.087	0.077	0.079	0.069	0.040	0.090	0.089
Ti	0.043	0.026	0.036	0.043	0.035	0.038	0.028	0.044	0.038
Fe ⁺³	0.086	0.055	0.083	0.094	0.095	0.074	0.071	0.088	0.072
Mg	0.742	0.829	0.728	0.728	0.741	0.758	0.827	0.711	0.719
Fe ⁺²	0.160	0.147	0.159	0.156	0.150	0.159	0.133	0.170	0.176
Mn	0.005	0.005	0.002	0.005	0.004	0.004	0.006	0.006	0.0
Ca	0.895	0.890	0.905	0.898	0.896	0.897	0.895	0.891	0.905
Mg	39.3	43.0	38.8	38.7	39.3	40.1	42.8	38.1	38.4
Fe**	13.3	10.8	13.0	13.6	13.2	12.5	10.9	14.1	13.3
Ca	47.4	46.2	48.2	47.7	47.5	47.4	46.3	47.8	48.3

* total iron as FeO

N.D. not detected

** (Fe⁺² + Fe⁺³ + Mn)

All specimens are salites from the Cat Cleuch Formation.

the concentric zones results in a curved boundary between the $\{100\}$ and $\{\bar{1}11\}$ sectors in the aforementioned acute angle, whilst the corresponding obtuse angle is normal and the boundary between the two sectors is straight. Within the $\{\bar{1}11\}$ sector there is a small curvature in the concentric zones in specimens with a concave $\{\bar{1}11\}$ edge. More commonly, however, there is no curvature in the concentric zones, but a line of dislocation runs close to the acute angle of the crystal across which there is a slight angular discordancy between concentric zones within the $\{\bar{1}11\}$ sector. The dislocation manifests itself on the crystal surface at the break of slope noted above.

The curvature of the boundary between the $\{100\}$ and $\{\bar{1}11\}$ sectors is well developed in simple-twinned crystals (see Plate 37) and closely resembles the feature described by Gray (1971) in sector-zoned pyroxenes from Quebec. Here, the curved boundary between sectors describes a perfect parabola and Gray (1971) suggests this reflects the different growth-controlling mechanisms of faces in different sectors. In the absence of a more detailed study of this feature in the pyroxenes of the Cat Cleuch Formation the interpretation of Gray (1971) is accepted.

7.3 AMPHIBOLES

The primary magmatic amphiboles occurring as phenocrysts and in xenoliths in the Bail Hill rocks are pargasites and ferroan pargasites in the classification of Leake (1979) (see Table 5). The Mg:Fe ratio shows considerable variation within individual crystals, among

Table 5. Pargasite and ferroan pargasite analyses (electron microprobe).

	1	2	3	4	5	6	7	8	9	10	11	12	13	14	15	16
SiO ₂	42.99	41.89	40.55	40.12	40.17	40.53	42.38	41.36	41.40	42.42	41.27	39.98	39.95	39.77	41.24	40.92
TiO ₂	0.56	1.63	1.88	1.66	2.24	1.61	1.15	1.33	2.74	2.51	2.39	1.50	1.39	1.40	1.53	2.74
Al ₂ O ₃	14.03	13.86	14.97	15.35	15.06	14.95	12.30	14.24	12.56	11.55	13.43	15.29	15.00	16.11	14.50	12.57
FeO*	8.02	8.11	8.46	9.72	8.96	10.27	12.00	12.41	12.45	13.40	11.89	12.90	12.88	12.90	9.56	13.51
MnO	0.24	0.10	0.08	0.18	N.D.	0.10	0.29	0.45	0.35	0.44	0.25	N.D.	0.29	0.28	N.D.	0.29
MgO	15.57	15.41	15.09	14.20	14.82	13.98	14.44	13.00	12.91	12.75	13.21	12.28	12.54	12.01	15.14	12.39
CaO	12.36	12.34	12.30	12.16	12.27	11.99	11.67	11.37	11.86	11.59	12.01	11.96	11.81	11.90	12.29	11.73
Na ₂ O	2.18	2.29	1.69	1.86	1.55	2.09	2.54	2.74	2.20	2.44	2.34	2.35	2.25	2.84	1.99	2.27
K ₂ O	0.75	1.16	1.44	1.23	1.45	1.07	0.63	0.69	0.98	0.91	0.97	0.96	0.97	0.91	0.87	0.82
Total	96.70	96.79	96.46	96.48	96.52	96.59	97.40	97.59	97.45	98.01	97.76	97.22	97.08	98.12	97.12	97.24

Number of ions on the basis of 23 oxygens

Si	6.242	6.130	5.939	5.904	5.888	5.977	6.229	6.114	6.153	6.295	6.092	5.935	5.931	5.878	5.993	6.115
Al ^{iv}	1.758	1.870	2.061	2.096	2.112	2.023	1.771	1.886	1.847	1.705	1.908	2.065	2.069	2.122	2.007	1.885
Al ^{vi}	0.643	0.521	0.523	0.566	0.490	0.576	0.361	0.596	0.354	0.316	0.430	0.611	0.556	0.685	0.478	0.329
Ti	0.061	0.179	0.207	0.184	0.247	0.179	0.127	0.148	0.306	0.280	0.265	0.168	0.155	0.156	0.167	0.308
Fe ⁺³	0.240	0.125	0.375	0.401	0.416	0.292	0.314	0.078	0.061	0.0	0.095	0.260	0.371	0.141	0.472	0.126
Mg	3.369	3.361	3.294	3.114	3.237	3.072	3.163	2.864	2.860	2.820	2.906	2.717	2.775	2.645	3.279	2.759
Fe ⁺²	0.734	0.868	0.661	0.795	0.682	0.975	1.161	1.456	1.487	1.663	1.373	1.342	1.228	1.454	0.690	1.563
Mn	0.030	0.012	0.010	0.022	0.0	0.013	0.036	0.056	0.044	0.055	0.031	0.0	0.037	0.035	0.0	0.037
Ca	1.923	1.935	1.930	1.917	1.927	1.895	1.838	1.801	1.889	1.843	1.900	1.903	1.879	1.885	1.914	1.878
Na	0.614	0.650	0.480	0.531	0.441	0.598	0.724	0.785	0.634	0.679	0.670	0.677	0.648	0.814	0.561	0.658
K	0.139	0.217	0.269	0.231	0.271	0.201	0.118	0.130	0.186	0.172	0.183	0.182	0.138	0.172	0.161	0.156

100Mg/(Mg+Fe⁺²)+Fe⁺³+Mn) 77.04 76.98 75.90 71.88 74.67 70.59 67.67 64.30 64.24 62.14 65.97 62.91 62.91 61.87 73.84 61.52

* total iron as FeO

N.D. Not detected

1. Average of 3 analyses in gabbroic xenolith (27/23). 2. Average of 5 analyses in gabbroic xenolith (27/5).
 3. Average of 9 analyses in basalt (16W). 4. & 5. Centre and edge of zoned crystal in basalt (16W).
 6. Average of 6 analyses in dioritic xenolith (27/X). 7. Average of 4 analyses in ultramafic xenolith (103/51).
 8. Average of 3 analyses in xenolith (27/19). 9. Average of 6 analyses in xenolith (103/7). 10. Single analysis, brown crystal in xenolith (103/7). 11. Single analysis, green crystal in xenolith (103/7). 12. Average of 3 analyses in dioritic xenolith (27/1). 13. Average of 13 analyses in hawaiite (27/2). 14. & 15. Centre and edge of zoned phenocryst in hawaiite (27/2). 16. Average of 8 analyses in dioritic xenolith (79/2).
- Analyses 1-7, pargasite; analyses 8-16, ferroan pargasite.

Table 6. Secondary amphibole in xenoliths (electron microprobe).

	1	2	3	4	5	6	7
SiO ₂	45.93	47.42	47.84	46.62	49.24	53.84	56.37
TiO ₂	0.90	1.51	1.30	0.75	0.82	0.29	0.31
Al ₂ O ₃	8.69	7.39	7.31	8.83	6.50	3.30	7.14
FeO*	10.30	9.53	9.53	8.10	7.31	5.04	4.11
MnO	0.33	0.21	0.25	0.21	0.27	0.19	N.D.
MgO	16.59	17.56	17.77	17.86	18.94	20.38	19.97
CaO	11.15	11.11	11.05	11.03	11.02	12.27	9.82
Na ₂ O	1.92	2.25	2.20	2.24	1.56	0.15	0.91
K ₂ O	0.61	0.46	0.23	N.D.	0.34	0.15	0.16
Total	96.42	97.44	97.50	95.64	96.00	95.61	98.79

Number of ions on the basis of 23 oxygens

Si	6.727	6.865	6.904	6.791	7.109	7.630	7.603
Al ^{iv}	1.273	1.135	1.096	1.209	0.891	0.370	0.397
Al ^{vi}	0.227	0.126	0.148	0.307	0.215	0.181	0.738
Ti	0.099	0.164	0.141	0.082	0.089	0.031	0.031
Fe ⁺³	0.188	0.0	0.003	0.106	0.0	0.058	0.0
Mg	3.621	3.789	3.822	3.877	4.075	4.304	4.014
Fe ⁺²	1.073	1.154	1.148	0.881	0.883	0.539	0.464
Mn	0.041	0.026	0.031	0.026	0.033	0.023	0.0
Ca	1.750	1.723	1.709	1.722	1.705	1.863	1.419
Na	0.545	0.614	0.621	0.633	0.436	0.041	0.238
K	0.114	0.085	0.042	0.0	0.063	0.027	0.028
100Mg/(Mg+Fe ⁺² +Fe ⁺³ +Mn)	73.55	76.29	76.38	79.29	81.65	87.41	89.64

* total iron as FeO N.D. not detected

1. Single analysis of amphibole rim to chlorite clusters in ultramafic xenolith (103/51). 2. Single analysis of amphibole replacing pyroxene in ultramafic xenolith (103/51). 3. Average of 5 analyses in ultramafic xenolith (103/51). 4. Single analysis of amphibole replacing pyroxene in ultramafic xenolith (103/70). 5. Single analysis of amphibole rim to chlorite cluster in ultramafic xenolith (103/70). 6. Average of 6 analyses in gabbroic xenolith (27/8). 7. Single analysis in gabbroic xenolith (27/1/1).

Analyses 1-4, Edenite; 5, Magnesio-hornblende; 6 & 7, Actinolite.

crystals and between xenoliths and/or lavas, suggesting crystallisation took place over a range of physicochemical conditions.

Crystal colour is related to the total iron content. Those containing over 12% total iron (as FeO) are brown or olive-green in colour and are pleochroic to straw yellow or pale olive-green, respectively. Those with under 12% total iron are green or yellow-green and are pleochroic to pale-green. Crystals commonly show a decrease in the Mg:Fe ratio from core to margin, although this is only occasionally visible as a colour-change within the crystal itself. Sharp colour discontinuities from dark-green interiors to pale-green margins were also observed, across which there is a marked increase in the Mg:Fe ratio.

The phenocrysts (Table 5, analyses 3-5, 13-15) have compositions overlapping those of the xenolith amphiboles, suggesting that the former are extrusive equivalents of the latter.

When compared with analyses in Deer et.al. (1963) the Bail Hill pargasites have above-average concentrations of TiO_2 (1.77% in the Bail Hill rocks, against 0.58% for analyses in Deer et.al., 1963), although they are still well below the TiO_2 concentration of kaersutites (average 6.7% for analyses in Deer et.al. (1963)). The substitution of Si by Al is close to the theoretical maximum limit of .2 Al per formula unit (Deer et.al., 1963). The Ca-content of Bail Hill primary amphiboles is close to or within the value of 1.8 ± 0.1 Ca atoms per formula unit, within which

the majority of analyses presented in Deer et.al. (1963) fall. The sub-silicic character, high Ti and Fe^{3+} suggest relatively high temperature crystallisation (Deer et.al., 1963; Lewis, 1973).

Pargasite is known to be incompatible with free silica (Boyd, 1956; Deer et.al., 1963) and the sub-silicic, feldspathoid-normative nature of the Bail Hill crystals is in agreement with this. The widespread occurrence of pargasitic amphibole in the Bail Hill Volcanic Group reinforces the conclusion that the parental magma of the extrusives and intrusives was undersaturated with respect to silica, i.e. alkaline in character.

Secondary amphiboles replacing pyroxenes in gabbroic and ultramafic xenoliths include edenites, magnesio-hornblendes and actinolites in the classification of Leake (1979) (see Table 6). The main difference between the primary and secondary amphiboles is that pargasite is sub-silicic and aluminous, whilst the secondary amphiboles are silicic and sub-aluminous. The variation in the composition of the secondary amphiboles may be due to variation in the composition of the original pyroxene and/or hydrothermal fluids from which the material crystallised (see Chapter 9), or it may reflect non-equilibration of the amphiboles due to their transportation and extrusion at the surface. The nature and association of the secondary amphiboles is consistent with an origin by hydrothermal alteration (Deer et.al., 1963) (see Chapter 9).

Table 7. Biotite and chlorite analyses (electron microprobe).

	1	2	3	4	5	6	7	8	9
SiO ₂	33.58	35.28	29.32	29.45	30.28	29.74	29.44	28.65	27.99
TiO ₂	3.74	5.40	N.D.						
Al ₂ O ₃	16.12	15.88	18.92	17.00	17.06	16.08	18.31	11.82	11.75
FeO*	18.80	13.72	9.75	13.16	13.21	13.97	11.10	27.21	28.37
MnO	1.18	0.20	0.85	0.30	0.33	0.35	0.28	N.D.	0.27
MgO	11.95	15.63	25.14	24.31	24.98	23.75	25.75	19.52	18.38
Na ₂ O	0.24	0.92	N.D.						
K ₂ O	7.69	7.17	N.D.						
Total	92.20	94.00	83.13	83.92	85.53	83.54	84.60	87.20	86.49
Si	5.241	5.274	5.930	6.043	6.087	6.155	5.924	6.168	6.118
Al ^{iv}	2.759	2.726	2.070	1.957	1.913	1.845	2.076	1.832	1.882
Al ^{vi}	0.207	0.073	2.442	2.156	2.130	2.078	2.267	1.168	1.145
Ti	0.439	0.607	0.0	0.0	0.0	0.0	0.0	0.0	0.0
Fe ²⁺	2.454	1.715	1.649	2.258	2.221	2.418	1.868	4.900	5.186
Mn	0.156	0.253	0.146	0.052	0.056	0.061	0.048	0.0	0.050
Mg	2.780	3.482	7.578	7.434	7.484	7.326	7.722	6.263	5.987
Na	0.073	0.267	0.0	0.0	0.0	0.0	0.0	0.0	0.0
K	1.531	1.367	0.0	0.0	0.0	0.0	0.0	0.0	0.0

* total iron as FeO

N.D. not detected

Analysis 1, Biotite, average of 5 analyses from dioritic xenolith (27/1);
 analysis 2, phlogopite, average of 3 analyses from dioritic xenolith (103/7);
 analysis 3, clinocllore, average of 4 analyses in gabbroic xenolith (27/8);
 analyses 4-9, chlorites in ultramafic xenolith (103/70).
 4, 5 & 7, clinocllore; 6, 8 & 9, pycnochlorite.

7.4 PRIMARY MICAS AND SECONDARY CHLORITES

Primary micas of magmatic origin include Mg-rich biotites (Table 7, analysis 1) and phlogopites (Table 7, analysis 2). When compared with analyses in Deer et.al. (1963) both Bail Hill analyses have below average SiO_2 and K_2O , and above average TiO_2 concentrations. The K_2O deficiency may be due to secondary processes as many apparently pristine micas gave low totals on the electron microprobe, with partial or complete loss of K_2O being the most noticeable feature. Analysis 1 is also characterised by an above average MnO concentration, a feature reflected in pyroxenes from the same xenolith (Table 3, analysis 16).

No analyses of phenocryst biotite/phlogopites were obtained because of the unsuitability of the material for microprobe studies. The phenocrysts are, however, optically similar to the xenolith biotites and contain pods of prehnite along the cleavage, a feature believed to be formed at depth (see Section 7.8 and Chapter 9). It is inferred from this that the phenocrysts are of cumulate origin and are compositionally similar to the xenolithic micas (i.e. Mg-rich biotites and phlogopites). Deer et.al. (1963) indicate that these are the typical varieties found in basic and intermediate lavas.

The chlorites replacing clinopyroxene in the gabbroic and ultramafic xenoliths (Table 7, analyses 3-9) show considerable variation in the Mg:Fe ratio. This is reflected in crystal colour, with high Mg:Fe corresponding to weakly pleochroic pale-green crystals, whilst low

Mg:Fe ratios correspond to dark-green and brown varieties, pleochroic to pale-green. Such variations can occur within a single crystal, with bands of strongly coloured Fe-rich material lying parallel to the cleavage-trace in otherwise pale-green crystals. The chlorites display anomalous purple and grey interference colours.

Chlorites are common products of hydrothermal alteration of magmatic pyroxenes (Deer et.al., 1963), a paragenesis similar to that envisaged for the Bail Hill chlorites (see Chapter 9). Their characteristic association with actinolitic amphibole at Bail Hill is well-documented from elsewhere (Winkler, 1976; Coleman, 1977).

7.5 FELDSPARS

Primary alkali feldspars are not found in the Bail Hill rocks. Plagioclase feldspar is very common and varies from bytownite to albite in composition. Secondary albitisation has not taken place and the composition of the plagioclase is therefore believed to be that of the original rocks. With the exception of crystals in the gabbroic xenoliths the feldspars are all zoned, with both simple and concentric varieties present.

The gabbroic xenoliths contain bytownite (An_{70} - An_{80}) which has partially altered to white mica. Pristine material is found between the micaceous alteration patches (see Table 8, analyses 1-4). In one specimen (BCC27/8) the gabbro is veined by feldspar of andesine composition (Table 8, analysis 5), although the host feldspar is calcic bytownite (Table 8, analysis 1). In another specimen

Table 8. Plagioclase feldspar analyses (electron microprobe).

	1	2	3	4	5	6	7	8	9	10	11	12	13	14	15	16
SiO ₂	48.03	48.76	50.35	54.66	57.25	58.49	61.58	64.45	67.51	49.93	48.17	51.09	48.23	48.33	60.68	64.44
TiO ₂	N.D.	N.D.	0.03	0.12	0.25	0.21	0.14	0.24	N.D.	0.19						
Al ₂ O ₃	32.51	32.32	31.45	28.21	26.83	26.15	24.67	21.22	20.21	30.79	32.30	30.01	32.31	32.19	24.41	17.99
FeO*	0.19	0.24	0.21	0.28	0.11	0.33	0.13	N.D.	N.D.	1.13	0.93	1.22	0.95	0.95	0.15	0.21
CaO	15.97	15.89	14.58	10.09	8.48	7.35	5.57	2.41	0.83	14.65	16.24	13.45	15.79	15.94	6.38	N.D.
Na ₂ O	2.54	2.14	3.37	5.42	6.25	7.00	7.47	9.06	11.34	2.40	1.81	3.57	2.19	1.79	7.91	N.D.
F ₂ O	N.D.	N.D.	0.05	0.23	0.38	0.40	0.56	1.09	N.D.	0.38	0.11	0.40	0.24	0.25	0.18	16.01
Total	99.24	99.35	100.04	99.01	99.55	99.93	100.12	98.47	99.99	99.28	99.56	99.74	99.71	99.45	99.71	98.84

Number of ions on the basis of 32 oxygens

Si	8.870	8.969	9.183	9.948	10.304	10.472	10.907	11.532	11.828	9.208	8.886	9.374	8.891	8.921	10.831	12.034
Al	7.078	7.008	6.762	6.053	5.693	5.520	5.151	4.476	4.175	6.694	7.025	6.492	7.022	7.005	5.137	3.961
Ti	0.0	0.0	0.004	0.016	0.034	0.028	0.019	0.032	0.0	0.0	0.0	0.0	0.0	0.0	0.0	0.027
Fe ⁺²	0.029	0.037	0.032	0.043	0.017	0.049	0.019	0.0	0.0	0.174	0.144	0.187	0.147	0.147	0.022	0.033
Na	0.910	0.763	1.192	1.913	2.181	2.430	2.565	3.143	3.852	0.858	0.647	1.270	0.783	0.641	2.738	0.0
Ca	3.160	3.132	2.849	1.968	1.635	1.410	1.057	0.462	0.156	2.895	3.210	2.644	3.119	3.153	1.220	0.0
K	0.0	0.0	0.012	0.053	0.087	0.091	0.127	0.249	0.0	0.089	0.026	0.094	0.056	0.059	0.041	3.815
Ab	22.3	19.6	29.4	48.6	55.9	61.8	68.4	81.6	96.1	22.3	16.7	31.7	19.8	16.7	30.5	0.0
MoI. % An	77.7	80.4	70.3	50.0	41.9	35.9	28.2	12.0	3.9	75.4	82.7	66.0	78.8	81.8	68.5	0.0
Or	0.0	0.0	0.3	1.4	2.2	2.3	3.4	6.4	0.0	2.3	0.6	2.3	1.4	1.5	1.0	100.0

* total iron as FeO N.D. not detected

1. Average of 2 analyses in gabbroic xenolith (27/8). 2. Average of 3 analyses in gabbroic xenolith (27/1/1). 3. Average of 4 analyses in gabbroic xenolith (27/4). 4. Single analysis from gabbroic xenolith (27/5). 5. Single analysis for vein mineral in gabbroic xenolith (27/8). 6. & 7. Centre and edge of zoned crystal in dioritic xenolith (27/1). 8. & 9. Single analyses from dioritic xenolith (27/12). 10, 11. & 12. Traverse, centre to edge in zoned phenocryst in basalt (145C). 13. & 14. Centre and edge of zoned phenocryst in basalt (111). 15. Single analysis in hawaiite (27/2). 16. Partial analysis of adularia feldspar in basalt (24). (Barium not included).

Analyses 1-3, 10, 11, 13-15, bytownite; analyses 4, 12, labradorite; analyses 5 & 6, andesine; analyses 7 & 8, oligoclase; analysis 9, albite; analysis 16, adularia.

(BCC27/3) some of the feldspar is pseudomorphed by prehnite (see Section 7.8).

Dioritic xenoliths contain feldspar varying in composition from albite to andesine (see Table 8, analyses 6-9). Often a single crystal is zoned from an andesine core to an albite rim. Concentric zoning was also observed. In some dioritic xenoliths feldspar is occasionally pseudomorphed by prehnite (see Section 7.8), although more typically it has partially altered to white mica.

The feldspars of the Cat Cleuch Formation and the petrographically identical Penfrau Member are strongly zoned labradorites and bytownites (see Table 8, analyses 10-14), although the basal lavas in the Cat Cleuch contain transitional andesine/labradorite feldspars. Simple zoning is subordinate to concentric zoning.

Some of the feldspars in the vicinity of the Cat Cleuch have altered from labradorite/bytownite to alkali feldspar. In view of the secondary nature of the feldspar and its close association with zeolites in the same rocks (see Section 7.7) it has been interpreted as adularia, a variety known to have this association and paragenesis (Coombs et.al., 1959; Deer et.al., 1963). Analytical totals for this material are generally low, but exclude barium which is often present in adularia in significant quantities (Deer et.al., 1963) and is present in anomalously high concentrations in the Cat Cleuch rocks (see Section 8.3.11). In thin section the adularia feldspars are dusty brown and although untwinned retain "ghosts" of albite twins. Optically similar material was observed

in phenocrysts of the Peat Rig Formation, although the material was unsuitable for microprobe analysis. An analysis from the Cat Cleuch Formation is given in Table 8 (analysis 16). This specimen has an unusually high analytical total, although the low calcium and sodium values (below detection limits) and the high potassium concentration are fairly typical of other specimens from the same lithology.

The lava matrix of the Bught Craig Member (Table 8, analysis 15) contains simple and concentrically zoned feldspars of oligoclase and andesine composition.

The feldspars of the Peat Rig Formation and the Grain Burn Member have been identified optically. Their cloudy, turbid appearance is reminiscent of the adularia feldspars in the Cat Cleuch Formation (see above), although they also show alteration to carbonate material. Where material was fresh enough to allow identification by optical techniques crystals of oligoclase and andesine composition were observed. Petrographically similar rocks in three of the outlying tuff members contain pristine oligoclase/andesine feldspars displaying simple and concentric zoning.

No pseudomorphs of prehnite or albite after calcic plagioclase were observed in the extrusive rocks, suggesting a lack of alteration due to very low grade (zeolite facies) metamorphism (see Section 7.7 and Chapter 8).

7.6 APATITES

Partial analyses of apatites (Table 10) indicate that the apatites in the "apatite rock" are similar to

varieties found in the lavas and xenoliths. The low analytical totals are due to the absence of fluorine from the analyses. The presence of this element in the apatites from Bail Hill has been substantiated by Kennedy (1936).

Fluor-apatite is the typical variety found in igneous rocks (Deer et.al., 1963). Its presence as inclusions in ferromagnesian minerals in the extrusive rocks implies a primary magmatic origin and the secondary origin proposed by Kennedy (1936) is rejected. The "apatite rock" itself is very similar to accumulations of igneous origin described by Philpotts (1967) and believed by him to be typical of crystallisation from alkaline magmas.

7.7 ZEOLITES

Zeolites were observed as amygdale and vein minerals in the extrusive rocks, often with associated calcite, analcite and clinzoisite.

The analysis presented (Table 9, analysis 1) is of thomsonite, which occurs as radiating bladed crystals in amygdales in the basalts of the Cat Cleuch Formation. This crystal form is characteristic of thomsonites with low silica contents (Wise and Tschernich, 1978) and the Bail Hill analysis is very similar to analyses presented by Wise and Tschernich (1978) for similar bladed crystals.

The silica content of zeolites is related to the silica content of the system from which they crystallised and both thomsonite and analcite are characteristically found in silica-undersaturated rocks (Deer et.al., 1963). The Bail Hill rocks are undersaturated with silica

and nepheline-normative, in agreement with this association (see Section 8.4).

There is no equivocal evidence to substantiate whether the zeolites were formed by hydrothermal alteration soon after extrusion of the volcanic rocks by volcanically-related fluids, or by burial metamorphism long after the volcanic pile had cooled and consolidated (Coombs et. al., 1959). On balance, the former alternative is preferred as evidence elsewhere suggests that circulation of hydrothermal fluids was contemporaneous with igneous activity (see Chapter 9).

7.8 PREHNITE

Prehnite is typically found in one of two associations in the gabbroic and dioritic xenoliths. The first is as lenses lying along the cleavage trace in biotite/phlogopite crystals (see Table 9, analyses 3, 5, 6). Contacts are sharp and in many instances the biotite cleavage is seen to bow round the prehnite outline. The second association is as pseudomorphs after plagioclase feldspar (see Table 9, analyses 2 and 4). Both of these associations have been described elsewhere in the literature, although to the present author's knowledge this is the first recorded occurrence of the two associations in the same rock.

Prehnite is found in biotite/phlogopite phenocrysts within the volcanic rocks but not within the groundmass of these rocks. Its presence in these micas is believed to be inherited from the plutonic environment in

which they crystallised.

Deer et.al. (1963) note the replacement of plagioclase by prehnite, whilst the biotite-prehnite association has been noted by Hall (1966), Moore (1976), Phillips and Rickwood (1977) and Tulloch (1979). Early reports suggested the prehnite was primary and of magmatic origin (Wells and Bishop, 1955), but recent experimental work on its stability field precludes this possibility (Liou, 1971) and it is widely regarded as a secondary "metamorphic" mineral.

The biotite-prehnite association is typically confined to rocks of dioritic nature (Wells and Bishop, 1955; Hall, 1965; Moore, 1976; Phillips and Rickwood, 1977; Tulloch, 1979). The petrography of the rocks in the examples cited is very similar to those of Bail Hill, typically consisting of biotite, plagioclase feldspar (commonly sericitised), amphibole, apatite and iron-titanium oxides. Recent reports conclude that the prehnite is formed by "deuteric alteration" involving plagioclase feldspar and biotite and/or amphibole (Moore, 1976; Phillips and Rickwood, 1977; Tulloch, 1979), in agreement with the origin by hydrothermal alteration proposed for the Bail Hill prehnites (see Chapter 9). From the similarity in the composition of the prehnites from the two associations (see Table 9 and compare analyses 2 and 3, 4 and 5) there is little doubt that they originated in a similar manner.

Deer et.al. (1963) indicate that the composition of prehnite is fairly constant and although analyses 2-6

Table 9. Zeolite and prehnite analyses (electron microprobe).

	1	2	3	4	5	6
SiO ₂	36.24	43.14	43.17	43.15	43.71	43.15
TiO ₂	N.D.	0.14	0.23	N.D.	0.12	N.D.
Al ₂ O ₃	30.29	22.00	23.14	25.10	23.44	23.10
FeO*	N.D.	3.23	1.89	N.D.	1.15	N.D.
MgO	N.D.	0.29	0.18	N.D.	N.D.	N.D.
CaO	11.35	26.71	26.58	26.90	26.59	26.90
Na ₂ O	3.23	N.D.	N.D.	N.D.	N.D.	N.D.
Total	81.24	95.51	95.19	95.15	95.01	95.15
Si	10.243	6.039	6.014	5.951	6.067	5.951
Ti	0.0	0.015	0.024	0.0	0.013	0.0
Al	10.093	3.631	3.800	4.081	3.836	4.081
Fe ⁺²	0.0	0.378	0.220	0.0	0.134	0.0
Mg	0.0	0.061	0.037	0.0	0.0	0.0
Ca	3.438	4.007	3.967	3.976	3.955	3.975
Na	1.770	0.0	0.0	0.0	0.0	0.0

* total iron as FeO

N.D. not detected

1. Thomsonite. Average of 2 analyses in amygdales in basalt (17) (Includes 0.05 MnO, 0.08 S). 2. Analysis of prehnite pseudomorphing plagioclase in dioritic xenolith (27/1). 3. Average of 3 analyses of prehnite along biotite cleavage in dioritic xenolith (27/1). 4. Analysis of prehnite pseudomorphing plagioclase in dioritic xenolith (27/X). 5. Analysis of prehnite along biotite cleavage in dioritic xenolith (27/X). 6. Analysis of prehnite along biotite cleavage in dioritic xenolith (27/5).

Analysis 1. Number of ions on the basis of 40 oxygens.

Analyses 2-6. Number of ions on the basis of 22 oxygens.

Table 10. Partial analyses of apatites
(electron microprobe).

	1	2	3	4
SiO ₂	0.19	0.38	0.37	N.D.
TiO ₂	0.18	N.D.	N.D.	N.D.
FeO*	N.D.	0.10	N.D.	0.38
MgO	0.26	0.12	0.28	N.D.
CaO	53.36	52.77	53.91	52.98
Na ₂ O	0.36	N.D.	N.D.	N.D.
P ₂ O ₅	40.15	39.93	40.94	40.09
Cl	0.34	0.11	0.47	0.93
Total	94.84	93.62	95.97	94.38

* total iron as FeO N.D. not detected

Analysis 1, average of 2 analyses from "apatite-rock" (Kennedy, 1936); analysis 2, average of 2 analyses in dioritic xenolith (27/1) (includes NiO 0.21); analysis 3, phenocryst in hawaiite lava (27/2); analysis 4, crystal in dioritic xenolith (103/7).

show minor differences from those presented in Deer et.al. (1963) (notably in Al and total iron concentrations), this is not thought to be significant. The Bail Hill analyses are very similar to electron microprobe analyses given by Tulloch (1979) for prehnites associated with biotites in dioritic rocks.

7.9 CONCLUSIONS

From the foregoing discussions and from the data presented in Tables 3-10 three main conclusions can be made :-

1. There is a genetic relationship between the coarse-grained xenoliths and the volcanic rocks. The gabbroic and ultramafic rocks contain the direct antecedents of the pyroxenes found as phenocrysts in the volcanics. The pargastic amphiboles, plagioclase feldspars and apatites show compositional overlap between xenolith and phenocryst varieties. The primary micas in the volcanic rocks are optically identical to Mg-rich biotites and phlogopites found in the xenoliths. From this, it is inferred that all the phenocrysts, with the exception of clinopyroxenes and plagioclase feldspars in the Cat Cleuch Formation which show signs of disequilibrium growth, are of cumulate origin and that the coarse-grained xenoliths are cognate.

2. The magma from which the xenoliths and volcanic rocks crystallised was undersaturated with respect to silica (i.e. alkaline in character). The evidence for this includes the nature and association of the xenolith

pyroxenes, the trend of xenolith and phenocryst pyroxenes on the pyroxene quadrilateral, the nature of the sector-zoning in the pyroxenes of the Cat Cleuch Formation, the pargasitic nature of the primary amphiboles and the sub-silicic character of the primary micas and secondary zeolites.

3. Alteration products in the xenoliths (amphiboles, chlorites and prehnite) show characteristics and associations compatible with an origin by hydrothermal activity. Alteration products in the extrusive rocks (zeolites, adularia) may be contemporaneous with the volcanism or related to subsequent burial metamorphism. The former alternative is preferred in view of the hydrothermal association present in the coarse-grained rocks.

CHAPTER 8 : GEOCHEMISTRY8.1 INTRODUCTION

Major and trace-element concentrations of 39 whole-rock samples are considered (see Tables 11-15) together with major-element concentrations of 6 ground-mass analyses (see Table 16). The 39 whole-rock analyses include 5 coarse-grained xenoliths of cognate origin. The remaining samples are classified according to their silica content.

Grid sampling was not feasible because of intermittent and weathered exposures. Preference was given to samples with relatively pristine mineralogies. The following samples were collected: 6 from the Cat Cleuch Formation, 1 from the Grain Burn Member, 12 from the Peat Rig Formation, 6 from the Bught Craig Member, 3 from shallow undifferentiated intrusions and 6 from outlying tuff members. In addition, the 5 coarse-grained xenoliths were taken from the Bught Craig Member (3) and the Peat Rig Formation (2). An analysis of a syenitic xenolith given by Mrs. Eyles is also presented in Table 11.

An account of the analytical techniques, accuracy and precision of data and sample localities is given in Appendices 4-6.

Table 11 Chemical compositions (oxides, wt %) and trace-element abundances (ppm) of xenoliths from the Bail Hill Volcanic Group.

	1	2	3	4	5	6
SiO ₂	34.18	46.49	49.15	50.73	53.79	60.19
TiO ₂	0.30	0.09	0.19	0.90	0.43	0.06
Al ₂ O ₃	11.74	27.15	21.98	18.39	22.16	19.94
Fe ₂ O ₃	3.09	0.58	0.66	0.04	1.79	0.52
FeO	6.92	1.57	1.90	4.74	4.04	0.68
MnO	0.27	0.12	0.16	0.17	0.13	0.05
MgO	12.80	4.93	6.70	6.46	2.82	0.60
CaO	17.21	5.92	8.62	6.45	5.70	3.22
Na ₂ O	0.63	1.56	2.25	3.67	6.74	9.08
K ₂ O	0.12	5.66	3.97	2.54	0.44	0.35
P ₂ O ₅	0.03	0.02	0.02	0.21	0.56	0.21
H ₂ O	5.24	3.62	2.58	3.82	3.38	1.45
LOI	6.15	1.25	0.26	1.29	1.87	1.43
Total*	87.29	94.09	95.86	94.30	95.23	97.49
Li	21	72	30	44	55	
Cr	2070	345	345	230	11	
Ni	744	190	183	194	27	
Rb	2	53	62	31	N.D.	
Sr	374	2783	1583	4220	2883	
Y	10	16	N.D.	19	17	
Zr	46	147	61	88	100	
Ba	5075	2070	3290	2435	6900	

* excluding H₂O and LOI

1. Ultramafic xenolith (103/70). 2. Gabbroic xenolith (30/2).
 3. Gabbroic xenolith (27/3). 4. Gabbroic xenolith (103/2).
 5. Dioritic xenolith (M9). 6. Soda syenite (Eyles, 1932; includes SrO 0.32, BaO 2.27).

Analyses 1 & 4, from Peat Rig Formation.
 Analyses 2, 3 & 5, from Bught Craig Member.

Table 12. Chemical compositions (oxides, wt %) and trace-element abundances (ppm) of basalts from the Bail Hill Volcanic Group.

	1	2	3	4	5	6	7
SiO ₂	43.81	44.19	44.84	45.44	43.04	44.96	46.96
TiO ₂	1.00	0.91	0.97	0.91	0.89	0.95	0.90
Al ₂ O ₃	14.65	16.78	17.20	16.51	16.95	17.81	15.85
Fe ₂ O ₃	1.84	0.48	2.67	4.74	2.22	3.89	0.69
FeO	5.67	6.56	4.83	2.57	4.81	3.97	5.79
MnO	0.17	0.17	0.17	0.13	0.22	0.13	0.13
MgO	9.01	6.24	6.33	5.07	5.46	5.14	5.34
CaO	12.57	10.57	9.34	13.36	9.38	10.96	13.29
Na ₂ O	1.78	3.09	3.74	3.33	2.59	2.59	2.10
K ₂ O	2.49	1.95	2.29	1.02	3.73	2.14	0.63
P ₂ O ₅	1.07	0.57	0.66	0.49	0.84	0.89	0.53
H ₂ O	3.62	4.68	4.90	3.06	3.64	2.66	2.44
LOI	2.57	3.23	1.80	2.18	4.67	3.39	4.51
Total*	94.06	91.81	93.04	96.63	94.80	93.43	92.21
Li	55	30	49	20	69	28	36
Cr	65	22	7	21	14	7	18
Ni	53	26	35	30	22	39	31
Rb	36	19	31	11	62	22	2
Sr	1184	1836	1577	2854	1526	2700	1892
Y	28	26	24	20	24	20	14
Zr	168	93	139	100	158	186	129
Ba	2385	1925	2470	2020	1800	1670	800

* excluding H₂O and LOI

1. Basalt (16W). 2. Basalt (17). 3. Basalt (26).
 4. Basalt (33). 5. Basalt (63/2). 6. Basalt (GBC111).
 7. Basalt (145C).

Analyses 1-6, from Cat Cleuch Formation.
 Analysis 7, lava clast in Penfrau Member.

Table 13. Chemical compositions (oxides, wt %) and trace element abundances (ppm) of intermediate lavas from the Bail Hill Volcanic Group.

	1	2	3	4	5	6	7	8	9	10	11	12	13	14
SiO ₂	45.13	48.95	48.67	48.25	49.51	49.92	47.99	49.09	49.59	50.44	50.44	51.02	52.10	56.44
TiO ₂	1.00	0.65	0.64	0.68	0.60	0.61	0.61	0.67	0.60	0.67	0.57	0.67	0.46	0.52
Al ₂ O ₃	18.35	17.90	18.54	17.44	18.01	17.72	18.00	16.47	18.14	17.87	20.24	19.84	19.04	18.56
Fe ₂ O ₃	3.24	0.13	0.27	0.55	0.79	1.70	2.95	1.28	1.50	0.36	2.84	2.17	0.61	1.65
FeO	6.34	5.25	5.09	5.41	5.08	4.02	3.35	4.81	4.47	5.73	2.77	3.78	4.73	1.87
MnO	0.14	0.15	0.13	0.15	0.16	0.18	0.13	0.24	0.16	0.18	0.13	0.12	0.17	0.09
MgO	7.21	5.08	4.48	5.09	4.10	4.14	3.56	4.71	4.11	3.94	4.08	4.47	4.47	3.97
CaO	6.24	7.67	9.63	6.48	7.30	8.41	7.80	8.93	7.36	6.55	6.62	5.97	4.54	3.85
Na ₂ O	2.80	3.99	4.38	5.46	4.73	5.05	4.12	4.49	4.90	4.49	5.42	5.91	5.33	7.92
K ₂ O	0.81	2.77	1.04	2.65	1.79	1.38	3.07	1.95	1.81	2.71	1.63	1.56	2.04	2.55
P ₂ O ₅	0.79	0.98	0.96	1.05	0.87	0.87	1.05	0.85	0.88	0.84	0.61	0.65	0.64	0.75
H ₂ O	4.44	3.86	4.34	3.48	3.76	3.84	2.70	3.12	4.16	3.32	2.48	2.64	3.48	2.06
LOI	3.08	3.05	1.12	1.18	1.54	2.10	4.25	3.05	0.46	1.29	0.96	0.47	0.22	0.21
Total*	92.03	93.52	93.83	93.21	92.94	94.00	92.63	93.42	93.52	93.78	95.35	96.16	94.13	98.17
Li	76	34	31	33	18	9	26	12	119	21	25	35	70	30
Cr	33	35	40	29	50	54	14	65	14	14	35	38	17	25
Ni	41	38	40	26	40	58	39	52	30	22	43	35	30	48
Rb	12	37	38	31	24	3	49	15	13	35	10	12	25	114
Sr	2411	1837	1911	2435	1671	1584	3922	1990	1290	2223	1088	4439	3253	2608
Y	14	29	19	24	21	21	30	18	32	27	31	23	22	30
Zr	91	127	159	191	163	148	126	153	225	129	135	206	114	116
Ba	1475	3290	1176	3550	3000	2140	2860	4000	3310	3805	1960	2400	2800	870

* excluding H₂O and LOI

1. (?) Basalt (GB60). 2.-8. Hawaiites/mugearites (GB 103/20, 21, 30, 40, 50, 6R, 71). 9. Hawaiiite/mugearite (MRD 102).
 10. Hawaiiite/mugearite (LK 114). 11. Hawaiiite/mugearite (BCC 28/1). 12. Hawaiiite/mugearite (27/2).
 13. Hawaiiite/mugearite (BHC 146). 14. Hawaiiite/mugearite (BCC32).

Analyses 1-8, 10, 13 & 14 from Peat Rig Formation; analysis 9 from Grain Burn Member; analyses 11 & 12 from Bught Craig Member.

Table 14. Chemical compositions (oxides, wt %) and trace element abundances (ppm) of pyroclastic rocks from the Bail Hill Volcanic Group.

	1	2	3	4	5	6	7	8	9	10
SiO ₂	42.26	44.10	49.42	50.45	52.03	37.65	46.99	49.03	49.50	48.33
TiO ₂	0.98	1.03	0.90	1.08	0.76	0.87	0.84	0.44	0.62	0.28
Al ₂ O ₃	17.32	16.74	18.17	18.49	18.01	16.97	18.16	20.50	19.51	19.47
Fe ₂ O ₃	0.34	1.38	0.85	0.67	1.71	N.D.	0.24	-	-	0.64
FeO	6.49	5.73	5.71	7.00	5.38	7.97	7.60	5.98	7.09	5.95
MnO	0.14	0.14	0.16	0.14	0.12	0.17	0.12	0.13	0.11	0.08
MgO	5.72	7.00	4.97	4.16	4.06	2.44	5.42	3.33	6.05	6.59
CaO	12.38	9.37	7.58	6.80	5.17	15.13	7.44	4.90	2.92	3.23
Na ₂ O	1.63	4.03	5.29	5.15	5.98	1.29	3.42	4.84	5.28	5.18
K ₂ O	1.27	1.54	0.39	1.41	0.65	0.89	0.57	2.04	1.73	1.20
P ₂ O ₅	0.71	0.75	0.69	0.66	0.75	1.06	0.86	0.59	0.84	0.62
H ₂ O	4.46	6.00	4.26	3.40	2.92	5.56	4.60	2.98	3.38	3.54
LOI	6.75	2.58	0.75	2.50	1.39	12.92	5.20	-	-	-
Total*	89.24	96.81	94.13	92.61	96.01	84.44	91.66	91.78**	93.65**	91.57**
Li	45	35	40	60	17	113	174	61	39	60
Cr	21	41	28	27	16	14	16	14	17	27
Ni	40	97	34	33	26	34	27	33	44	50
Rb	17	40	13	19	-	24	4	25	17	14
Sr	2109	1428	1480	1903	3537	403	1557	2430	1474	1872
Y	25	28	47	32	22	34	31	30	28	30
Zr	106	64	148	176	190	130	125	150	125	160
Ba	1470	70	1730	2100	850	280	970	2300	2270	1695

* excluding H₂O and LOI ** LOI and Fe₂O₃ : FeO not determined

Analysis 1, basaltic tuff from Penfrau Member;
 Analyses 2-5, hawaiite/mugearite tuffs from Bught Craig Member;
 Analyses 6&7, hawaiite/mugearite lava clasts in Stoodfold Member.
 Analyses 8-10, hawaiite/mugearite tuffs from Stoodfold Member.

Table 15. Chemical compositions (oxides, wt %) and trace-element abundances (ppm) of intrusives from the Bail Hill Volcanic Group.

	1	2	3
SiO ₂	49.43	56.85	56.80
TiO ₂	0.52	0.34	0.22
Al ₂ O ₃	19.58	19.97	19.57
Fe ₂ O ₃	1.64	N.D.	N.D.
FeO	4.41	4.37	4.60
MnO	0.13	0.16	0.12
MgO	5.17	2.19	1.98
CaO	3.74	1.74	1.71
Na ₂ O	5.64	7.21	7.50
K ₂ O	1.26	2.36	2.19
P ₂ O ₅	0.69	0.38	0.26
H ₂ O	4.36	2.58	2.18
LOI	3.40	1.98	1.77
Total*	92.21	95.57	94.95

Li	69	46	62
Cr	7	14	3
Ni	35	23	28
Rb	31	-	21
Sr	5293	1996	2875
Y	40	29	10
Zr	138	269	202
Ba	32	2800	3780

* excluding H₂O and LOI

N.D. not detected

Analysis 1, hawaiite/mugearite from Cat Cleuch.

Analyses 2 & 3, sodic trachytes from Cat Cleuch and Grain Burn.

Table 16. Groundmass analyses (electron microprobe).

	1	2	3	4	5	6
SiO ₂	45.40	48.04	45.93	51.26	54.17	54.49
TiO ₂	1.16	1.20	1.17	0.67	0.29	0.35
Al ₂ O ₃	15.63	19.48	19.32	22.04	22.39	22.73
FeO*	6.93	3.91	6.21	4.35	3.75	3.31
MnO	0.21	N.D.	0.23	0.06	N.D.	0.06
MgO	6.12	1.28	4.41	3.00	2.65	2.26
CaO	8.71	7.89	8.28	4.15	3.54	4.46
Na ₂ O	1.85	8.22	2.65	5.52	6.56	6.59
K ₂ O	4.72	0.39	3.88	2.50	2.19	1.24
P ₂ O ₅	2.39	0.80	0.68	0.59	0.22	0.24
S	0.15	0.26	0.11	0.09	N.D.	N.D.
Total	93.27	91.47	92.87	94.23	95.76	95.73

Normative Minerals**

C	0.0	0.0	0.0	4.4	3.5	3.1
Or	30.0	2.5	24.7	15.7	13.5	7.7
Ab	12.9	37.9	12.6	46.2	51.6	57.2
An	21.9	16.6	31.6	17.7	16.8	21.5
Ne	2.1	20.8	6.3	1.9	3.4	0.5
Di	3.9	7.2	3.6	0.0	0.0	0.0
He	2.5	10.2	2.9	0.0	0.0	0.0
Ol	18.5	0.3	14.2	11.3	10.0	8.7
Il	2.0	2.5	2.4	1.4	0.6	0.7
Ap	5.9	2.0	1.7	1.4	0.6	0.6

1. Average of 2 analyses groundmass of basalt (16W).
2. Average of 2 analyses groundmass of basalt (24).
3. Average of 2 analyses groundmass of basalt (17).
4. Average of 2 analyses groundmass of hawaiiite (27/2).
5. Average of 2 analyses hawaiiite clast in (27/2).
6. Average of 2 analyses groundmass of hawaiiite (27/12).

* total iron as FeO

** Cation norm of Baragar and Irvine (1971).

8.2 ALTERATION

8.2.1 Geochemical constraints

It is necessary to evaluate the nature and degree of any alteration in the Bail Hill rocks in order to establish which elements can be used to characterise the original composition of the rocks and provide information on their petrogenesis.

The presence of zeolites as amygdales in the lavas and the fact that plagioclase feldspar in the extrusive rocks has not been albitised indicates that the volcanic rocks have been metamorphosed to zeolite facies. The zeolites may be contemporaneous with the volcanic activity, forming as a result of the circulation of volcanically-related hydrothermal fluids, or they may be related to burial metamorphism on a regional scale, long after the volcanics had cooled and consolidated. Distinguishing between these two modes of formation has been recognised as a major problem in interpreting very low-grade metamorphic rocks (Coombs et.al., 1959), although the non-albitisation of plagioclase feldspar in the Bail Hill rocks clearly indicates that at no time in its history has the succession been above zeolite facies grade.

In addition to very low-grade metamorphism the rocks are inferred to have undergone submarine weathering on extrusion (see Section 6.8) and subaerial weathering at the present day.

In analyses, totals for non-volatile major oxides range between 84 and 99%. The remainder consists

largely of H_2O , CO_2 and S, although Ba and Sr form significant portions of some rocks (e.g. Table 13, analysis 12). The presence of calcite as veins, amygdales and infillings has been noted in the field and in thin-section, indicating mobility of Ca. In addition, zeolite and clinzoisite infillings suggest mobility of Si, Al, Ca and Na. Plagioclase feldspar shows alteration to white mica, carbonate and K-feldspar (adularia?), suggesting loss of Ca and Na, gain of K and Ba and gain or loss of Si from the crystal structure. Ferromagnesian minerals are pseudomorphed by chlorite, carbonate, epidote and iron oxides, although in this instance the preservation of the crystal outline and the chemistry of the secondary assemblage does not preclude the possibility that major elements have been redistributed within the crystal structure.

8.2.2 Petrographical constraints

Further constraints on the interpretation of the geochemical data are suggested by the petrography of the Bail Hill rocks. The extrusive rocks are all strongly porphyritic, with phenocrysts constituting up to 40% of the total rock. Phenocrysts display simple and concentric zoning and contain inclusions of other phases. The presence of cognate blocks and other igneous xenoliths suggest that accumulative and/or xenocryst mineralogies are present. Therefore, whole-rock analyses are not likely to represent an evolved-liquid composition and trends in variation diagrams can only show relative relationships and not an absolute liquid line of descent (Carmichael et.al., 1974).

The geochemistry of the coarse-grained xenoliths is strongly dependent on the feldspar:ferromagnesian mineral ratio and this is expected to be the major control on their location and/or classification in any discriminant functions used.

8.3 MAJOR AND TRACE-ELEMENT DATA

In view of the fairly specific SiO_2 contents of petrographically similar rocks, irrespective of their location or degree of alteration (see Tables 12-15), it is suggested that the silica content is close to the original concentration of the rocks and is a valid criterion in their classification. The absence of secondary quartz and the dominance of carbonate over silicate minerals in secondary assemblages further suggest that SiO_2 was restricted in mobility.

In Figures 7 and 8 major and trace-element concentrations have been plotted against SiO_2 . Using SiO_2 as an index of differentiation the relative trends of the major and trace-elements are discussed below with regard to primary and secondary mineralogies. Two analyses (Table 11, analysis 1 and Table 14, analysis 6) have silica percentages below the threshold of Figures 7 and 8. The former is an ultramafic xenolith and the latter a desilicified lava-clast in an agglomerate.

8.3.1 Aluminium

Although there is some scatter of points an overall trend of increasing Al_2O_3 with differentiation

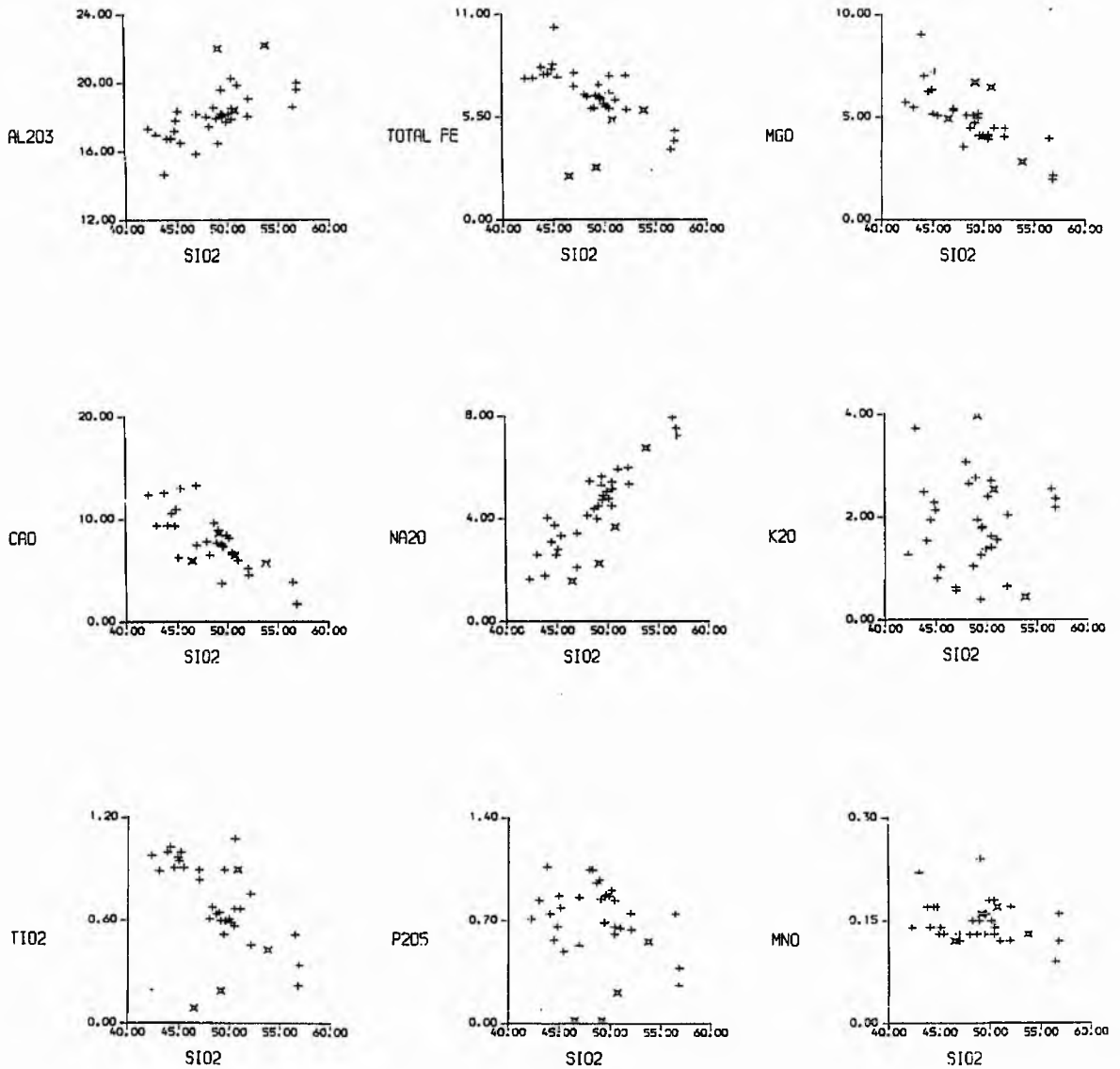


Figure 7: Major-element oxide concentrations vs. SiO_2 . Al_2O_3 and K_2O concentrations for one gabbroic xenolith lie above maximum values for respective plots. Stellate symbols, coarse-grained xenoliths; crosses, extrusive rocks.

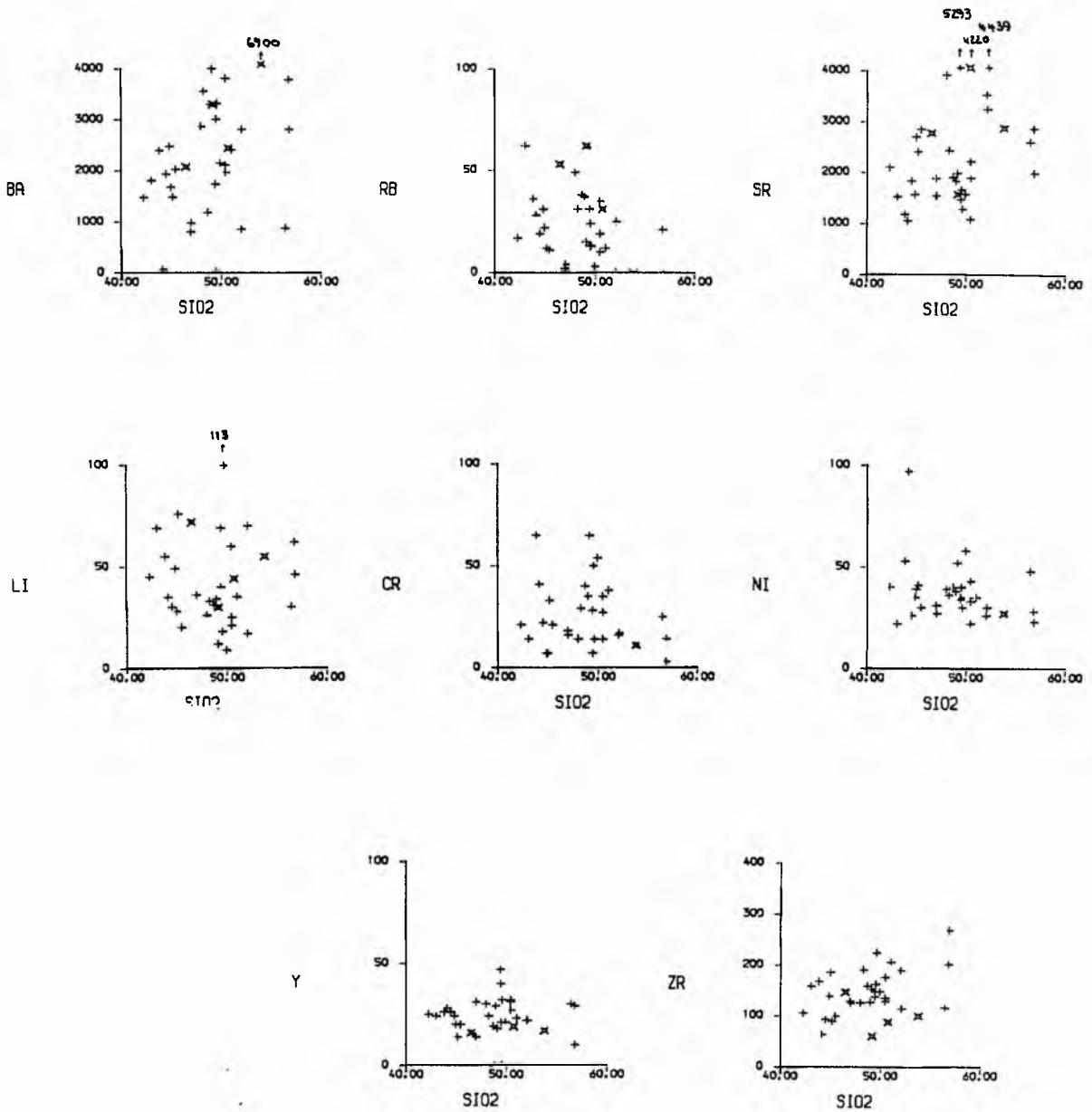


Figure 8: Trace-element concentrations (ppm) vs. SiO_2 (wt %) for the Bail Hill rocks. Cr and Ni analyses for gabbroic and ultramafic xenoliths not included.

can be seen. This trend and the scatter in points, particularly the two high xenolith values, reflects the concentration of the main Al-bearing phase in the rocks, plagioclase feldspar. Significant amounts of Al_2O_3 are also found in ferromagnesian minerals (up to 20%), iron-titanium oxides (up to 12%) and in the felsic groundmass of lavas (15-24%).

Alteration of plagioclase feldspar and to a lesser extent ferromagnesian minerals has resulted in release of Al_2O_3 and its subsequent recrystallisation in white mica, zeolites, epidote and, in the xenoliths, prehnite. The restricted scatter of points on the SiO_2 - Al_2O_3 plot might be anticipated from its known restricted mobility during weathering processes (Wedepohl, 1970) and suggests that redistribution of Al_2O_3 within the system (a whole-rock sample) has been more important than overall gain or loss.

8.3.2 Iron and Magnesium

Total iron (as Fe_2O_3) and MgO both show decreasing concentrations with differentiation, reflecting the diminishing role of the ferromagnesian minerals with increasing silica. The low total-iron and slightly above-average MgO concentrations in two of the xenoliths reflect the absence of iron-titanium oxides and the Mg-rich nature of the pyroxenes in these lithologies.

Localised redistribution of total iron by alteration of ferromagnesian minerals to iron oxides and epidote is common in some lithologies. Chlorite is the only

significant Mg-bearing secondary mineral in the extrusive rocks, although Mg-bearing amphiboles and chlorites replace pyroxenes in the coarse-grained xenoliths.

Mg:Fe ratios show an overall decrease with differentiation, although petrographically similar rocks often show a range of values, suggesting the ratio may be affected by the concentration and/or composition of the ferromagnesian phenocrysts in a particular rock.

The trends in Figure 7 suggest redistribution of Fe and Mg within the system predominates any overall gain or loss.

8.3.3 Calcium

CaO shows an overall decrease with differentiation, reflecting its decreasing concentration in plagioclase feldspar. Significant concentrations are also found in pyroxenes (20-24%), amphiboles (up to 12%) and apatites (48-52%), although these minerals are not present in sufficient concentrations to affect the overall trend.

Field and petrographic evidence indicates loss of Ca from some plagioclase feldspars, pyroxenes and amphiboles. However, the presence of carbonates, zeolites and clinozoisite in the same rocks together with the linear trend of CaO against SiO₂ indicate redistribution of calcium within whole-rock samples.

The concentration of CaO in the Bail Hill rocks is in good agreement with average values for modern alkali andesites (9.4% CaO, 47.6% SiO₂) and alkali basalts (12.42% CaO, 46.8% SiO₂) (Wedepohl, 1978).

8.3.4 Sodium

The linear trend of increasing Na_2O with differentiation reflects its concentration in plagioclase feldspar and the increasing Na-content of the feldspar with differentiation. Minor amounts of Na_2O are also found in amphiboles (up to 3%) and in the felsic groundmass of lavas (up to 8%).

The presence of Na_2O in zeolites and analcite indicates that some mobilisation has taken place. The source is likely to be the plagioclase feldspar in the same rock that has altered to adularia and released Na_2O (see Section 7.5), indicating a redistribution of Na within the whole-rock sample.

The trend of increasing Na_2O with differentiation is typical of the alkaline magma series and in marked contrast to the calc-alkaline series in which it remains almost constant (Wedepohl, 1970).

8.3.5 Potassium

The expected increase in potassium with differentiation (Wedepohl, 1970) is not evident in the Bail Hill rocks. The wide scatter of points, lack of any systematic trend and the variation in concentration in petrographically similar rocks imply substantial potassium mobility, with K_2O being added to or lost from whole-rock samples. In the absence of any knowledge of the original K_2O concentration it is not possible to assess the extent to which this mobility reflects redistribution of potassium within the volcanic pile or its introduction from an external source.

However, the absence of primary alkali feldspar (the main K-bearing phase) together with the relatively high K_2O concentrations of the Bail Hill rocks suggest that some potassium has been added to the system.

The only significant K-bearing primary minerals in the Bail Hill rocks are biotite/phlogopites (6-8%) and amphiboles (up to 1.5%), although values of 2-5% were found in the groundmass of lavas. The highest concentrations, however, were found in adularia feldspars of secondary origin (up to 16% K_2O) replacing primary labradorite/bytownite. There is no apparent internal K-bearing primary mineral phase in the rocks containing the adularia feldspar and an external source for the potassium seems probable.

8.3.6 Manganese

MnO remains fairly constant with differentiation. It is found in pyroxenes, amphiboles and primary micas. Anomalously high concentrations of over 3% were found in pyroxenes from a dioritic xenolith. In the same specimen biotites contain over 1% MnO . However, this does not appear to be a feature of the dioritic xenoliths as can be seen from the slightly below average concentration in xenolith M9 (Table 11, analysis 5).

The anticipated trend of decreasing MnO with differentiation (Wedepohl, 1978) is not observed in the Bail Hill rocks. No explanation for this is offered, although a similar trend of constant MnO with differentiation is observed in the alkaline volcanic suite of Tristan da Cunha (Baker et.al., 1964).

8.3.7 Titanium

Titanium shows a decrease in concentration with differentiation, in agreement with its anticipated variation in a differentiated magma (Wedepohl, 1978). It is found in decreasing abundance in iron-titanium oxides, sphene, primary micas, amphiboles and pyroxenes. The low values in two of the gabbroic xenoliths reflects the absence of iron-titanium oxides in these rocks.

The absolute concentration of TiO_2 is low for an alkaline magma and is more typical of the subalkaline series (Miyashiro, 1978). The linear trend, restricted scatter of points and the lack of any significant Ti-bearing secondary mineral phases in the rocks all suggest the present values reflect its original concentration in the rocks and that titanium has been relatively immobile.

8.3.8 Phosphorus

Apatite is the main P-bearing phase in the Bail Hill rocks and the P_2O_5 - SiO_2 plot reflects the distribution of this mineral in the rocks. The Bail Hill rocks display P-enrichment in the middle stages of differentiation, in agreement with the expected precipitation of apatite in the middle stages of fractionation (Wedepohl, 1976). The scatter of points is believed to be of primary (magmatic) origin and, in corroboration of this, there are no secondary P-bearing mineral phases in the rocks. The gabbroic xenoliths contain no apatite and have very low P_2O_5 concentrations, whilst the apatite-bearing diorite xenolith has a P_2O_5 concentration of the same order as the volcanic rocks.

The high P_2O_5 concentrations are typical of rocks crystallising from an alkaline magma (Wedepohl, 1976; Miyashiro, 1978).

8.3.9 Chromium and Nickel

The similarity in the behaviour of these two elements during magmatic differentiation (Prinz, 1967; Wedepohl, 1978) and their sympathetic variation in the Bail Hill rocks allows them to be considered together. The restricted scatter of points and the similarity in values of petrographically similar rocks suggest the present values reflect their original concentration in the rocks, in corroboration of their relatively immobile nature (Hart et.al., 1974).

Cr and Ni are known to be preferentially incorporated in early-formed ferromagnesian minerals (Prinz, 1967; Wedepohl, 1978). Significant amounts of Cr_2O_3 were observed in xenolith pyroxenes (see Section 7.2.1), whilst pseudomorphs after olivine, the main Ni-bearing phase (Wedepohl, 1978), were observed in melanocratic gabbros (see Section 6.3.3). In accordance with this the gabbroic and ultramafic xenoliths are strongly enriched in both elements relative to the extrusive rocks.

The Bail Hill basalts are exceptionally low in Cr and Ni when compared with their modern equivalents (ocean-island basalts, 245 ppm Cr; Hawaiian basalts, 191 ppm Ni; alkali-olivine basalts, 145 ppm Ni), although the more differentiated rocks show much closer agreement with their modern equivalents (hawaiite, 30 ppm Cr; mugearite, 11 ppm Cr)

(see Wedepohl, 1978, for Cr and Ni values).

The scatter in the values of Cr and Ni and in particular the slight peak for samples with 48-52% SiO_2 may reflect the presence of xenocrysts of Cr and Ni-bearing pyroxenes in the extrusive rocks.

8.3.10 Strontium

The highest concentrations of strontium in modern volcanics are found in mugearites (3400 ppm Sr), although their average value is much lower (Wedepohl, 1978). The anomalously high values, wide scatter of points and the lack of any systematic trend with differentiation for the Bail Hill rocks suggest that the Sr-concentrations are not of primary (magmatic) origin but secondary, with introduction of substantial amounts of Sr into the volcanic pile.

Sr is known to substitute for K and Ca in minerals (Wedepohl, 1972). In view of this it is inferred that the introduction of Sr was contemporaneous with the K-mobilisation (see Section 8.3.5). If the formation of the secondary K-feldspars was synchronous with the release of Ca from the original calcic plagioclase then there would be two possible sites for the concentration of Sr. Firstly, in the secondary adularia (where it would substitute for K) and, secondly, in the carbonate veins, amygdales and infillings (where it would substitute for Ca). In accordance with this paragenesis, the only sample without a significant plagioclase feldspar component has the lowest Sr-content (Table 11, analysis 1).

8.3.11 Barium

The Bail Hill rocks rarely contain less than 1000 ppm Ba, in marked contrast to the average value for alkali basalts of 613 ppm (Wedepohl, 1972) and values of less than 1200 ppm Ba in alkalic rocks with 45-50% SiO₂ (Miyashiro, 1978). In view of the anomalously high values, the lack of systematic variation and the wide scatter for petrographically similar rocks the barium values of the Bail Hill rocks are believed to reflect secondary processes that have acted on the volcanic pile.

At least some of the Ba is found as barytes, which has been reported in the Bail Hill rocks (Kennedy, 1936). However, its dissipated nature and ambiguous optical properties make it difficult to assess the amount of barytes in the rocks. It is almost certainly of secondary origin, being typically associated with hydrothermal deposits (Deer et.al., 1963). Ba is also known to substitute for K in K-feldspars (Prinz, 1967; Wedepohl, 1972) and substantial amounts of Ba may be contained in the secondary feldspars of the Bail Hill rocks. Zeolites could also serve as sites for concentration of Ba (Wood et.al., 1976).

Haynes (1973) suggests that the anomalously high Ba-values in the Bail Hill rocks is due to the introduction of Ba-rich fluids along the Sanquhar Fault. However, the outlying tuff members, which are situated well away from the Sanquhar Fault, also show anomalously high Ba-concentrations, whilst material situated at or near the fault show below average values (e.g. Table 12, analysis 6 and Table 15, analysis 1). This precludes the origin suggested by

Haynes (1973), and it is inferred that, in view of their ionic similarities, the introduction of Ba was coeval with the K-mobilisation (see Section 8.3.5).

8.3.12 Rubidium

There is no evidence for the expected systematic increase in Rb with magmatic differentiation (Wedepohl, 1970). Petrographically similar rocks show a wide scatter in values and, overall, there is no systematic trend with differentiation. It is inferred from this that the present-day concentrations of Rb reflect secondary processes that have affected the volcanic pile and do not reflect the primary (magmatic) concentrations.

The substitution of Rb for K in minerals (Prinz, 1967; Wedepohl, 1970) suggest Rb-mobilisation may be related to the K-mobilisation noted above (see Section 8.3.5). The absolute values are within the range for modern alkaline rocks (Miyashiro, 1978), suggesting Rb has been redistributed within the volcanic pile as a whole and not introduced from an external source.

8.3.13 Lithium

The lack of systematic variation with differentiation and the wide scatter for petrographically similar rocks suggest mobilisation of Li has taken place. In accordance with this, the values for the Bail Hill rocks are substantially greater than those found in pristine alkali basalts (11 ppm Li) and alkali andesites (12 ppm Li) (Wedepohl, 1970).

Although it is known to be present in significant

amounts in ferromagnesian minerals, particularly micas (Wedepohl, 1970), there is no evidence for any systematic variation or concentration in the Bail Hill volcanic rocks and/or minerals.

8.3.14 Zirconium and Yttrium

The zirconium and yttrium analyses of the Bail Hill rocks show a restricted scatter of points and values typical of pristine igneous material, in agreement with their relatively immobile nature (Pearce and Cann, 1973). The slight scatter of points on the Zr-SiO₂ plot may reflect the greater inaccuracy of the Zr-analyses in relation to those of the other trace elements. This scatter tends to mask any overall trend, although there is probably some increase in Zr with differentiation, a feature observed in other oceanic alkaline suites (LeMaitre, 1962; Baker et.al., 1964). Yttrium shows a more or less constant value with differentiation.

The Zr and Y values are believed to represent their original concentrations in the rocks, a conclusion apposite with the absence of Zr and Y-bearing secondary assemblages in the Bail Hill rocks.

8.4 INTERPRETATION

8.4.1 Nature of alteration

The chemistry of the secondary minerals of the Bail Hill rocks implies that mobility of SiO₂, Al₂O₃, CaO, MgO, Na₂O and total iron has taken place. However, the

linear trends of these elements with differentiation and their similar concentrations in petrographically similar rocks indicate that they have been redistributed within a whole-rock system. This element mobility closely resembles that produced by basalt-seawater interaction at elevated temperatures (Humphris and Thompson, 1978a).

In addition, it is apparent that substantial amounts of Ba and Sr, and, to a lesser degree, K_2O and Li have been introduced into the Bail Hill volcanic pile. In addition Rb has undergone large-scale redistribution within the volcanic pile as a whole. These elements are known to be present in hydrothermal fluids (Humphris and Thompson, 1978b; Wedepohl, 1979) and are concentrated in zeolite minerals (Wood et.al., 1976). The secondary feldspars and carbonate minerals in the Bail Hill rocks have also been inferred as potential sites for the concentration of these elements (see Section 8.3). Three of these elements (K, Rb and Sr) have been experimentally precipitated from seawater-related hydrothermal systems to give anomalous concentrations in volcanic rocks (Menzies and Seyfried, 1979). In addition, barium-deposits and barium-bearing fluids have been directly observed in seawater-based hydrothermal systems in modern oceanic environments (Lonsdale, 1979, and references therein).

It is tentatively concluded that the Bail Hill rocks show signs of hydrothermal alteration involving seawater. SiO_2 , Al_2O_3 , MgO, CaO, Na_2O and total iron were mobilised but retained within whole-rock systems. K_2O , Ba, Sr, Rb and Li were introduced to the volcanic

pile and are concentrated in secondary minerals. TiO_2 , MnO , P_2O_5 , Cr, Ni, Zr and Y show no signs of mobility and were relatively unaffected by the hydrothermal alteration.

8.4.2 Igneous spectrum and alkali elements

According to Hughes (1973) the majority of fresh igneous rocks plot in an "igneous spectrum" in the diagram of $\text{Na}_2\text{O} + \text{K}_2\text{O}$ versus $(\text{K}_2\text{O}/\text{Na}_2\text{O} + \text{K}_2\text{O}) \times 100$. The majority of the Bail Hill rocks plot within the spectrum close to the expected values for the alkali basalt trend (see Figure 9(a)). Those samples plotting to the right of the spectrum are enriched in K_2O relative to Na_2O , whilst those plotting to the left of spectrum are enriched in Na_2O relative to K_2O . However, in view of the strong linear trend of Na_2O with differentiation (see Figure 7) the two fields are believed to correspond to potassium-gain and potassium-loss respectively. All the points plotting to the left of the spectrum are from the late and middle-stage activity of the Bail Hill volcanic episode (see Section 6.8), suggesting the main mobilisation of K may have preceded the later stages of volcanic activity.

The great majority of the Bail Hill samples fall in the alkaline field in the alkalies-silica diagram (see Figure 8(b)), in agreement with conclusions based on mineralogical criteria that the parent magma was alkaline in character (see Section 7.9). The reasonably linear trend suggests that the mobilisation and introduction of K has not unduly affected the total alkali content. The scatter of points is greater at low silica values indicating

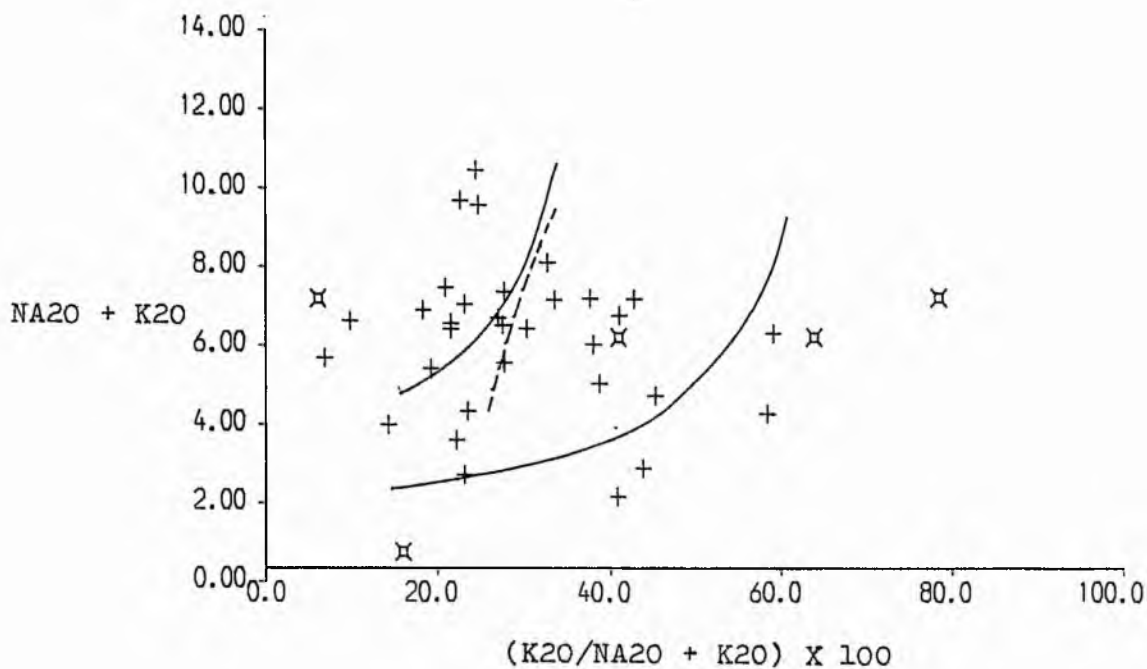


Figure 9(a): Bail Hill rocks in relation to the igneous spectrum of Hughes (1973). Trend of sodic alkaline rocks indicated by dashed line. Stellate symbols, coarse-grained xenoliths; crosses, extrusive rocks.

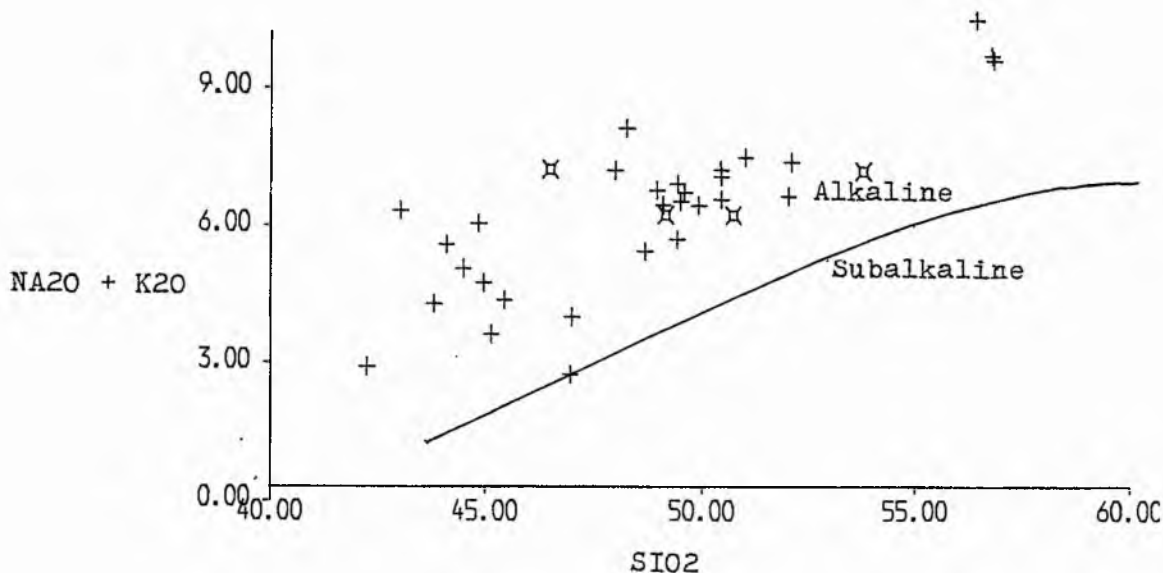


Figure 9(b): Plot of total alkalis vs. SiO₂. The field boundaries are those proposed by Miyashiro (1978). Stellate symbols, coarse-grained xenoliths; crosses, extrusive rocks.

the main mobilisation of K has not affected the late and middle-stage rocks to the same degree as the early basalts and hawaiites.

8.4.3 Normative analyses

Whole-rock and groundmass analyses have been classified according to the "cation norm" of Baragar and Irvine (1971). In view of the restricted mobility of most major elements the results are believed to be representative of the original nature of the rocks.

All but five of the volcanic rocks are undersaturated with silica and contain normative nepheline. In addition, all samples contain normative olivine; normative diopside is found in all samples except two late-stage intrusives and three of the samples lacking normative nepheline. All samples contain normative oligoclase, albite, anorthite, apatite, magnetite and ilmenite. Minor amounts of normative corundum and hypersthene are found in a few specimens.

The samples without normative nepheline show a higher degree of alteration than the other rocks in the group. Phenocrysts have been replaced by secondary minerals and the groundmass contains abundant secondary iron oxides and chlorite. This would suggest that the rocks became less undersaturated with alteration.

Four of the five xenoliths contain normative nepheline, although this never exceeds 4%, and all contain over 10% normative olivine.

In the volcanic rocks the basalts contain the

greatest amounts of normative nepheline (commonly 6-10%), whilst the intermediate lavas and intrusives contain less than 6%, suggesting the volcanics became less undersaturated with differentiation. Olivine content varies between 8 and 15% in the extrusives and shows no systematic variation with differentiation.

In the rock classification of Baragar and Irvine (1971) the great majority of the Bail Hill rocks belong to the alkali olivine basalt series. Only specimens with substantial alteration belong to other series (tholeiitic and calc-alkaline). Among the alkaline rocks, the majority belong to the sodic series rather than the potassic series. Those that belong to the sodic series are less altered than their potassic equivalents. In view of this and the knowledge that some potassium may have been introduced to the system, it is believed that the Bail Hill rocks differentiated along the sodic alkaline series (alkali basalt - hawaiite - mugearite - benmoreite - trachyte) rather than the potassic alkaline series (alkali basalt - trachybasalt - tristanite - K-rich trachyte).

In order to ascertain the influence of phenocrysts on the normative composition of the rocks a number of groundmass analyses were obtained by using a defocussed beam on the electron microprobe. Although this technique is subject to large errors it is clear from Table 16 that these analyses substantiate the undersaturated nature of the volcanic rocks. In all cases the rocks classification of Baragar and Irvine (1971) for the groundmass was the same as that for the whole rock from which it was taken,

indicating the porphyritic nature of the rocks has not significantly affected the normative mineral content or the rock classification.

8.4.4 AFM data

The Bail Hill rocks show a scatter of points on an AFM diagram, although an overall trend towards the 'A' apex can be seen (see Figure 10(a)). The absence of any significant iron enrichment in the extrusive rocks and the very low iron contents of the gabbroic xenoliths are readily apparent on this diagram. The Bail Hill values are close to the trends for alkaline (Tristan da Cunha) and calc-alkaline (Cascades) volcanic suites, although in view of the scatter of points it is not possible to resolve which of these trends they most closely resemble. It is noted, however, that the majority of the Bail Hill rocks are depleted in iron when compared with modern volcanic suites.

8.4.5 Minor oxides and trace elements

Ba, Sr, Rb and Li cannot be used to define the nature of the parental magma as these elements have been introduced and/or redistributed within the volcanic pile by secondary "metamorphic" processes. They are not considered hereafter. Cr, Ni, Zr and Y, however, show a restricted scatter and their values in rocks agree closely with their modern counterparts. These elements can therefore be used to define the nature and affinities of the parent magma and to elucidate the petrogenesis of

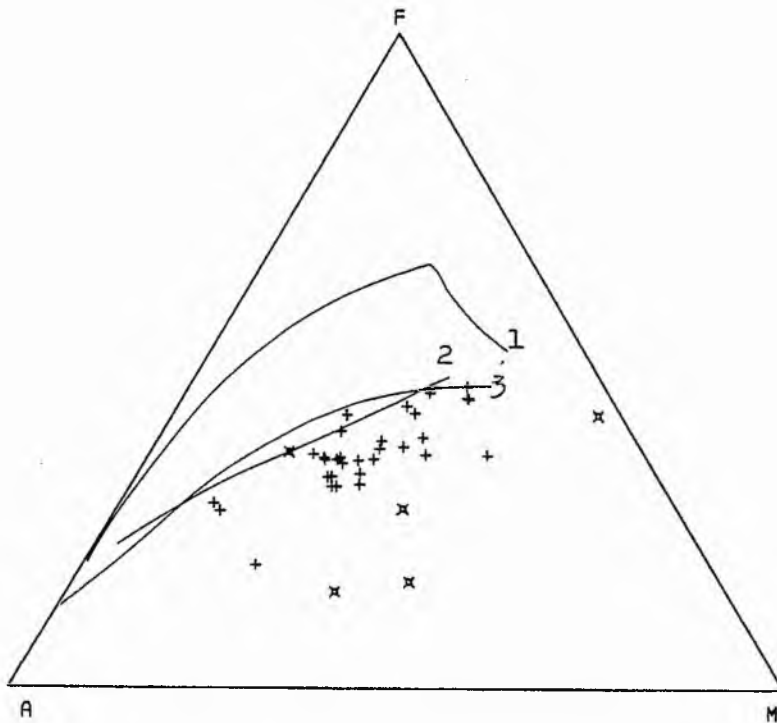


Figure 10(a): Iron-magnesium-alkali variation in the Bail Hill rocks. Tholeiitic, calc-alkaline and alkaline trends are included for comparison. 1, tholeiitic; 2, calc-alkaline; (Carmichael, 1964); 3, alkaline (LeMaitre, 1962).

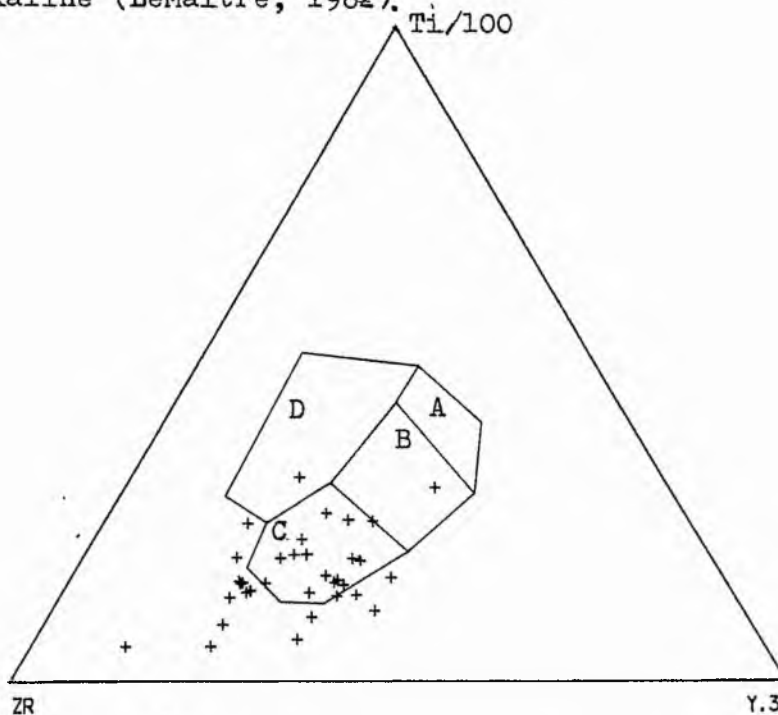


Figure 10(b): Ti-Y-Zr plot for Bail Hill extrusive rocks (after Pearce and Cann, 1973). "Within-plate" basalts normally fall in field D, whilst field C corresponds with calc-alkali basalts. Half of the Bail Hill samples lie outside all four recognised fields.

the Bail Hill rocks. In addition to these four elements the concentrations of P_2O_5 and TiO_2 are considered below.

Using the appropriate data (rocks with 45-50% SiO_2) from Bail Hill for the six relatively immobile elements mentioned above, it is clear that the Bail Hill rocks are typically alkaline in their low Cr and Ni, high P_2O_5 and Zr and moderately low Y values (Miyashiro, 1978). The TiO_2 values, however, are typical of the subalkaline series, and an explanation for this is given below.

It has already been observed that the gabbroic and ultramafic xenoliths are strongly enriched in Cr and Ni relative to the extrusive rocks (Section 8.3.9). This is interpreted in the following manner. Concentration of these two elements in early precipitating ferromagnesian minerals (now found in the gabbroic and ultramafic xenoliths) resulted in the remaining liquid(s) being strongly depleted in these two elements. These liquids are now represented by the extrusive rocks of Bail Hill.

In an analogous manner the anomalous TiO_2 contents of the Bail Hill rocks can be explained by precipitation of iron-titanium oxides. Evidence for this is as follows. The decreasing concentration of TiO_2 with differentiation (Figure 7) reflects precipitation of iron-titanium oxides rather than Ti-bearing silicates (amphiboles and micas), as the latter are concentrated in the middle-stage volcanic activity and would produce middle-stage TiO_2 enrichment on Figure 7. The iron-titanium oxides do not form significant portions of the volcanic rocks, but are common in xenoliths with pargasitic amphibole and subordinate biotite/phlogopite,

plagioclase feldspar and apatite. Although no xenoliths of this type have been analysed as whole-rock, it is inferred from the mineralogy that the TiO_2 concentrations of such rocks must be substantially higher than that of the volcanic rocks as 50-80% of the rock consists of iron-titanium oxides (up to 50% TiO_2), amphiboles (1-3% TiO_2) and micas (4-6% TiO_2). Precipitation of this assemblage would leave the resulting liquid(s) depleted in TiO_2 , although the continuing precipitation of small amounts of iron-titanium oxide could produce the trend illustrated in Figure 7. In corroboration of this the early crystallising pyroxenes and the cumulate amphiboles and micas contain above average concentrations of TiO_2 (see Sections 7.2.1, 7.3 and 7.4), suggesting that the magma from which they crystallised was not depleted in titanium. It is further noted that this model could also explain the below average iron-concentrations of the extrusive rocks (see Section 8.5.4), as the iron-titanium oxides contain above average iron-concentrations and their precipitation could cause iron-depletion in the residual liquid(s).

As a result of the anomalously low totals of TiO_2 in the Bail Hill rocks many of the plots used for distinguishing the tectonic setting of volcanic rocks are expected to give spurious results for the Bail Hill data. For example, on the Ti-Zr-Y diagram (see Figure 10(b)) many of the Bail Hill samples lie outside the four fields designated by Pearce and Cann (1973). The points lie close to the Zr-apex of the diagram and scatter across to the Y-apex, suggesting that the rocks are depleted in Ti relative

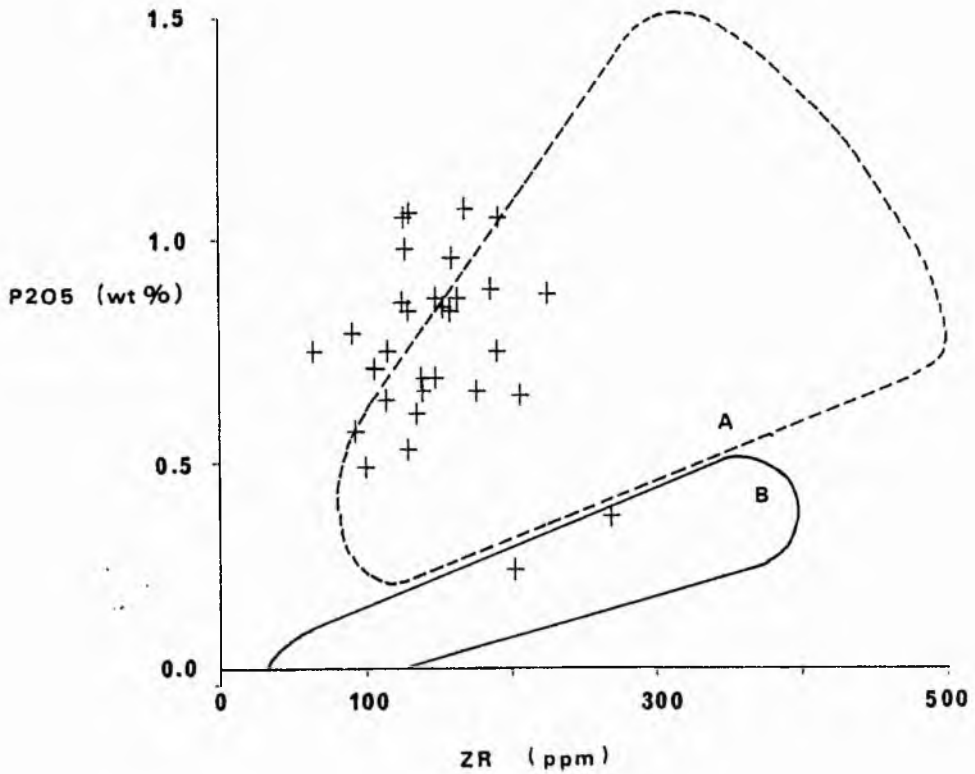
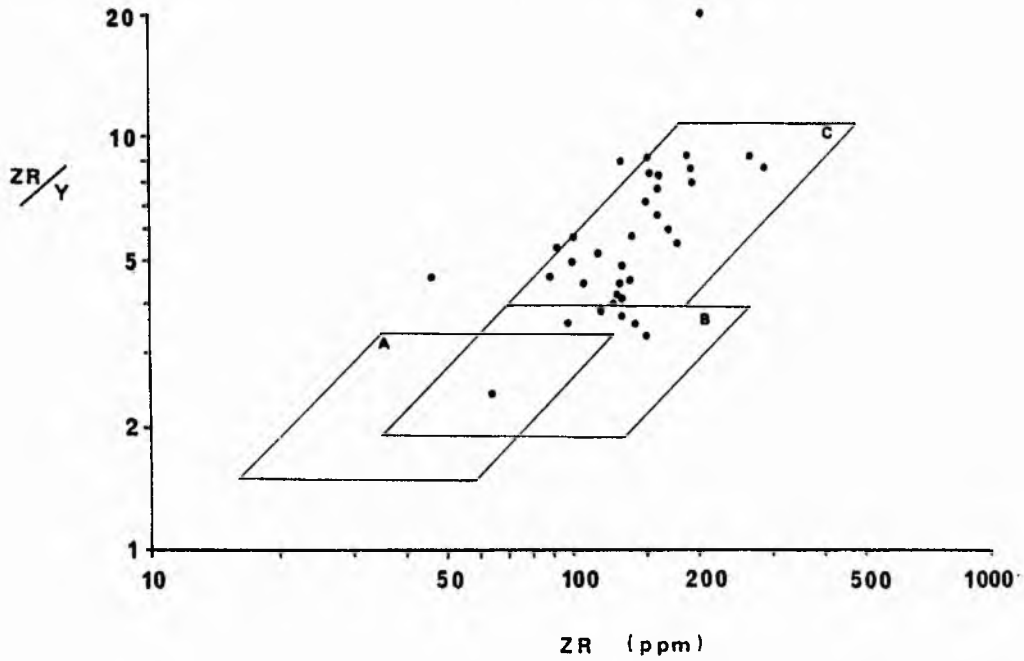


Figure 11(a): (top). Zr vs. Zr/Y plot for Bail Hill extrusive rocks (after Pearce and Norry, 1979). Field A, island arc basalts; Field B, mid-ocean ridge basalts; Field C, within plate basalts.

Figure 11(b): (bottom). Zr vs. P₂O₅ plot for Bail Hill extrusive rocks (after Floyd and Winchester, 1975). Field A, oceanic-alkali basalts; Field B, oceanic tholeiitic basalts.

to Zr and Y. In a similar manner the Bail Hill rocks fall outside the recognised fields on the Zr-TiO₂ plot of Floyd and Winchester (1975). The statistical analyses of Pearce (1974) on major-element concentrations in basalts rely mainly on the TiO₂ and K₂O values of the rocks. The mobility of K₂O and the anomalously low TiO₂ values in the Bail Hill rocks preclude the use of this discriminant.

The unsuitability of TiO₂ as a parameter in classifying the rocks and the absence of Nb data severely restricts the number of techniques that can be used to discriminate between the various magma-types and tectonic environments. However, on the Zr-Zr/Y plot (see Figure 11(a)) the majority of the Bail Hill rocks fall in the "within-plate basalt" field of Pearce and Norry (1979), whilst the majority of points fall in the "ocean alkali basalt" field of Floyd and Winchester (1975) (see Figure 11(b)).

8.5 CONCLUSIONS

Three main conclusions can be made from the foregoing discussion and the analyses presented in Tables 11-16 :-

1. A genetic relationship exists between the extrusive rocks of the Bail Hill Volcanic Group and is exemplified by the continuity in geochemical trends for most elements:
2. The igneous rocks of Bail Hill were derived from a silica-undersaturated magma and are alkaline in character. Normative mineral compositions suggest the rocks differentiated along the sodic alkaline series

(alkali basalt - hawaiite - mugearite - benmoreite - trachyte).

3. The nature of the alteration in the Bail Hill rocks is consistent with formation by circulation of seawater-based hydrothermal fluids. It is possible to discriminate between elements that have been mobilised but retained within the system, elements that have remained relatively immobile and elements that have been introduced to the system from external sources. However, it is not possible to resolve the timing or the environment in which the alteration took place.

CHAPTER 9 : PETROGENESIS

It is proposed that the intrusive and extrusive rocks at Bail Hill were derived by fractional crystallisation of a basaltic parent magma under low pressure. A silica-poor parent magma was generated in the mantle and rose intermittently to the upper mantle/lower crust where it differentiated in a high-level magma chamber. Periodic tapping of this magma chamber resulted in the extrusion of the Bail Hill Volcanic Group, whilst fractional crystallisation resulted in the formation of a cumulate body at depth. The introduction of new magma into the high-level chamber caused partial disruption of the cumulate material, some of which was incorporated in the extrusive rocks as coarse-grained xenoliths.

The overall framework of this model is similar to the evolution of an ocean-island volcano by fractional crystallisation in an open system (O'Hara, 1977). The model is capable of providing a series of genetically related liquids, such as those from which the Bail Hill rocks crystallised, by fractional crystallisation in a periodically refilled magma chamber (O'Hara, 1977; Pankhurst, 1977).

The earliest precipitates in the Bail Hill rocks are the gabbroic xenoliths, which contain the most refractory phases found in the igneous rocks and are enriched in Cr and Ni. The presence of possible pseudomorphs after olivine in melanocratic gabbros suggests that olivine was

an early crystallising phase, preceding the diopside-bytownite assemblage.

From consideration of the petrography of the xenoliths the following assemblages were precipitated, in order, by a process of fractional crystallisation :-

1. (?) olivine + diopside + bytownite:
2. diopside/salite + bytownite:
3. pargasitic amphibole + iron-titanium oxides ± plagioclase feldspar (labradorite/andesine/oligoclase), phlogopite/biotite, apatite, clinopyroxene (salite/augite):
4. plagioclase feldspar (andesine/oligoclase/albite) + phlogopite/biotite + apatite ± pargasitic amphibole, iron-titanium oxides.

The ultramafic xenoliths are believed to be transitional between assemblages 2 and 3, as petrographic evidence indicates that the clinopyroxene and plagioclase feldspar precipitated before the pargasitic amphibole and iron-titanium oxides.

Volcanic activity did not take place at Bail Hill prior to precipitation of assemblage 3 at depth, as phenocrysts of pargasite are found in the basal lavas and are believed to be of cumulate origin. The clinopyroxene and plagioclase feldspars in these basal lavas show features typical of disequilibrium growth and are not of cumulate origin.

Coarse-grained xenoliths are not found in the basal lavas, although assemblages 1-4 are present as blocks in the subsequent middle-stage volcanic activity. This indicates that disruption of the cumulate body took place

prior to extrusion of the middle-stage volcanics and that by this time a body of material ranging from gabbro, through diorite, to rocks with syenitic affinities, existed at depth. It is suggested that this disruption was due to the introduction of a fresh batch of magma into the high-level chamber, in the manner envisaged by O'Hara (1977). O'Hara (1977) indicates that this material would mix with any remaining liquid in the chamber to produce a new homogeneous liquid. However, it is thought that there was very little liquid left in the Bail Hill sub-volcanic chamber by this stage. The evidence for this is twofold. Firstly, a differentiated plutonic body must have existed prior to the middle-stage volcanic activity and any residual liquid would be highly differentiated and relatively small in volume compared with the cumulate pile that produced it. Secondly, evidence suggests the coarse-grained material in the plutonic body had undergone low-grade metamorphism prior to incorporation in the extrusive rocks at temperatures well below the solidus for basic igneous rocks. These conditions are therefore incompatible with the presence of magma in the same chamber. This is considered in more detail below.

Actinolitic amphibole and chlorites have been observed replacing clinopyroxenes in the gabbroic xenoliths, whilst prehnite is found pseudomorphing plagioclase feldspar in gabbros and diorites and is also present along the cleavage in phlogopite/biotite crystals in dioritic xenoliths.

Actinolite-chlorite facies metamorphism takes place at 300-500°C (Winkler, 1976), whilst prehnite has

an upper stability of 400-500°C between 0 and 7 kb (Liou, 1971). In contrast to this the zeolite facies grade of the volcanic rocks and the non-albitisation of plagioclase indicates temperatures below 200°C (Liou and Ernst, 1979). Clearly the metamorphism of the xenoliths predates their incorporation in the extrusive rocks.

The secondary minerals are consistent in nature and association with an origin by hydrothermal alteration. Actinolite and chlorite are common replacement products of clinopyroxenes in Layer 2 of the oceanic crust (Bonatti *et.al.*, 1975; Coleman, 1977). Similarly the biotite-prehnite association has been ascribed by various authors to the action of circulating fluids on dioritic material (see Section 7.8).

It is therefore suggested that the cumulate pile containing assemblages 1-4 had cooled to temperatures below 500°C and was undergoing low-grade metamorphism as a result of hydrothermal fluid circulation, prior to the extrusion of the middle-stage volcanics. The interlocking vein-like nature of the secondary amphiboles and chlorites (see Section 6.3.3) is interpreted as a fracture system along which the fluids could migrate.

Spooner and Fyfe (1973) indicate that juvenile water is unlikely to be the aqueous fluid in such hydrothermal systems and suggest seawater as a more likely contaminant. The alteration of the coarse-grained lithologies may mark the initiation of a seawater geothermal system such as that envisaged by Spooner and Fyfe (1973) for sub-sea-floor metamorphism. This could also act as the

source for the zeolites, K-feldspars and carbonate minerals found in the extrusive rocks, suggesting the alteration was contemporaneous with volcanism and not related to subsequent regional burial metamorphism (see Sections 7.7, 7.9, 8.4.1 and 8.5).

The introduction of a fresh batch of magma into the high-level chamber resulted in fragmentation of material in conduit walls and on the sides of the high-level chamber itself. Some of this material may have been assimilated by the new liquid, although the coarse-grained xenoliths are interpreted as the non-assimilated or partially assimilated remnants of this material.

O'Hara (1977) envisages extrusion at the surface as an indication that new material has been added at depth. In his model material would be added to the high-level body at fairly regular intervals. In contrast, the model for the Bail Hill area necessitates addition of material at relatively infrequent intervals, allowing material in the high-level chamber to differentiate and cool to temperatures characteristic of low-grade metamorphism. It is stressed, however, that uncertainties over the detailed history of the Bail Hill episode do not permit the resolution of events required by O'Hara's (1977) model.

Some indication of the depth at which fractionation took place can be gleaned from the xenolith mineralogies. The occurrence of plagioclase as the aluminous phase places an upper limit of 15 kb (50 km) on the site of fractionation (Wyllie, 1971), in agreement with the 30-50 km maximum depth estimate for differentiation of oceanic alkaline

suites (Carmichael et.al., 1974). In an experimental alkali basalt-water system amphibole precipitates before plagioclase at water pressures above 1.5 kb (Yoder and Tilley, 1962), whilst phlogopite is unstable in "basaltic" rocks at pressures below 2 kb (Yoder and Eugster, 1954). Wyllie (1971) indicates that amphibole and plagioclase feldspar cannot co-exist at pressures above 12 kb in a gabbro system under hydrous conditions. Although these experimental systems can only approximate to that of Bail Hill, it is inferred from the above data that fractional crystallisation of the Bail Hill rocks occurred at pressures between 2 and 12 kb. A depth of between 7 and 40 km is implied, which places the site of fractionation, assuming oceanic crust, in the upper mantle or lower crust. It is noted that in the model of O'Hara (1977) fractional crystallisation is expected to take place over a range of pressures, and further definition of the site of fractionation for the Bail Hill rocks may be misleading and is therefore not attempted.

No estimate can be made of the original parent magma composition as all lithologies derived from this material have undergone extensive changes in major and trace-element chemistry as a result of fractional crystallisation (O'Hara, 1977). Furthermore, no estimate can be made of the relative volumes of phases fractionated for three reasons. Firstly, incomplete exposure of the volcanic rocks at Bail Hill results in a lack of knowledge of the relative volumes of present-day lithologies. Secondly, the presence of lithologies not found at outcrop as clasts in

the Bught Craig Member and Peat Rig Formation indicates that the present-day exposures are not representative of the igneous products in Ordovician times. Thirdly, the possibility that Bail Hill was only one of a number of vents stemming from a single deep-seated source (see Section 10.3) suggests that the igneous history of the Southern Uplands in N. gracilis times would have to be considered and not just the history of the Bail Hill vent.

In view of these uncertainties no attempt has been made to define the physicochemical conditions of crystallisation. However, the nature of the minerals in assemblages 3 and 4, together with the ubiquitous zoning of phenocrysts, suggest crystallisation under relatively hydrous conditions.

The Bail Hill rocks show petrogenetic affinities with those of the modern Tristan da Cunha islands, situated on the flanks of the Mid-Atlantic Ridge (Baker, 1973). Here, as at Bail Hill, fractional crystallisation in a periodically refilled, sub-volcanic magma chamber has produced a variety of genetically related intrusive and extrusive rocks (Baker et. al., 1964). The Tristan rocks, however, have differentiated along the potassic alkaline series (alkali basalt - trachybasalt - trachyandesite - trachyte), rather than the sodic series of Bail Hill. The major and trace-element variation with differentiation for the extrusive rocks of Tristan (Baker et. al., 1964) is similar to that for those elements in the Bail Hill rocks that have not been introduced to the system (see Sections 8.4.1 and 8.4.5). In particular, both Bail Hill and Tristan

are characterised by low Cr and Ni concentrations in the extrusive rocks, a feature said to be atypical of ocean island suites by Baker et.al. (1964). At Bail Hill their low concentrations is a direct result of their concentration in the ferromagnesian minerals of the gabbroic xenoliths. The limited data available on the concentration of these elements in the Tristan xenoliths is equivocal. LeMaitre (1969) provides data on two Tristan xenoliths which contain low Cr and Ni, although he admits the data is of poor quality. In view of this the possibility that these elements are concentrated in the Tristan xenolith minerals must remain unsupported.

The xenoliths at Bail Hill and Tristan are characterised by an absence of hypersthene, scarcity of olivine and the presence of clinopyroxene, brown amphibole, iron-titanium oxides, plagioclase feldspar, apatite and biotite (Tristan data from Baker et.al., 1964). In contrast to the Bail Hill rocks, the clinopyroxene of the Tristan xenoliths is titanaugite and the brown amphibole is kaersutite (a Ti-rich pargasite) (LeMaitre, 1969). This suggests the Tristan magma was enriched in Ti relative to the Bail Hill magma, or that differences in the physico-chemical conditions of crystallisation of two magmas with similar Ti-contents resulted in Ti entering the silicate minerals in one (Tristan), and the iron-titanium oxides in the other (Bail Hill).

The phenocrysts at both Bail Hill and Tristan show compositional overlap with xenolith mineralogies, although in both cases the xenolith pyroxenes are more

refractory than the phenocryst varieties (Tristan data from Baker et.al., 1964; LeMaitre, 1969).

It is concluded that the petrogenesis of the Bail Hill rocks is consistent with differentiation by fractional crystallisation in an open system, as modeled by O'Hara (1977). The particular history of the Bail Hill rocks is similar in several respects to that of the modern Tristan da Cunha islands, indicating that such processes are currently active in oceanic environments. It is noted, however, that the Tristan rocks formed on the flanks of a mid-ocean ridge, well away from the influence of terrigenous sedimentation, whereas the Bail Hill volcano was active at the same time as land-derived turbiditic sediments were being deposited on the adjacent ocean floor.

Finally, it is noted that although the coarse-grained xenoliths in the volcanic rocks are believed to be fragments of a cumulate body that once underlay the Bail Hill volcano, there is no trace of this body in the present-day Southern Uplands. An explanation for this is given in Section 10.4.

CHAPTER 10 : DISCUSSION10.1 INTRODUCTION

The postulated existence in Lower Palaeozoic times of an ocean situated between the northwestern and southeastern forelands of the Caledonian/Appalachian orogen (Wilson, 1966) has been supported by faunal evidence (Williams, 1976; McKerrow and Cocks, 1976), palaeomagnetic evidence (Briden et.al., 1973; Piper, 1978) and structural evidence (Phillips et.al., 1976). Harland and Gayer (1972) proposed the term "Iapetus Ocean" for this in preference to the ambiguous "proto-Atlantic Ocean" of Wilson (1966).

Most authorities now agree that the Southern Uplands succession was deposited on an oceanic plate lying to the south of a northwestern continent (Wilson, 1966; Dewey, 1969, 1971), although on the basis of geophysical evidence Powell (1970) argues that the Southern Uplands is underlain by sialic crystalline basement and that there is no evidence for any oceanic crust. Although this problem is beyond the scope of this discussion, it is noted that the present-day structure under the Southern Uplands may be totally unrelated to crustal structure in Lower Palaeozoic times and the apparent absence of oceanic crust at present does not preclude its existence in former times. Bamford et.al. (1978) indicate the presence of a crustal anomaly under the present-day Southern Uplands, supporting arguments that it represents the zone of ocean closure.

Numerous models for the area in Lower Palaeozoic

times exist in the literature, differing in the times, directions and sites for destruction of oceanic crust. Dewey (1969, 1971) proposes northerly subduction, with an ocean trench situated near the line of the Southern Uplands fault: Fitton and Hughes (1970) postulate southerly subduction under the broad area of the Paratectonic Caledonides of Dewey (1969): Gunn (1973) invokes paired subduction zones in the vicinity of the Highland Boundary and Southern Uplands Faults, with the Midland Valley representing oceanic crust: Mitchell and McKerrow (1975) reiterate the northerly subduction system of Dewey (1971): Phillips et.al. (1976) suggest oblique closure of the Iapetus Ocean, progressively later to the southwest, with subduction systems on the northwest and southeast margins of the ocean.

The postulated northwesterly dipping subduction system has led to interpretations of the Southern Uplands succession as material offscraped at a continent-ocean interface (Mitchell, 1974; Floyd, 1975; McKerrow et.al., 1977), reminiscent of modern "accretionary prisms" formed by "imbricate thrusting" (Seely et.al., 1974; Kulm and Fowler, 1974).

It is within this framework that the data and conclusions presented in this thesis are discussed.

10.2 THE VOLCANIC ROCKS

Dewey (1971) and Church and Gayer (1973) suggest the Bail Hill rocks are of island-arc origin on the basis of their "andesitic" nature and their position within the Southern Uplands succession. Evidence herein shows that

the Bail Hill "andesites" are in fact hawaiites and mugearites, the suite having differentiated along the alkali basalt - hawaiite - mugearite - trachyte trend, and not the basalt - andesite - dacite - rhyolite trend of the calc-alkaline series, typical of island-arcs.

The Bail Hill rocks have been shown to be alkaline in character, and although such rocks are found in island-arc environments they are relatively uncommon and generally confined to the continental interior, landward of the trench (Miyashiro, 1973). This is incompatible with the tectonic position of the Bail Hill Volcanic Group within the sedimentary succession of the Iapetus Ocean. Furthermore, the alkaline rocks of island-arcs are generally shoshonitic, with K_2O/Na_2O close to unity and $(K_2O + Na_2O)$ showing little variation with differentiation (Jakes and White, 1969). In contrast, the Bail Hill rocks have $Na_2O > K_2O$ and $(Na_2O + K_2O)$ shows a marked increase with differentiation.

Alkaline rocks are very rarely found in intra-oceanic island-arcs and even when they are present are subordinate to subalkaline varieties (DeLong et.al., 1975). These centres generally contain a single alkaline rock-type (e.g. alkali basalt or mugearite) (DeLong et.al., 1975) rather than a suite of related rock-types as found at Bail Hill.

It is concluded that there is no evidence, tectonic, geochemical or petrographic, to support the concept of an island-arc origin for the Bail Hill Volcanic Group.

A more plausible explanation for the nature and tectonic setting of the Bail Hill Volcanic Group is that it

represents the remnants of a "within-plate" volcano of ocean-island type. The volcano never broke through sea-level so the Bail Hill volcano would have been a seamount rather than an ocean-island. Modern seamounts have, for reasons of accessibility, received relatively little attention when compared with ocean islands, even though they are numerically more abundant (Batiza, 1977). However, the work that has been carried out suggests they are smaller submarine equivalents of ocean islands and their volcanic origin is not in doubt (Batiza, 1977; Hall et.al., 1977; Sullivan and Keen, 1977; D.S.D.P. reports).

The nature of the volcanism at Bail Hill and in particular the increase in pyroclastic activity with time is analogous to the sequence of events anticipated during the formation of a typical seamount (Tazieff, 1971). Early extrusion of basaltic lavas would build up a volcanic cone to a height where the level of hydrostatic pressure was sufficiently low to allow pyroclastic activity to take place (Tazieff, 1971). At Bail Hill early activity was of basalt-lava extrusion (Cat Cleuch Formation), whilst the later activity was dominantly pyroclastic, with subordinate amounts of lava (Peat Rig Formation). Tazieff (1971) indicates that the flat-topped profile of modern seamounts is congenital, indicative of eruption under considerable hydrostatic pressure rather than subsequent subaerial erosion. The configuration of the Bail Hill Volcanic Group, with its relatively planar upper surface, may be a representative cross-section through the volcano as it existed in Ordovician times, immediately after the final

activity. In agreement with this there is no evidence of subaerial erosion at the top of the volcanic pile.

Further evidence for a seamount-type origin for the Bail Hill rocks comes from consideration of the lavas themselves. Bonatti (1970) states that granulation of volcanic products by lava-seawater interaction is typical of the submarine, central-type volcanism of seamounts and contrasts with the quiet fissural eruptions of a mid-ocean ridge environment. Such a process of lava-seawater interaction has been invoked to explain the auto-brecciation of lavas in the Bail Hill Volcanic Group.

Lithologically similar material to that of Bail Hill has been dredged from seamounts off the Canadian coast, which are partially or wholly buried by contemporaneous clastic sedimentation (Hall et.al., 1977). This is reminiscent of the burial of the Bail Hill volcano beneath the sediments of the Kiln and Spothfore Formations. Zeolite-facies metamorphism and hydrothermal alteration, similar to processes altering the Bail Hill rocks, have been observed in material from the Muir Seamounts, off Bermuda (Hall et.al., 1977).

Further evidence for contemporaneous clastic sedimentation and volcanism is provided by Sullivan and Keen (1977) in a study of the Newfoundland Seamounts. Their studies indicate the seamounts are composed of a suite of alkaline rocks, from basalts, through hawaiites and mugearites, to trachytes, similar to the lithologies found at Bail Hill. The Newfoundland Seamounts also show signs of hydrothermal alteration and rocks are in the zeolite-

facies grade of metamorphism (Sullivan and Keen, 1977). The summits of these seamounts are commonly 1500-2000 m above the adjacent ocean floor (Sullivan and Keen, 1977). If, as has been suggested, the present-day configuration of the Bail Hill Volcanic Group is a representative cross-section through the original volcano, then its original dimensions would have been approximately 3 km wide (at the base) by 1.5 km high (assuming half to be buried under the Sanquhar Coal Basin), a figure of the same order of magnitude as the Newfoundland Seamounts.

Present-day ocean-island volcanoes also provide interesting parallels to the Bail Hill rocks. For example, plutonic masses, similar to that inferred beneath Bail Hill, have been exposed by deep erosion beneath the volcanic rocks of Fuerteventura and Tahiti (Carmichael et.al., 1974). The presence of coarse-grained xenoliths is a characteristic feature in alkaline rocks of ocean-island type (Borley, 1974) and the xenoliths have been cited as evidence for the presence of plutonic material at shallow depths below the volcanoes. (Carmichael et.al., 1974, and references therein.). Although petrographically similar xenoliths have been found in some island-arc volcanics, the host lavas are subalkaline (Yamazaki et.al., 1966; Lewis, 1973) and bear little affinity with those of Bail Hill.

The Bail Hill rocks show petrographical and geochemical similarities to the "moderately alkaline" group of Baker (1973), for volcanic islands in the South Atlantic. The three island groups represented (Tristan da Cunha, St.Helena and Gough Island) have potassic affinities,

in contrast to the sodic series of Bail Hill. However, the similarity in the alkalis-silica variation between Bail Hill and Baker's (1973) Group 2 is manifest when Figure 9(b) is compared with his Figure 4. The rocks of these three island groups are nepheline and olivine-normative, similar to Bail Hill, and are believed to be the products of fractional crystallisation (Baker, 1973, and references therein.). The presence of petrographically similar xenoliths, the silica-undersaturated nature of the lavas and the compositional range of lithologies produced from a single magma by differentiation suggest a similar petrogenesis for the four volcanic suites (South Atlantic data from Baker (1973)).

It is concluded that the nature of the volcanism at Bail Hill, the lithologies present, the secondary processes affecting them and their position within the Southern Uplands succession are consistent with the interpretation of Bail Hill as a seamount within the Iapetus Ocean. Processes analagous to those inferred for the formation and setting of the Bail Hill volcano are active in modern ocean basins.

10.3 SEDIMENTATION AND FOREARC TECTONICS

In recent models the sedimentary rocks of the Southern Uplands have been interpreted as a typically oceanic succession (Dewey, 1969, 1971; Mitchell and McKerrow, 1975; McKerrow et.al., 1977). These models envisage radiolarian oozes (now cherts) being deposited on basal volcanics (the alleged Iapetus Ocean crust, not preserved in the

Bail Hill area), and being in turn succeeded by hemipelagic muds (black shales) and clastic sediments derived from a northwesterly (Laurentian) continent.

It has been shown in Chapter 4 that the clastic rocks of the Bail Hill area are the deposits of turbidity currents and related sediment gravity flows coming from the northeast or northwest. Local reworking of sedimentary and volcanic material by bottom currents produced thin arenaceous units. Although the basal stratigraphy is complicated by folding and faulting, the evidence suggests the clastic rocks were deposited on black shales and cherts. Thus the sedimentary succession in the Bail Hill area is consistent with an interpretation of the Southern Uplands sedimentary succession as Layer 1 of the Iapetus Ocean crust.

Piper (1972) drew analogies between the Southern Uplands succession and the deposits found in the present-day Aleutian Trench off Alaska. He concluded that the clastic rocks of the Southern Uplands were similar to turbidites found in the Aleutian Trench. This analogue is developed and modified below.

According to Piper (1972), the sediment distribution patterns in the Southern Uplands and in particular the axial palaeocurrent directions are indicative of trench sedimentation. However, modern trenches are characterised by a lack of volcanic activity and the presence of interbedded volcanics in the turbidite succession at Bail Hill indicates that sedimentation was not confined to a trench. The earliest volcanic activity at Bail Hill was erupted on

to hemipelagic muds (black shales), but during the subsequent volcanic activity the area moved within the compass of clastic sedimentation. This coincidence in the onset of volcanic activity with the change from hemipelagic to clastic (turbiditic) sedimentation can be explained by consideration of the structure of modern forearc regions. The terminology of Dickinson and Seely (1979) is used throughout.

In modern forearc systems the "trench" and "outer slope" pass seaward into a bathymetric high known as the "outer rise" ("outer swell" of Karig and Sharman, 1975). This has an arch-like profile, rising gently from the abyssal plain and bending more steeply into the trench (see Dickinson and Seely, 1979, Figure 2). The outer rise is up to 1 km above the neighbouring abyssal plain and is situated 100-200 km from the trench axis. The geometry of its arch-like profile produces a tensional regime in the upper crust and this area has been postulated as a region of igneous activity (Segawa and Tomoda, 1976).

Volcanic activity taking place in this region over a period of time would coincide with the transition from abyssal-plain sedimentation to sedimentation within the trench system (trench and outer slope). It is proposed that the igneous activity now represented by the Bail Hill Volcanic Group took place in this region, and that clastic sedimentation was ponded in the trench and outer slope, landward of the outer rise, whilst hemipelagic muds and radiolarian oozes were deposited seaward of the outer rise in the abyssal plain of the Iapetus Ocean.

The presence of sediments on the outer slope obviates the problem of the anomalous thickness of material in the postulated Lower Palaeozoic trench when compared with thicknesses in modern trenches. Von Huene (1974) states that modern trenches rarely contain more than 1000 m of sediment and typically contain less than 500 m. In contrast to this, the Kiln and Spothfore Formations in the Bail Hill area attain a thickness of 1.8 km and have been interpreted as a continuous stratigraphic sequence with little internal repetition of strata. On uniformitarian grounds it is unlikely that this 1.8 km could represent trench-fill. If, however, part or all of the Kiln Formation was deposited on the outer slope, then the thickness of trench-fill (the Spothfore Formation) would decrease to between 300 and 800 m. These figures are compatible with trench-fill thicknesses in modern environments (Von Huene, 1974).

The apparent absence of distal turbidites from the Bail Hill area suggests the confinement of turbidites to a trench system precluded the development of a deep-sea fan system (Schweller and Kulm, 1978). If clastic sedimentation was confined to the trench system then distal turbidites would not be found seaward of the feeder system (as in a deep-sea fan), but within the trench itself at some considerable distance from the point source. Therefore, the nature of the material succeeding the abyssal plain sediments in any given area would depend on the distance of that area from the point source supplying sediment to the trench. The dominance of proximal turbidites in the Bail Hill area

suggests it was situated relatively close to the feeder system(s).

The provenance of the sediments is considered next. The petrography of the greywackes consists of varying amounts of igneous, sedimentary and metamorphic rock-fragments, together with quartz and feldspar in an argillaceous matrix. Palaeocurrent directions, although scarce, are consistent in indicating currents flowing to the southwest or southeast, in agreement with the concept of turbidity currents originating on the northwestern Laurentian continent and transporting detritus into the trench system via submarine canyon feeder-systems. However, some of the material is clearly of intrabasinal origin (e.g. greywacke, siltstone, shale and chert clasts) and arenaceous units suggest local reworking of earlier deposited material by bottom currents. In the light of this the nature and source of "andesitic" detritus and ferromagnesian grains in the greywackes of the Northern Belt and Longford-Down are assessed.

The presence of "andesitic" and/or ferromagnesian detritus in greywackes of the Northern Belt and their Irish equivalents has been well documented (Welsh, 1961; Kelling, 1961, 1962; Floyd, 1975; Sanders and Morris, 1978). "Andesitic" detritus has also been recognised in the greywackes and rudites of the Bail Hill area, although ferromagnesian minerals are scarce or absent. Recent models suggest that this material was derived from a chain of volcanoes on the Laurentian continent in Ordovician times, directly related to the northwesterly subduction system (Mitchell and McKerrow, 1975; Sanders and Morris, 1978).

The suggestion of Mitchell and McKerrow (1975) that the "andesitic" material was derived from volcanoes in the Midland Valley is in direct contrast to detailed studies of the petrography of the greywackes which suggest intrabasinal sources for this material (Ritchie and Eckford, 1935; Kelling, 1962; Walton, 1965b). Furthermore, there are no known examples of Ordovician volcanics in the Midland Valley that could have acted as sources for this material. A third factor against an extrabasinal origin for this volcanic material is its pristine nature, which would argue against significant weathering, erosion or transportation prior to incorporation in the greywackes.

The clinopyroxene and amphibole analyses presented by Sanders and Morris (1978) are very similar in composition and association to material found at Bail Hill. Sanders and Morris (1978) suggest the parent magma to these crystals was subalkaline, on the basis of pyroxene chemistry. However, it was noted in Chapter 7 that under certain conditions alkaline magmas crystallise pyroxenes with subalkaline affinities (see also Barberi et.al., 1971; Gibb, 1973; Nisbet and Pearce, 1978). Furthermore, Sanders and Morris (1978) have plotted zoned phenocrysts on diagrams designed for unzoned groundmass pyroxenes, a method known to produce spurious results (Gibb, 1973). In view of this their suggestion of a subalkaline parent magma for the "andesitic" and ferromagnesian detritus is unsupported. A more plausible explanation in view of the chemical similarities with Bail Hill material and its pristine nature, is that the detritus was derived from "intrabasinal" volcanism similar to that of

Bail Hill.

Further evidence for an intrabasinal source for the ferromagnesian detritus is inferred from the present author's observations of material in Blackcraig Formation greywackes (Floyd, 1975). Clinopyroxene and amphibole fragments in the Blackcraig greywackes are remarkably fresh and optically similar to varieties found in the Bail Hill Volcanic Group. The presence of calcic plagioclase in these rocks (Floyd, 1975) further suggests affinities with Bail Hill. This must remain unsubstantiated, however, as a result of the apparent absence of palaeocurrent indicators in the Blackcraig greywackes (Floyd, 1975), although it is noted that the southwesterly-flowing currents implied by this model have been observed in the Bail Hill area and elsewhere in the Northern Belt. Compositional similarity between igneous clinopyroxenes in intrabasinal igneous rocks and grains in greywackes has been noted in the Leadhills area, within the Northern Belt (B.C.Hepworth, pers. comm., 1979), in corroboration of the above model.

The presence of intrabasinal clasts of sedimentary material has been reported by many authors working in the Southern Uplands and Sanders and Morris (1978) recognise similar material in the Longford-Down greywackes. Reworking of sedimentary and volcanic detritus has been recognised in arenaceous units within the Kiln Formation in the Bail Hill area. Clearly currents were able to erode, transport and redeposit earlier deposits inside the basin. In view of this there seems little need to look for hypothetical

extrabasinal sources for the volcanic detritus, particularly when a petrographically similar suite of rocks is known to have existed in the Bail Hill area. The "andesitic" detritus in the greywackes is therefore interpreted as alkaline basalts, hawaiites, mugearites and trachytes derived from "within-plate" ocean island or seamount sources.

The nature of the eroding currents and the location of the original material is problematical. The erosive power of turbidity currents is widely believed to be confined to the submarine canyon system, although Crook (1959) suggests that currents may retain some erosive power within the basin of deposition. Bottom currents in modern-day oceans are capable of eroding and transporting large amounts of material (Heezen, 1959; Johnson, 1972) and the arenaceous units in the Kiln Formation attest to the presence of such currents in the Bail Hill area. It seems unlikely, however, that these currents would be capable of anything other than localised redistribution. An alternative explanation for intrabasinal reworking is that material was accreted onto the facing edge of the continent and subsequently eroded by sediment gravity flows, thereby mixing extrabasinal and intrabasinal material. This is considered in more detail below.

The nature and source of the clasts in the Spothore Formation are considered next. The clasts are all of intrabasinal material and vary from brittle (fully lithified) to unconsolidated plastic masses (non-lithified). The absence of shallow-water lithologies, the nature and association of the rudites themselves and the apparent

absence of a subaerial landmass containing such lithologies in N. gracilis times, suggest the clasts were eroded and transported in a submarine environment. A graptolite fauna from a shale clast in the rudites is from lower down in the N. gracilis zone than any of the in situ faunas collected in the area. Taken together with the solitary palaeocurrent indicator in the Spothfore rudites it suggests the clasts were eroded from older abyssal plain, outer slope and trench sediments lying to the northwest of the present area. A mechanism for the formation of the Spothfore rudites is presented below.

In the accretionary-prism model the successions lying to the northwest of the present area were sequentially stripped from the ocean crust and accreted on to the Laurentian continental margin prior to the succession in the Bail Hill area. Recycling of this earlier-accreted material would provide the intrabasinal clasts of the Spothfore rudites. Two alternatives are proposed, both of which involve obstruction of feeder systems. The first requires obstruction of a submarine canyon by the accretion of material at its base. In this case it is assumed that the currents flowing down these canyons would be partially obstructed and would cut through this material. The erosive power of the currents in submarine canyons is well documented (e.g. Shepard and Dill, 1966) and the resultant material would be transported a short distance into the trench where it would be deposited as "chaotic" units. The second mechanism requires the accretion of material on to the inner wall of the trench to be followed by the slumping

of material back into the trench. Currents flowing axially along the trench would erode, transport and redeposit this material as rudaceous units. A similar situation has been envisaged in the Aleutian Trench, where the erosion of the slumped material is due to the presence of the main channel followed by turbidity currents being close to the inner wall of the trench (Piper et.al., 1973).

A similar situation may have existed in the Southern Uplands trench.

In both instances the rudite deposits would be localised within the trench itself and would pass laterally into sand or silt turbidites. This model is also capable of recycling sand-grade material and as such is a potential mechanism for the redistribution of intrabasinal volcanic detritus inferred above. A critical point with regard to this is the presence of volcanic clasts in the Spothore rudites. If, as has been alleged, the clasts in the rudites are older than the succession in the Bail Hill area, then the lava-clasts in the rudites represent an earlier volcanic event than that at Bail Hill. Petrographically the clasts are similar to the middle stage hawaiiite/mugearite activity of Bail Hill. The presence of prehnite along the cleavage in biotite/phlogopite phenocrysts suggests the rocks may have a similar petrogenesis to those of Bail Hill.

Ritchie and Eckford (1935), Kelling (1961, 1962), Floyd (1975) and Kelling and Holroyd (1978) have described similar material in conglomerates and granule sandstones from other localities in the Northern Belt. It is evident

that although this material may be confined to N.gracilis times, it is not confined to a single stratigraphic horizon. From consideration of the stratigraphy of this area it is evident that the Bail Hill volcano was only in existence for a small part of N.gracilis time, which may span 8 m.y. (Churkin and Carter, 1977).

It is therefore suggested that volcanism related to the Bail Hill episode took place prior to and possibly after the extrusion of the Bail Hill Volcanic Group itself. The tendency for modern seamounts to occur in groups rather than existing as isolated centres is well documented (e.g. Hall et.al., 1977) and it seems plausible that Bail Hill should represent only one of a number of volcanic centres, stemming from a single tectonic regime and ranging over a time-span of the order of millions of years. Each of these centres could have provided material for recycling and incorporation in the sedimentary succession. Material would be expected to be of an alkaline nature, similar to Bail Hill, but would show petrographical differences dependent on the degree of differentiation and the individual histories of volcanic centres. The suggestions of Ritchie and Eckford (1935) and Kelling (1962) that centres similar to Bail Hill existed as sources for detritus in the "Haggis Rock" and Corsewall rocks, respectively, are consistent with these conclusions. Indeed, the volcanic clasts in the Spothore rudites are inferred to come from an earlier centre than nearby Bail Hill. Similar intrabasinal sources could be proposed to account for volcanic phenocrysts and detritus in the Marchburn and Blackcraig Formations of

Floyd (1975), the Portpatrick rocks of Kelling (1962) and the Red Island Formation of Sanders and Morris (1978).

Despite the indication above that a number of volcanic centres may have existed in N. gracilis times on the northern margin of the Iapetus Ocean, it is evident that very few traces of in situ volcanic activity are found in the present-day Northern Belt of the Southern Uplands. Three possible explanations are given. Firstly, the volcanic centres were not detached from the downgoing oceanic plate and were subducted rather than accreted. Secondly, the centres were accreted, but lie above or below the present-day erosion level in the Southern Uplands. Thirdly, the centres were detached from the downgoing plate, but had too great a relief to be incorporated in the accretionary prism. In this instance the volcanic material above the sediment-water interface would be detached from the sedimentary succession and would remain as a large block in the trench or inner-wall environment and would eventually be eroded away.

The depositional environment of the Glenflossh and Guffock Formations is problematical. Although they have been identified as proximal sand turbidites there are few features of use in delineating their position within the postulated forearc system. Although basal exposures are poor it seems probable that the change from abyssal plain muds and oozes to coarse-sand turbidites is fairly sharp. The apparent absence of distal turbidites and the axial palaeocurrent directions are indicative of trench sedimentation rather than sedimentation in a deep-sea

fan (Piper, 1972). However, it is not possible to resolve whether these turbidites are outer slope deposits or trench-fill material.

In the eastern Aleutian trench sand turbidites are found in an axial channel which abuts against the inner wall of the trench (Piper et.al., 1973). In the absence of more detailed studies of the sand turbidites of the Glenflossh and Guffock Formations they are tentatively interpreted as deposits in an axial channel possibly located close to the inner wall of the trench.

10.4 MODEL FOR THE BAIL HILL AREA

The geological history of the Bail Hill area is consistent with the concept of an oceanic plate moving towards a destructive margin at a continent-ocean interface. Successive events at Bail Hill record the transition from the abyssal plain of the Iapetus Ocean, through the outer slope and into the region of trench fill itself. As such, analogues to the sequence of events at Bail Hill can be found in modern environments by examination of a succession of areas, progressively closer to a destructive margin. The model outlined below demonstrates the similarity in sedimentation, volcanism and tectonics between the Bail Hill area and the modern Alaskan Abyssal Plain and eastern Aleutian Trench.

The sequence at the base of the Kiln Formation has been tentatively inferred as cherts followed by black shales. These are believed to represent radiolarian oozes and hemipelagic muds respectively, that accumulated on the

the Iapetus abyssal plain. Subduction of oceanic crust beneath the Laurentian continent caused the area to migrate towards this northwesterly landmass. During N. gracilis time the area moved into the tensional regime of the outer rise, where igneous activity took place. Initially the activity was intrusive, forming a high-level magma chamber which differentiated by fractional crystallisation. Eventually, however, extrusive basaltic activity took place, building up a small volcanic edifice on top of black graptolitic muds. The modern Miller Seamount in the Alaskan Abyssal Plain is in an analogous position to that envisaged for Bail Hill, being situated on the fringe of turbiditic and hemipelagic sedimentation (Kulm, von Huene et.al., 1973).

As the Bail Hill area migrated through the outer rise into the outer slope it moved within the compass of clastic sedimentation. Here, a sequence of rapidly accumulating silt turbidites, with occasional sandy units, built up on top of the earlier hemipelagic deposits. At the same time volcanic activity, representing the middle and late-stage activity at Bail Hill, built a seamount up to 1500 m above the contemporaneous turbidite deposits.

The situation is analogous to D.S.D.P. sites 178/179. Here, silt turbidites dominate a 777 m sedimentary succession which includes interbedded volcanic-ash units (Kulm, von Huene et.al., 1973). The Bail Hill seamount was situated in an environment similar to that of the present-day Giacomini Seamount (Kulm, von Huene et.al., 1973). Following the cessation of volcanism at Bail Hill

(still within N. gracilis times), turbidite deposits (middle and upper Kiln Formation) built up around the seamount, gradually diminishing its relief. At some stage the area moved into the region of trench-fill. This may have occurred during deposition of the upper part of the Kiln Formation (channel-mouth sands and silts), or at the boundary between the Kiln and the Spothfore Formations. The extremely coarse nature of the Spothfore rudites suggest they are trench-fill deposits, located close to the inner wall.

At the onset of deposition of the Spothfore rudites the Bail Hill seamount would have been situated within the trench itself, in an analogous position to the Kodiak Seamount in the Aleutian Trench (Kulm, von Huene et. al., 1973). Unlike the Kodiak Seamount, however, the Bail Hill seamount would have had little bathymetric relief at this time, having been swamped by the sandstones and siltstones of the middle and upper Kiln Formation. Eventually the Bail Hill seamount was buried beneath the rudites of the Spothfore Formation.

At the time the Spothfore rudites were being deposited the area was in an analogous position to D.S.D.P. site 180, although the Spothfore Formation is inferred to have been deposited close to the inner wall (i.e. landward of D.S.D.P. site 180). The coarse nature of the Spothfore Formation reflects its alleged deposition close to the inner wall of the trench and its derivation from a nearby feeder system or slump. In contrast the finer grained rocks of the D.S.D.P. site 180 reflect their location away

from the inner wall of the trench and outside the main axial channel as well as the absence of nearby feeder systems and/or slumps (Kulm, von Huene et.al., 1973; Piper et.al., 1973).

Following the deposition of the Spothfore Formation the Bail Hill area was accreted on to the facing edge of the Laurentian continent. Decollement took place along the black shale horizon, with the result that underlying material, excepting a few thin slivers of chert, were subducted rather than accreted. The postulated Iapetus oceanic crust, together with the bulk of the chert horizon, are not preserved in the Bail Hill area, suggesting they have been subducted. The cumulate body inferred to have existed in the upper mantle or lower crust beneath Bail Hill would have been subducted along with Layers 2 and 3 of the Iapetus ocean-crust.

ACKNOWLEDGMENTS

The project was originally suggested by Professors J.B.Dawson and E.K.Walton. I would like to thank my supervisor, Professor E.K.Walton for his advice and encouragement at all stages of the project.

Among the staff members of the Department of Geology at St.Andrews I am particularly indebted to Dr.W.E.Stephens for his help in setting up the catanorm computer programme, and Dr.G.J.Oliver and Dr.C.H.Donaldson for critically appraising parts of the manuscript.

The identification of the graptolites was carried out by Dr.R.B.Rickards, University of Cambridge, and is gratefully acknowledged.

Electron microprobe work was carried out at the Grant Institute of Geology, University of Edinburgh, and the help of Messrs. P.G.Hill and C.Begg was instrumental to this.

Among the technical staff of the University of St.Andrews I wish to acknowledge Messrs. D.Pirie, A.Barman and A.Mackie for thin-section work, Mr.R.A.Batchelor for help with the geochemical work and Mr.J.Allen for his excellent photographic work.

The manuscript was typed by Anne Bennett and the tables by Lyndsey Oliver and the fact that they never once mis-read my writing speaks volumes for their diligence.

Last, but certainly not least, I am particularly grateful to Peg Miller and family in Crawick for looking after me during my field-work seasons. The excellent

catering of Peg Miller was especially appreciated and made many a wet, windy field-work day quite bearable.

The award of a grant in support of this work by the Natural Environment Research Council is gratefully acknowledged.

REFERENCES

- ANDERSON, T.B. & CAMERON, T.D.J. (in press). A structural profile of Caledonian deformation in Down. In: The Caledonides of the British Isles reviewed. I.G.C.P. Conference 1978.
- AOKI, K.I. 1959. Petrology of alkali-rocks of the Iki Islands and Higashi-matsuura district, Japan. Tohoku Univ. Sci. Repts., 3rd ser., 6, 261-311.
- BAKER, I. 1969. Petrology of the volcanic rocks of Saint Helena island, South Atlantic. Bull. geol. Soc. Am. 80, 1283-1310.
- BAKER, P.E. 1973. Islands of the South Atlantic. In: Nairn and Stehli (eds.), The Ocean Basins and Margins. Vol.1. Plenum Press. pp. 493-551.
- BAKER, P.E., GASS, I.G., HARRIS, P.G. & LEMAITRE, R.W. 1964. The volcanological report of the Royal Society Expedition to Tristan da Cunha, 1962. Philos. Trans. R. Soc. London, ser.A. 256, 439-578.
- BAMFORD, D., NUNN, K., PRODEHL, C. & JACOBS, B. 1977. Upper Crustal structure of Northern Britain. J. geol. Soc. London. 133, 481-488.
- BARAGAR, T.N. & IRVINE, W.R.A. 1971. A guide to the chemical classification of the common volcanic rocks. Can. J. Earth Sci. 8, 523-548.
- BARBERI, F., BIZOUARD, H. & VARET, J. 1971. Nature of the clinopyroxene and iron-enrichment in alkalic and transitional basaltic magmas. Contrib. Mineral. Petrol.

33, 93-107.

- BATIZA, R. 1977. Age, volume, compositional and spatial relations of small, isolated oceanic central volcanoes. Mar. Geol. 24, 169-183.
- BONATTI, E. 1970. Deep sea volcanism. Naturwissenschaften. 57, 379-384.
- BONATTI, E., HONNOREZ, J., KIRST, P. & RADICATI, F. 1975. Metagabbros from the Mid-Atlantic ridge at 06°N: Contact-hydrothermal-dynamic metamorphism beneath the axial valley. J. Geol., Chicago. 83, 61-78.
- BORLEY, G.D. 1974. Oceanic islands. In: Sorensen (ed.), The Alkaline Rocks. John Wiley and Sons. 311-329.
- BOUMA, A.H. 1962. Sedimentology of Some Flysch Deposits. Elsevier, Amsterdam.
- BOUMA, A.H. & HOLLISTER, C.D. 1973. Deep ocean basin sedimentation. In: G.V.Middleton and A.H.Bouma (eds.), Turbidites and Deep-Water Sedimentation. Soc. Econ. Palaeont. Mineral. Pacific Section, Short Course, Anaheim. pp. 79-118.
- BOYD, F.R. 1956. Hydrothermal investigation of amphiboles. In: P.H.Abelson (ed.), Researches in Geochemistry. Wiley, New York. p.377-396.
- BRIDEN, J.C., MORRIS, W.A. & PIPER, J.D.A. 1973. Palaeo-magnetic studies in the British Caledonides - VI Regional and global implications. Geophys. J. R. astron. Soc. 34, 107-134.
- CAMPBELL, C.V. 1967. Lamina, laminaset, bed and bedset. Sedimentology. 8, 7-26.

- CARMICHAEL, I.S.E. 1964. The petrology of Thingmuli, a Tertiary volcano in eastern Iceland. J. Petrol. 5, 435-460.
- CARMICHAEL, I.S.E., TURNER, F.J. & VERHOOGEN, J. 1974. Igneous Petrology. McGraw Hill.
- CHURCH, W.R. & GAYER, R.A. 1973. The Ballantrae Ophiolite. Geol. Mag. 110, 497-510.
- CHURKIN, M., CARTER, C. & JOHNSON, B.R. 1977. Subdivision of Ordovician and Silurian time scale using accumulation rates of graptolitic shales. Geology 5, 452-456.
- COLEMAN, R.G. 1977. Ophiolites. Springer-Verlag, Berlin.
- COOMBS, D.S., ELLIS, A.J., FYFE, W.S. & TAYLOR, A.M. 1959. The zeolite facies, with comments on the interpretation of hydrothermal syntheses. Geochim. cosmochim. Acta. 17, 53-107.
- CRAIG, G.Y. & WALTON, E.K. 1959. Sequence and structure in the Silurian rocks of Kirkudbrightshire. Geol. Mag. 96, 209-220.
- CROOK, K.A.W. 1959. Unconformities in turbidite sequences. J. Geol., Chicago. 67, 710-713.
- DAVIES, I.C. & WALKER, R.G. 1974. Transport and deposition of resedimented conglomerates : the Cap Enrage Formation, Cambro-Ordovician, Gaspe, Quebec. J. Sediment. Petrol. 44, 1200-1216.
- DEER, W.A., HOWIE, R.A. & ZUSSMAN, J. 1962, 1963. Rock-Forming Minerals. Vols. 1-5. First Edition. London (Longman).
- DEER, W.A., HOWIE, R.A. & ZUSSMAN, J. 1978. Rock-Forming Minerals. Vol. 2A. Second Edition. London (Longman).

- DELONG, S.E., HODGES, F.N. & ARCULUS, R.J. 1975. Ultramafic and mafic inclusions, Kanaga Island, Alaska, and the occurrence of alkaline rocks in island arcs. J. Geol., Chicago. 83, 721-736.
- DEWEY, J.F. 1969. Evolution of the Appalachian/Caledonian orogen. Nature. London. 222, 124-129.
- DEWEY, J.F. 1971. A model for the Lower Palaeozoic evolution of the southern margin of the early Caledonides of Scotland and Ireland. Scott. J. Geol. 7, 219-240.
- DICKINSON, W.R. & SEELY, D.R. 1979. Structure and stratigraphy of forearc regions. Bull. Am. Assoc. Petrol. Geol. 63, 2-31.
- DOTT, R.L. 1964. Wacke, greywacke and matrix - what approach to immature sandstone classification? J. sediment. Petrol. 34, 625-632.
- DOWNES, M.J. 1974. Sector and oscillatory zoning in calcic augites from Mt. Etna, Sicily. Contrib. Mineral. Petrol. 47, 187-196.
- DOWTY, E. 1976. Crystal structure and crystal growth: II. Sector zoning in minerals. Am. Mineral. 61, 460-469.
- EALLES, M.H. 1978. The Moffat Shale Group of the Southern Uplands of Scotland : Structure, stratigraphy and palaeontology. Univ. Glasgow Ph.D. thesis (unpubl.).
- EYLES, J.M. An account of the igneous rocks in the neighbourhood of Bail Hill, Sanquhar. (Unpubl. account in I.G.S. building, Edinburgh).
- FERGUSON, A.K. 1973. On hour-glass sector zoning in clinopyroxene. Mineralog. Mag. London. 39, 321-325.

- FISKE, R.S. 1963. Subaqueous pyroclastic flows in the Ohanpecosh Formation, Washington. Bull. geol. Soc. Am. 74, 391-406.
- FISKE, R.S. & MATSUDA, T. 1964. Submarine equivalents of ash flows in Tokiwa Formation, Japan. Am. J. Sci. 262, 76-106.
- FITTON, J.G. & HUGHES, D.J. 1970. Volcanism and plate tectonics in the British Ordovician. Earth planet. Sci. Lett. 8, 223-228.
- FLOYD, J.D. 1975. The Ordovician Rocks of West Nithsdale. Univ. St. Andrews Ph.D. thesis (unpubl.).
- FLOYD, P.A. & WINCHESTER, J.A. 1975. Magma type and tectonic setting discrimination using immobile elements. Earth planet. Sci. Lett. 27, 211-218.
- FYFE, T.B. & WEIR, J.A. 1976. The Ettrick Valley Thrust and the upper limit of the Moffat Shales in Craigmichan scaurs. Scott. J. Geol. 12, 93-102.
- GEOLOGICAL SURVEY OF SCOTLAND MEMOIRS. 1871. Explanation of Sheet 15. H.M.S.O.
- GIBB, F.G.F. 1971. Clinopyroxene crystallisation from a basic magma of alkaline affinity. Nature (phys. Sci.) 230, 153-154.
- GIBB, F.G.F. 1973. The zoned clinopyroxenes of the Shiant Isles Sill, Scotland. J. Petrol. 14, 203-230.
- GRAY, N.H. 1971. A parabolic hourglass structure in titanaugite. Am. Mineral. 56, 952-958.
- GREIG, D.C. 1971. British Regional Geology. The South of Scotland. (3rd edition). H.M.S.O.

- GUNN, P.J. 1973. Location of the proto-Atlantic suture in the British Isles. Nature. London. 242, 111-112.
- HALL, A. 1966. The occurrence of prehnite in appinitic rocks from Donegal, Ireland. Mineralog. Mag. London. 35, 234-236.
- HALL, J.M., BARRETT, D.L. & KEEN, C.E. 1977. The volcanic layer of the ocean crust adjacent to Canada - a review. In: T.N.Baragar, R.G.Coleman and J.M.Hall (eds.), Volcanic Regimes in Canada. Geol. Soc. Canada Sp. Paper 16, 425-444.
- HARLAND, W.B. & GAYER, R.A. 1972. The Arctic Caledonides and earlier Oceans. Geol. Mag. 109, 289-314.
- HARRIS, P.M., FARRAR, E., MACINTYRE, R.M., YORK, D. & MILLER, J.A. 1965. Potassium-argon age measurements on two igneous rocks from the Ordovician system of Scotland. Nature. London. 205, 352-353.
- HART, S.R., ERLANK, E.J. & KABLE, E.J.D. 1974. Sea floor basalt alteration : some chemical and Sr isotopic effects. Contrib. Mineral. Petrol. 44, 219-230.
- HAYNES, L. 1973 Mineralogic assessment of geochemical drainage anomalies at Bail Hill, Dumfriesshire. Instit. of Geol. Sci. (Geochem. Division) Mineralogy Unit Report no. 135.
- HEEZEN, B.C. 1959. Deep-sea erosion and unconformities. J. Geol. Chicago. 67, 713-714.
- HENDRY, H.E. 1972. Sedimentation of deep water conglomerates in the Lower Ordovician rocks of Quebec - composite bedding produced by progressive liquefaction of sediment? J. sediment. Petrol. 43, 125-136.

- HESSE, R. 1975. Turbiditic and non-turbiditic mudstone of Cretaceous flysch sections of the East Alps and other basins. Sedimentology. 22, 387-416.
- HOLLISTER, L.S. & GANCARZ, A.J. 1971. Compositional sector-zoning in clinopyroxene from the Narce area, Italy. Am. Mineral. 56, 959-979.
- HOLLISTER, L.S. & HARGRAVES, R.B. 1970. Compositional zoning and its significance in pyroxenes from two coarse grained Apollo 11 samples. Proc. Apollo 11 Lunar Sci. Conf. 1, 541-550.
- HUGHES, C.J. 1972. Spilites, keratophyres and the igneous spectrum. Geol. Mag. 109, 513-527.
- HUMPHRIS, S.E. & THOMPSON, G. 1978a. Hydrothermal alteration of oceanic basalts by seawater. Geochim. cosmochim. Acta. 42, 107-125.
- HUMPHRIS, S.E. & THOMPSON, G. 1978b. Trace element mobility during hydrothermal alteration of oceanic basalts. Geochim. cosmochim. Acta. 42, 127-136.
- JAKES, P. & WHITE, A.J.R. 1969. Structure and distribution of the Melanesian arcs and correlation with the distribution of magma types. Tectonophysics. 8, 223-236.
- JOHNSON, D.A. 1972. Ocean floor erosion in the equatorial Pacific. Bull. geol. Soc. Am. 83, 3121-3144.
- KARIG, D.E. & SHARMAN, G.F. 1975. Subduction and accretion in trenches. Bull. geol. Soc. Am. 86, 377-389.
- KELLING, G. 1961. The stratigraphy and structure of the Ordovician rocks of the Rhinns of Galloway. J. geol. Soc. London. 117, 37-75.

- KELLING, G. 1962. The petrology and sedimentation of Upper Ordovician rocks in the Rhinns of Galloway, south-west Scotland. Trans. R. Soc. Edinburgh. 65, 107-137.
- KELLING, G. & HOLROYD, J. 1978. Clast size, shape and composition in some ancient and modern fan gravels. In: D.J.Stanley and G.Kelling (eds.), Sedimentation in Submarine Canyons, Fans and Trenches. Dowden, Hutchinson & Ross, Stroudsburg. Pa., p.138-159.
- KENNEDY, W.Q. 1936. An apatite rock from Dumfriesshire. Progr. Geol. Surv. Gt. Britain. 1935 pt.II, 53-59.
- KUENEN, P.H. 1964. The shell pavement below oceanic turbidites. Mar. Geol. 2, 236-246.
- KULM, L.D., VON HUENE, R. et.al. 1973. Initial Reports of the Deep Sea Drilling Project, Volume 18, Washington (U.S. Government Printing Office). 1077p.
- KULM, L.D. & FOWLER, G.A. 1974. Oregon continental margin structure and stratigraphy : A test of the imbricate thrust model. In: C.A.Burk and C.L.Drake (eds.), The Geology of Continental Margins. Springer-Verlag. pp. 261-283.
- KUSHIRO, I. 1960. Si-Al relations in clinopyroxenes from igneous rocks. Am. J. Sci. 258, 548-554.
- LEAKE, B.E. 1978. Nomenclature of amphiboles. Can. Mineral. 16, 501-520.
- LEBAS, N.J. 1962. The role of aluminium in igneous pyroxenes with relation to their parentage. Am. J. Sci. 260, 267-288.

- LEMAITRE, R.W. 1962. Petrology of volcanic rocks, Gough Island, South Atlantic. Bull. geol. Soc. Am. 73, 1309-1340.
- LEMAITRE, R.W. 1969. Kaersutite-bearing plutonic xenoliths from Tristan da Cunha, South Atlantic. Mineralog. Mag. London. 37, 185-197.
- LEWIS, J.F. 1973. Petrology of the ejected plutonic blocks of the Soufriere Volcano, St.Vincent, West Indies. J. Petrol. 14, 81-112.
- LIU, J.G. 1971. Synthesis and stability relations of prehnite. Am. Mineral. 56, 507-531.
- LIU, J.G. & ERNST, W.G. 1979. Oceanic ridge metamorphism of the East Taiwan ophiolite. Contrib. Mineral. Petrol. 68, 335-348.
- LONSDALE, P. 1979. A deep-sea hydrothermal site on a strike-slip fault. Nature. London. 281, 531-534.
- McKERROW, W.S. & COCKS, L.R.M. 1976. Progressive faunal migration across the Iapetus Ocean. Nature. London. 263, 304-305.
- McKERROW, W.S., LEGGETT, J.K. & EALES, M.H. 1977. Imbricate thrust model of the Southern Uplands of Scotland. Nature. London. 267, 237-239.
- MENZIES, M & SEYFRIED, W.E. 1979. Basalt-seawater interaction : trace element and strontium isotopic variations in experimentally altered glassy basalt. Earth planet. Sci. Lett. 44, 463-472.
- MIDDLETON, G.V. & HAMPTON, M.A. 1973. Sediment gravity flows : Mechanics of flow and deposition. In: G.V.Middleton and A.H.Bouma (eds.), Turbidites and

- Deep Water Sedimentation. Soc. Econ. Palaeont. Mineral., Pacific Section, Short Course, Anaheim. pp. 1-38.
- MITCHELL, A.H.G. 1974. Flysch-ophiolite successions : polarity indicators in arc and collision-type orogens. Nature. London. 248, 747-749.
- MITCHELL, A.H.G. & MCKERROW, W.S. 1975. Analogous evolution of the Burma orogen and the Scottish Caledonides. Bull. geol. Soc. Am. 86, 305-315.
- MIYASHIRO, A. 1974. Volcanic rock series in island arcs and active continental margins. Am. J. Sci. 274, 321-355.
- MIYASHIRO, A. 1978. Nature of Alkalic volcanic series. Contrib. Mineral. Petrol. 66, 91-104.
- MOORE, A.C. 1976. Intergrowth of prehnite and biotite. Mineralog. Mag. London. 40, 526-529.
- MURRAY, R.J. 1954. The clinopyroxenes of the Garbh Eilean Sill, Shiant Isles. Geol. Mag. 91, 17-31.
- MUTTI, E. 1977. Distinctive thin-bedded turbidite facies and related depositional environments in the Eocene Hecho Group (South-central Pyrenees, Spain). Sedimentology. 24, 107-131.
- NAKAMURA, Y. 1973. Origin of sector-zoning in igneous clinopyroxenes. Am. Mineral. 58, 989-990.
- NELSON, C.H., MUTTI, E. & RICCI-LUCCHI, F. 1975. Comparison of proximal and distal thin-bedded turbidites with current-winnowed deep-sea sands. IXth Int. Congr. of Sedimentology. 317-324.
- NISBET, E.G. & PEARCE, J.A. 1977. Clinopyroxene composition in mafic lavas from different tectonic settings.

- Contrib. Mineral. Petrol. 63, 149-160.
- O'HARA, M.J. 1977. Geochemical evolution during fractional crystallisation of a periodically refilled magma chamber. Nature. London. 266, 503-507.
- PANKHURST, R.J. 1977. Open system crystal fractionation and incompatible element variation in basalts. Nature. London. 268, 36-38.
- PAPIKE, J.J., CAMERON, K.I. & BALDWIN, K. 1974. Amphiboles and pyroxenes - characterisation of other than quadrilateral components and estimates of ferric iron from microprobe data. Abstr. Prog. geol. Soc. Am. 6, 1053-1054.
- PEACH, B.N. & HORNE, J. 1899. The Silurian Rocks of Britain, vol.1, Scotland. H.M.S.O.
- PEARCE, J.A. 1974. Statistical analysis of major element patterns in basalts. J. Petrol. 17, 15-43.
- PEARCE, J.A. & CANN, J.R. 1973. Tectonic setting of basic volcanic rocks determined using trace element analysis. Earth planet. Sci. Lett. 19, 290-300.
- PEARCE, J.A. & NORRY, M.J. 1979. Petrogenetic implications of Ti, Zr, Y and Nb variations in volcanic rocks. Contrib. Mineral. Petrol. 69, 33-47.
- PETTIJOHN, F.J. 1957. Sedimentary Rocks. (2nd edition). Harper and Row.
- PHILLIPS, E.R. & RICKWOOD, P.C. 1977. The biotite-prehnite association. Lithos. 8, 275-281.
- PHILLIPS, W.E.A., STILLMAN, C.J. & MURPHY, T. 1976. A Caledonian plate tectonic model. Jl. geol. Soc. Lond. 132, 579-609.

- PIPER, D.J.W. 1972. Trench sedimentation in the Lower Palaeozoic of the Southern Uplands. Scott. J. Geol. 8, 289-291.
- PIPER, D.J.W., VON HUENE, R. & DUNCAN, J.R. 1973. Late Quaternary sedimentation in the active eastern Aleutian Trench. Geology. 1, 19-22.
- PIPER, D.J.W. 1978. Turbidite muds and silts on deepsea fans and abyssal plains. In: D.J.Stanley & G.Kelling (eds.), Sedimentation in Submarine Canyons, Fans and Trenches. Dowden, Hutchinson & Ross, Stroudsburg, Pa. pp. 163-176.
- PIPER, J.D.A. 1978. Palaeomagnetism and palaeogeography of the Southern Uplands in Ordovician times. Scott. J. Geol. 14, 93-107.
- POWELL, D.W. 1970. Magnetised rocks within the Lewisian of Western Scotland and under the Southern Uplands. Scott. J. Geol. 6, 353-369.
- PRINGLE, J. 1948. British Regional Geology. The South of Scotland. (2nd edition). H.M.S.O.
- PRINZ, M. 1967. Geochemistry of basaltic rocks : Trace elements. In: H.H.Hess and A.Poldevaart (eds.), Basalts, vol.1. Wiley, New York. pp. 271-324.
- RAHMAN, S. 1975. Some aluminous clinopyroxenes from Vesuvius and Monte Somma, Italy. Mineralog. Mag. London. 40, 43-52.
- REINECK, H.E. & SINGH, I.B. 1973. Depositional Sedimentary Environments. Springer-Verlag, Berlin.
- RITCHIE, M & ECKFORD, R.J.A. 1935. The "Haggis Rock" of the Southern Uplands. Trans. geol. Soc. Edinburgh.

13, 371-377.

- ROCHLEAU, M. & LAJOIE, J. 1974. Sedimentary structures in resedimented conglomerate of the Cambrian flysch, L'Islet, Quebec Appalachians. J. sediment. Petrol. 44, 826-836.
- RUPKE, N.A. & STANLEY, D.J. 1974. Distinctive properties of turbiditic and hemipelagic mud layers in the Algero-Balearic Basin, western Mediterranean Sea. Smithson. Contrib. Earth Sci. no.13, 40pp.
- RUST, B.R. 1965. The stratigraphy and structure of the Whithorn area of Wigtownshire, Scotland. Scott. J. Geol. 1, 101-133.
- SANDERS, I.S. & MORRIS, J.H. 1978. Evidence for Caledonian subduction from greywacke detritus in the Longford-Down inlier. J. Earth Sci. R. Dubl. Soc. 1, 53-62.
- SCHWELLER, W.J. & KULM, L.D. 1978. Depositional patterns and channelized sedimentation in active eastern Pacific trenches. In: D.J.Stanley and G.Kelling (eds.), Sedimentation in Submarine Canyons, Fans and Trenches. Dowden, Hutchinson & Ross, Stroudsburg, Pa. p.311-324.
- SCOTT, A. 1914. Augite from Bail Hill, Dunfriesshire. Mineralog. Mag. London. 17, 100-110.
- SEELY, D.R., VAIL, P.R. & WALTON, G.G. 1974. Trench slope model. In: C.A.Burke and C.L.Drake (eds.), The Geology of Continental Margins. Springer-Verlag. p.249-260.
- SEGAWA, J. & TOMODA, Y. 1976. Gravity measurements near Japan and study of the upper mantle beneath the oceanic trench-marginal sea transition zones. Geophys. Monogr. Washington. 19, 35-52.

- SHEPARD, F.P. & DILL, R.F. 1966. Submarine Canyons and Other Sea Valleys. Rand, McNally and Co. Chicago.
- SPOONER, E.T.C. & FYFE, W.S. 1973. Sub-sea-floor metamorphism, heat and mass transfer. Contrib. Mineral. Petrol. 42, 287-304.
- STANLEY, D.J. 1964. Large mudstone-nucleus sand spheroids in submarine channel deposits. J. sediment. Petrol. 34, 672-676.
- STANLEY, D.J., PALMER, H.D. & DILL, R.F. 1978. Coarse sediment transport by mass flow and turbidity current processes and downslope transformation in Annot Sandstone canyon fan valley systems. In: D.J.Stanley and G.Kelling (eds.), Sedimentation in Submarine Canyons, Fans and Trenches. Dowden, Hutchinson & Ross, Stroudsburg, Pa. p.85-115.
- STOW, D.A.V. & BOWEN, A.J. 1978. Origin of lamination in deep sea, fine-grained sediments. Nature. London. 274, 324-328.
- STOW, D.A.V. & LOVELL, J.P.B. 1979. Contourites : Their recognition in modern and ancient sediments. Earth. Sci. Rev. 14, 251-290.
- SULLIVAN, K.D. & KEEN, C.E. 1977. Newfoundland seamounts : petrology and geochemistry. In: T.N.Baragar, R.G.Coleman & J.M.Hall (eds.), Volcanic Regimes in Canada. Geol. Soc. Canada Sp. Paper 16, 461-476.
- TAZIEFF, H. 1971. About deep-sea volcanism. Geol. Rdsch. 61, 470-480.
- THOMPSON, R.N. 1972. Oscillatory and sector zoning in augite from a Vesuvian lava. Carnegie Instit. Yrbook.

- Washington. 71, 463-470.
- TULLOCH, A.J. 1979. Secondary Ca-Al silicates as low-grade alteration products of granitoid biotite. Contrib. Mineral. Petrol. 69, 105-117.
- VERHOOGEN, J. 1962. Distribution of titanium between silicates and oxides in igneous rocks. Am. J. Sci. 260, 211-220.
- VON HUENE, R. 1974. Modern Trench Sediments. In: C.E.Burk and C.L.Drake (eds.), The Geology of Continental Margins. Springer-Verlag. p.207-211.
- WAGER, L.R. & BROWN, G.M. 1967. Layered Igneous Rocks. Oliver and Boyd, Edinburgh.
- WALKER, R.G. 1975. Generalised facies models for resedimented conglomerates of turbidite association. Bull. geol. Soc. Am. 86, 737-748.
- WALKER, R.G. 1976. Facies Models 2. Turbidites and associated coarse clastic deposits. Geoscience Can. 3, 25-36.
- WALKER, R.G. & MUTTI, E. 1973. Turbidite facies and facies associations. In: G.V.Middleton and A.H.Bouma (eds.), Turbidites and Deep Water Sedimentation. Soc. Econ. Palaeont. Mineral., Pacific Section, Short Course, Anaheim. p.119-158.
- WALTON, E.K. 1961. Some aspects of the succession and structure in the Lower Palaeozoic rocks of the Southern Uplands of Scotland. Geol. Rdsch. 50, 63-77.
- WALTON, E.K. 1963. Sedimentation and structure in the Southern Uplands. In: M.R.W.Johnston and F.H.Stewart (eds.), The British Caledonides. Oliver & Boyd,

- Edinburgh. p.71-97.
- WALTON, E.K. 1965a. Lower Palaeozoic Rocks - stratigraphy. In: G.Y.Craig (ed.), Geology of Scotland. Oliver & Boyd, Edinburgh. p.161-200.
- WALTON, E.K. 1965b. Lower Palaeozoic Rocks - palaeogeography and structure. In: G.Y.Craig (ed.), Geology of Scotland. Oliver & Boyd, Edinburgh. p.201-227.
- WEDEPOHL, K.H. (ed.). 1969, 1970, 1972, 1974, 1978. Handbook of Geochemistry. Vol.II/1-5. Springer-Verlag, Berlin.
- WELLS, A.K. & BISHOP, A.C. 1955. An appinitic facies associated with certain granites in Jersey, Channel Islands. J. geol. Soc. Lond. 111, 143-166.
- WELSH, W. 1964. The Ordovician Rocks of Northwest Wigtownshire. Univ. Edinburgh Ph.D. thesis (unpubl.).
- WILKINSON, J.F.G. 1956. Clinopyroxenes of alkali-basalt magma. Am. Mineral. 41, 724-743.
- WILKINSON, J.F.G. 1967. The petrography of basaltic rocks. In: H.H.Hess and A.Poldevaart (eds.), Basalts. Vol.1. John Wiley & Sons, New York. p.163-215.
- WILKINSON, J.F.G. 1974. The mineralogy and petrography of alkali basaltic rocks. In: H.Sorensen (ed.), The Alkaline Rocks. John Wiley & Sons, New York. p.67-95.
- WILLIAMS, A. 1976. Plate tectonics and biofacies evolution as factors in Ordovician correlation. In: M.G.Bassett (ed.), The Ordovician System. Univ. of Wales Press and National Museum. p.29-66.

- WILSON, J.T. 1966. Did the Atlantic close and then re-open? Nature. London. 211, 676-681.
- WINKLER, H.G.F. 1976. Petrogenesis of Metamorphic Rocks. 4th edition. Springer-Verlag.
- WINN, R.D. & DOTT, R.H. 1977. Large-scale traction-produced structures in deep-water fan-channel conglomerates in southern Chile. Geology. 5, 41-44.
- WISE, W.S. & TSCHERNICH, R.W. 1978. Habits, crystal forms and composition of thomsonite. Can. Mineral. 16, 487-493.
- WOOD, D.A., GIBSON, I.L. & THOMPSON, R.N. 1976. Element mobility during zeolite facies metamorphism of the Tertiary basalts of eastern Iceland. Contrib. Mineral. Petrol. 55, 241-254.
- WYLLIE, P.J. 1971. The Dynamic Earth. John Wiley & Sons, New York.
- YAMAZAKI, T., ONUKI, H. & TIBA, T. 1966. Significance of hornblende gabbroic inclusions in calc-alkaline rocks. Jap. Assoc. Min. Petrol. Econ. Geol. 55, 87-103.
- YODER, H.S. & EUGSTER, H.P. 1954. Phlogopite synthesis and stability range. Geochim. cosmochim. Acta. 6, 157-185.
- YODER, H.S. & TILLEY, C.E. 1962. Origin of basalt magmas : An experimental study of natural and synthetic rock systems. J. Petrol. 3, 342-532.

APPENDIX 1. LIST OF GRAPTOLITE SPECIMENS.

All specimens have been identified by Dr.R.B. Rickards.
Specimen numbers refer to the Sedgwick Museum collection where the
specimens are kept.

CAT CLEUCH TRIBUTARY (NS75781314)

Climacograptus bicornis (Hall)Corynoides sp.Dicranograptus rectus (Hopkinson)Didymograptus superstes (Lapworth)Glyptograptus teretiusculus (Hisinger) s.l.Orthograptus calcaratus (Lapworth) s.l.

Specimen nos. A.101956-101974

CAT CLEUCH (NS75861326)

? Amplexograptus perexcavatus (Lapworth)Corynoides sp.Cryptograptus tricornis (Carruthers)Dicellograptus aff. intortus (Lapworth)Dicranograptus aff. tardiusculus (Lapworth)? Didymograptus superstes (Lapworth)Glyptograptus aff. euglphus (Lapworth)? Nemagraptus gracilis (Hall)Orthograptus calcaratus (Lapworth)Pseudoclimacograptus scharenbergi (Lapworth) s.l.

Specimen nos. A.103935-103962

APPENDIX 1.

LIST OF GRAPTOLITE SPECIMENS

KILN BURN (NS77151350)

- Climacograptus bicornis (Hall)
Cryptograptus tricornis (Carruthers)
Dicranograptus brevicaulis (Elles and Wood)
Didymograptus superstes (Lapworth)
Glossograptus hincksi (Hopkinson)
Orthograptus calcaratus (Lapworth)

Specimen nos. A.101910-101921

KILN BURN (NS76891386)

- Climacograptus bicornis (Hall)
Climacograptus sp.
Corynoides sp.
Dicranograptus ramosus longicaulis (Lapworth)
or
Dicranograptus ramosus spirifer (Lapworth)
Glyptograptus ? euglyphus (Elles and Wood)
Orthograptus calcaratus (Lapworth) s.l.
Pseudoclimacograptus scharenbergi (Lapworth) s.l.

Specimen nos. A.103843-103859

APPENDIX 1. LIST OF GRAPTOLITE SPECIMENS

STOODFOLD BURN (NS76731384)

Cryptograptus tricornis (Carruthers)Dicellograptus aff. intortus (Lapworth)Glossograptus hincksi (Hopkinson)Glyptograptus aff. teretiusculus (Hisinger) s.l.Leptograptus validus incisus (Lapworth)?Orthograptus calcaratus (Lapworth)

Specimen nos. A.101899-101909

POLCRAIGY BURN (NS78181419)

Cryptograptus tricornis (Carruthers)Dicellograptus divaricatus salopiensis (Elles and Wood)Dicellograptus sextans exilis (Elles and Wood)Dicranograptus aff. ramosus (Hall)Dicranograptus rectus (Hopkinson)Didymograptus superstes (Lapworth)Glyptograptus teretiusculus (Hisinger) s.l.Nemagraptus gracilis (Hall)Orthograptus calcaratus (Lapworth) s.l.Pseudoclimacograptus scharenbergi (Lapworth) s.l.

Specimen nos. A.101838-101878

APPENDIX 1.

LIST OF GRAPTOLITE SPECIMENS

SPOTHFORD BURN (NS78681506)

?Amplexograptus perexcavatus (Lapworth)Cryptograptus tricornis (Carruthers)Dicellograptus cf. divaricatus salopiensis (Elles and Wood)Dicranograptus rectus (Hopkinson)Nemagraptus gracilis (Hall)

Specimen nos. A.101879-101886

SPOTHFORD BURN (NS78671506)

Dicellograptus cf. divaricatus salopiensis (Elles and Wood)Dicellograptus cf. sextans exilis (Elles and Wood)?Didymograptus superstes (Lapworth)Dicranograptus aff. tardiusculus (Lapworth)Hallograptus mucronatus (Hall)Pseudoclimacograptus scharenbergi (Lapworth) s.l.

Specimen nos. A.103761-103775

APPENDIX 1.

LIST OF GRAPTOLITE SPECIMENS

POLHOLM BURN (NS78001539)

?Amplexograptus perexcavatus (Lapworth)Climacograptus bicornis (Hall)Cryptograptus tricornis (Hopkinson)Corynoides sp.Dicellograptus cf. divaricatus salopiensis (Elles and Wood)Dicellograptus ? salopiensis rigens (Elles and Wood)Dicellograptus cf. sextans exilis (Elles and Wood)Dicranograptus ? ramosus (Hall)Dicranograptus aff. tardiusculus (Lapworth)?Didymograptus aff. superstes (Lapworth)Hallograptus mucronatus (Hall)Nemagraptus gracilis (Hall)Orthograptus calcaratus (Lapworth) s.l.Pseudoclimacograptus scharenbergi (Lapworth)s.l.

Specimen nos. A.103963-103996

APPENDIX I.

LIST OF GRAPTOLITE SPECIMENS

BACK BURN (NS791159)

- Climacograptus bicornis (Hall)
Corynoides sp.
Cryptograptus tricornis (Carruthers)
Dicellograptus divaricatus salopiensis (Elles and Wood)
Dicellograptus sextans exilis (Elles and Wood)
Dicranograptus ? ramosus (Hall)
Dicranograptus rectus (Hopkinson)
Dicranograptus aff. tardiusculus (Lapworth)
Dicranograptus sp. nov.
Didymograptus superstes (Lapworth)
Diplograptus arctus (Elles and Wood)
Glossograptus hincksi (Hopkinson)
Glyptograptus cf. euglyphus (Lapworth)
Glyptograptus teretiusculus (Hisinger) s.l.
Hallograptus mucronatus (Hall)
Leptograptus ? ascendens (Elles and Wood)
Nemagraptus gracilis (Hall)
Orthograptus calcaratus (Lapworth) s.l.
Pseudoclimacograptus scharenbergi (Lapworth) s.l.
Pseudoclimacograptus scharenbergi (Lapworth) cf stenostama
(Bulman)
Pseudoclimacograptus sp. nov.

Specimen nos. A.101780-101837 and A.103648-103760

APPENDIX 1.

LIST OF GRAPTOLITE SPECIMENS

B740 SANQUHAR-CRAWFORDJOHN ROAD

(NS80571561)

Climacograptus bicornis (Hall)? Climacograptus antiquus lineatus (Elles and Wood)Corynoides sp.Cryptograptus tricornis (Carruthers)Dicellograptus aff. intortus (Lapworth)? Dicellograptus divaricatus salopiensis (Elles and Wood)Dicellograptus sextans exilis (Elles and Wood)Didymograptus superstes (Lapworth)Diplograptus sp. s.s.Glossograptus cf. hincksi (Hopkinson)Glyptograptus euglyphus (Lapworth)Glyptograptus teretiusculus (Hisinger) s.l.Hallograptus mucronatus (Hall)Lasiograptus harknessi costatus (Lapworth)Leptograptus validus incisus (Lapworth)Nemagraptus gracilis (Hall)Orthograptus calcaratus (Lapworth)Pseudoclimacograptus cf. scharenbergi (Lapworth)Pseudoclimacograptus cf. scharenbergi stenostoma (Bulman)

Specimen nos. A.101936-101955 and A.103860-103934

APPENDIX 1.

LIST OF GRAPTOLITE SPECIMENS

POLTHISTLY BURN

(NS79561626)

Dicranograptus ? ramosus (Hall)Didymograptus superstes (Lapworth)cf. Diplograptus arctus (Elles and Wood)Glyptograptus tertiusculus (Hisinger) s.l.? Nemagraptus gracilis (Hall)Orthograptus calcaratus (Lapworth)Pseudoclimacograptus cf. scharenbergi scharenbergi (Lapworth)Pseudoclimacograptus cf. scharenbergi stenostoma (Bulman)

Specimen nos. A.101922-101935

KILN BURN

(NS76731449)

CLAST IN CONGLOMERATE

Climacograptus bicornis (Hall)Corynoides sp.Dicellograptus ? intortus (Lapworth)Dicranograptus aff. tardiusculus (Lapworth)? Didymograptus superstes (Lapworth)? Glyptograptus euglyphus (Elles and Wood)Nemagraptus gracilis (Hall)Orthograptus calcaratus (Lapworth)Pseudoclimacograptus scharenbergi (Lapworth) s.l.

Specimen nos. A.103807-103820 and A.103841-2

APPENDIX 1.

LIST OF GRAPTOLITE SPECIMENS

SPOTHFORD BURN (NS77931521) CLAST IN CONGLOMERATE

Corynoides sp.

Dicellograptus ? divaricatus rigidus (Lapworth)

Dicellograptus cf. intortus (Lapworth)

Diplograptus sp.

Glyptograptus teretiusculus (Hisinger)

? Orthograptus calcaratus (Lapworth)

Pseudoclimacograptus aff. scharenbergi stenostoma (Bulman)

Specimen nos. A.103776-103790

All assemblages belong to the N. gracilis zone, although assemblages from the Cat Cleuch, Kiln Burn, Stoodfold Burn and Polthistly Burn do not contain the characteristic fossil, Nemagraptus gracilis (R.B. Rickards, written communication). The assemblage from a shale clast in a conglomerate from the Spothford Burn comes from the lower part of the N. gracilis zone (R.B. Rickards, written communication).

APPENDIX 2.

GREYWACKE POINT COUNTING DATAGLENFLOSH FORMATION

	Specimen	Q	F	B	A	Met	Sed	Fm	Mx	Grid	Ref.
1	SPB1	443	40	25	5	12	54	-	421	7942	1412
2	SPB3	444	45	40	17	31	64	1	358	7923	1430
3	SPB4	434	44	23	21	32	55	1	390	7921	1443
4	SPB5	370	41	42	20	33	35	1	458	7918	1449
5	SPB9	412	63	40	19	20	83	-	353	7894	1488
6	BB1	369	84	49	8	15	50	-	425	7985	1511
7	BB61	404	106	62	4	14	26	-	384	7985	1513
8	BB63	444	68	14	18	23	35	-	398	7975	1515
9	BB64	355	108	66	3	9	73	-	386	7970	1520
10	NC	386	99	51	-	7	65	-	392	8062	1531
11	PB152	438	10	-	11	15	55	-	471	7803	1435
12	CRD5	450	107	21	22	30	35	2	333	8032	1508
	Mean	412	69	36	12	20	53	-	398		

Q - Quartz; F - Feldspar; B - Basic and intermediate igneous;
A - Acid igneous; Met - Metamorphic rock fragments;
Sed - Sedimentary rock fragments; Fm - Ferromagnesian minerals;
Mx - Matrix (including micas and heavy minerals).

APPENDIX 2.

GREYWACKE POINT COUNTING DATAKILN FORMATION

	Specimen	Q	F	B	A	Met	Sed	Fm	Mx	Grid Ref.
1	M67	354	143	61	10	20	72	1	328	7702 1337
2	SPB15/2	433	54	42	41	22	81	-	327	7867 1504
3	BB65	345	133	140	14	17	62	-	289	7967 1522
4	KB123	414	80	228	27	28	35	-	388	772 135
5	KB123	315	155	107	3	19	59	2	340	772 135
6	KB125	387	15	69	5	15	80	-	429	7710 1360
7	KB125	373	167	68	6	10	87	1	288	7710 1360
8	BCC153	370	60	20	16	17	43	1	473	7787 1442
9	SPB25	340	172	52	60	8	81	1	256	7849 1518
10	BB71	447	141	19	37	25	43	-	288	7937 1555
11	BB74	312	175	120	35	9	61	-	288	7925 1569
12	BB23	282	224	61	10	19	93	-	311	7932 1559
13	CRD101/1	395	160	51	24	14	44	-	312	8063 1666
14	CRD101/2	442	144	18	12	20	34	-	330	8062 1666
15	CRD106/1	429	165	46	19	14	45	-	282	8086 1630
16	CRD106	412	194	85	10	9	96	-	194	8086 1630
17	KB137	315	277	78	43	9	31	-	247	7681 1415
	Mean	375	145	63	22	16	62	-	317	

APPENDIX 2.

GREYWACKE POINT COUNTING DATASPOTHPORE FORMATION (MATRIX)

	Specimen	Q	F	B	A	Met	Sed	Fm	Mx	Grid Ref.
1	SPBA	235	124	124	9	7	51	1	449	7828 1528
2	SPB31	323	212	63	68	13	91	2	228	7830 1527
3	SPB34	307	183	58	37	17	57	2	339	7820 1530
4	SPB45M	259	201	7	20	12	23	-	478	7800 1523
5	SPB45M	264	202	88	13	11	45	-	377	7800 1523
6	SPB46M	245	166	40	17	20	39	-	473	7794 1521
7	SPB47M	88	315	19	27	5	13	1	532	7787 1519
8	NR51R	240	216	72	10	10	30	-	422	7756 1520
9	BB25M	237	88	48	5	14	48	-	560	7923 1579
10	BB27M	243	77	42	17	13	40	4	564	7923 1579
11	GBC103/1	343	177	57	47	9	30	-	337	746 142
12	KB138	202	205	24	24	14	29	-	502	7680 1423
13	KB139	290	112	86	44	13	136	-	319	7680 1429
14	KB143	231	89	30	4	11	42	-	593	7676 1442
15	KB143M	350	145	40	36	25	61	-	343	7676 1442
16	KB166/6	368	163	74	6	12	64	-	313	7613 1450
17	GBC94	419	149	41	21	33	44	3	290	7533 1436
	Mean	273	166	54	24	14	50	1	418	

APPENDIX 2.

GREYWACKE POINT COUNTING DATASPOTTHORE FORMATION (CLASTS)

	Specimen	Q	F	B	A	Met	Sed	Fm	Mx	Grid Ref.
1	SPB45C	183	312	23	13	22	48	-	399	7800 1523
2	SPB46C	167	75	13	16	10	18	-	701	7794 1521
3	SPB56	240	187	125	15	15	52	-	366	7707 1526
4	BB26C	234	87	56	26	7	28	7	555	7923 1579
5	BB28	333	168	175	12	7	65	-	240	7923 1579
6	BB29	278	149	81	18	7	45	1	421	7923 1579
7	KB177	188	42	16	9	11	31	-	703	7676 1442
8	GB90/1	286	94	162	7	12	27	9	403	7537 1430
9	GB90/3	270	163	101	14	21	62	1	368	7537 1430
10	KB143C	324	129	48	14	20	32	1	432	7676 1442
II	KB164	292	120	91	15	23	36	1	422	760 140
	Mean	254	139	81	15	14	40	2	455	

APPENDIX 2.

GREYWACKE POINT COUNTING DATAGUFFOCK FORMATION

	Specimen	Q	F	B	A	Met	Sed	Fm	Mx	Grid Ref.
1	SPB39/1	314	204	9	49	23	54	-	347	7800 1540
2	SPB39/2	286	265	25	26	20	35	-	343	7800 1540
3	SPB40	293	234	61	53	24	44	-	291	7796 1550
4	BB32	296	224	180	12	14	51	1	222	7870 1599
5	BB78	350	126	19	22	22	35	-	426	7898 1595
6	BB85DS	370	144	37	31	15	59	-	344	7884 1599
7	GHB122	282	95	6	33	18	34	2	530	7433 1435
8	GHB123	275	152	27	12	21	23	1	489	7414 1426
9	GHB124	308	117	4	9	13	11	2	586	7411 1426
10	KB155	240	164	72	20	9	55	-	440	7558 1488
11	KB169	292	154	91	7	18	30	-	378	756 148
	Mean	301	174	48	24	18	39	1	395	

APPENDIX 3.

ORIENTATION OF FOLDS IN THE AREA.

<u>ORIENTATION</u>	<u>FORMATION</u>	<u>GRID REFERENCE</u>
055°E/30°SW	Kiln. Fm.	76421403
055°E/35°SW	Kiln. Fm.	76761382
050°E/45°SW	Kiln. Fm.	78801498
078°E/32°SW	Kiln. Fm.	76911385
037°E/15°SW	Kiln. Fm.	81001621
057°E/45°NE	Kiln. Fm.	80881572
047°E/32°NE	Kiln. Fm.	80881572
055°E/30°SW	Kiln. Fm.	79561536
065°E/25°SW	Kiln. Fm.	77111356
090°E/25°NE	Kiln. Fm.	77021369
087°E/32°NE	Kiln. Fm.	77021369
059°E/59°NE	Kiln. Fm.	80801574
055°E/37°SW	Guffock Fm.	79111591
083°E/30°SW	Guffock Fm.	78051532
065°E/45°NE	Spothfore Fm.	76231457
085°E/30°SW	Glenflosk. Fm.	80801570
115°E/55°NW	Kiln. Fm.	79511541

APPENDIX 4. PREPARATION OF SAMPLES AND CHEMICAL ANALYSIS
OF IGNEOUS ROCKS.

Whole-rock samples were analysed by a combination of X-ray fluorescence spectrometry and Atomic absorption spectrometry. Polished thin sections were analysed using an electron-microprobe analyser.

Major elements were analysed at the Grant Institute of Geology, University of Edinburgh, on a Phillips PW1450 automatic spectrometer. Rb, Sr, Zr and Y were analysed on a similar instrument in the Department of Geology, University of St. Andrews. Cr, Ni, Ba and Li were analysed on a Atomic absorption spectrometer Techtron AA4 at the Department of Geology, University of St. Andrews.

Electron microprobe studies were carried out at the Grant Institute of Geology, University of Edinburgh, on a Cambridge Instruments Microscan V coupled to a Link Systems Energy Dispersive Spectrometer.

For whole-rock analysis the weight of each sample was 2-5 kg. The rocks were broken down to 5 cm lumps and weathered surfaces removed with a Gemtek grit wheel. Material was then crushed to chips (1-2 cms) and weathered material discarded. The chips were washed in distilled water, dried and crushed in a Tema-mill for approximately 1 minute (2 x 30 secs) per 75 g load. The resultant powder was mixed by "coning and quartering" and stored.

For electron microprobe analysis carbon coated polished thin sections were used.

APPENDIX 4.PREPARATION OF SAMPLES AND CHEMICAL ANALYSIS
OF IGNEOUS ROCKS.

XRF analytical conditions

Line	Crystal	kV	mA	Collimator	Counter
SiK _α	PE	50	45	C	F
AlK _α	PE	60	45	C	F
FeK _α	LiF200	50	45	F	F
MgK _α	TIAP	60	45	C	F
CaK _α	LiF200	50	30	F	F
NaK _α	TIAP	60	45	C	F
KK _α	LiF200	50	45	F	F
TiK _α	LiF200	50	45	F	F
MnK _α	LiF200	60	45	F	F
PK _α	Ge	50	45	C	F
RbK _α	LiF200	32	14	F	S
SrK _α	LiF200	32	14	F	S
YK _α	LiF200	32	14	F	S
ZrK _β	LiF200	32	14	F	S

Crystals

PE, Pentaerythritol

TIAP, Thallium acid phthalate

Ge, Germanium

LiF, Lithium fluoride.

Collimators

C, Coarse; F, Fine

Counters

F, gas flow proportional counter

S, scintillation counter.

Electron microprobe analyses were carried out with an accelerating voltage of 20kV and a probe current of 6 nanoamps (as measured in the Faraday Cage).

APPENDIX 5.ACCURACY AND PRECISION OF THE GEOCHEMICAL
AND MINERALOGICAL DATA.

A measure of the precision and accuracy of the geochemical and mineralogical data can be derived from the tables below.

	Mean	<u>+2σ</u>
SiO ₂	59.62	0.240
Al ₂ O ₃	17.12	0.062
Fe ₂ O ₃	6.92	0.035
MgO	1.59	0.030
CaO	4.96	0.020
Na ₂ O	4.37	0.124
K ₂ O	2.96	0.013
TiO ₂	1.06	0.006
MnO	0.10	0.009
P ₂ O ₅	0.48	0.007

Data from Grant Institute of Geology, University of Edinburgh.
Values in wt.%. 16 cycles per sample.

	Mean	<u>+2σ</u>
Rb	89	5.8
Sr	65	5.2
Y	28	1.5
Zr	136	2.0 *
Cr	40	5.7
Ni	33	11.0
Ba	734	44
Li	140	6.1

Data from Geochemical Laboratory, Department of Geology, University of St. Andrews. Values in ppm.

* Zr data for Bail Hill rocks is subject to greater imprecision as the ZrK_β peak has been measured. No estimate of the precision can be made.

APPENDIX 5.ACCURACY AND PRECISION OF THE GEOCHEMICAL
AND MINERALOGICAL DATA.

	XRF	Abbey (1977)
SiO ₂	66.09	65.98
Al ₂ O ₃	14.81	14.71
Fe ₂ O ₃	3.82	3.75
MgO	2.30	2.31
CaO	2.45	2.51
Na ₂ O	3.60	3.78
K ₂ O	4.687	4.64
TiO ₂	0.662	0.68
MnO	0.060	0.06
P ₂ O ₅	0.269	0.28
Cr	10	12
Li	10	14
Ni	30	19
Ba	1114	1208*
Rb	114	120**
Sr	198	190**
Zr	87	91**
Y	38	40**

Analyses of standard samples run as unknowns, not included in calibrations, compared with values from Abbey (1977) and *Flanagan (1973). Major elements in wt.%, trace elements in ppm.

**Values from Report 1, Geochemistry Lab. University of Southampton.

For the electron microprobe analyses the calibration was monitored by a Co standard and an estimate of accuracy was obtained by analysing a Jd standard as an unknown at the beginning of each session.

The precision of the electron microprobe data varies according to the atomic no. and concentration of the elements. Major elements (greater than 10%) are believed precise to approximately 1-2% of the actual concentration, whilst minor elements (under 10%) are precise to approximately 5% of the actual concentration. Precision of the lighter elements is poorer than

APPENDIX 5.ACCURACY AND PRECISION OF THE GEOCHEMICAL
AND MINERALOGICAL DATA.

the above figures and sodium was not usually detected at concentrations below 0.5%.

A beam width of 1 micron was used for all mineral analyses. A defocussed beam of approximately 150 microns width was used for groundmass analyses and these analyses are subject to greater inaccuracies than the narrow beam analyses.

APPENDIX 6.IGNEOUS ROCK SAMPLE LOCALITIES.

Rock number	Baragar & Irvine classification	Occurrence	Grid Ref
CC6E	Sodic trachyte, SS	Int	75871317
CC9W	Mugearite, SS	Int	75751309
CC16W	Ankaramite, PS	CCF	75781329
CC17	Alkali basalt, PS	CCF	757133
CC26	Alkali basalt, PS	CCF	75651333
BCC27/2	Mugearite, SS	BCM	75741352
BCC27/3	Alkali basalt, PS	Xen	75741352
BCC28/1	Hawaiite, SS	BCM	75731345
BCC30/2	Alkali basalt, PS	Xen	75741356
Bcc32	Benmoreite, SS	PRF	75681375
BCC33	Alkali basalt, PS	CCF	75731341
BCC34/1	Hawaiite, SS	BCM	75781341
BCC35/1	Mugearite, SS	BCM	75741345
BCC36	Hawaiite, SS	BCM	757134
GB60	Calc-alkali basalt	PRF	74621367
GB63/2	Alkali basalt, PS	CCE	74681371
GB85P2	Benmoreite, SS	Int	75351412
MRD102	Hawaiite, SS	GBM	75651437
GBC103/2	Trachybasalt, PS	Xen	746142
GBC103/20	Trachybasalt, PS	PRF	746142
GBC103/21	Hawaiite, SS	PRF	746142
GBC103/30	Trachybasalt, PS	PRF	746142
GBC103/40	Hawaiite, SS	PRF	746142
GBC103/50	Hawaiite, SS	PRF	746142
GBC103/6	Trachybasalt, PS	PRF	746142
GBC103/70	Alkali picrite basalt, SS	Xen	746142
GBC103/71	Hawaiite, SS	PRF	746142
GBC111	Alkali basalt, PS	CCF	74521375
LK114	Trachybasalt, PS	PRF	759144
STB135/2	Ankaramite, SS	SM	76771381
SPB145M	Ankaramite, SS	PM	78671504
SPB145C	Calc-alkali basalt	PM	78671504
BHC146	Mugearite, SS	PRF	76101415
M9	Mugearite, SS	Xen	75741352
M91	Calc-alkali basalt	SM	76771381
M127	Hawaiite, SS	BCM	757134

APPENDIX 6.IGNEOUS ROCK SAMPLE LOCALITIES.

Rock number	Baragar and Irvine classification	Occurrence	Grid Ref
StB9	Hawaiite, SS	SM	76701381
KBR142/1	Hawaiite, SS	SM	769138
KBR142/3	Hawaiite, SS	SM	769138

In the Baragar and Irvine (1971) classification SS refers to lithologies belonging to the sodic alkaline basalt series, whilst PS refers to lithologies in the potassic alkaline series.

Occurrence: CCF= Cat Cleuch Formation; BCM= Bught Craig Member; Int= Intrusion; Xen= xenolith; PRF= Peat Rig Formation; GBM= Grain Burn Member; SM= Stoodfold Member; PF= Penfrau Member.

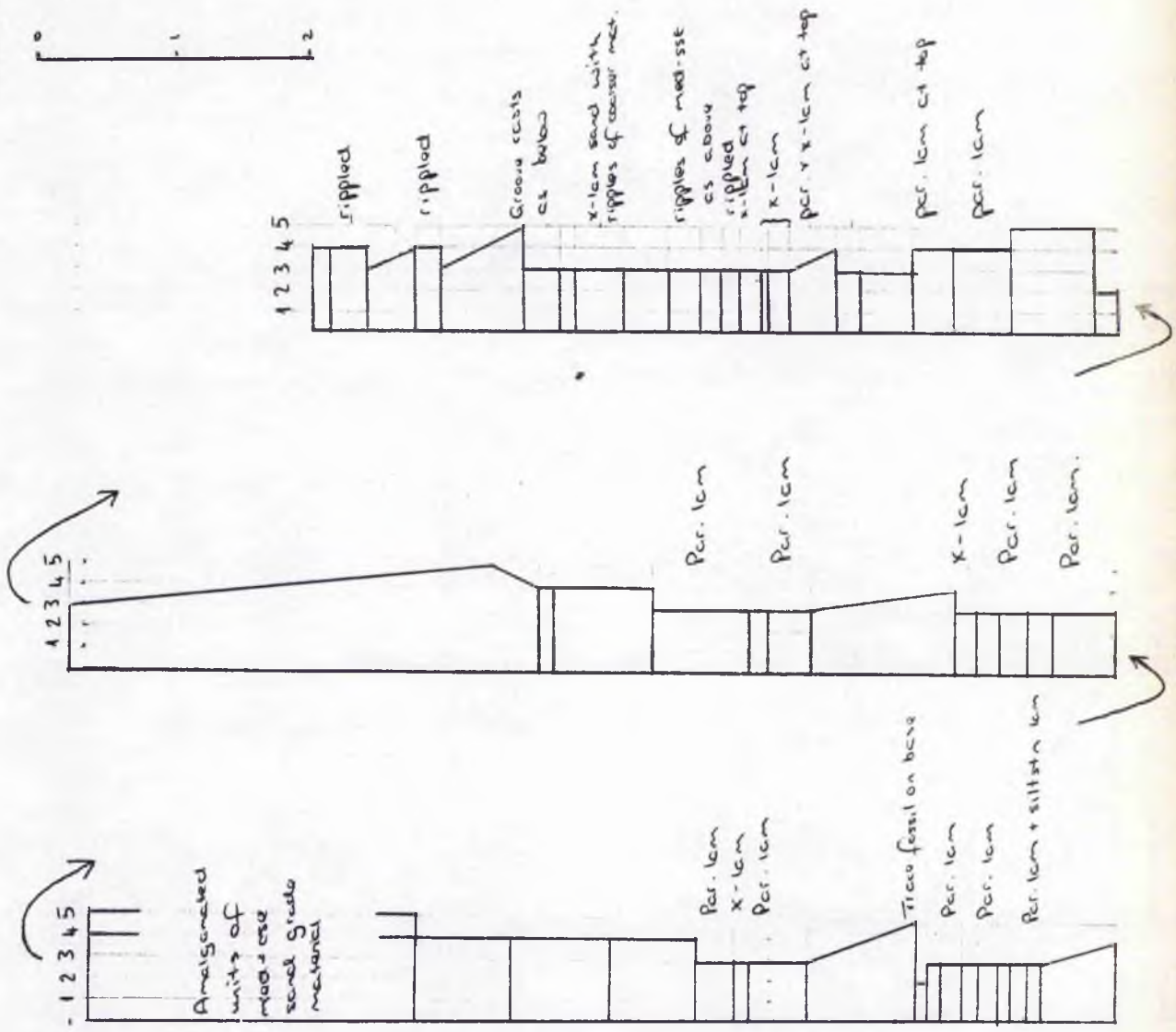
Polished thin section number	Occurrence	Grid Ref
CC16W	CCF	75781329
CC17 (2 spec)	CCF	757133
CC24	CCF	75501334
BCC27/1 (2 spec)	BCM	75741352
BCC27/1/1 (2 spec)	BCM	75741352
BCC27/2	BCM	75741352
BCC27/3	BCM	75741352
BCC27/4	BCM	75741352
BCC27/5	BCM	75741352
BCC27/7	BCM	75741352
BCC27/12	BCM	75741352
BCC27/19	BCM	75741352
BCC27/23	BCM	75741352
BCC27X	BCM	75741352
BCC28/4	BCM	75731345
GB79 (3 spec)	GBM	75131401
GBC103/51	PRF	746142
GBC103/7	PRF	746142
GBC103/70	PRF	746142
GBC111	CCF	74521375
SPB145C	PF	78671504
S31278	"Apatite rock"	749140

APPENDIX 7. LOGGED SEQUENCES IN THE GLENFLOSH AND KILN FORMATIONS

KILN FORMATION: Sequence from the lower part of the Kiln Formation logged in the Kiln Burn section.

1 = shale; 2 = siltstone; 3 = fine-grained sandstone; 4 = medium-grained sandstone; 5 = coarse-grained sandstone.

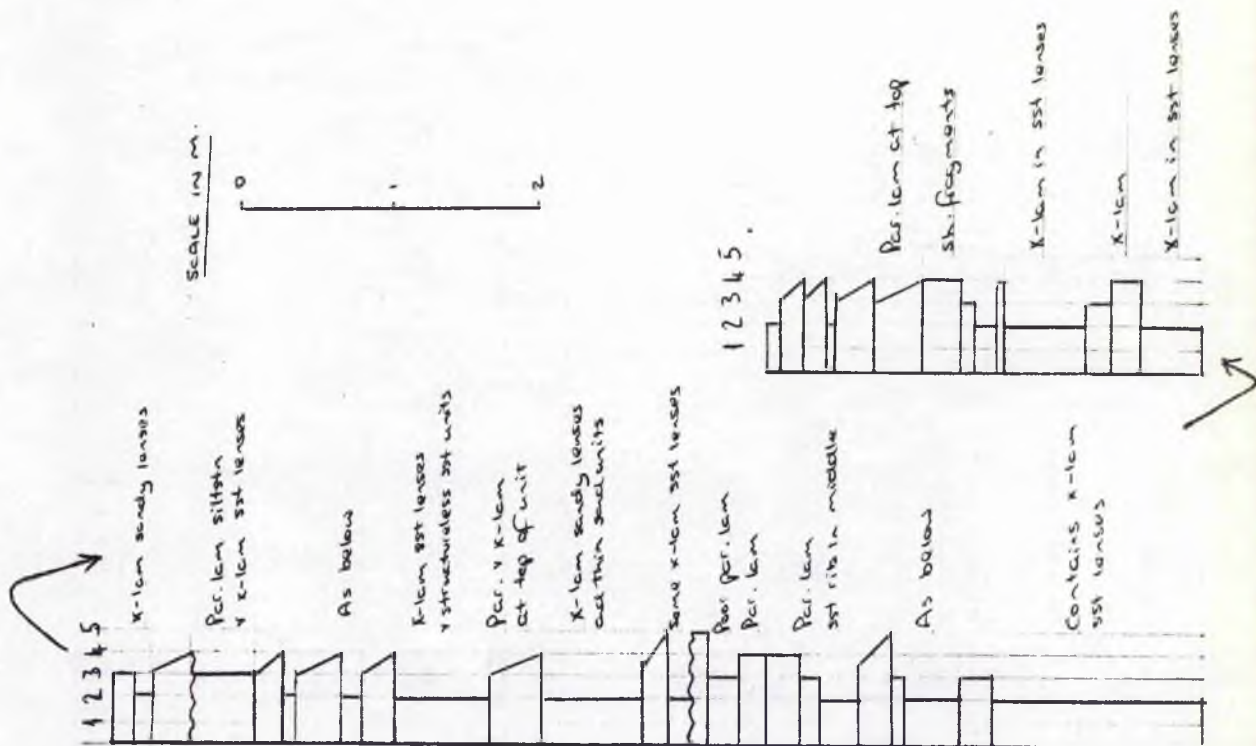
SCALE IN M.



APPENDIX 7. LOGGED SEQUENCES IN THE GLENFLOSH AND KILN FORMATIONS

KILN FORMATION: Sequence from the middle part of the Kiln Formation logged in the Kiln Burn 150 m downstream from the Stoodfold Burn.

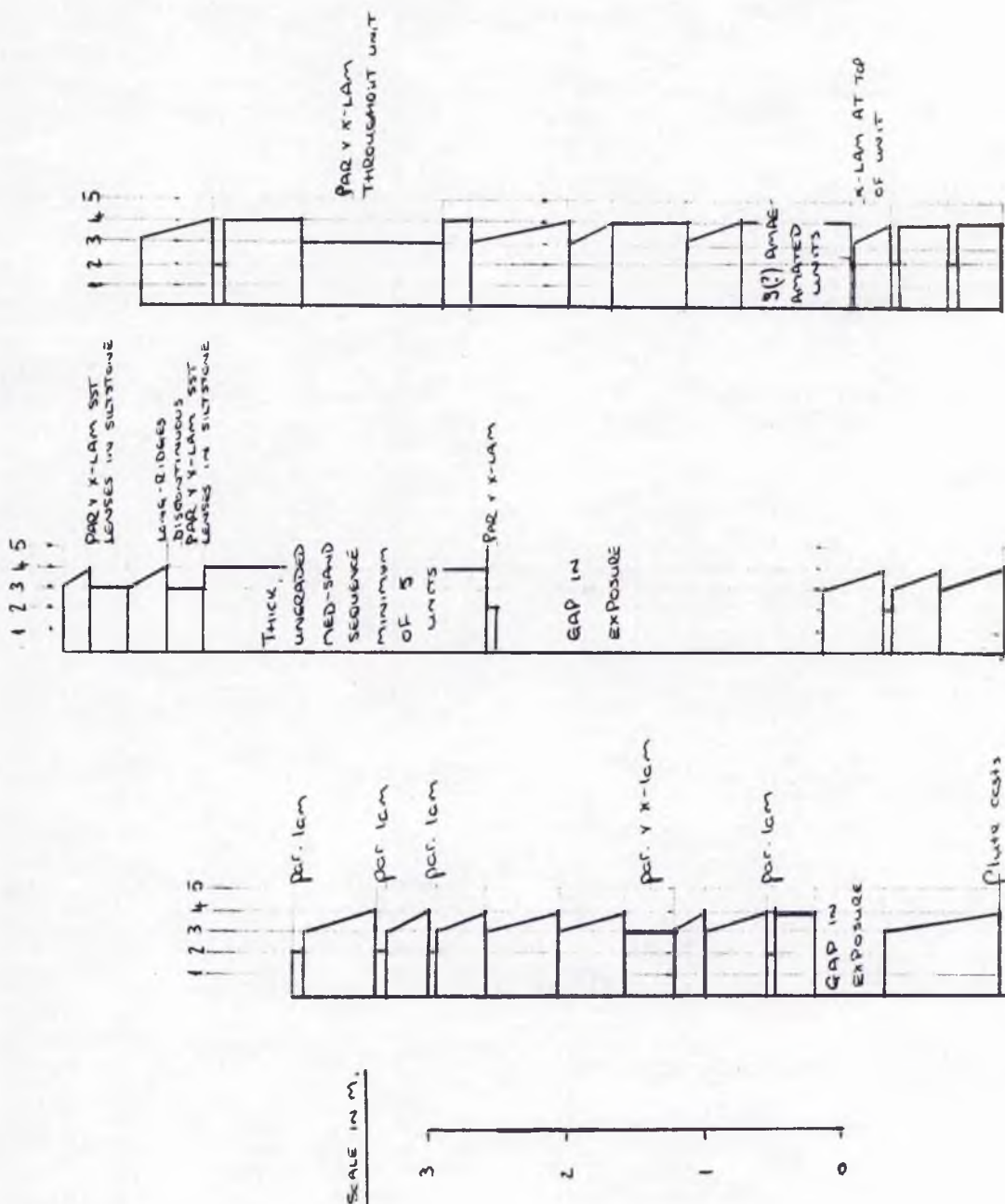
See (i) for explanation.



APPENDIX 7. LOGGED SEQUENCES IN THE GLENFLOSH AND KILN FORMATIONS

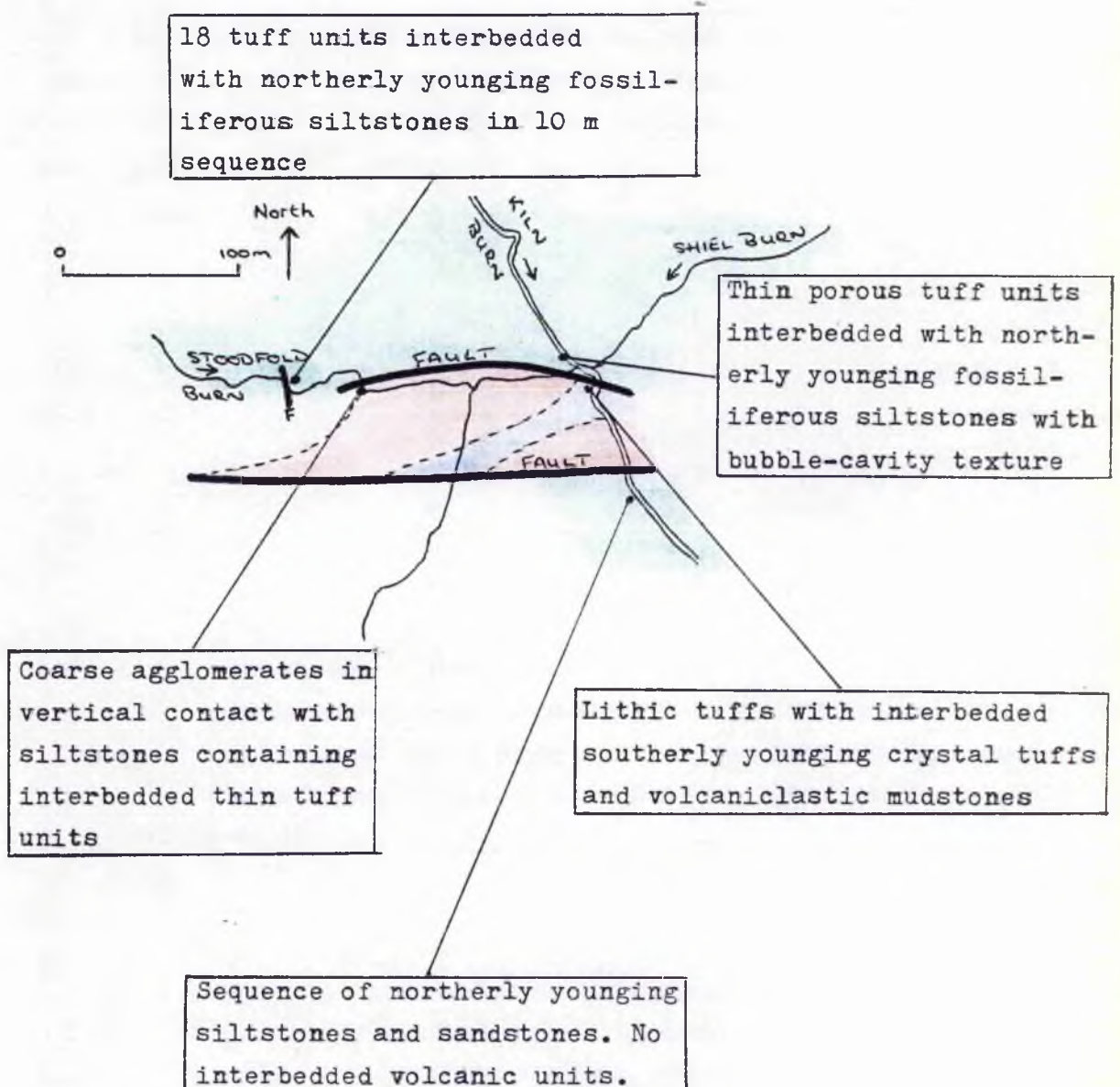
GLENFLOSH FORMATION: Three sequences from exposures in the Spothfore Burn.

See (i) for explanation.



STOODFOLD MEMBER: The largest and best exposed of the tuff members. It crops out near the confluence of the Kiln and Stoodfold Burns. The tuffs and agglomerates are of hawaiite/mugearite composition and originate from the middle-stage activity of the Bail Hill volcano.

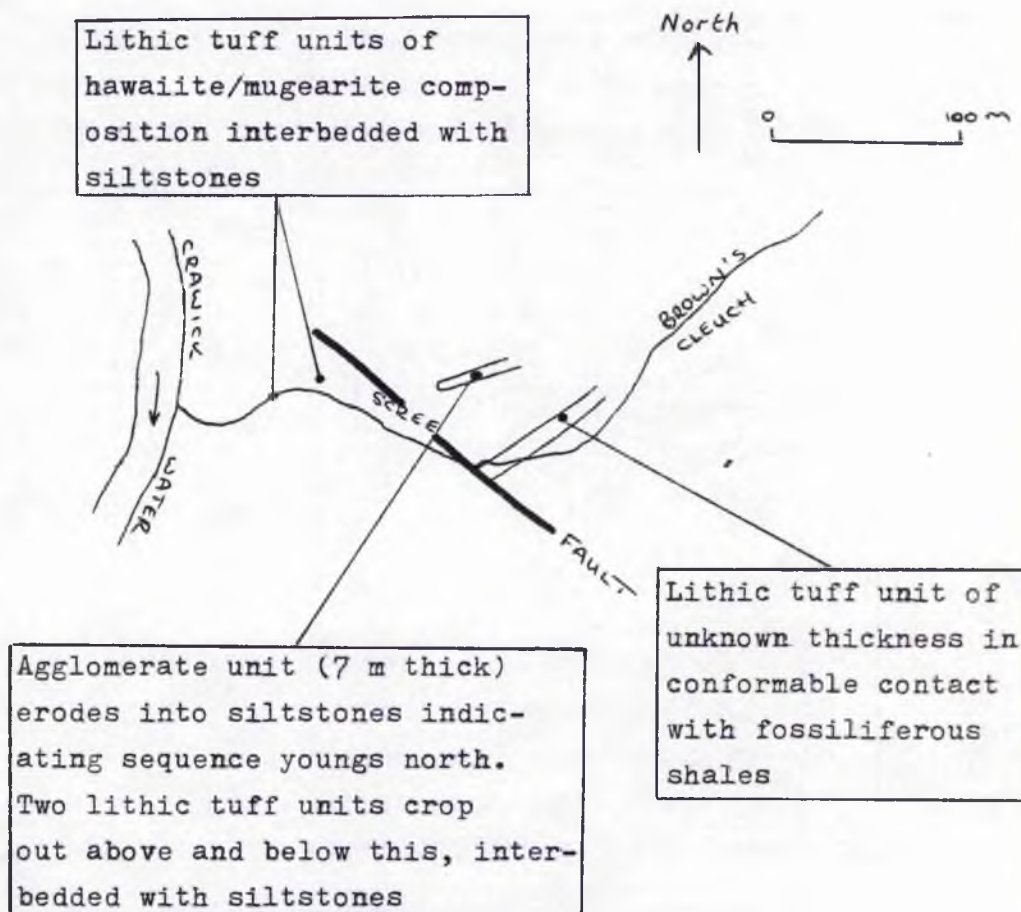
In the sketch-map below green = Kiln Formation sediments (+ interbedded volcanics); red = agglomerates; blue = crystal and lithic tuffs and volcanoclastic mudstones.



APPENDIX 8.

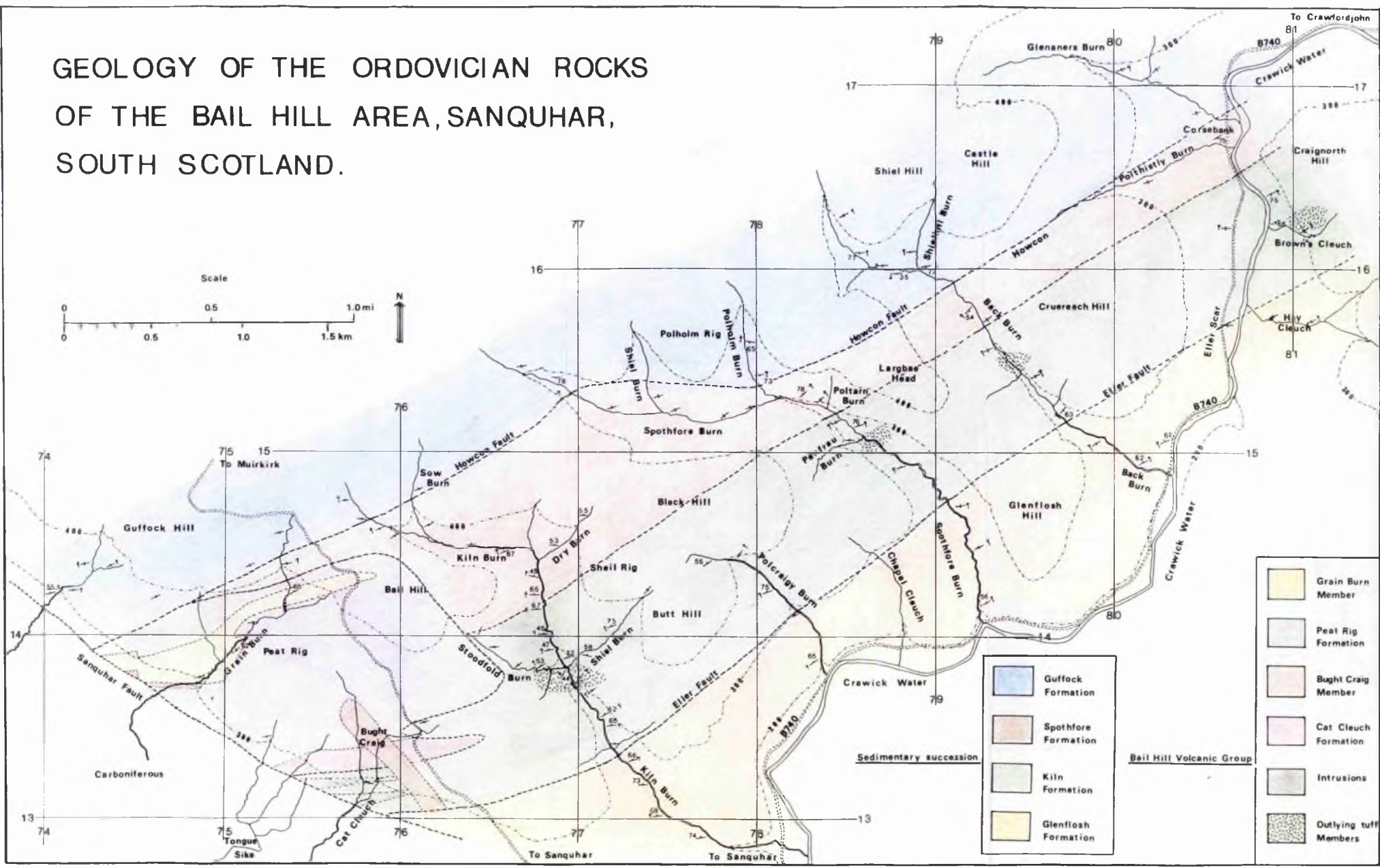
FIELD MAPS OF OUTLYING TUFF MEMBERS

CRAIGNORTH MEMBER: The Craignorth Member crops out in the stream draining the southern flank of Craignorth Hill - Brown's Cleuch. The sequence is strongly complicated by folding and faulting and the field relations in the sketch are therefore oversimplified. The salient outcrops and features should however be detectable by using this map.



BACK BURN MEMBER: The Back Burn Member, a hitherto undiscovered outcrop of the volcanic horizon, is too small and too poorly exposed to be mapped. It crops out as a single 1.5 m thick unit in the stream at (79441547) and is in conformable and vertical contact with sand-grade turbidites.

GEOLOGY OF THE ORDOVICIAN ROCKS OF THE BAIL HILL AREA, SANQUHAR, SOUTH SCOTLAND.



- | | |
|--|-----------------------|
| | Guffock Formation |
| | Spothfore Formation |
| | Kiln Formation |
| | Glenfloss Formation |
| | Grain Burn Member |
| | Peat Rig Formation |
| | Bught Craig Member |
| | Cat Cleuch Formation |
| | Intrusions |
| | Outlying tuff Members |

Sedimentary succession

Bail Hill Volcanic Group

Offprint from

JOURNAL OF
EARTH SCIENCES

ROYAL DUBLIN SOCIETY



ROYAL DUBLIN SOCIETY

*Founded in 1731 for the Promotion
of Agriculture, Industry, Science and Art*

DISCUSSION OF: EVIDENCE FOR CALEDONIAN SUBDUCTION FROM GREYWACKE DETRITUS IN THE LONGFORD-DOWN INLIER

M.J. McMURTRY

In their recent paper Sanders and Morris (1978) suggest that volcanic detritus found in Irish greywackes of the Red Island Formation was derived from a calc-alkaline volcanic arc situated on a northwestern continent. Euhedral crystals of pyroxene, amphibole and feldspar occurring in the greywackes are interpreted as volcanic phenocrysts incorporated soon after eruption. Although feldspars are albitised and the whole rock chemistry is not known, the volcanic clasts are identified as andesites of the calc-alkaline magma series on the evidence of pyroxene chemistry. The greywackes pass up into rocks containing a *Nemagraptus gracilis* fauna and a tentative Llandeilo age is suggested.

It is my contention that the fragments were not derived from an extrabasinal calc-alkaline volcanic arc but from an intrabasinal, within-plate alkaline magma. My work suggests that the Bail Hill volcanics represent one such source for the volcanic detritus.

The Bail Hill volcanics crop out in the Northern Belt of the Southern Uplands of Scotland. Although truncated by the Carboniferous rocks of the Sanquhar coal basin, they form the single largest volcanic area in the three belts of the Southern Uplands. The volcanic rocks are interbedded with sediments yielding a *N. gracilis* fauna.

The volcanic rocks are highly porphyritic auto-brecciated lavas and pyroclastics. Early

activity was basaltic and became more siliceous with time. My unpublished data suggest that there is a genetic relationship between the basalts and the more siliceous members of the series. The presence in the volcanics of cumulate blocks and lava-types not found in outcrop suggest that the Bail Hill pile represents only a small portion of a larger intrusive and extrusive episode.

Phenocrysts and cumulate minerals in pristine condition have been analysed on the electron microprobe at the Grant Institute of Geology, University of Edinburgh. Pyroxene and amphibole analyses very similar to those presented by Sanders and Morris (1978, Table 2) are presented in Table 1. Al-'poor' and Al-'rich' pyroxenes occur and the latter co-exist with brown pargasite similar to the Al-'rich' pyroxene and brown hornblende association of Sanders and Morris (1978, Table 2). In the same specimen a green amphibole of edenitic composition is seen to replace the pyroxene and is similar to the green hornblende of Sanders and Morris (1978, Table 2), which they suggest is derived from a metamorphic clinopyroxenite.

In view of the similarity of mineral compositions and associations I suggest that the detritus in the Irish greywackes was derived from a magmatic episode similar to that from which came the Bail Hill rocks.

Feldspars in the Bail Hill rocks have not

Table 1. E.D.S. probe analyses of selected minerals from the Bail Hill volcanics.

	DIOPSIDE	SALITE	PARGASITE	EDENITE
SiO ₂	53.16	50.63	42.38	47.84
TiO ₂	0.26	0.42	1.15	1.30
Al ₂ O ₃	1.91	5.10	12.30	7.31
Cr ₂ O ₃	0.33	0.38	—	—
iFeO	4.49	5.96	12.00	9.53
MnO	0.21	0.25	0.29	0.25
MgO	16.14	15.16	14.44	17.77
CaO	23.07	21.23	11.67	11.05
Na ₂ O	—	0.47	2.54	2.22
K ₂ O	—	—	0.63	0.23
TOTAL	99.87	99.60	97.40	97.50
STRUCTURAL FORMULAE				
Si	1.958	1.863	6.23	6.90
Al ^{iv}	0.042	0.137	1.77	1.10
Al ^{vi}	0.041	0.084	0.36	0.15
Ti	0.007	0.012	0.13	0.14
Fe ²⁺	0.138	0.131	1.16	1.15
Fe ³⁺	—	0.052	0.31	—
Mn	0.007	0.008	0.04	0.03
Mg	0.881	0.831	3.16	3.82
Ca	0.906	0.837	1.84	1.71
Na	—	0.034	0.73	0.62
K	—	—	0.12	0.04
CATIONS	3.990	4.000	15.85	15.66
OXYGEN	6.00	6.00	23.00	23.00

ⁱAll iron treated as ferrous.

been albitised and classification has been based on mineralogical and geochemical criteria as suggested by Hatch, Wells and Wells (1972). Although oligoclase- and andesine-bearing rocks are volumetrically abundant at Bail Hill, the silica percentage of the rocks is always less than 54 per cent, much lower than for calc-alkaline andesites. Furthermore, it is clear from the early basaltic activity and the presence of cumulate blocks that the oligoclase- and andesine-bearing rocks have evolved from liquids of basaltic composition. Whole rock and groundmass norms are undersaturated and contain nepheline. The liquid has differentiated along the basalt – hawaiite – mugearite – trachyte trend, typical of mildly alkalic magmas and is not related to the calc-

alkaline series.

Sanders and Morris (1978) have based their evidence for a subalkalic magma source for the volcanic clasts on pyroxene chemistry. However, it has been noted that pyroxenes from evolved basalt and mildly alkaline magmas are not reliable indicators of magma type (Nisbet and Pearce 1977, Gibb 1973). The diagram used by Sanders and Morris (1978, Fig. 2a) was developed for groundmass pyroxenes only and Le Bas (1962) indicated that phenocrysts frequently plotted outside their respective magma fields. The zoning in the pyroxenes of Sanders and Morris (1978) is also likely to complicate the interpretations of such plots.

Intrabasinal clasts of volcanic origin in

rocks from the Southern Uplands were originally recognised by Ritchie and Eckford (1936). Kelling (1962) also suggested an intrabasinal origin for volcanic clasts in the Corsewall Group of the Rhinns of Galloway. Sedimentary clasts, such as shales, siltstones and greywackes, have been reported by many authors working on rocks from the Southern Uplands and Longford-Down, including Sanders and Morris (1978, p. 57). These have been identified as intrabasinal 'rip-up' clasts, indicative of submarine erosion.

In view of this widespread intrabasinal contribution to the sedimentary clasts found in rocks from the Southern Uplands and Longford-Down, there seems little need to look for possible extrabasinal sources for the volcanic detritus, particularly when a petrographically identical suite of rocks was known to exist in the sedimentary basin.

M.J. McMURTRY
Department of Geology,
University of St. Andrews,
Fife, Scotland.

References

- GIBB, F.G.F. (1973). The zoned pyroxenes of the Shiant Isles Sill, Scotland. *J. Petrol.* **14**, 203-220.
- HATCH, F.H., WELLS, A.K. and WELLS, M.K. (1972). *Petrology of the igneous rocks*. George Allen & Unwin Ltd. London, 551 pp.
- KELLING, G. (1962). The petrology and sedimentation of Upper Ordovician rocks in the Rhinns of Galloway, south-west Scotland. *Trans. R. Soc. Edinburgh*, **65**, 107-137.
- LE BAS, M.J. (1962). The role of aluminium in igneous rocks with relation to their parentage. *Am. J. Sci.* **260**, 267-288.
- NISBET, M.G. and PEARCE J.A. (1977). Clinopyroxene composition in mafic lavas from different tectonic settings. *Contrib. Mineral. Petrol.* **63**, 149-160.
- RITCHIE, M. and ECKFORD, R.J.A. (1935). The "Haggis Rock" of the Southern Uplands. *Trans. geol. Soc. Edinburgh*, **13**, 371-377.
- SANDERS, I.S. and MORRIS, J.H. (1978). Evidence for Caledonian subduction from greywacke detritus in the Longford-Down inlier. *J. Earth Sci. R. Dubl. Soc.* **1**, 53-62.

REPLY TO DISCUSSION

I.S. SANDERS and J.H. MORRIS

We find McMurtry's revised interpretation of our data plausible and stimulating, particularly since the Bail Hill volcanic rocks and the Red Island Formation are about the same age. However, we would wish to see much more evidence in support of his case than space permits in a short discussion article. In particular, we would like to see a comparison of the full range of pyroxene and amphibole chemistry from the two suites of rocks, and

also a comparison of their petrography. We would also welcome a fully argued case for the suggested within-plate origin of the Bail Hill volcanic rocks.

For the present we prefer to stand by our original view, and in support of it we would make the following additional comments.

The Red Island Formation is the oldest of three formations comprising the Gowna Group, which is estimated to be, very approx-

imately, 6000 m thick (Leggett *et al.* in press, Morris 1979). Gowna Group greywackes are generally similar in composition to those of the Red Island Formation, although plagioclase rich varieties are common in the two younger formations. The formation overlying the Red Island Formation contains both *Nemagraptus gracilis* Zone graptolite localities and spilitic lavas. We consider it reasonable to infer that the Gowna Group ranges in age from Llandeilo to Caradoc, an inference based on the time span of the *N. gracilis* Zone, the stratigraphical location of *N. gracilis* faunas, and the thickness of the group. Protracted influx of andesitic debris through such a time span is more easily reconciled with a volcanic arc source, rather than temporally, and perhaps spatially, restricted ocean island sources. Moreover, the spilitic lavas exposed in the group, and which might be termed 'intrabasinal', are of tholeiitic affinity (Leggett *et al.* in press) and are non-porphyritic; they do not represent a possible source of andesitic debris in enclosing greywackes.

Greywackes petrographically similar to those of the Red Island Formation occur elsewhere in the Longford-Down inlier and in the Rhinns of Galloway, Scotland (Leggett *et al.* in press). Research by one of us (J.H.M.) subsequent to publication of our paper, in-

dicates that greywackes of the Portpatrick Group Basic Clast Division (Kelling 1961, 1962) are, in fact, petrographically identical to those of the Red Island Formation, although Portpatrick Group greywackes are slightly younger. The wide distribution, over a strike length of about 200 km, of greywackes rich in distinctive volcanic detritus is, again, more readily attributed to a regionally extensive volcanic arc source, than to spatially isolated oceanic islands. It might also be noted that Kelling (1962) specifically rejects Bail Hill as a possible source of the andesitic debris in the Basic Clast Division, even though the age difference of the rocks in the two areas does not preclude such a possibility.

Additional references

- KELLING, G. (1961). The stratigraphy and structure of the Ordovician rocks of the Rhinns of Galloway. *Q. J. geol. Soc. Lond.* **117**, 37-75.
- LEGGETT, J.K., McKERROW, W.S., MORRIS, J.H., OLIVER, G.J.H., and PHILLIPS, W.E.A. (1980). The north-western margin of the Iapetus Ocean. In Harris, A.L., Holland, C.H. and Leake, B.E. (Eds.) *The Caledonides of the British Isles - reviewed*. Geol. Soc. Lond. in press.
- MORRIS, J.H. (1979). *The geology of the western end of the Lower Palaeozoic Longford-Down inlier, Ireland*. Unpubl. Ph.D. thesis, Univ. of Dublin.

I.S. SANDERS and J.H. MORRIS
Department of Geology,
Trinity College,
Dublin 2.